

Deciphering the redox signalling pathway in long-lived mitochondrial mutant

Inaugural-Dissertation

Zur
Erlangung des Doktorgrades
der Mathematisch-Naturwissenschaftlichen fakultät
der Universität zu Köln



vorgelegt von
Johannes Christiaan Wilhelmus Hermeling
aus Arnhem, die Niederlande

Köln 2021

Berichterstatter: **Prof. Dr. Aleksandra Trifunovic**

Prof. Dr. David Vilchez

Tag der mündlichen Prüfung: 21.01.2022

“Happiness can be found
even in the darkest of times,
if only one remembers to
turn on the light.”

J.K. Rowling, *The Prisoner of Azkaban*

To my beloved family and friends

List of Content

List of Content.....	iv
Abbreviations	x
Abstract	xvi
1. Introduction	17
1.1. Ageing	17
Fig. 1.1. Hallmarks of ageing and their functional interconnections	18
1.2. Mitochondria and ageing.....	19
1.2.1 Mitochondria	19
1.2.2 Mitochondria genome.....	20
1.2.3 Mitochondria structure and OXPHOS.....	20
Fig. 1.2. Mitochondrial architecture	21
Fig. 1.3. Overview of mitochondrial respiratory chain complexes	22
Fig. 1.4. Schematic overview of Q cycle	23
1.2.4 Mitochondria and their role in ageing	24
1.3. ROS.....	26
1.3.1 ROS molecules	26
Fig. 1.5. ROS generation, reduction and signalling.	26
1.3.2 H ₂ O ₂ as second messenger.....	27
1.3.3 Mitochondrial ROS.....	29
Fig. 1.6. Possible sites of ROS generation	29
1.4. <i>C. elegans</i> and aging research	30
1.4.1 <i>C. elegans</i> research model.....	30
Fig. 1.7. Schematic overview of <i>C. elegans</i> lifespan.....	31
1.4.2 <i>C. elegans</i> ageing research.....	31
1.4.3 <i>C. elegans</i> mitomutants.....	33
1.4.3 Longevity assurance pathways	36
1.5.1 KLF-1: regulator of mitomutant <i>isp-1;ctb-1</i> lifespan	37
Fig. 1.8. KLF-1 is necessary during early adulthood for mitomutant-induced longevity.	38
1.5.2 Conserved function of mammalian KLFs.....	39
1.6 Aim of this study.....	41
2. Material and methods.....	42
2.1. <i>C. elegans</i> methods	42
2.1.1. Strains and maintenance	42
Table. 2.1 <i>C. elegans</i> strains used	42

2.1.2. Microinjection and X-ray integration of transgenic strains	43
2.1.3. Crossing of <i>C. elegans</i> strains	44
2.1.4. Genotyping of <i>1(qm150);ctb-1(qm189)</i> strain	44
Table 2.2 Primers for genotyping	45
2.1.5. Synchronization of worm populations	45
2.1.6. RNAi treatment	45
Table 2.3 RNAi clones	46
2.1.7. KLF-1 nuclear localisation	46
Table 2.4 Drugs	47
2.1.8. Lifespan analysis	48
2.1.9. ROS measurements	48
2.1.10. H ₂ O ₂ resistance assay	48
2.1.11. BODIPY 493/503 staining	49
2.1.12. Xenobiotic resistance assays	49
2.2. Molecular biology and biochemistry	49
2.2.1. Real-Time qPCR	49
Table 2.5 Primers for real-time PCR	50
2.2.2. Protein isolation	51
2.2.3. Western blot	51
Table 2.6 Primary antibodies used for western blot	52
Table 2.7 Secondary antibodies used for western blot	52
2.2.4. Shift assay	52
2.2.6. Site-directed mutagenesis	53
Table 2.8 Primers for site-directed mutagenesis	54
2.3. Microscopy	54
2.4. Statistical Analysis	54
2.5. Chemicals, equipment and biological materials	55
Table 2.9 Chemicals and supplier	55
2.5.2. Buffers and solutions	57
Table 2.10 Buffer and solutions	57
2.5.3. Commercial and Assay kits	61
Table 2.11 Commercial and Assay kits	61
2.5.4. Equipment	62
Table 2.12 Equipment	62
2.5.5. Software	62
Table 2.13 Software	62
3. Results	64
3.1 ROS is mediating KLF-1 activation	64

Fig. 3.1 <i>Isp-1;ctb-1</i> animals have mainly nuclear localized KLF-1	65
Fig. 3.2 Oxidative stress activates and translocate KLF-1 to the nucleus. .	65
Fig. 3.3 Oxidative stress-induced longevity is inhibited by KLF-1 suppression during adulthood.....	66
Fig. 3.4 <i>Isp-1;ctb-1</i> animals showed elevated H ₂ O ₂ levels during L4.....	67
Fig. 3.5 Antioxidant treatment abolishes oxidative stress-induced KLF-1 nuclear localization.....	68
3.2 L3/L4-dependent ROS signalling is required for KLF-1 nuclear localization	68
Fig 3.6 Complex III-ROS-production site inhibitor S3QEL-2 blocks KLF-1 nuclear localization during larvae stages.....	69
Fig 3.7 Redox signal is required during L3/L4	70
3.3 KLF-1 nuclear translocation is induced by mitochondrial produced ROS	70
Table 3.1. Overview of drugs and RNAi used for inducing mild mitochondrial dysfunction	70
Fig 3.8 ROS-producing ETC complexes are responsible for KLF-1 nuclear localization.	72
Fig 3.9 Peroxisomal and ER-derived ROS are unable to induce KLF-1-mediated longevity.....	73
Fig 3.10 KLF-1 is translocated to the nucleus by mtROS.....	74
3.4 E3 ligase WWP-1 is activating KLF-1, however it is not part of the KLF-1-induced longevity pathway	75
Fig. 3.11 <i>Wwp-1</i> depletion subcellular translocate KLF-1 in a non-redox dependent manner	75
Fig 3.12 KLF-1 is not regulated by WWP-1-induced proteasomal degradation	76
Fig 3.13 WWP-1-mediated KLF-1 nuclear localization is not inducing <i>cyps</i>	77
Fig 3.14 WWP-1 interaction with KLF-1 is not responsible for the increased lifespan in <i>isp-1;ctb-1</i> worms	78
3.5 The role of mitochondrial SOD-3 and PRDX-3 in KLF-1 nuclear translocation	79
Fig 3.15 ROS molecule H ₂ O ₂ translocate KLF-1 to the nucleus	79
Fig 3.16 Mitomutant-induced longevity is mediated by <i>sod-3</i>	80
Fig 3.17 KLF-1-independent increased <i>sod-2</i> and <i>sod-3</i> expression in D1 <i>isp-1;ctb-1</i> mutant	81
Fig 3.18 KLF-1 is translocated to the nucleus when <i>prdx-3</i> is depleted.....	82
Fig 3.19 <i>Prdx-3</i> depletion results in ROS-induced and KLF-1-mediated longevity	83
3.6 L4 <i>isp-1;ctb-1</i> animals have increased mitochondrial H ₂ O ₂ release what results in increased oxidative cytosolic redox state.....	83

Fig 3.20 <i>Isp-1;ctb-1</i> mutants demonstrate increased oxidative roGFP2 in muscle	84
Fig 3.21 <i>Isp-1;ctb-1</i> mutants demonstrate increased oxidative roGFP2 in muscle	85
Fig 3.22 Increased mitochondrial H ₂ O ₂ excretion into cytosol during L4 in <i>isp-1;ctb-1</i> mutant.	86
Fig 3.23 Increased mitochondrial H ₂ O ₂ excretion into cytosol during L4 in <i>isp-1;ctb-1</i> mutant.	87
Fig 3.24 One-day-old <i>isp-1;ctb-1</i> animals have increased oxidized cytosolic environment	88
Fig 3.25 <i>Vdac-1</i> depletion inhibits KLF-1 nuclear translocation and diminish increased <i>isp-1;ctb-1</i> lifespan.....	90
3.8 SOD-3, PRDX-3 and VDAC-1 regulates CYPs-induced xenobiotic detoxification response.....	90
Fig 3.26 VDAC-1 may be part of mitochondrial H ₂ O ₂ transport across OMM.	91
Fig 3.27 Schematic overview of proposed mitochondrial signalling cascade	91
Fig 3.28 SOD-3, PRDX-3 and VDAC-1 regulates <i>cyp34a8</i> expression	92
Fig 3.29 <i>Prdx-3</i> depletion induce, whereas <i>sod-3</i> and <i>vdac-1</i> depletion inhibits xenobiotic detoxification response	93
3.9 Indirect thiol modification is responsible for KLF-1 nuclear translocation	93
Fig 3.30 Formation of disulphide bonds are required for KLF-1 nuclear translocation	94
Fig 3.31 Schematic illustration showing protocol of shift assay	95
Fig 3.32 Shift assay resulted in inconclusive results	95
Fig 3.33 H ₂ O ₂ -induced KLF-1 nuclear translocation is dependent on the NLS and cysteine 419	96
Fig 3.34 Mutagenesis of NLS and cysteine 419 decreases WWP-1-mediated KLF-1 nuclear translocation	98
3.10 Thiol alteration-sensitive p38 MAPK components: SEK-1 and NSY-198	
Fig 3.35 Schematic overview of the p38 MAPK signalling cascade	99
Fig 3.36 p38 MAPK signalling pathway is mediated KLF-1 nuclear translocation	99
Fig 3.37 TRX-1 and TRX-4 may regulate KLF-1 nuclear translocation via NSY-1	100
3.11 KLF-1 nuclear translocation is regulated by conserved MAPK component; PMK-3.....	100
Fig 3.38 PMKs mediate the nuclear localization of KLF-1 in <i>isp-1;ctb-1</i> mutant.....	102
Fig 3.39 PMK-3 is mediating cyps-induced longevity.....	102

Fig 3.40 PMK-3 is regulating KLF-1 nuclear translocation by phosphorylation of serine 39	103
4. Discussion	105
4.1 Identification of mtROS as inducer of KLF-1-mediated mitohormesis ...	105
Fig 3.41 Overview of KLF-1 activation in <i>C. elegans</i>	106
4.2 WWP-1: an alternative pathway of KLF-1 activation	108
4.3 Regulation of mtROS release	110
4.4 PMK pathway regulates KLF-1-mediated longevity	113
4.6 Summary	116
References	118
Acknowledgements	152
Appendix	155
Supplementary Table 1. Lifespan data and statistical analysis	155
Supplementary Table 2. Potential KLF-1 interaction partners	157
Erklärung	160
Curriculum vitae	161

Abbreviations

°C	Degree Celsius
%	Percent
3'	Three prime end of DNA sequence
5'	Five prime end of DNA sequence
A	Alanine
AA	Antimycin A
AB	Antibody
ADP	Adenosine diphosphate
Am	Ampere
Amp	Ampicillin
ATP	Adenosine triphosphate
BSA	Bovine Serum Albumin
BTE	Basic transcription element
BTEB	BTE binding
C	Cysteine
CI-CIV	Complex I – complex IV
CaCl ₂	Calcium chloride
CCO	Cytochrome c oxidase
cDNA	Complementary DNA
<i>C. elegans</i>	<i>Caenorhabditis elegans</i>
CGC	<i>Caenorhabditis</i> Genetics Center
cm	Centimetre
co-IP	Co-immunoprecipitation
CTL	Catalase

CYC	Cytochrome C
CYP	Cytochrome P450
D	Aspartic acid
D1	Day one of adulthood
DCF	Dichlorofluorescein
DCFH	Dichlorodihydrofluorescein
DIC	Differential interference contrast
DMSO	Dimethyl sulfoxide
DNA	Deoxyribonucleic acid
dNTPs	Deoxynucleotides
DR	Dietary restriction
dsRNA	Double-stranded RNA
DTT	Dithiothreitol
<i>E. coli</i>	<i>Escherichia coli</i>
ECL	Enhanced chemiluminescence
EDTA	Ethylenediaminetetraacetic acid
ER	Endoplasmic reticulum
EtBr	Ethidium bromide
ETC	Electron transport chain
EV	Empty vector
FADH	Flavin adenine dinucleotide
FCCP	Carbonyl cyanide-4-(trifluoromethoxy) phenylhydrazone
Fw	Forward
FUdR	Floxuridine
g	G force
GFP	Green fluorescent protein

GPX	Glutathione peroxidase
GRX	Glutaredoxin
GSH	Glutathione
GST	Glutathione S-transferases
h	Hour
H ₂ O	Water
H ₂ O ₂	Hydrogen peroxide
HCL	Hydrochloric acid
HECT	Homologous to the E6-AP carboxyl terminus
HEt	Hydroethidine
HO•	Hydroxyl radical
HOO•	Hydroperoxyl radical
IMM	Inner mitochondrial membrane
IMS	Intermembrane space
IPTG	Isopropyl-β-D-thiogalactopyranosid
K	Lysine
K ₂ HPO ₄	Dipotassium phosphate
KH ₂ PO ₄	Monopotassium phosphate
KLF	Krüppel-like factor
KPI	Phosphate buffer
L	Litre
L1-L4	Larval stage 1 – larval stage 4
L4440	Plasmid with EV
LB	Luria broth media
M	Molar
MAPK	Mitogen-activated protein kinase

Mal	Malonate
MgCl ₂	Magnesium chloride
MgSO ₄	Magnesium sulphate
min	Minute
ml	Millilitre
mm	Millimetre
mM	Millimolar
MRC	Mitochondrial respiratory chain
mRNA	Messenger RNA
mtDNA	Mitochondrial DNA
mtROS	Mitochondrial ROS
Myxo	Myxothiazol
NAC	N-acetyl-L-cysteine
NaCl	Sodium chloride
NADH	Nicotinamide adenine dinucleotide
NADPH	Nicotinamide adenine dinucleotide phosphate
NaOH	Sodium hydroxide
nDNA	Nuclear DNA
NLS	Nuclear localisation sequence
ng	Nanogram
NGM	Nematode growth medium
nm	Nanometre
NUO	NADH ubiquinone oxidoreductase
O ₂	Oxygen
O ₂ ^{•-}	Superoxide anion radical
OD595	Optic density at 595 nm

OE	Overexpression
OH ⁻	Hydroxyl anion
OMM	Outer mitochondrial membrane
OXPHOS	Oxidative phosphorylation
PBS	Phosphate-buffered saline
PBST	Phosphate-buffered saline supplemented with Tween
PCR	Polymerase chain reaction
pH	Potential of hydrogen
PMK	Mitogen-activated protein kinase
PQ	Paraquat
PRDX	Peroxiredoxin
PRX	Putative peroxisome assembly protein
qPCR	Quantitative polymerase chain reaction
Q _o	Quinol oxidation
RC	Respiratory chain
RNA	Ribonucleic acid
RNAi	RNA interference
ROS	Reactive oxygen species
Rot	Rotenone
rpm	Revolutions per minute
RT	Room temperature
Rv	Reverse
S	Serine
SDS	Sodium dodecyl sulphate
SEM	Standard error of the mean
SOD	Superoxide dismutase

t-Test	Students t-Test
TBS	Tris-buffered saline
TBST	Tris-buffered saline supplemented with Tween
TCA	Tricarboxylic acid
Tet	Tetracycline
TOMM	Translocator of the OMM
TIMM	Translocator of the IMM
Tris	Tris(hydroxymethyl)aminomethane
TRX	Thioredoxin
UGT	Glucuronosyltransferases
UV	Ultra violet
V	Volt
VDAC	Voltage-dependent anion channel
Vit C	Vitamin C
vol/vol	Volume per volume
VLCFA	Very long chain fatty acid
WT	Wild-type
Wt/vol	Weight per volume
WWP	WW domain protein
YFP	Yellow fluorescent protein
μg	Microgram
μl	Microliter
μm	Micrometre

Abstract

Most manipulations that extend lifespan also increase cytoprotective mechanisms to various stress in a range of animals from yeast to mammals. However, the underlying signalling cascades regulating stress resistance and longevity are still largely unknown. Here, we identified a mitochondrial ROS (mtROS) pulse during L4 as novel activator of transcriptional factor Krüppel-like factor-1 in *isp-1(150);ctb-1(189)* mitomutant. For this purpose, we created a *de novo* outer mitochondrial membrane (OMM) H₂O₂ sensor by adding a TOMM20 targeting sequence to the roGFP2-Orp1 probe. We further show that H₂O₂ signalling is dependent on superoxide dismutase-1 (SOD-1), peroxiredoxin-3 (PRDX-3) and voltage-dependent anion channel-1 (VDAC-1). Upon the ROS signal, KLF-1 is activated by the p38 MAPK signalling cascade and translocates to the nucleus where it activates genes involved in phase I of xenobiotic detoxification programme, the cytochrome P450 oxidases (CYPs). Collectively, these findings underline the importance of ROS, especially H₂O₂, as signalling molecule and identify the p38 MAPK signalling cascade as a key regulator of mitomutant lifespan.

1. Introduction

1.1. Ageing

The average lifespan has steadily been increasing in humans (Oeppen and Vaupel 2002). However, with the prolonged lifespan, many diseases remain prevalent and without a cure. Therefore, the field of Geroscience is coupling the concept that ageing is a disease and the fact that elevated age enhances the occurrence of chronic diseases (Sierra 2016; Mitchell et al. 2015). Thus, treating or preventing ageing would be beneficial in the fight against age-related diseases, like cardiovascular diseases, arthritis, diabetes, heart failure, cancer and neurodegenerative diseases such as Alzheimer's disease and Parkinson's disease. This would be more beneficial than finding treatments or trying to cure single chronic disease (Sierra 2016). However, ageing is a multifactorial complex, interconnecting process at molecular, cellular, tissue and system levels (Gems and Partridge 2013; Cohen 2018). Nowadays, there are more than 300 different concepts and theories to explain why we age. However, we still know little about the regulation of lifespan. The fundamental question remains: why do we age?

To better understand the ageing process, others have attempted to identify and categorize the cellular and molecular processes in hallmarks of ageing (López-Otín et

al. 2013). The proposed hallmarks are: 1. Genomic instability, 2. Telomere attrition, 3. Epigenetic alterations, 4. Loss of proteostasis, 5. Deregulated nutrient sensing, 6. Mitochondrial dysfunction, 7. Cellular senescence, 8. Stem cell exhaustion and 9. Altered intercellular communication (Fig.1.1) (López-Otín et al. 2013). Here, we further elaborate on some of these hallmarks.

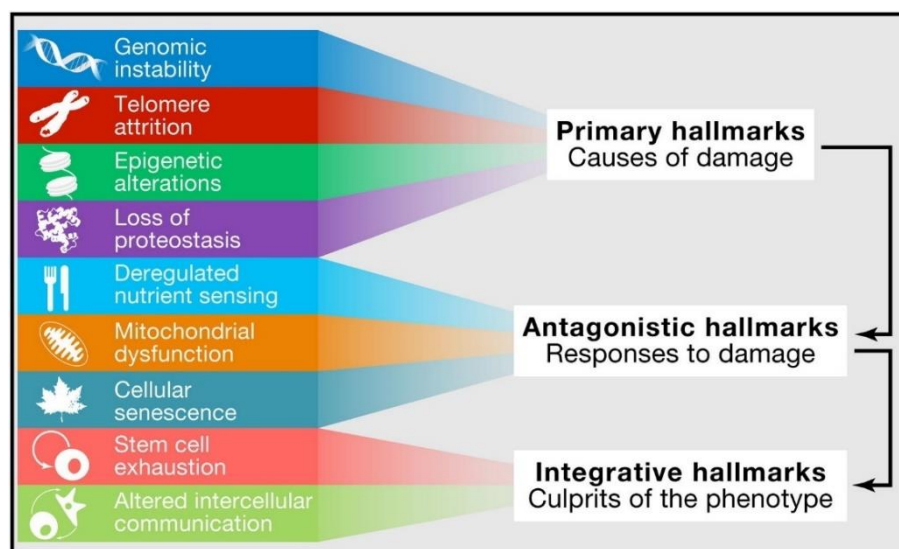


Fig. 1.1. Hallmarks of ageing and their functional interconnections

The proposed nine hallmarks of ageing divided into three categories based on their contribution on ageing: primary hallmarks, which are negative contributors, antagonistic hallmarks, which are either beneficial or harmful, and integrative hallmarks. Figure obtained from López-Otín et al. 2013.

Genomic instability is the change of genomic information through alterations in DNA, either by DNA damage or mutations. These alterations might affect essential genes and transcriptional pathways and therefore disrupt cell and tissue homeostasis. It was observed that DNA damage was accumulated in ageing (Forsberg et al. 2012; Faggioli et al. 2012) and premature ageing diseases, for example Werner syndrome (Muftuoglu et al. 2008).

Telomere attrition is refereeing to the declining length of this DNA-protein structure. Telomeres are located at the end of chromosomes and protect the genome against degradation (van Steensel, Smogorzewska, and de Lange 1998) and intrachromosomal fusion (Griffith et al. 1999). During cell division telomere length is decreased (Brouillette et al. 2003) and this is progressively upon ageing (Takubo et al. 2000). This results in short telomeres, which might lead to cell senescence or apoptotic cell death (Cawthon et al. 2003). Interestingly, transgenic induction of a telomerase gene extends cellular lifespan (Bodnar et al. 1998). Moreover, increased telomere

length was observed in long-lived stem and cancer cells (Hande et al. 1999; Horn et al. 2013).

Protein homeostasis or proteostasis is a complex network of chaperones (Y. E. Kim et al. 2013) and degradation machinery (Cichanover 2005), which monitor protein concentration, quality and correct subcellular location (Ulloa-Aguirre et al. 2020). Proteostasis dysfunction results in accumulation of misfolded protein (Balchin, Hayer-Hartl, and Hartl 2016) and protein aggregates (Mukherjee et al. 2015). The proteostasis efficiency is age-dependent declined, which results in cellular dysfunction (Mukherjee et al. 2015) and degenerative disease, such as Alzheimer's disease (Alzheimer et al. 1991) and Parkinson's disease (Powers et al. 2009).

Deregulation of nutrient sensing was the first pathway demonstrated to regulate lifespan through insulin/IGF-1 signalling (Brunet et al. 1999). Nowadays, also three other nutrient sensing signalling pathways, namely mTOR (Vellai et al. 2003), Sirtuins (Rogina and Helfand 2004; Y. Li et al. 2008) and AMP-activated kinase (AMPK) (Greer et al. 2007), are observed to alter lifespan. Downstream of these signalling pathways is the mammalian forkhead transcription factor (FOXO), which is altering multiple biological processes, such as cell cycle and metabolism (X. Sun, Chen, and Wang 2017).

1.2. Mitochondria and ageing

1.2.1 Mitochondria

Mitochondria are eukaryotic organelles and most famous for their ability to produce adenosine triphosphate (ATP). Historically, mitochondria were identified as “bioblasts”, vital organisms within the cell (Altmann 1890). Later, these “bioblasts” were redefined as organelles and named mitochondria, after the Greek “mitos” for thread and “chondrion” for granule (Brenda 1898). Nowadays, we understand the endosymbiotic origin of the mitochondria and that they are from bacterial origin (Roger, Muñoz-Gómez, and Kamikawa 2017). In fact, mitochondria possess their own DNA (mtDNA) and both mitochondrial and bacteria share circular DNA. Moreover, they have double membranes and the mitochondrial proteome is a mixture of bacterial and eukaryotic-derived proteins. Besides energy production (Pfanner, Warscheid, and Wiedemann 2019), mitochondria are key regulators of: (I) multiple metabolic pathways,

like the metabolism of amino acids, lipids, nucleotides and TCA metabolites (Spinelli and Haigis 2018), (II) biosynthesis of iron-sulphur (Fe-S) clusters (Stehling and Lill 2013), (III) calcium homeostasis (Giorgi, Marchi, and Pinton 2018), (IV) quality control and degradation, for example mitophagy and apoptosis (Ashrafi and Schwarz 2013), (V) inflammation (Vringer and Tait 2019) and (VI) reactive oxygen species (ROS) generation (P. K. Jensen 1966) and homeostasis (Scialò, Fernández-Ayala, and Sanz 2017).

1.2.2 Mitochondria genome

mtDNA is a relatively small, abundant and highly conserved DNA molecule and, as mentioned, mtDNA is circular. The mammalian mtDNA molecule is about 16.6 kb (Chinnery and Hudson 2013) and encodes 13 polypeptides of the electron transport chain (ETC), two rRNAs and 22 tRNAs, which are essential for mitochondrial protein synthesis. mtDNA is highly efficient as around 93% represents a coding region (Chinnery and Hudson 2013). The rest of the mitochondrial proteome, that is not transcribed from the mtDNA, is encoded by nuclear DNA (nDNA), translated in the cytosol and imported into the mitochondria (N.-G. Larsson and Clayton 1995). This includes machinery necessary for mtDNA replication, transcription and translation. Therefore, a highly multifaceted cross-talk between the nucleus and mitochondria is required (Poyton and Mcewen 1996).

1.2.3 Mitochondria structure and OXPHOS

The mitochondria are surrounded by a double-membrane, consisting of the outer and inner mitochondrial membranes (OMM, IMM) (Fig.1.2) (Kühlbrandt 2015). In between the OMM and IMM is the intermembrane space (IMS) and the IMM is surrounding the matrix and forming cristae (Fig.1.2). The amount and morphology of mitochondria differs between cells and might be different in the same tissue. While the levels of ions and small molecules in the IMS are similar as in the cytosol, due to porins in the OMM, other molecular or protein transport is regulated by various transport machinery, like the translocases of the outer- and inner mitochondrial membrane (TOMM/TIMM) complex, voltage-dependent anion channel (VDAC) or mitochondrial permeability transition pore (Briston et al. 2017; Schmidt, Pfanner, and Meisinger 2010;

Camara et al. 2017). The matrix contains the mtDNA, translation machinery and the enzymes of the tricarboxylic acid (TCA) cycle or Krebs cycle, required for metabolizing metabolites and electron transporters nicotinamide adenine dinucleotide (NAD^+) and flavin adenine dinucleotide (FAD^+). The distinct compartmentation within the mitochondria is crucial to utilize their key functions (Kühlbrandt 2015).

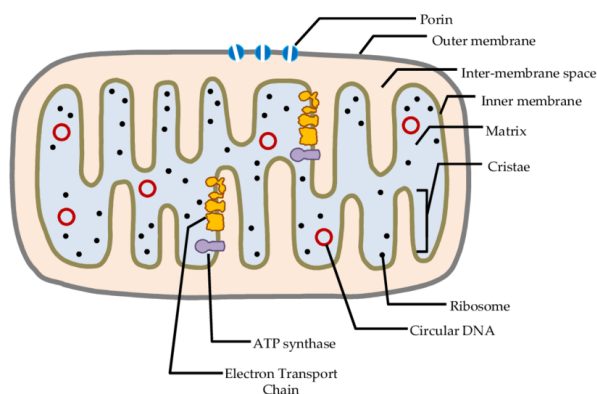


Fig. 1.2. Mitochondrial architecture

Schematic overview of the mitochondrial compartmentation: the intermembrane space and matrix segregated by the inner membrane (IMM). The mitochondria and cytosol are segregated by the outer membrane (OMM). Figure obtained from Yusoff et al. 2015.

As mentioned, one of the functions of mitochondria is the metabolic energy production, in the form of ATP, by the mitochondrial oxidative phosphorylation or OXPHOS. The OXPHOS system is embedded in the IMM and consists of five protein complexes and two electron carriers (Fig.1.3) (Papa et al. 2012; Matsuno-Yagi and Hatefi 1985). The first four complexes, also named the electron transport chain (ETC), transfer electrons across the ETC and couples this transfer to proton transport across the IMM. Thereby, creating a proton gradient across the IMM, which produces a proton motive force driving complex V, an ATP synthase, to generate ATP. The ETC and complex V are named the mitochondrial respiratory chain (MRC). The electrons are passed from Krebs cycle-derived NADH or succinate via complex I or complex II, respectively, into OXPHOS (Fig.1.3). For a long time, it was proposed that the OXPHOS complexes diffuse freely across the IMM, also referred to as the fluid-state model (Hackenbrock, Chazotte, and Shaila Gupte 1986; Dudkina et al. 2008). Nowadays, it appears that the OXPHOS organization is according to the solid-state model, which describes the formation of OXPHOS supercomplexes (Dudkina et al. 2008). Here, we further elaborate in detail on the OXPHOS complexes.

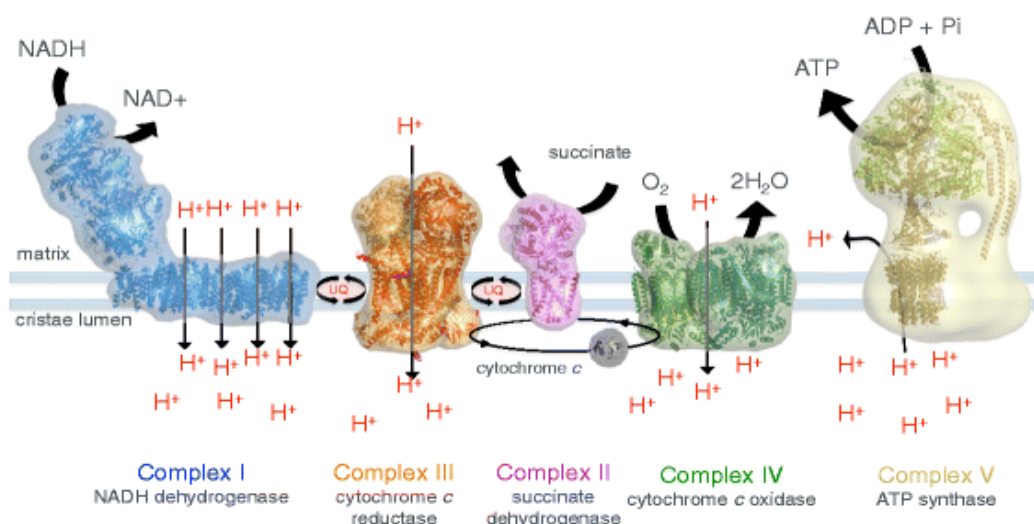


Fig. 1.3. Overview of mitochondrial respiratory chain complexes

Schematic overview of the mitochondrial respiratory chain complexes, composed of complex I, a NADH dehydrogenase, complex II, a succinate dehydrogenase, complex III, a cytochrome c reductase, complex IV, a cytochrome c oxidase, complex V, an ATP synthase, and ubiquinol (UQ). Complex I to IV are grouped together as electron transport chains (ETC). The respiratory chain complexes are fuelled by NADH at complex I and succinate at complex II and the electron transport through the ETC is creating a proton gradient, which is utilized by complex V. Figure obtained from Kühlbrandt, 2015.

Complex I is a “L-shaped” NADH dehydrogenase and a major electron entry point into the ETC (Lencina et al. 2018). While the hydrophobic arm is bedded in the IMM, the soluble peripheral arm is in the matrix. This soluble arm contains the flavoprotein and iron protein subunits, which are necessary for electron acceptance from NADH (Distelmaier et al. 2009). These electrons are transferred to the electron carrier ubiquinone. The function of the hydrophobic arm is proton transport across the IMM. Mammalian complex I is the largest of the OXPHOS complexes and consists of 44 subunits (Carroll et al. 2003). The genes of these subunits are frequent targets for mitochondrial disease-causing mutations (Koopman et al. 2012) and complex I dysfunction was connected to mitochondrial diseases, such as Parkinson’s disease (Morais et al. 2009) and dementia (Gatt et al. 2016).

Succinate dehydrogenase or complex II consists of four nuclear encoded protein subunits (F. Sun et al. 2005). Matrix-localized SDHA and SDHB are the succinate dehydrogenase domain (Dourado, Swart, and Carvalho 2018) and SDHC and SDHD, the hydrophobic anchors to the IMM, are necessary for electron transfer (Bandara, Drake, and Brown 2021). Complex II has a dual role in respiration by catalysing the oxidation of succinate to fumarate in the TCA cycle (Cecchini 2003; F.

Sun et al. 2005) and transferring electron transfer to ubiquinol in the ETC (Cecchini 2003; Miyadera et al. 2003).

Complex III is a cytochrome c reductase and it is involved in electron transfer by accepting electrons from complex I and II and transferring to complex IV via cytochrome c (Solmaz and Hunte 2008) and transporting protons across the IMM. As cytochrome c can only accept a single electron per transfer, this process happens in two steps in the Q cycle (Fig. 1.4) (Meinhardt et al. 1987; Zhu et al. 2007).

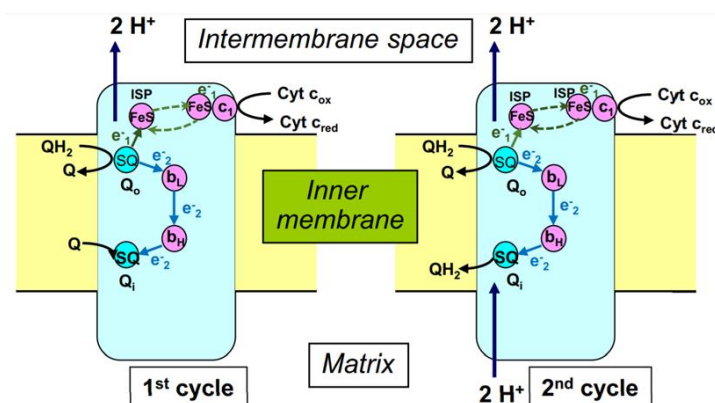


Fig. 1.4. Schematic overview of Q cycle

In the first cycle, ubiquinol at Q_o donates one of its electrons to the Rieske Fe-S subunit and consequently cytochrome c. The other electron is transferred to cytochrome b to ubiquinone to form an unstable semiquinone at Q_i . In the second cycle, another ubiquinol donates again its electrons resulting in two reduced cytochrome c, four proton transport and the semiquinone is oxidized to ubiquinol and dislocates. Figure obtained from Mazat, Devin, and Ransac 2020

The mammalian complex IV (cytochrome c oxidase) is formed by 14 subunits and it is the rate limiting complex of the OXPHOS (E. Cadenas et al. 2000; Kadenbach 2021). It transfers the electrons from cytochrome c to molecular oxygen, hereby transporting protons across the IMM. The catalytic core is formed by three mitochondrial DNA-encoded subunits, namely COX1-3 (Timón-Gómez et al. 2018).

The different concentration of protons across the IMM induce a chemical gradient (pH) and electric gradient (membrane potential) (Neupane et al. 2019). This electrochemical energy is utilized by ATP synthase (complex V) to generate ATP. The protons are transferred back in the matrix through the proton specific channels in the F_o domain, while the F_1 domain catalysed ADP and P_i to ATP (Capalde et al. 1994; Nijtmans et al. 1995).

1.2.4 Mitochondria and their role in ageing

Declining of mitochondrial function is a widely accepted concept during aging. This decline has been observed in common mitochondrial features, such as respiration (Alemany et al. 1988; Figueiredo et al. 2009), ATP production (Jang et al. 2009; Capozza et al. 1994), membrane potential (Chabi et al. 2008; Garcia-Fernandez et al. 2011) and ROS generation. Moreover, mitochondria have altered morphology (Shigenaga, Hagen, and Ames 1994), decreased mtDNA copy number and mitochondrial proteins (Stocco, Cascarano, and Wilson 1977) and the mitochondrial numbers are declined during ageing (Herbener 1976). Here, we focus on three main characteristics of mitochondrial function and their effect on lifespan determination: ROS, mtDNA and metabolic rates.

ROS was first observed as free radicals, which were proposed to be mediator of all oxidative reactions involving organic molecules (Bisby 1990; Michaelis 1939). In the early 1950s, free radicals were first observed in biological material (Commoner, Townsend, and Pake 1954), which were rapidly connected to pathological processes and ageing theories (Harman 1956; Gerschman et al. 1954). Their role in ageing theories was mostly described as a source of molecular damage, as ROS, such as hydrogen peroxide (H_2O_2), could damage macromolecules (Stadtman 1992). This led to the free radical theory of ageing (Sohal et al. 1994; Harman 1956). In short, this theory suggests that aging occurs due to accumulation of ROS-induced damaged molecules. In agreement with this theory, it was observed that increased ROS generation can shorten lifespan (Kirkwood and Kowald 2012). Others dispute that oxidative damage is just one type of damage and expand this theory to various types of damage, including translation or transcriptional damage on DNA, protein and metabolites (Gladyshev 2014; Barondes et al. 1963).

Interestingly, free radicals were also implicated in beneficial processes, such as reducing infection (Babior, Kipnes, and Curnutte 1973; Rossi, Bianca, and de Togni 1985) and vasodilation (Geletyuk et al. 1982; Furchgott and Zawadzki 1980). Nowadays, it is more commonly accepted that free radicals and especially ROS have a dual role in physiological processes proliferation (Geiszt and Leto 2004; Foreman et al. 2003; Sauer et al. 2000; J. Li et al. 2006; Ushio-Fukai 2006). Moreover, low levels of mtROS can also induce long-term beneficial responses by inducing adaptive

responses and increasing biological plasticity (Calabrese, 2018; Ristow & Zarse, 2010; Tapia, 2006).

As mitochondria have their own genome and are responsible for ROS generation, it was suggested that mtDNA could be exposed to ROS. This might lead to accumulation of damage in the mtDNA and mutations. It was suggested that these mtDNA alterations would result in decreased mitochondrial function, through impairment of the MRC and consequently increased ROS generation and more ROS-induced damage (Harman 1972). Nowadays, the impact of mtDNA mutations on ageing are extensively investigated (A. Bratic and Larsson 2013) and indeed, a causative connection between mutations in mtDNA and ageing was established in mtDNA mutator mice (Trifunovic et al. 2004). These mice express a homozygous knock-in proof-reading-deficient version of polymerase gamma (POLG) leading to an accelerated ageing phenotype caused by a three-fold to five-fold increase in the levels of point mutations in mtDNA (Trifunovic et al. 2004). Interestingly, despite the increase in mtDNA mutations in the mtDNA mutator mice, there was no increase in ROS production observed (Trifunovic et al. 2005). In addition, it was proposed that mutations in mtDNA are rather occurring when DNA repair systems are not repairing errors originating from mtDNA replication and synthesis (Stewart et al. 2008; N. G. Larsson 2010; Ameer et al. 2011). This argues against a direct role of ROS in mtDNA mutations-derived ageing.

As mentioned, one of the mitochondrial functions that declines during ageing is a respiration rate. Therefore, this suggests a role of metabolic rate in lifespan regulation. In the rate of living theory (Pearl 1928), the role of metabolic rate on lifespan is described to be inversely correlated (Loeb and Northrop 1911). Organisms have a limited amount of energy, which is consumed during life (Pearl 1928). Altogether, this theory suggests that long-lived organisms should have reduced basal respiration and metabolic rate than shortened lived organisms. However, the role of ATP, a production of the mitochondrial respiration, and lifespan seems to be conflicting. Pathways that induce longer lifespan, such as nutrient sensing, can both increase and decrease ATP production (Kharade et al. 2005; Houthoofd et al. 2002; Lambert and Merry 2004; I. Bratic and Trifunovic 2010). Others even observed no difference in ATP levels between caloric restriction, a dietary intervention without malnutrition that extend lifespan (Chapman and Partridge 1996; E J Masoro 2002; Edward J Masoro 2009; Lakowski and Hekimi 1998), and control conditions (Khraiwesh et al. 2013). As our

understanding of the precise molecular pathway of caloric restriction-induced remains unclear, also the exact role of metabolic rate in lifespan regulation (C. L. Green, Lamming, and Fontana 2021). Likely the mitochondrial energy metabolism is a key regulator of this process, together with mTOR (Vellai et al. 2003), Sirtuins (Rogina and Helfand 2004; Y. Li et al. 2008) and AMP-activated kinase (AMPK) (Greer et al. 2007).

1.3. ROS

1.3.1 ROS molecules

ROS molecules are reduced oxygen derivatives, which have accepted extra electrons and can oxidize various molecules. The three primary forms of ROS are: superoxide radical ($O_2^{\bullet-}$), H_2O_2 and hydroxyl radical (OH^{\bullet}) (Fig.1.5) (Sullivan and Chandel 2014). Other ROS molecules are hydroxyl ion (OH^-), peroxy radicals (ROO^{\bullet}), nitric oxide (NO), lipid hydroperoxide (LOOH), alkoxy radical (RO^{\bullet}) and sulphate radical ($SO_4^{\bullet-}$). As they all have different reactivities, this led to different effect on cellular physiology (Sullivan and Chandel 2014). For example, studies of peroxy radicals are an emerging field of ROS as they are linked to ferroptosis and Alzheimer's disease (Gaschler and Stockwell 2017). ROS molecules are produced under physiologic conditions but also as by-products in mitochondria, peroxisomes, endoplasmic reticulum (ER) (Mignolet-Spruyt et al. 2016) and by several cytosolic enzymes, like the NADPH oxidases (Hole et al. 2013; Bedard and Krause 2007), cyclooxygenases (Martínez-Revelles et al. 2013) and lipoxygenases (Cho, Seo, and Kim 2011).

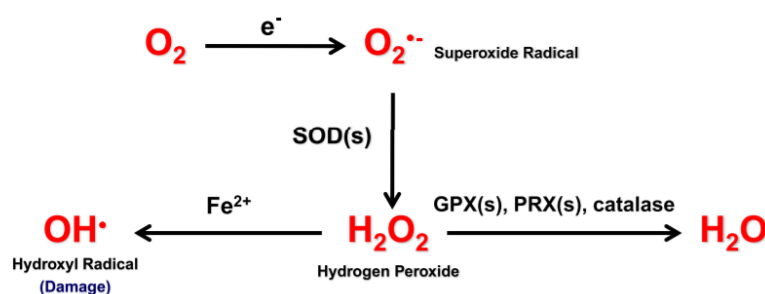


Fig. 1.5. ROS generation, reduction and signalling.

Superoxide radical ($O_2^{\bullet-}$) is formed by gaining an electron from electron leak in the ETC and reduced by superoxide dismutase (SOD) in hydrogen peroxide (H_2O_2). H_2O_2 can either be reduced to water by redox enzymes glutathione peroxidases (GPX), peroxiredoxins (PRDX) or catalase (CTL) or undergo Fenton reaction to form hydroxyl radical. Figure obtained and modified by Sullivan and Chandel 2014.

1.3.2 H₂O₂ as second messenger

H₂O₂ was first proposed to act as potential second messenger due to its relatively long half-life, in comparison with other ROS molecules (Sies, 1993). This is further highlighted by its low molecular weight, relatively high cellular concentrations (range of nM till μ M) and its capacity of transporting across membranes and through tissues (di Marzo, Chisci, and Giovannoni 2018; Sies 2014). Furthermore, the catalytic reduction of H₂O₂ involves oxidation of cysteine residues (Winterbourn and Hampton 2008), which enables H₂O₂ to oxidize thiol residues to sulfenic, sulfinic and sulfonic acid on target proteins (Nagy and Ashby 2007; Poole, Karplus, and Claiborne 2004; John Barton, Packer, and Sims 1961). Reversible oxidizing of these thiolates on target proteins can switch the protein's activity, localization or stability (Riemer et al. 2015; D'Autréaux and Toledano 2007). This mechanism is considered to be fundamental for the redox signalling. Nowadays, H₂O₂ has been reported to activate antioxidant gene expression (Sablina et al. 2005; An and Blackwell 2003), cell proliferation (Geiszt and Leto 2004; Foreman et al. 2003), differentiation (Sauer et al. 2000; J. Li et al. 2006), migration (Ushio-Fukai 2006), apoptosis (Gechev and Hille 2005; Cai 2005) and, modulation of transcription factors (Delaunay, Isnard, and Toledano 2000; Pedre et al. 2018; Pearson, Morf, and Singh 2013; J. W. Lee and Helmann 2006).

One of the main reasons H₂O₂ was not fully understood as second messenger was the limited methods to visualize or measure ROS (Cheng et al. 2018). In most cases low levels of mtROS was linked to promoting cell division, modulating MAPKs, phosphatases and transcriptional factors, without specifying the exact nature and location of the ROS molecules (Ogrunc et al. 2014; P. Li et al. 2016; Ge et al. 2017). Due to limited ROS visualizing methods, investigators often used various redox-active probes, namely dichlorodihydrofluorescein (DCFH) (Kubben et al. 2016; Lin et al. 2015), hydroethidine (HET) (B. Zhang et al. 2021), mitochondrial HET or Mito-SOX (Hu et al. 2020) and CellROX reagents (Cacialli et al. 2021; Esterberg et al. 2016). However, interpretation of the exact mechanism of detection and nature of detected ROS molecules are challenging. For example, the redox-active probe DCFH was suggested to visualize intracellular H₂O₂ via oxidizing of DCFH into the green fluorescent product dichlorofluorescein (DCF). However, it has been shown that DCFD is also catalysed into DCF by peroxidases or via intracellular iron-dependent processes (Tampo et al. 2003; Karlsson et al. 2010; Kotamraju et al. 2004). Moreover, DCF can

undergo redox cycling which forms artefactual formation of H_2O_2 and some even report DCFD does not react with H_2O_2 (Rota, Chignell, and Mason 1999; Bonini et al. 2006; Tampo et al. 2003). Therefore, the final readout of these redox-active probes remains challenging to interpret. Furthermore, when using ROS probes it is necessary to verify the cellular uptake of some probes as this may vary between cell types or treatment conditions (Cheng et al. 2018).

Recent development in redox-active probes has led to *de novo* genetically encoded ROS and H_2O_2 sensors, namely the OxyR-based HyPer family reporters and roGFP2 family; roGFP2-Orp1 and roGFP2-Tsa probes (B. Morgan et al. 2016; Nietzel et al. 2019; Belousov et al. 2006). These sensors are both successfully tested *in vitro* and *in vivo* (Gutscher et al. 2009; Markvicheva et al. 2011). While redox-active probes, such as DCFD and MitoSOX, have the advantages of being easy in handling and having high dynamic range, these sensors benefit from being highly specific, genetic-derived, subcellular targeted and redox reversible (Markvicheva et al. 2011). Thus, they are providing a specific localized real-live time H_2O_2 sensor. The H_2O_2 -sensitive HyPer family is designed by integrating a YFP into the regulatory domain of the bacterial H_2O_2 sensing protein OxyR, which contains a redox active thiolate of C199 (Belousov et al. 2006; Zheng, Aslund, and Storz 1998; Åslund et al. 1999; Choi et al. 2001). Nowadays, the sequels HyPer-2 and HyPer-3 have been replaced by HyPer (Belousov et al. 2006), HyPerRed (Ermakova et al. 2014) and HyPer-7 (Pak et al. 2020). The peroxidase-based Orp1 promotes the oxidation into disulphide bridges on redox-sensitive GFP (roGFP2) in present of H_2O_2 (Maiorino et al. 2007; Gutscher et al. 2009).

Thiol redox signalling upon ROS exposure has a dual role, it protects against ROS-induced damage and transfers ROS signalling. ROS is metabolized by enzymatic antioxidants, such as superoxide dismutase (SOD), catalase (CAT), glutathione peroxidases (GPX) and peroxiredoxins (PRDX). Transfer of H_2O_2 signalling has been suggested to be performed by GPX (Margis et al. 2008) and PRDX (Winterbourn 2018; Z. A. Wood et al. 2003). Both redox enzymes use their cysteines to reduce H_2O_2 by forming dithiols. Afterward, GPX is reduced by glutathione (Margis et al. 2008), while PRDX is reduced by the thioredoxin redox (TRX) system (Lu and Holmgren 2014).

1.3.3 Mitochondrial ROS

Mitochondrial produced ROS (mtROS) was first described in 1966 as a molecule that consumes oxygen in mitochondria (P. K. Jensen 1966). As this reaction was catalase dependent, it was concluded that this molecule was H_2O_2 (P. K. Jensen 1966). Now, it is generally assumed mitochondria are responsible for around 90% of the total cellular ROS production (Wenjia Zhang et al. 2019; Balaban, Nemoto, and Finkel 2005). The main production sites of ROS, especially $\text{O}_2^{\cdot -}$, are complex I and III of the ETC (Fig. 1.6). The major ROS producers on complex I are the Flavin site and ubiquinone reducing site (I_Q) (Brand 2016). ROS generated at the I_Q site was observed during reverse electron transport (RET). Due to the high ubiquinol/ ubiquinone ratio and consumption of the proton electron force (Chance 1961; Chouchani et al. 2014), the electrons are driven backwards in complex I and produce ROS (Chouchani et al. 2014). Complex III located ROS production happens at the Q-cycle (Q_o) and depends on the location of Q_o site if ROS is released either into the mitochondrial matrix or into the IMS (Brand 2016). Between the Q-cycle, the second electron can be prematurely transferred to oxygen instead of cytochrome c to generate $\text{O}_2^{\cdot -}$ (Salo, Husen, and Solov'Yov 2017; Muller et al. 2003). It has been suggested that the ROS production level of complex III is much smaller than complex I (Brand 2010). This is emphasized by the major role of complex I in diseases, like Leigh syndrome and hydrotopic cardiomyopathy (Rodenburg 2016). In complex II-related mutations or diseases, ROS

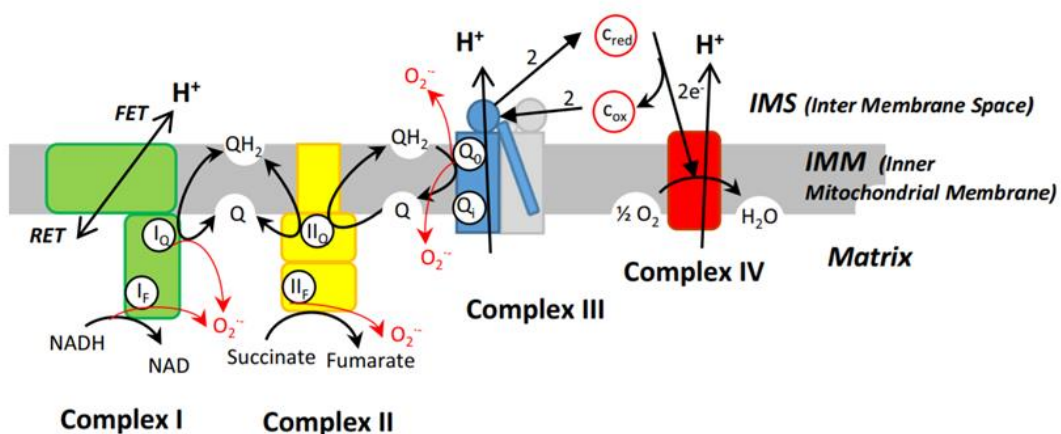


Fig. 1.6. Possible sites of ROS generation

ROS is produced at sites on complex I, II and III and extrude in the matrix, except the ROS produced at complex III Q_o site which extrudes in the IMS. Forward electron transport (FET) and Reverse electron transport (RET). Figure obtained from Mazat, Devin, and Ransac 2020.

production is produced at the IIF site and associated with succinate dehydrogenase (Cecchini 2013; Hoekstra and Bayley 2013). Under normal conditions, complex II ROS production is minimum (Fig. 1.6) (Cecchini 2013).

1.4. *C. elegans* and aging research

1.4.1 *C. elegans* research model

To unravel mechanisms of lifespan regulation researchers have utilized various model organisms. The common characteristics of these organisms are that they are relatively short lived, have well-described genomes and are easily genetically manipulated. Therefore, the classical models used are yeast (*Saccharomyces cerevisiae*), fly (*Drosophila melanogaster*), mouse (*Mus musculus*) (Mitchell et al., 2015) and the emerging models of the naked mole rat (*Heterocephalus glaber*) (Buffenstein 2005) and killifish (Harel and Brunet 2016). Another model that is popular due to its size, easy handling, transparency and genomic toolbox is the roundworm *Caenorhabditis elegans* (*C. elegans*), an optimal model for lifespan and aging research.

50 years ago, the nematode *C. briggsae* was cultivated and utilized for investigating developmental biology and nervous system (Sydney Brenner 2002; S. Brenner 1988). Later, *C. elegans* was used as this strain grew better in laboratory conditions (Félix et al. 2011). Nowadays, the *C. elegans* model is worldwide studied in over a thousand laboratories and responsible for over 1800 published research articles in 2020 alone.

C. elegans is a small, free-living organism, which lives in soil and feeds on different species of bacteria (Avery and Shtonda 2003; Félix and Duveau 2012). They have a rapid life cycle, as they develop from egg through 4 larval developmental stages to egg-laying adults in around 3 days at 20°C (Fig.1.7). Adults are a primarily self-fertilizing hermaphrodites, although males exist in low frequency in the population (0.2%) (Corsi, Wightman, and Chalfie 2015). Besides the four larval developmental stages, *C. elegans* larvae can undergo dauer arrest during the second molt (Fielenbach and Antebi 2008). Dauer larvae exhibit increased stress resistance and altered metabolism and are therefore considered a survival mechanism during harsh environments. These features, combined with the fact that *C. elegans* was the first

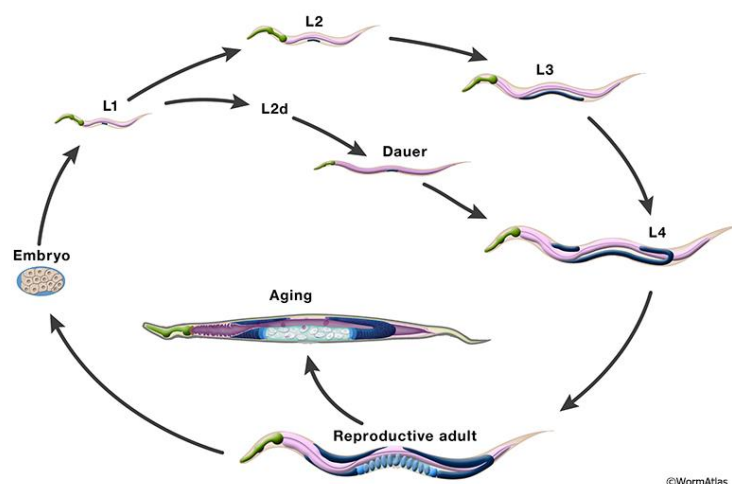


Fig. 1.7. Schematic overview of *C. elegans* lifespan.

C. elegans larvae are hatching from eggs and go through four developmental larval stages by molting (L1 till L4), until they become a reproductive adult. Under harsh conditions, like low food availability or crowdedness, L2 stage can activate an alternative L3 stage, namely dauer larvae for survival. Adult worms lay eggs in the first 5 days of adulthood and afterwards they age. Figure obtained from WormAtlas (Corsi, Wightman, and Chalfie 2015).

whole genomic sequenced organism, makes these roundworms a powerful model for eukaryotic genetic studies. Moreover, 60-80% of human genes have an ortholog in the roundworm DNA (Kandoth and Mitchum 2013) and about 40% of nematode genes have orthologs associated with human diseases (Culetto and Sattelle 2000). Another feature that emphasize *C. elegans* as powerful research model is that they are easily visualized by microscope. Phenotypes are observed by assessment of movement, eating rate, developmental rate, reproduction rate and number of progeny (Corsi, Wightman, and Chalfie 2015). Nematodes being transparent, are ideal for single cell visualization and protein localization studies through expression of fluorescently tagged proteins (R. A. Green et al. 2008; Chamberlain and Benian 2000). The use of fluorescent protein tags enables tracking of protein and cell function and investigates protein interactions *in vivo*. Altogether, these features highlight the roundworm *C. elegans* as a prominent model for lifespan regulation research.

1.4.2 *C. elegans* ageing research

For the past decade, the aging field was largely broadened and enlightened by various *de novo* discoveries. Especially experimental work in the *C. elegans* model

has led to successful breakthroughs in identifying genes involved in lifespan, either as novel fundamental knowledge of signalling cascades that regulate normal lifespan or as better understanding of healthy aging processes. What started with research on dauer formation, nutrient sensing or insulin handling has led to the remarkable field of prolonging lifespan by mutations in genes affecting nutrient sensors or stress-response signalling cascades (C. J. Kenyon 2010). Nowadays, we know nutrient sensing can induce long lifespan by altering signalling cascades involving the kinase target of TOR (Hansen et al. 2007; Kaeberlein, Powers, and Steffen 2005; Kapahi et al. 2004), AMP kinase (Greer et al. 2007), sirtuins (Rogina and Helfand 2004; Y. Li et al. 2008) and insulin/IGF-1 signalling (Arum et al. 2009; Honjoh et al. 2009). Furthermore, we know that DR-induced longevity is not limited to the *C. elegans* model, as mutations in the insulin/IGF-1 signalling induce long lifespans in *Drosophila melanogaster* and mice (Grandison, Piper, and Partridge 2009; Clancy et al. 2002; Bartke 2008; Arum et al. 2009). The list of genes implied in stress-induced genes and longevity is still expanding, now including heat- (Shama et al. 1998; Lithgow et al. 1995; Kumsta et al. 2019) and oxidative stress (Heidler et al. 2010), signalling of homeostasis from germline tissue (Di Chen et al. 2013; C. Kenyon 2010; Khodakarami et al. 2015), mRNA translation (Pan et al. 2007; Derisbourg et al. 2021), proteostasis balance (Koyuncu et al. 2021; Kevei and Hoppe 2014) and alteration in mitochondrial activity (Dancy, Sedensky, and Morgan 2014). While the pathway of germline-induced longevity is well studied, the others and especially the involvement of mitochondrial activity in longevity remain poorly understood. As mentioned, the mitochondria have been proposed to alter lifespan via ROS signalling, mutation in mtDNA or altered metabolic rates (Miranda-Vizuete and Veal 2017; Z. Wu et al. 2018; Dancy, Sedensky, and Morgan 2014).

Due to their short lifespan, the effects of single gene loss-of-function or overexpression are easily observed. Genes that affect lifespan in *C. elegans* can be roughly divided into at least three classes, genes that regulate: dauer formation (e.g. *daf*), dietary pathways (e.g. *eat*) and physiological rates (e.g. *clk*) (Feng, Bussière, and Hekimi 2001). Dauer formation genes are interesting as they mediate the formation of longer lived and stress-resistant larval stage and induce the signalling cascade involving the insulin receptor-like transmembrane tyrosine kinase (*daf-2*) and forkhead-like transcription factor (*daf-16*) (X. Sun, Chen, and Wang 2017). Dietary pathways, like *eat* genes, are mainly responsible for the function of the pharynx and thereby

prolonging lifespan by mimicking dietary restriction (DR) (Lakowski and Hekimi 1998). Physiological rates regulating genes, like *clk*, are a group of genes affecting rates of many processes, like embryonic and postembryonic development, reproduction and behavioural rhythms (Lakowski and Hekimi 1996). Interesting, *clk-1* was the first mitochondrial dysfunction mutant (mitomutant) discovered (Wong et al. 1995) and encodes the nematode ortholog of demethoxyubiquinone hydrolase, which is necessary for the ubiquinone synthesis (Miyadera et al. 2001).

1.4.3 *C. elegans* mitomutants

A systemic RNA interference (RNAi) screen for gene inactivation that prolongs lifespan observed a majority of genes encoding mitochondrial proteins, like mitochondrial carriers, ETC components and mitochondrial ribosomal subunits (S. S. Lee et al. 2003). The phenotype of most of these mitomutants was that they were smaller, had altered mitochondrial morphology, lower oxygen consumption rates and reduced ATP levels (S. S. Lee et al. 2003). Direct disruption of the ETC either in mitomutant, such as *isp-1(qm150)* (iron sulphur protein) mutant (Feng, Bussi re, and Hekimi 2001), or RNAi knockdown of MRC subunits, like complex I, III, IV and V (Dillin et al. 2002) induces longevity in these animals. Interestingly, MRC suppression, for example by *atp-3* and *cyc-1* RNAi, during larval development is sufficient to induce longevity (Dillin et al. 2002). However, these long-lived animals have delayed developmental rates, decreased fertility and reduced fecundity (Rea, Ventura, and Johnson 2007). Here, we introduce interesting ETC mutants that led to remarkable insights on the role of mitochondrial dysfunction, ROS production and generation on lifespan (Dancy, Sedensky, and Morgan 2014).

Complex I:

The *C. elegans* nuclear-encoded *gas-1* gene is the ortholog of human NDUFS2. This 49 kDa subunit is part of nematode complex I of ETC and was first described as a crucial gene in controlling and maintaining volatile anaesthetics (P. G. Morgan, Sedensky, and Meneely 1990; P. G. Morgan, Margaret, and Sedensky 1994). *Gas-1(fc21)* mutants have reduced complex I activity, fewer offspring, delayed development, are highly sensitive to oxidative stress and have a shortened lifespan (Hartman et al. 2001). The reduced complex I activity is associated with an increased

complex III-dependent activity, probably as compensatory mechanisms (E. B. Kayser et al. 2001). Remarkably, these phenotypes are dependent on oxygen levels, as low oxygen concentrations diminish the *gas-1* phenotypes while high oxygen concentrations reduce survival and fecundity (Hartman et al. 2001; E. B. Kayser et al. 2001). However, survival, fecundity and lifespan of wild-type (WT) animals are also affected upon high oxygen concentrations. Additionally, WT animals become hypersensitive to volatile anaesthetics (E.-B. Kayser, Morgan, and Sedensky 2004; Hartman et al. 2001), suggesting anaesthetics sensitivity and lifespan are linked to mitochondrial activity. In agreement, mitochondrial ROS production (Muñoz-Tremblay 2015) and oxidative damage are increased in *gas-1* mutants (E.-B. Kayser, Morgan, and Sedensky 2004).

Contradictory to *gas-1* mutant, all members of the NADH ubiquinone oxidoreductase (*nuo*) gene family have prolonged lifespans upon suppression (Munkácsy and Rea 2014). All members are encoding complex I subunits and especially, *nuo-2*, ortholog of human NDUFS3 (Grad and Lemire 2004), and *nuo-6*, ortholog of human NDUFB4, are described as inducers of longevity (Dillin et al. 2002). Notably, mitochondria isolated from *nuo-6* mutant show increased mtROS generation (Yang and Hekimi 2010a), which is not accompanied by oxidative stress or damage (Yang and Hekimi 2010b). The authors suggested this mtROS is sensed by components of the intrinsic apoptosis signalling pathway, namely CED-9, CED-4 and CED-3 (Yee, Yang, and Hekimi 2014). While *gas-1* and *nuo-6* mutants have opposite effects on lifespan, our lab observed no difference in activated longevity assurance pathways (Pujol et al. 2013).

Complex II:

Remarkably, complex II dysfunction is the only disruption of ETC that has never been reported to increase lifespan (Kuang and Ebert 2012; Ichimiya et al., n.d.). Rather than long lived, *mev-1(kn1)* mutant, ortholog of succinate dehydrogenase complex subunit C (SDHC) has a shorter lifespan (Naoaki Ishii et al. 1990; Yanase, Yasuda, and Ishii 2002). Contradictory to the other mitomutants, *mev-1* mutants are hypersensitive to molecular oxygen, have increased oxidative damage and decreased SOD levels (Naoaki Ishii et al. 1990; Hartman et al. 2001). In addition, the steady state and production levels of $O_2^{\cdot-}$ are elevated in adult *mev-1* mutants (Yanase, Yasuda, and Ishii 2002; Naoaki Ishii et al. 1990), which is contradicting other ETC mutants, like

isp-1;ctb-1, *nuo-6* and *clk-1* mutants (Yang and Hekimi 2010a). These differences from the other ETC mutants could be explained by dual role of complex II in TCA cycle, as succinate dehydrogenase, and in ETC, as electron transporter.

Complex III:

Single point-mutation of nematode Rieske iron sulphur protein-1 (*isp-1*) at proline residue 225 of mitochondrial complex III was reported to be sufficient to increase lifespan (Feng, Bussi re, and Hekimi 2001). While WT has a mean lifespan of 20,3 days, *isp-1(qm150)* has a mean lifespan of 33,0 days. However, the drawback was that the physiological rates are highly reduced in comparison with WT worms. Especially, reproduction characteristics, like egg production rate, embryonic development and brood size were affected. Interestingly, despite these decreased physiological rates, the animals appear healthy as embryonic and postembryonic lethality remained low and similar to WT animals. Similar to *nuo-6* mutant, *isp-1* suppression results in different activated longevity assurance pathways. *Isp-1* suppression via RNAi activates the autophagy and HSF-1-mediated heat-shock response (Yang and Hekimi 2010b), while *isp-1* mutation activates a specific mtROS response pathway (Yang and Hekimi 2010a).

Others observed that double mutant *isp-1(qm150);ctb-1(qm189)* suppress the *isp-1* fecundity phenotypes and restore the postembryonic development as slow behavioural features (Feng, Bussi re, and Hekimi 2001). Remarkably the long lifespan of *isp-1* was not altered in *isp-1(qm150);ctb-1(qm189)* (Suthammarak, Morgan, and Sedensky 2010; Feng, Bussi re, and Hekimi 2001). The *ctb-1(qm189)* mutation is a single-point mutation in cytochrome b of alanine to valine (Iwata et al. 1998). From now on, the double mutant *isp-1(qm150);ctb-1(qm189)* will be referred as *isp-1;ctb-1*.

Depletion of nematode cytochrome c reductase (*cyc-1*) was one of the RNAi observed in the screen for ETC subunits (S. S. Lee et al. 2003; Dillin et al. 2002). *Cyc-1* RNAi-treated animals have increased expression of cell-protective genes, like chaperones, SOD and glucuronosyltransferases (UGTs) (Cristina et al. 2009), which has been suggested to be the primary reason for longer lifespan.

Complex IV:

Depletion of the nuclear-encoded cytochrome c oxidase-1 (*cco-1*) via RNAi increases lifespan (Dillin et al. 2002). Remarkably, until now there is no complex IV

mutant described that prolongs lifespan. Previously, longer lifespan by *cco-1* suppression was reported to be mediated by mitochondrial unfolded protein response (mtUPR), as in *cco-1* mutant the mtUPR is activated. However, *cco-1* RNAi treatment still prolongs lifespan in mtUPR *atfs-1(tm4525)* mutant (Bennett, vander Wende, et al. 2014). Similarly, mtUPR is not required in *isp-1* mutant (Yang and Hekimi 2010b). Altogether, the role of mtUPR in longevity phenotype remains unclear (Bennett and Kaerberlein 2014). The exact mechanism of CCO-1 in lifespan regulations remains unclear.

Complex V:

Besides the ETC, also ATP synthase has been linked to longevity. Suppression of ATP synthase subunits *atp-2* (ortholog of human ATP synthase F1 subunit beta), *atp-3* (ortholog of human ATP synthase peripheral stalk subunit), *atp-4* (ortholog of human ATP synthase peripheral stalk subunit F6) *atp-5* (ortholog of human ATP synthase peripheral stalk subunit d) and *asb-2* (ortholog of human ATP synthase peripheral stalk-membrane subunit b) were found in genome-wide RNAi screen to induce prolonged lifespan in *C. elegans* (C. Xu et al. 2018). *Atp-2(ua2)* mutants are enlisted as long-lived (Tsang et al. 2001). However, the exact role of ATP synthase in promoting lifespan remains unclear. Surprisingly, complex V-mediated long lifespan is independent of altered ATP levels, has decreased complex I activity and higher levels of mtDNA (C. Xu et al. 2018). Moreover, TCA metabolite α -ketoglutarate was shown to inhibit complex V and promote longevity (Chin et al. 2014).

1.4.3 Longevity assurance pathways

Lifespan extension in long-lived animals was achieved by either switching to alternative metabolic pathways (Butler et al. 2010) or activating cytoprotective mechanisms (Shore, Carr, and Ruvkun 2012). Long-lived mitomutants alter their metabolism from respiratory metabolism towards more anaerobic pathways, like glycolysis, which is regulated by mTOR and hypoxia-inducible factor 1 α (HIF-1 α) (Butler et al. 2010; Hudson et al. 2002). Cytoprotective mechanisms were observed during disruption of insulin/IGF-1 signalling, which induces heat shock, antioxidant and pathogen response (C. T. Murphy et al. 2003). Nematode mitochondrial mutants, such as *isp-1*, *clk-1* and *cyc-1*, have been shown to induce mtUPR (Cristina et al. 2009).

This upregulation of mitochondrial chaperones and proteases, like ClpP could restore protein homeostasis (Q. Zhao et al. 2002). Also the activation of xenobiotic detoxification by upregulating different drug-metabolizing enzymes, like UGTs and glutathione S-transferases (GSTs), have been described in nematode long-lived mutants (C. T. Murphy et al. 2003; Shore, Carr, and Ruvkun 2012) and mammalian long-lived mutants (Amador-Noguez et al. 2004; Steinbaugh et al. 2012).

In agreement with the increased cytoprotective processes in long-lived animals, the concept of hormesis has been described as a mechanism in which increased resistance to stress factors is achieved by early exposure to mild stress and activation of cytoprotective mechanisms. (Yang and Hekimi 2010a). This led to the implication of ROS as mild stressor and inducer of resistance response, which is named the mitohormetic response or mitohormesis (Ristow and Schmeisser 2014; Yun and Finkel 2014; Calabrese 2018).

1.5. KLF-1-mediated longevity

1.5.1 KLF-1: regulator of mitomutant *isp-1;ctb-1* lifespan

To elucidate the signalling cascade that was responsible for mitochondrial dysfunctional-induced longevity, we performed a genome-wide RNAi screen on long lived mitomutant *isp-1;ctb-1* (Herholz et al. 2019). The screen was started with chromosome III of the existing feeding library (Kamath and Ahringer 2003) and focussed on transcription factors, since they are key regulators of genetic reprogramming and cellular signalling cascades. Here, transcriptional factor Krüppel-like factor-1 or KLF-1 was the only candidate to fulfil the criteria of being able to suppress longevity in *isp-1;ctb-1* mutant, while not having any effect on WT lifespan (Fig.1.8) (Herholz et al. 2019). Remarkably, KLF-1 depletion only during early adulthood was sufficient to fully suppress the longer lifespan in *isp-1;ctb-1* animals (Fig.1.8). Above all, *klf-1* suppression on day one of adulthood (D1) was crucial for blocking longer lifespan, as *klf-1* RNAi started later than D1 had less of a strong effect on the phenotype (Herholz et al. 2019). Remarkably, in agreement with a previous observation that both long- and short-lived mutants activate the same longevity-assurance responses (Pujol et al. 2013), KLF-1 depletion also led to shorter lifespan in *gas-1(fc21)* and *mev-1(kn1)* mutants (Herholz et al. 2019).

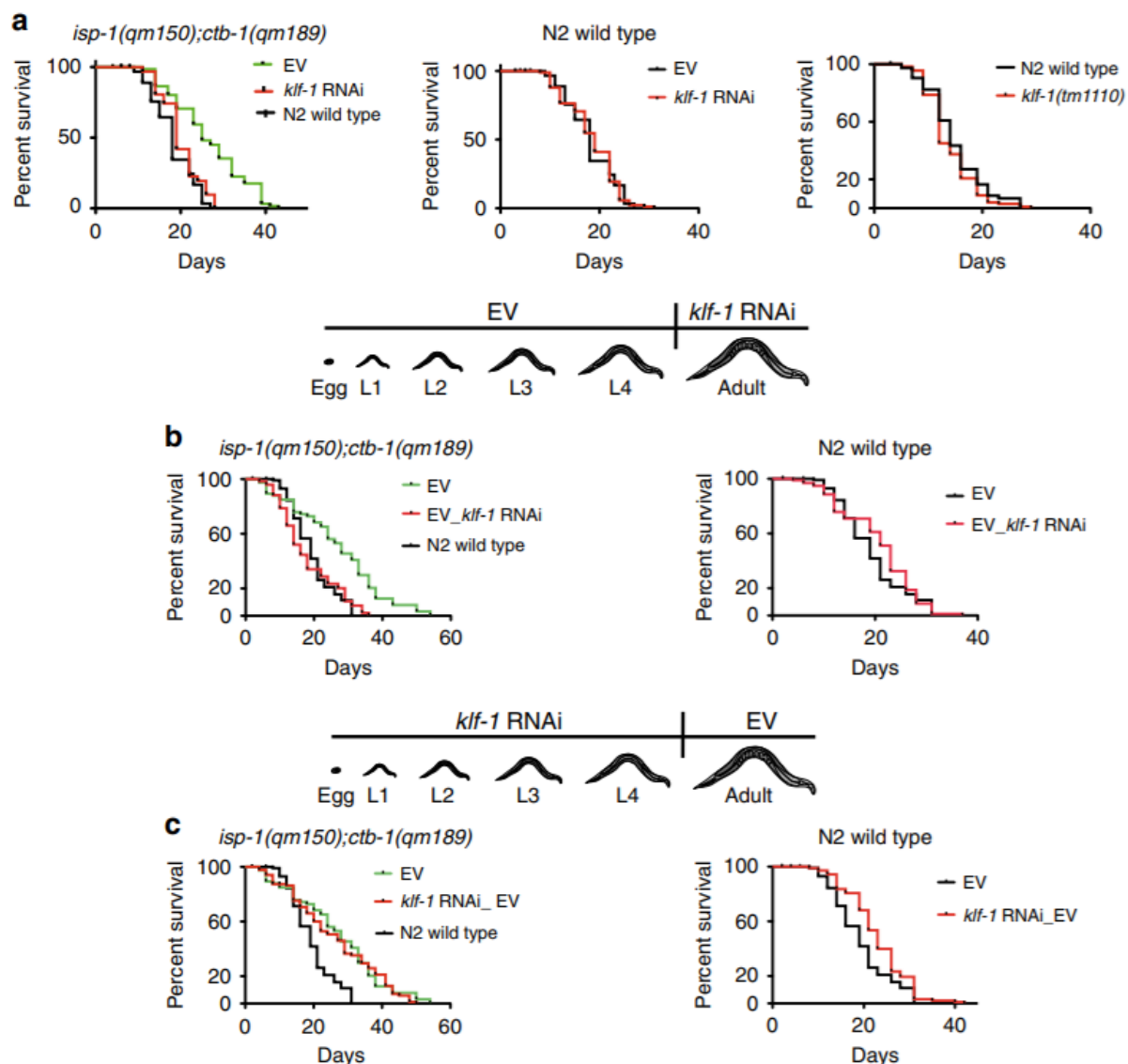


Fig. 1.8. KLF-1 is necessary during early adulthood for mitomutant-induced longevity.

Lifespan of N2 and *isp-1;ctb-1* animals grown on control (empty vector, EV) and *klf-1* RNAi plates. **A.** *Klf-1* RNAi on *isp-1;ctb-1* animals (left), WT animals (middle) and *klf-1(tm1110)* mutant lifespan (right) with WT on EV as control. **B.** Animals were only exposed to *klf-1* RNAi during adulthood, starting with D1 animals. **C.** Animals were only exposed to *klf-1* RNAi during larval development, from egg stage till late L4 stage. Figure obtained and modified from (Herholz et al. 2019)

KLF-1-induced longevity was achieved via upregulation of the xenobiotic detoxification transcriptional program during adulthood in *isp-1;ctb-1* mutant (Herholz et al. 2019). The majority of upregulated genes encoded proteins involved in phase I xenobiotic detoxification, particularly cytochrome P450 oxidases (CYPs) (Herholz et al. 2019). In agreement, many long-lived mutants of different species have upregulated gene programmes involved in xenobiotic detoxification (McElwee et al. 2004; Shore

and Ruvkun 2013), including the Snell dwarf mice and Little mice (Steinbaugh et al. 2012). KLF-1 is a direct regulator as it binds the GC-rich DNA motifs in the *cyps* promoter. The upregulation of CYPs was fully dependent on KLF-1, as KLF-1 depletion in *isp-1;ctb-1* animals suppress all increased xenobiotic resistance (Herholz et al. 2019). This xenobiotic resistance should give the mitomutant an advantage over WT animals and therefore explain the longer lifespan. However, still little is known about the signalling pathway that underlies this increased resistance to various stressors.

1.5.2 Conserved function of mammalian KLFs

Nematode KLF-1 belongs to the Krüppel-like factors (KLFs) proteins, which are part of the specificity proteins (SPs)/KLFs family of zinc-finger transcription factors involved in various biological pathways, like development, differentiation and growth (McConnell and Yang 2010). In fact, the name of this transcription factor originates from *Drosophila* protein Krüppel, which means cripple and is associated with development (Pollak et al. 2018). The members of the KLFs family have a high similarity as all members have three C-terminal located C2H2-type zinc fingers for binding GC-rich DNA motifs, preferably CACCC sequence (McConnell and Yang 2010). Whereas the C-terminal is highly conserved, the N-terminal regions before the zinc fingers are highly variable between members. They contain short sequence motifs for potential post-translation modifications and protein binding partners (Pollak et al. 2018). Moreover, the KLFs are conserved across mammals and some lower organisms, for example *Danio rerio* (zebrafish), *Xenopus laevis* (frog), *Gallus gallus* (chicken) and *C. elegans*. While the KLFs members in mice and humans contain at least 18 members (Pollak et al. 2018; Pei and Grishin 2013), nematodes only have three orthologous, namely KLF-1, KLF-2 and KLF-3 (Hsieh et al. 2017). These KLFs are described as mediators of lipid metabolism, cell death and phagocytosis (Hashmi et al. 2008).

Most of the 18 mammalian KLF homologues are involved in various stress responses or development and differential gene programmes (Cullingford et al. 2008; McConnell and Yang 2010). The closest homologues of *C. elegans* KLF-1 are KLF2, KLF4 and KLF5, as these KLFs are induced by oxidative stress and essential for switching the differential gene program (Cullingford et al. 2008; Hsieh et al. 2017). Intriguingly, KLF4, KLF6 and KLF15 are previously linked to mitochondria, as KLF4

and KLF15 seems to regulate cardiac mitochondrial biogenesis and function while KLF6 is a key regulator of mitochondrial gene expression morphology in kidney. Furthermore, *Klf6* expression levels are increased upon H₂O₂ (Mallipattu et al. 2015; Cullingford et al. 2008) and KLF15 control lipid metabolism (Prosdocimo et al. 2015; Fan et al. 2021; Matoba et al. 2017).

Mammalian *cyps* expression is a complex process, involving multiple transcription factors, cofactors and signalling cascades (Tralau and Luch 2013). One of these modulators is a basic transcription element (BTE), which is present in some of the *cyp* promoters. Intriguingly, KLF function as transcription factor was first described as BTE-binding (BTEB) protein (Black, Black, and Azizkhan-Clifford 2001). In fact, some of the KLFs are renamed after their identification, namely BETB2/KLF5, BTEB/KLF9, BTEB3/KLF13 and BTEB4/KLF16 (Imataka et al. 1992; Komori et al. 1993; Kaczynski et al. 2002). Interestingly, increased AA-induced *cyp* expression in Hepa1-6 cells are diminished when either *Klf4* or *Klf5* is inhibited via siRNA (Herholz et al. 2019). Moreover, some KLFs were observed regulating *cyp* expression by binding to the BTE promoter (Yanagida et al. 1990; Weiqing Zhang et al. 1998). This further emphasize the conserved role of KLFs on CYPs. However, the knowledge of this regulation and potential physiological relevance still needs to be explored. Until now, the only physiological roles observed are the regulatory role of KLF6 with binding partner aryl hydrocarbon receptor on *cyps* expression through binding of the xenobiotic response elements and of KLF9 modulation of CYP2D6 expression during pregnancy (Koh et al. 2014; Wilson, Joshi, and Elferink 2013). The role of *cyps* and other xenobiotic detoxification genes, like *ugt* and *gst*, have been established in long-lived nematode mutants (C. T. Murphy et al. 2003; Shore, Carr, and Ruvkun 2012; McElwee et al. 2004).

1.6 Aim of this study

As stated before, we identified the transcription factor KLF-1 as mediator of aging and lifespan determination in the context of mitochondrial (dys)function. While, KLF-1 is required during early adulthood, the exact mechanism of KLF-1 activation remains unclear. Therefore, the aim of this study is to gain deeper insights into the signalling cascade activated by mitochondrial dysfunction in nematode *isp-1;ctb-1* long-lived mutant. To this end, we utilized RNAi and mutants of WT and *isp-1;ctb-1* animals to further establish novel components of this signalling cascade. Moreover, we assayed potential signalling candidates by lifespan, *cyps* expression and xenobiotic resistance. In the end we defined the ROS origin that activates the signalling machinery, by developing and employing a strain expressing roGFP2-Orp1 localized to the OMM.

In summary, the objectives of this study are:

- To determine the initial activation signal in *isp-1;ctb-1* long-lived mutant
- To identify the major signalling components within the mitochondria and to define their possible role in lifespan determination
- To characterise the cytosolic mtROS-induced signalling cascade resulting in KLF-1 nuclear translocation

2. Material and methods

All used chemicals, equipment, software and (biological) materials are enlisted in chapter 2.5 with their respectively supplier.

2.1. *C. elegans* methods

2.1.1. Strains and maintenance

Strains were maintained at 20°C on nematode growth media (NGM) plates and fed with *Escherichia coli* OP50 and stored in air permeable boxes (S. Brenner 1974). Following strains were used:

Table. 2.1 *C. elegans* strains used

Strain	Genotype
N2, Bristol	Wild-type
MQ989	<i>isp-1(qm150);ctb-1(qm189)</i>
ATR1016	<i>klf-1(tm1110)</i>
ATR1045	<i>isp-1(qm150);ctb-1(qm189);prpl-17::grx1-rogfp2;unc-119</i>
ATR4081	<i>N2;(pvha-6::klf-1-yfp;prab-3::mCherry;rol-6(su1006))</i>

ATR4082	<i>isp-1(qm150);ctb-1(qm189);(pvha-6::klf-1-yfp;prab3::mCherry;rol-6(su1006))</i>
ATR4086	<i>N2;Ex(pvha-6::klf-1-yfp;prab-3::mCherry;rol-6(su1006))</i>
ATR4026	<i>isp-1(qm150);ctb-1(qm189);pcyp-34a8::gfp;prab-3::mCherry</i>
ATR4030	<i>N2;pcyp-34A8::gfp pGH8</i>
ATR4133	<i>N2;Ex(pmyo-3::rogfp2-ORP1; rol-6; prab-3::mCherry)</i>
ATR4135	<i>N2;Ex(pvha-6::rogfp2-ORP1; rol-6; prab-3::mCherry)</i>
ATR4138	<i>isp-1(qm150);ctb-1(qm189);Ex(pmyo-3::rogfp-ORP1; rol-6; prab-3::mCherry)</i>
ATR4139	<i>isp-1(qm150);ctb-1(qm189);Ex(pvha-6::rogfp2-ORP1; rol-6; prab-3::mCherry)</i>
ATR4140	<i>N2;(pvha-6::klf-1-yfp (*C419>S);prab3::mCherry;rol-6(su1006))</i>
ATR4141	<i>N2;(pvha-6::klf-1-yfp (*K411>A);prab3::mCherry;rol-6(su1006))</i>
ATR4142	<i>N2;Ex(pvha-6::klf-1-ha-flag;prab-3::mCherry;rol-6(su1006))</i>
ATR4143	<i>N2;(pvha-6::klf-1-yfp (*S39>A);prab3::mCherry;rol-6(su1006))</i>
ATR4144	<i>N2;(pvha-6::klf-1-yfp (*S39>D);prab3::mCherry;rol-6(su1006))</i>
ATR4146	<i>N2;(pvha-6::klf-1-ha-flag;prab-3::mCherry;rol-6(su1006))</i>
ATR4147	<i>isp-1(qm150);ctb-1(qm189);(pvha-6::klf-1-HA-FLAG;prab-3::mCherry;rol-6(su1006))</i>
JV2 (GRX)	<i>N2;prpl-17::grx1-rogfp2;unc-119</i>
VC1151	<i>prdx-3(gk529)</i>
VC289	<i>prdx-2(gk169)</i>

2.1.2. Microinjection and X-ray integration of transgenic strains

Plasmid mixtures were prepared and injected using standard procedures (Mello et al. 1991). Briefly, injection mixes were prepared as indicated with a final concentration of 100 ng/μl and injected into the gonad of D1 adults using a Zeiss Observer A.1 microscope equipped with AxioCam ERc5S camera, Eppendorf InjectMan Nlz injection pump and Eppendorf FemtoJet microinjector. After injection, animals were maintained on NGM plates and the appearance of transgenic progeny was analysed by the co-injection markers *pGH8* and *pRF4*. ATR4030 was generated by injecting the *pcyp-34a8::gfp* (50 ng/μl) and *pRF4* (50 ng/μl) plasmids into N2 wild-type (WT) animals and crossed into *isp-1(qm150);ctb-1(qm189)* to create ATR4026. ATR4086 was generated by injecting the *pvha-6::klf-1::yfp* (40 ng/μl), *pGH8* (20 ng/μl) and *pRF4* (40 ng/μl) plasmids into WT animals. ATR4142 was generated by injecting the *pvha-6::HA::FLAG* (40 ng/μl), *pGH8* (20 ng/μl) and *pRF4* (40 ng/μl) plasmids into WT animals. ATR4142 was generated by injecting the *pvha-6::HA::FLAG* (40 ng/μl), *pGH8* (20 ng/μl) and *pRF4* (40 ng/μl) plasmids into WT animals. ATR4086 and ATR4142 were subsequently integrated by X-ray and outcrossed to create ATR4081

and ATR4146 strains respectively. ATR4081 and ATR4146 were crossed into *isp-1(qm150);ctb-1(qm189)* to create ATR4082 and ATR4147 strains respectively. Plasmid *pvha-6::klf-1::yfp* was mutated by site-directed mutagenesis into *pvha-6::klf-1*C419>S::yfp*, *pvha-6::klf-1*K411>A::yfp* and *pvha-6::klf-1*S39>D::yfp* plasmids. ATR4140, ATR4141 and ATR4143 were generated by injecting the *pvha-6::klf-1*C419>S::yfp*, *pvha-6::klf-1*K411>A::yfp* and *pvha-6::klf-1*S39>D::yfp* (40 ng/μl), respectively, *pGH8* (20 ng/μl) and *pRF4* (40 ng/μl) into WT animals. ATR4133 and ATR4135 were generated by injecting the *pmyo-3::tomm20-roGFP2-ORP1* and *pvha-6::tomm20-roGFP2-ORP1* (40 ng/μl), respectively, *pGH8* (20 ng/μl) and *pRF4* (40 ng/μl) into WT animals. ATR4138 and ATR4139 were generated by crossing ATR4133 and ATR4135 respectively into *isp-1(qm150);ctb-1(qm189)*.

2.1.3. Crossing of *C. elegans* strains

In order to set up crossings, males were generated by exposing L4 hermaphrodites at 30 °C for 4h or by crossing four L4 WT hermaphrodites with eight WT males. To outcross a mutation or cross two different genotypes, males with the desirable genotype were generated by crossings four L4 hermaphrodites with desirable genotype with eight WT males. Desirable genotype was followed by checking for roller phenotype (*rol-6* gene) and red fluorescence signal (*prab-3::mCherry*). Then, twenty of these males were placed together with four L4 hermaphrodites with a different genotype. F1 progeny was checked for roller phenotype and animals were singled on NGM plates and allowed to lay eggs. Then, F1 generation worms were analysed for desired genotype by single worm polymerase chain reactions (PCR). Roller phenotype was analysed in the next generation and worms with desired genotype were maintained or frozen.

2.1.4. Genotyping of *1(qm150);ctb-1(qm189)* strain

Single worm PCR was performed by picking single worms into PCR tubes, which contain 10 μl single worm lysis buffer supplied with proteinase K. PCR tubes were frozen for 10 minutes (min) at -80 °C to break the worm's cuticles. Then samples were exposed to a cycle of 60 °C for one hour followed by 15 min at 95 °C by using the Veriti 96 well Thermal cycler. For genotyping, PCR amplification reactions were

performed by mixing 10,7 µl of H₂O, 3,2 µl of dNTPs, 0,1 µl of DreamTaq polymerase, 1 µl of each primer (Table 2.2) and 2 µl of DreamTaq buffer and 2 µl of the worm lysate in a final volume of 20 µl. Samples were exposed to 95 °C for 5 min, a fourthly long cycle consisting of 95 °C for 45 sec, 54 °C for 45 sec and 72 °C for 1 min, subsequently 72 °C for 10 min and cooling down samples to 4 °C. After PCR, samples were digested with restriction enzymes BsmAI and CutSmart buffer for 4 h at 55 °C. Samples were analysed by agarose gel electrophoresis. For this, 2% agarose gel supplied with ethidium bromide (EtBr) was made and Gene Ruler DNA Ladder Mix was used.

Table 2.2 Primers for genotyping

Allele	Primer	Restriction enzyme
<i>isp-1(qm150)</i>	Fw 5'-CAAATCGCGAACTTTTCTTCA-3'	BsmAI
	Rv 5'-AACGTCGTGCTCTTCCAAC-3'	

2.1.5. Synchronization of worm populations

Egg-containing adults were washed off the plate and collected in 7 ml M9 and synchronized by treatment with bleaching solution to extract the eggs from the worms. After 10 min incubation, while vortexing each 2 min, eggs were pelleted by centrifugation (3000 rpm, 1 min). Bleaching solution was removed and eggs were washed 4 to 5 times by adding 4.5 ml M9 and centrifugation (3000 rpm, 1 min). Egg suspension was placed on fresh NGM plates and incubated at 20°C

2.1.6. RNAi treatment

During experiments, worms were bleached or transferred on control plates or RNAi plates. RNAi treatment was performed as described previously (Kamath et al. 2003). In summary, both control and RNAi plates were NGM agar plates with the addition of 1 mM Isopropyl β-D-1-thiogalactopyranoside (IPTG) and antibiotics 100 µg/ml Ampicillin (Amp) and 25 µg/ml Tetracycline (Tet). Control plates contain the bacteria *E. coli* HT115 (DE3) strain which carries the empty vector (EV) L4440. Bacteria clones for RNAi plates were acquired from the Ahringer RNAi library or if stated from the Vidal library by growing the clones overnight at 37°C in Luria broth (LB) media which contains both antibiotics Amp and Tet (Table 2.3) (Kamath et al. 2003;

Rual et al. 2004; Kamath and Ahringer 2003). Bacterial clones were stored in glycerol stocks, isolated and sequenced or directly expanded. For storage, 100% glycerol was mixed with bacteria cultures to 15% glycerol and stored at -80°C. To determine the sequence, vector plasmid was isolated from bacteria cultures by Plasmid Miniprep skit, according to manufacturer's protocol, and sent for sequencing to Eurofins Genomics. For seeding bacteria on plates, bacterial cultures were grown in LB media, in the presence of antibiotics, until reaching OD₅₉₅ = 0.5. Then cultures were induced with 1 mM IPTG for three hours at 37°C and seeded on NGM plates with IPTG and antibiotics.

Table 2.3 RNAi clones

Name	Sequence	Ahringer RNAi library
<i>atp-5</i>	C06H2.1	V-7J03
<i>cco-1</i>	F26E4.9	I-4L08
<i>ctl-1</i>	Y54G11A.6	II-9I01
<i>ctl-2</i>	Y54G11A.5	II-9G23
<i>cyc-1</i>	C54G4.8	I-3P14
<i>klf-1</i>	F56F11.3	III-1J15
<i>nuo-1</i>	C09H10.3	II-7L05
<i>nsy-1</i>	F59A6.1	II-4M01
<i>pmk-1</i>	B0218.3	IV-9P08
<i>pmk-2</i>	F42G8.3	IV-4G23
<i>pmk-3</i>	F42G8.4	IV-4I01
<i>prdx-3</i>	R07E5.2	III-2O03
<i>prdx-6</i>	Y38C1AA.11	IV-10F05
<i>prx-5</i>	C34C6	II-6G16
<i>sek-1</i>	R03G5.2	X-4E03
<i>sod-1</i>	C15F1.7	II-10114 E6 (Vidal)
<i>sod-2</i>	F10D11.1	I-4K13
<i>sod-3</i>	C08A9.1	X-8F07
<i>wwp-1</i>	Y65B4BR.4	I-10090 A1 (Vidal)
<i>vdac-1</i>	R05G6.7	IV-3D24

2.1.7. KLF-1 nuclear localisation

Bleached eggs were placed on control plates or drug containing plates and grown until D1, when nuclear localization was visualized. In specific cases, worms were grown on control plates and transferred on drug containing plates during L4 and

nuclear localization was visualized on D1. Treatment with 10 mM N-Acetyl-L-cysteine (NAC), 10 mM L-Ascorbic acid (Vitamin C, Vit C), 10 μ M Bortezomib (Bor), paraquat (PQ) or 100 μ M S3QEL-2 was performed by adding the compounds in the NGM agar, before pouring the plates (Table 2.4). Other drug treatments were performed by adding compounds dissolved in M9 on the heat-inactivated bacteria of control plates and dried by air, one hour prior to transferring of worms. The following drugs concentration were used: 2 μ M Antimycin A (AA), 5 μ M Carbonyl cyanide-4-(trifluoromethoxy) phenylhydrazone (FCCP), 25 mM Malonate (MAL), 5 μ M mitoPQ, 2 μ M Myxothiazol (Myxo) 100 nM Rotenone (ROT), 50 μ M Tunicamycin (Table 2.4). For 1,4 Dithiothreitol (DTT) and H₂O₂ treatment, worms were collected in M9 and exposed to either 5 mM DTT or 10 mM H₂O₂ for 15 min before imaging (Table 2.4). Nuclear localization was characterized by dividing level of nuclei into three categories, namely low nuclear localization (0-2 nuclei), moderate nuclear localization (3-5 nuclei) and high nuclear localization (>6 nuclei), unless otherwise stated. For stage specific treatment, worms were transferred between control plates and control plates with drugs.

Table 2.4 Drugs

Name	Concentration	Mechanism
Antimycin A	2 μ M	Inhibitor of Qi site of Complex III
DTT	5 mM	Reducer of disulphide bonds
FCCP	5 μ M	Disrupts ATP synthesis by transporting protons across the mitochondrial inner membrane
H ₂ O ₂	10 mM	ROS compound
Malonate	25 mM	Inhibitor of succinate dehydrogenase
Mito-paraquat	2 μ M	Superoxide production by redox cycling at the matrix-complex I site
Myxothiazol	2 μ M	Inhibitor of Qq site of complex III
NAC	10 mM	Antioxidant
Paraquat	0.1 mM	Superoxide production by redox cycling
Rotenone	100 nM	Inhibitor of transfer of electrons from the iron-sulphur subunits of complex I to ubiquinone
S3QEL-2	100 μ M	Inhibitor of Qo site of complex III
Tunicamycin	50 μ M	Inhibitor of biosynthesis of N-linked glycans
Vitamin C	10 mM	Antioxidant

2.1.8. Lifespan analysis

Lifespan experiments were performed by growing the worms at 20°C. Day 1 of the lifespan was defined as D1 of adulthood. All lifespans were done in the absence of Floxuridine (FUdR), therefore worms were transferred during the first five days of adulthood to new plates, to remove the eggs. On day 0, 25 worms were transferred to NGM plate, for a total of 100 worms per condition, which results in four plates per condition. Worms were examined every two or three days and removed and defined as dead when there was no reaction by prodding with a platinum pick. Worms that escaped the plate or died due to protrusion or internal hatching were removed from the experiment. When stated that worms were only exposed to *klf-1*, *prdx-3*, *sod-3* or *vdac-1* RNAi during larvae stages, worms were transferred on D1 on control RNAi plates. When stated that worms were only exposed to *klf-1* during adult stage, worms were hatched and grown on control RNAi plates and transferred on D1 on *klf-1* RNAi plates. Compilation of lifespan assay is illustrated in Supplementary table 1.

2.1.9. ROS measurements

To determine mitochondrial (mito) mass and ROS levels, animals were stained with respectively Mitotracker Red CM-H₂XROS and Mitotracker Deep Red. L4 or D1 animals were transferred to plates containing dye solutions and incubated for 1 h in the dark. Plates were made day prior by seeding NGM plates with heat-inactivated bacteria and air-dried overnight at room temperature (RT). Heat-inactivated bacteria were used to reduce background intensity. On day of experiment, 200 µl of 10 µM Mitotracker was added on top of the bacteria and let air-dry. After incubation, animals were washed 3 times with M9 buffer and afterward transferred to NGM plates without dye solution for 2 h. Mitotracker intensity was analysed with Biosorter Instrument and FlowPilot™ software.

2.1.10. H₂O₂ resistance assay

WT and *isp-1;ctb-1* worms were grown on plates with EV RNAi and transferred at specific larvae stages to plates containing 1 µM AA or 100 µM S3QEL-2, respectively. At D1, worms were transferred into 96-well plate filled with M9 buffer, 8

worms per well. H₂O₂ was added to final concentration of 20 mM. Worms were assayed for survival after 4 h. For each condition, 12 wells were scored.

2.1.11. BODIPY 493/503 staining

To assay neutral lipids levels, WT and *isp-1;ctb-1* worms were grown on indicated RNAi plates and on D1 collected and washed in M9 buffer. Worms were stained by 5 µM BODIPY 493/503 at RM for 1 h in the dark. Then, worms were washed twice in M9, paralysed with 5 mM levamisole and mounted on an 2% agarose pad for imaging.

2.1.12. Xenobiotic resistance assays

To access xenobiotic resistance, worms were grown on indicated RNAi plates with or without Vit. C and at D1 worms were bleached. For the vinblastine assay, eggs were incubated overnight in S-Basal at shaker. Then, 20-30 synchronized L1 larvae per well were incubated in S-Basal with indicated bacteria and 1 mM IPTG. For antioxidant treatment 10 mM Vit. C was added to S-Basal. Wells were divided into controls without vinblastine and with 100 µM vinblastine. Worms were incubated at 450 rpm at the shaker on RT and checked every day. Development stage of worms in vinblastine was scored when worms in controls wells without vinblastine reached adulthood. For this, at least six wells per condition were used. For the Levamisole assay, synchronized D1 worms were transferred to 1 mM levamisole NGM plates. Animals were scored every 15 min for paralysis by prodding. When there was no movement observed, worms were scored as paralysed. At least eight plates were used per condition, each with 25 worms.

2.2. Molecular biology and biochemistry

2.2.1. Real-Time qPCR

RNA isolation

Animals were grown on RNAi plates and collected at D1. Per sample three full 9 cm plates were used and for each condition, five independent samples were

prepared. Total RNA was isolated by Trizol reagent in RNase free Eppendorf tubes. DNase treatment was performed using DNA-free, DNase and removal kit, according to manufacturer's protocol. Then supernatant was transferred to fresh RNase free Eppendorf tubes and RNA concentration was measured by spectrophotometry (NanoDrop) at 260 nm and 280 nm.

cDNA synthesis and real-time PCR

For the cDNA synthesis, 0,8 µg of total RNA was reversely transcribed using the High-Capacity cDNA Reverse Transcription Kit. The following PCR program was used: 25 °C for 10 min, 37 °C for 120 min, 85 °C for 5 sec, 4 °C until ready for use. Samples were diluted in 30 µl of RNase free water. For cDNA testing, 2 µl cDNA was used with 18 µl PCR Mix which contains 2 µl Dream Taq buffer, 3.2 µl dNTPs, 1 µl of Fw and Rv primer (Table 2.5), 0.05 µl Dream Taq polymerase in 10.75 µl water. The following PCR program was used: 95 °C for 3 min, followed by 40 cycles of 95 °C for 5 sec and 60 °C for 10 sec, afterwards 4 °C until ready for use. Samples were run on 2% agarose gel. qPCR was performed using the Step One Plus Real-Time PCR System. qPCR Master Mix contains 0.6 µl forward (Fw) primer, 0.6 µl reverse (Rv) primer, 6 µl SYBR Green, 0.18 µl ROS dye and 2.62 µl DEPC water for each condition. The following PCR program was used: 95 °C for 3 min, followed by 40 cycle of 95 °C for 5 sec and 60 °C for 15 sec. Amplified products were detected with SYBR Green and relative quantification was performed against Y45F10D.4

Table 2.5 Primers for real-time PCR

Gene	Primer
<i>cyp-13a7</i>	Fw 5'-AAAAATGGCAATGGGACAAG-3'
	Rv 5'-AATACTTTGAATATCGGTAG-3'
<i>cyp-34a9</i>	Fw 5'-AGCAAGGCAGAACTTCCAA-3'
	Rv 5'-ACCTGTGCCCAAAGTGTTTC-3'
<i>cyp-14a1</i>	Fw 5'-CCTTTCTTGGGGTCTCATCA-3'
	Rv 5'-AAGTAGCGGCTTGGATTGAA-3'
<i>cyp-14a3</i>	Fw 5'-CAGGCACTGGAGACAAATCA-3'
	Rv 5'-GCAAAAGAGAATGGGGGATT-3'
<i>cyp-13a11</i>	Fw 5'-GCAAATTCTCGCCGTTGTAT-3'
	Rv 5'-TCGTCTCCTGATTCCCATCT-3'

<i>sod-1</i>	Fw 5'-GGCGATCTAGGAAATGTGGA-3'
	Rv 5'-CTTCTGCCTTGTCTCCGACT-3'
<i>sod-2</i>	Fw 5'-GGTCTCCAAAGGAAACGTCA-3'
	Rv 5'-GATCCGAAGTCGCTCTTAATTGC-3'
<i>sod-3</i>	Fw 5'-TCGGTTCCCTGGATAACTTG-3'
	Rv 5'-AAAGTGGGACCATTCTTCC-3'
Y45F10D.4	Fw 5'-GTCGCTTCAAATCAGTTCAGC-3'
	Rv 5'-GTTCTTGTCAAGTGATCCGACA-3'

2.2.2. Protein isolation

For protein sample isolation from *C. elegans*, worms were collected from three full plates and washed with M9 and pelleted by gravity, to remove the bacteria. After centrifugation (3000 rpm, 1 min), worm pellet was frozen in liquid nitrogen and stored at -80°C or used directly. Worm pellet was thawed on ice and 100 – 200 µl worm lysis buffer (see 2.7.2) was added, followed by sonication. Then worm debris was removed by centrifugation (12.000 rpm, 4°C, 10 min) and transferring the supernatant to a fresh tube. The protein sample was stored at -80°C or directly used.

2.2.3. Western blot

Protein concentration was measured by Bradford assay and 30 µg proteins were boiled for 10 min in SDS-PAGE sample loading buffer. Samples were loaded and separated on an 10-12% polyacrylamide gradient gels. Separated proteins were transferred onto nitrocellulose membranes. Protein loading was checked by Ponceau staining. Then membranes were washed in PBS or TBS + 0.1% Tween-20 (PBST or TBST) and blocked in 5% (wt/vol) dried nonfat milk in PBST or TBST, depending on the antibody. Membranes were incubated for two hours at 20°C or overnight at 4°C in corresponding blocking solution and primary antibodies (Table 2.6). Following three times washing in PBST or TBST for 5 min, membranes were incubated with fluorescent secondary antibodies in PBST or TBST for one hour. Secondary antibody signal was detected by using ECL western blotting solution, according to manufacturer's protocol and developed using X-ray film (Table 2.7).

Table 2.6 Primary antibodies used for western blot

Antibody	Company	Product number	Blocking solution	Dilution	Host
Monoclonal Anti-FLAG M2	Sigma-Aldrich	F1804	MPBST	1:1000	Mouse
Polyclonal GFP-Tag	OriGene Technologies Inc.	TP401	MTBST	1:5000	Rabbit
Monoclonal HSC70 (B-6)	Santa Cruz Biotechnology Inc.	sc-7298	MPBST	1:4000	Mouse

Table 2.7 Secondary antibodies used for western blot

Antibody	Company	Product number	Solution	Dilution
HRP linked anti-mouse IgG	Sigma-Aldrich	A9044	PBST/TBST	1:2000
HRP linked anti-rabbit IgG	Jackson Immuno-Research	706035148	TBST	1:2000

2.2.4. Shift assay

For protein sample isolation from *C. elegans*, worms were collected from five full plates and washed with PBS and pelleted by gravity, to remove the bacteria. Worms for the H₂O₂ condition were exposed to 10 mM for 15 min while gently shaking. All samples, except minimum (min) and maximum (max) shift samples, were washed with PBS containing 20 mM *N*-Ethylmaleinimid (NEM). Then these conditions were resuspended in 1 ml PBS-NEM, while min and max shift samples were resuspended in 1 ml PBS, and broken by tissue Lyser. Samples were centrifuged (20.000 rcf, 15 min, 4°C), supernatant was transferred and frozen in liquid nitrogen. Samples were thawed at RT and protein precipitation was performed with 8% (w/v) trichloroacetic acid (TCA) and 5% (w/v) TCA. Supernatant was removed and sample pellet was dissolved in Laemmli buffer containing 20 mM Tris(2-carboxyethyl)phosphine - hydrochlorid (TCEP). Min shift sample was treated with 20 mM NEM for 1 h at RT, while the other samples were treated with 20 mM mm(PEG)24 for 1 h at RT. Following steps were performed as described in 2.2.3 Western blot.

2.2.5 CO-IP and Pull down

For protein sample isolation from *C. elegans*, worms were collected from at least twenty full plates and washed with PBS and pelleted by gravity, to remove the bacteria. Worm pellet was frozen in liquid nitrogen and then thawed on ice. All handlings were performed on ice and all solutions were at 4°C, unless otherwise stated. Worms were lysed using modified RIPA buffer and incubation for 20 min. Then samples were sonicated for 6 rounds in the Bioruptor at 30/60 cycles. Consequently, samples were centrifuged at full speed and supernatant was collected. After equilibrating the flag-antibody-coupled magnetic beads with modified RIPA buffer, samples were incubated with the beads for 120 min on a rotator. Beads were captured with a magnetic rack and washed once with modified RIPA buffer, three times with wash buffer 1 and four times with wash buffer 2. For the digestion step, beads were resuspended in elution buffer, 50 ng trypsin was added and beads were incubated for 30 min at RT. Then, digestion buffer was added and samples were incubated for 30 min at RT. Supernatant was collected and samples were digested overnight with 50 ng LysC and 100 ng Trypsin at 37°C at 1000 rpm. Next day, samples were acidified with formic acid (FA) to final concentration of 1% FA and analysed by Mass Spectrometry by the CECAD/CMMC Proteomics Facility.

2.2.6. Site-directed mutagenesis

Site-directed mutagenesis was performed by using the QuickChange II XL Site-Directed Mutagenesis kit according to manufacturer's protocol. In summary, sample reaction was prepared by mixing 50 ng *pvha-6::klf-1-yfp;prab-3::mCherry;rol-6(sy1006)* construct, 10x reaction buffer, 125 ng of each primer (Table 2.8), 1 µl dNTP mix, 3 µl QuickSolution and 1 µl *PfuUltra* HF DNA polymerase in water and mutant strand synthesis was performed by thermal cycling using a Step One Plus Real-Time PCR System. The following PCR program was used: 95°C for 1 min, followed by 18 cycles of 95°C for 50 sec, 60°C for 50 sec and 68°C for 90 sec, afterwards 68°C for 7 min and 4 °C until ready for use. Digestion of template strand was performed by adding 1 µl *Dpn* I restriction enzyme to each sample and incubation at 37°C for 1 h. Transformation in XL10-Gold ultracompetent cells, as provided in the kit with the

mutated amplification construct by using cold-shock and grown in NZY⁺ broth. Amp treatment was used for transformation control.

Table 2.8 Primers for site-directed mutagenesis

Construct	Mutation	Primer
<i>pvha-6::klf-1::yfp</i>	C419>S	Fw 5'-CAAGAGGCTTCACCATAGCACACATCCGAAATTGC-3'
		Fw 5'-GCAATTTTCGGATGTGTGCTATGGTGAAGCCTCTTG-3'
<i>pvha-6::klf-1::yfp</i>	K411>A	Fw 5'-GAACCATCTGTGCGAGGCTTCACCATTCGC-3'
		Fw 5'-GCAATGGTGAAGCCTCGCGACAGATGGTTC-3'
<i>pvha-6::klf-1::yfp</i>	S190>A	Fw 5'-GGATAGATCAGTACATTTGGCACCGTCTTTTTTTCAACCA GG-3'
		Fw 5'-CCTGGTTGAAAAAAGACGGTGCCAAATGTACTGATCTA TCC-3'

2.3. Microscopy

General handling and observations of worms were performed on the Olympus KL 1500 compact stereomicroscope. During experiments animals were immobilized in 5 mM levamisole and mounted on 2% agarose pads. For visualizing GFP, either for nuclear localization or expression levels of *pcyp34a8::gfp*, an Axiolmager Z.1 epifluorescence microscope, equipped with a Hammamatsu camera and AxioVision software 4.8 was used. Nuclear localization was assayed with a 10x objective and exposure time of 6 sec. Expression levels of *pcyp34a8::gfp* were assayed with a 5x objective and exposure time of 1 sec. For visualizing BODIPY 498/503 levels and *grx::rogfp2* a Spinning Disc Confocal microscope from the CECAD Imaging facility was used. For visualizing *tomm20::rogfp2* a gSTED Superresolution and Confocal microscope from the CECAD Imaging facility was used. Images were analysed using ImageJ.

2.4. Statistical Analysis

A two-tailed unpaired Student's t-test was used to determine statistical significance, unless it was stated that an one-way ANOVA with Tukey post hoc test was used. All *p* values below 0.05 were considered significant: **p*<0.05, ***p*<0.01 and ****p*<0.001. Error bars were represented as standard error of the mean (SEM). All

statistical analysis and generation of figures/graphs were performed in GraphPad Prism 6. Lifespan data and statistical analysis are enlisted in Supplementary Table 1

2.5. Chemicals, equipment and biological materials

2.5.1. Chemicals and biological materials

All chemicals are enlisted in Table 2.9 and stored according to manufactures' protocol.

Table 2.9 Chemicals and supplier

Chemical	Supplier
N-Acetyl-L-cysteine (NAC)	Sigma-Aldrich, Seelze, Germany
Acrylamide Bisacrylamide 40% (37.5:1)	Roth, Karlsruhe, Germany
Agar	VWR International GmbH, Darmstadt, Germany
Agarose	Roth, Karlsruhe, Germany
Ammonium persulfate	Sigma-Aldrich, Seelze, Germany
Ampicillin	Sigma-Aldrich, Seelze, Germany
Antimycin A	Sigma-Aldrich, Seelze, Germany
L-Ascorbic acid (Vitamin C, Vit. C)	Sigma-Aldrich, Seelze, Germany
Auranofin	Sigma-Aldrich, Seelze, Germany
BODIPY 493/503	Thermo Scientific, Braunschweig, Germany
Bortezomib (Bor)	Sigma-Aldrich, Seelze, Germany
Bradford Reagent	Sigma-Aldrich, Seelze, Germany
Bromophenol blue	Merck, Darmstadt, Germany
Buthionine sulfoximine (BSO)	Sigma-Aldrich, Seelze, Germany
Calcium chloride	Merck, Darmstadt, Germany
Carbonylcyanide-4-(trifluoromethoxy) phenylhydrazone (FCCP)	Sigma-Aldrich, Seelze, Germany
Carmustine / BCNU	Sigma-Aldrich, Seelze, Germany
Chloroacetamide (CAA)	Sigma-Aldrich, Seelze, Germany
Chloroform	Merck, Darmstadt, Germany
Cholesterol 95%	Applchem, Darmstadt, Germany
Deoxynucleotides (dNTPs)	Sigma-Aldrich, Seelze, Germany
Dimethyl sulfoxide (DMSO)	Sigma-Aldrich, Seelze, Germany
Dipotassium hydrogen phosphate	Merck, Darmstadt, Germany
Disodium phosphate	Sigma-Aldrich, Seelze, Germany
Dithiothreitol (DTT)	Sigma-Aldrich, Seelze, Germany

DNA-free™, DNase and removal	Ambion, Life Technologies, Karlsruhe, Germany
Dream Taq buffer	Promega, Wisconsin, USA
Dream Taq polymerase	Promega, Wisconsin, USA
ECL western blot solution	GE Healthcare, Munich, Amerham
Ethanol	Applichem, Darmstadt, Germany
Ethylenediaminetetraacetic acid (EDTA)	Sigma-Aldrich, Seelze, Germany
(anti-) Flag M2 magnetic beads	Sigma-Aldrich, Seelze, Germany
Formic acid	Sigma-Aldrich, Seelze, Germany
Gene Ruler DNA ladder mix	Thermo Scientific, Braunschweig, Germany
Glycerol	Sigma-Aldrich, Seelze, Germany
Glycine	Applichem, Darmstadt, Germany
HEPES	Applichem, Darmstadt, Germany
High-Capacity cDNA Reverse Transcription kit	Applied Biosystems, Massachusetts, US
Hydrochloric acid	Applichem, Darmstadt, Germany
Hydrogen peroxide (H ₂ O ₂)	Sigma-Aldrich, Seelze, Germany
IPTG	Applichem, Darmstadt, Germany
LysC protease	Thermo Scientific, Braunschweig, Germany
Levamisole (-hydrochloride)	Merck, Darmstadt, Germany
Magnesium chloride	Sigma-Aldrich, Seelze, Germany
Magnesium sulphate anhydrous	Applichem, Darmstadt, Germany
Malonate	Sigma-Aldrich, Seelze, Germany
Methanol	Applichem, Darmstadt, Germany
MitoTracker CH-H ₂ -XROS	Invitrogen, Karlsruhe, Germany
MitoTracker Deep Red	Invitrogen, Karlsruhe, Germany
mm(PEG)24 Methyl-PEG-Maleimide reagent	Sigma-Aldrich, Seelze, Germany
Monopotassium phosphate	Sigma-Aldrich, Seelze, Germany
N-Ethylmaleimide (NEM)	Thermo Scientific, Braunschweig, Germany
Nitrocellulose membranes	GE Healthcare, UK
Nitrogen (liquid)	Linde, Pullach, Germany
Non-fat Dried Milk powder	Sigma-Aldrich, Seelze, Germany
NP-40	Applichem, Darmstadt, Germany
Nystatin powder	Sigma-Aldrich, Seelze, Germany
Page Ruler Prestained Protein Ladder mix	Thermo Scientific, Braunschweig, Germany
Pepton	Merck, Darmstadt, Germany
Phosphatase inhibitor cocktail tablets (PhosStop)	Roche, Basel, Switzerland
Phosphate buffered saline (PBS)	Applichem, Darmstadt, Germany
Ponceau S	Sigma-Aldrich, Seelze, Germany
Protease Inhibitor Cocktail (PIC) tablets	Roche, Basel, Switzerland

Protease K	Applichem, Darmstadt, Germany
S3QEL-2	Cayman Chemical, Michigan, USA
Sodium chloride (NaCl)	Sigma-Aldrich, Seelze, Germany
Sodium (Na)-deoxycholate	Applichem, Darmstadt, Germany
Sodium dodecyl sulphate (SDS)	Applichem, Darmstadt, Germany
Sodium Fluoride (NaF)	Applichem, Darmstadt, Germany
Sodium hypochlorite 14%	VWR International GmbH, Darmstadt, Germany
Sodium hydroxide	Sigma-Aldrich, Seelze, Germany
SYBR Green (Brilliant III Ultra-Fast SYBR Green qPCR Master Mix)	Agilent Technologies, California, US
Tetracycline Hydrochloride (Tet)	Applichem, Darmstadt, Germany
Tetramethylethylenediamine (TEMED)	Sigma-Aldrich, Seelze, Germany
Tris(2-carboxyethyl)phosphine-hydrochloride (TCEP)	Thermo Scientific, Braunschweig, Germany
Trizma Base (Tris)	Sigma-Aldrich, Seelze, Germany
Trizol	Invitrogen, Karlsruhe, Germany
Trypsin	VWR International GmbH, Darmstadt, Germany
Trypton	Applichem, Darmstadt, Germany
Tween-20	VWR International GmbH, Darmstadt, Germany
UltraPure™ DEPC-Treated water	Thermo Scientific, Braunschweig, Germany
Urea	Sigma-Aldrich, Seelze, Germany
X-ray film super RX, FUJI medical	FUJIFILM, Tokyo, Japan
Yeast extract granulate for	Merck, Darmstadt, Germany
β-mercaptoethanol	Sigma-Aldrich, Seelze, Germany

2.5.2. Buffers and solutions

All compounds used for the preparation of these buffers and solutions were enlisted in Table 2.10.

Table 2.10 Buffer and solutions

Bleaching solution	Compound	Concentration / amount
For 7.0 ml sample	Sodium hypochlorite 14%	714 µl
	Sodium hydroxide 5 M	1.0 ml
CaCl₂	Compound	Concentration / amount
For 200 ml	CaCl ₂	29.4 g

	H ₂ O	Up to 200 ml
Cholesterol	Compound	Concentration / amount
For 200 ml	Cholesterol	1 g
	Ethanol	Up to 200 ml
dNTP solution	Compound	Concentration / amount
	Each dNTP	1.25 mM
	H ₂ O	9.5 ml
Digestion buffer	Compound	Concentration / amount
For 1 ml	Urea	2 M
pH 8.0	HEPES	50 mM
	Chloroacetamide (CAA)	50 mM
	H ₂ O	1 ml
Elution buffer	Compound	Concentration / amount
For 1 ml	Urea	2 M
pH 8.0	HEPES	50 mM
	DTT	5 mM
	H ₂ O	1 ml
Freezing solution 2x	Compound	Concentration / amount
For 500 ml	NaCl	2.92 g
	KH ₂ PO ₄	3.4 g
	Glycerol	30% (v/v)
	NaOH 1M	2.8 ml
	H ₂ O	Up to 500 ml
After autoclave	MgSO ₄ 1M	150 µl
KPI buffer	Compound	Concentration / amount
For 50 ml	K ₂ HPO ₄	1 M
pH 6.0	KH ₂ PO ₄	1 M
	H ₂ O	Up to 50 ml
Laemmli buffer	Compound	Concentration / amount
For 50 ml	Tris	60 mM
pH 6.8	SDS	1 g
	Glycerol	10%
	Bromophenol blue	0.02%
	H ₂ O	Up to 50 ml
LB agar	Compound	Concentration / amount
For 1 L	Trypton	10 g
	Yeast Extract	10 g
	NaCl	5 g
	Agar	10 g

	H ₂ O	Up to 1 L
LB medium	Compound	Concentration / amount
For 1 L	Yeast Extract	
	H ₂ O	Up to 1 L
Lysis buffer	Compound	Concentration / amount
For 500 ml	Tris-HCL, pH 7.4	50 mM
	NP-40	5 ml
	Na-deoxycholate	2.5 g
	SDS	0.5 g
	NaCl	150 mM
	EDTA	2 mM
	NaF	1.05 g
	H ₂ O	Up to 500 ml
Freshly added before use	Protease inhibitor cocktail	1x
M9 buffer	Compound	Concentration / amount
For 1 L	K ₂ HPO ₄	3 g
	Na ₂ HPO ₄	6 g
	NaCl	6 g
	H ₂ O	Up to 1 L
After autoclave	MgSO ₄	1 mM
Modified RIPA buffer	Compound	Concentration / amount
For 50 ml	Tris	50 mM
pH 7.4	NaCl	150 mM
	Sodium-deoxycholate	0.25 %
	SDS	0.1 %
	NP-40	1 %
	H ₂ O	Up to 50 ml
Freshly added before use	Protease inhibitor cocktail	1x
	PhosStop	1x
NGM agar	Compound	Concentration / amount
For 1 L	Pepton	2.5 g
	NaCl	3 g
	Agar	17 g
	H ₂ O	Up to 1 L
After autoclave	Cholesterol	1 ml
	CaCl ₂	1 ml
	MgSO ₄	1 ml
	KPI buffer	25 ml
	Nystatin	2.5 ml

	Ampicilin	2 ml (50 µg/ml)
	Tetracycline	1 ml (25 µg/ml)
	IPTG	1 mM
PBS buffer 10x	Compound	Concentration / amount
For 1 L	PBS	2.5 g
	H ₂ O	Up to 1 L
Running buffer 10x	Compound	Concentration / amount
2 L	Tris	302 g
	Glycine	142 g
	SDS	10 g
	H ₂ O	Up to 2 L
S Basal	Compound	Concentration / amount
For 1 L	NaCl	5.9 g
	H ₂ O	Up to 1 L
After autoclave	KPI buffer	50 ml
	Cholesterol	1 ml
SDS-PAGE sample loading buffer	Compound	Concentration / amount
50 ml	Tris	50 mM
pH 6.8	SDS	2%
	Glycerol	10%
	β-mercaptoethanol	1%
	EDTA	12.5 mM
	Bromophenol blue	0.02%
	H ₂ O	Up to 50 ml
Separating buffer	Compound	Concentration / amount
300 ml	Tris	54.46 g
pH 8.8	H ₂ O	Up to 300 ml
Single worm lysis buffer	Compound	Concentration / amount
10 ml	Tris	30 mM
pH 8.8	EDTA	8 mM
	NaCl	100 mM
	NP-40	0.7%
	Tween	0.7%
	H ₂ O	Up to 10 ml
Freshly added before use	Proteinase K	100 µg/ml
Stacking buffer	Compound	Concentration / amount
300 ml	Tris	18.171 g
pH 6.8	H ₂ O	Up to 300 ml

TBS buffer 10x	Compound	Concentration / amount
1 L	Tris	24 g
pH 7.5	NaCl	88 g
	H ₂ O	Up to 1 L
Transfer buffer 10x	Compound	Concentration / amount
2 L	Tris	60.6 g
	Glycine	288,2 g
	H ₂ O	Up to 2 L
Transfer buffer 1x	Compound	Concentration / amount
1 L	Transfer buffer 10x	100 ml
	Methanol	200 ml
	H ₂ O	Up to 1 L
Tris-HCL, pH 7.4	Compound	Concentration / amount
50 ml	Tris	6.057 g
pH 7.4	H ₂ O	Up to 50 ml
Wash buffer 1	Compound	Concentration / amount
50 ml	Tris	50 mM
pH 7.4	NaCl	150 mM
	Glycerol	5 %
	NP-40	0.05 %
	H ₂ O	Up to 50 ml
Freshly added before use	Protease inhibitor cocktail	1x
	PhosStop	1x
Wash buffer 2	Compound	Concentration / amount
50 ml	Tris	50 mM
pH 7.4	NaCl	150 mM
	H ₂ O	Up to 50 ml
Freshly added before use	Protease inhibitor cocktail	1x
	PhosStop	1x

2.5.3. Commercials and Assay kits

Commercials and Assay kits are enlisted in Table 2.11. They are used and stored according to manufactures' protocol, otherwise it was stated.

Table 2.11 Commercials and Assay kits

Commercials and Assay kits	Supplier
High capacity cDNA Reverse Transcription kit	Thermo Fisher, USA

LightRun DNA sequencing Eurofins Genomics	Eurofins Scientific, Luxembourg
QuickChange II XL Site-Directed Mutagenesis kit	Agilent Technologies, California, USA
Turbo DNA-free™ kit	Thermo Fisher, USA

2.5.4. Equipment

Equipment was enlisted in Table 2.12 and used according to manufactures' protocol, otherwise it was stated

Table 2.12 Equipment

Equipment	Supplier
Axiolmager Z.1 epifluorescence microscope, equipped with a Hammamatsu camera	Carl Zeiss Microscopy Deutschland GmbH, Koln, Germany
Biosorter Instrument	Union Biometrica
Bioruptor ^R Sonication device	Diagenode, Liege, Belgium
Eppendorf InjectMan N1z injection pump	Eppendorf, Hamburg, Germany
Eppendorf FemtoJet microinjector	Eppendorf, Hamburg Germany
gSTED Superresolution and Confocal microscope	Leica Microsystems GmbH, Wetzlar, Germany
NanoDrop 8000 spectrophotometer	Thermo Fisher, USA
Olympus KL 1500 compact stereomicroscope	Olympus Corporation, Tokyo, Japan
Spinning Disc Confocal microscope	PerkinElmer, Massachusetts, USA
Step One Plus Real-Time PCR System	Applied Biosystems, Massachusetts, USA
Zeiss Observer A.1 microscope equipped with AxioCam ERc5S camera	Zeiss, Oberkochen, Germany

2.5.5. Software

Software was enlisted in Table 2.13 and used according to manufactures' protocol, otherwise it was stated

Table 2.13 Software

Software	Supplier / developer(s)
ApE – plasmid Editor	M. Wayne Davis
AxioVision	Carl Zeiss Microscopy, USA
BioRender	BioRender.com
Fiji/ImageJ2	National Institutes of Health. Johannes Schindelin, Ignacia Arganda-Carreras, Albert

	Cardona, Mark Longair, Benjamin Schmid, and others
FlowPilot™	Union Biometrica
GraphPad Prism 6	GraphPad Software, USA
Mendeley	Mendeley company, London, UK
Microsoft Excel 2016 for Mac	Microsoft Corporation, USA
Microsoft Powerpoint 2016 for Mac	Microsoft Corporation, USA
Microsoft Word 2016 for Mac	Microsoft Corporation, USA
Volocity	PerkinElmer, Massachusetts, USA

3. Results

3.1 ROS is mediating KLF-1 activation

In order to identify the signal that is behind the activation of KLF-1-induced longevity, we analysed the KLF-1 expression pattern in WT and *isp-1;ctb-1* mitomutant. To assay the KLF-1 expression pattern, our lab designed a reporter strain with KLF-1 tagged to yellow fluorescent protein (YFP) (Herholz et al. 2019). As KLF-1 is mainly expressed in the gut (Herholz et al. 2019), we designed *klf-1::yfp* under the control of gut promoter *vha-6*. As our lab has shown that KLF-1 is required during adulthood for longevity, not during larval development, we focused on D1. D1 WT worms exhibit mainly cytosolic *klf-1-yfp* expression, whereas in D1 *isp-1;ctb-1* worms, the KLF-1 localizes mainly in the nucleus (Fig. 3.1).

As mitochondrial dysfunction results in increased oxidative stress, which has also been shown for mitomutants, we evaluated WT worms with PQ or AA treatment to further investigate the mode of KLF-1 nuclear translocation. PQ induces oxidative stress by undergoing cyclic reduction-oxidation reactions at ETC complex I (Cochemé and Murphy 2008; Sampayo, Olsen, and Lithgow 2003; N. Ishii 2000). AA induces oxidative stress by binding to the Qi site of cytochrome c and inhibiting the oxidation of ubiquinone and therefore disrupting the proton flow

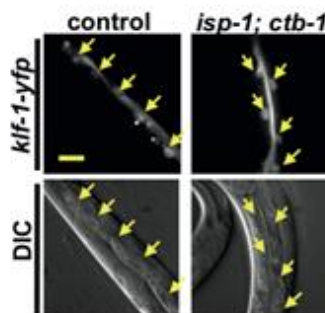


Fig. 3.1 *isp-1;ctb-1* animals have mainly nuclear localized KLF-1

Reprehensive fluorescence and Differential interference Contrast (DIC) images of *klf-1* expression in WT and *isp-1;ctb-1* worms expressing *pvha-6::klf-1::YFP*. Arrows represent *klf-1-yfp* positive gut nuclei. Scale bar is 200 μ M. Data and figures obtained by Herholz et al. 2019. Figure is modified.

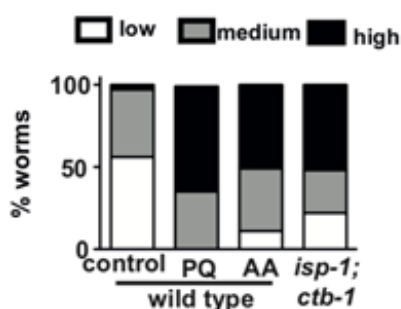


Fig. 3.2 Oxidative stress activates and translocate KLF-1 to the nucleus.

Quantification of the amount of KLF-1 nuclear localization in WT and *isp-1;ctb-1* worms upon control, 0.1mM PQ and 1 μ M Antimycin A (AA) at day 1 of adulthood. Worms were assayed by number of KLF-1-positive nuclei and categorized by “low” as less than 2 nuclei, “medium” as 3-10 nuclei and “high” as higher than 10 nuclei per worm. $n=20$ animals per condition. Data and figures obtained by Herholz et al. 2019.

(Slater 1973; Rieske et al. 1967; Melo and Ruvkun 2012). Both treatments result in increased free $O_2^{\cdot -}$ synthesis. Interestingly, low amount of PQ has been shown to induce longevity by similar mechanisms as mitomutants (Yang and Hekimi 2010a). Nuclear localization of *klf-1-yfp* was increased in WT worms under oxidative stress-inducers PQ and AA (Fig. 3.2). Remarkably, we could show that WT worms have increased lifespan induced by oxidative stress, which is only suppressed by KLF-1 depletion during adulthood (Fig. 3.3) (Herholz et al. 2019). Altogether, these suggest that KLF-1 in *isp-1;ctb-1* animals have a similar nuclear translocation mechanism as the WT animals under oxidative stress.

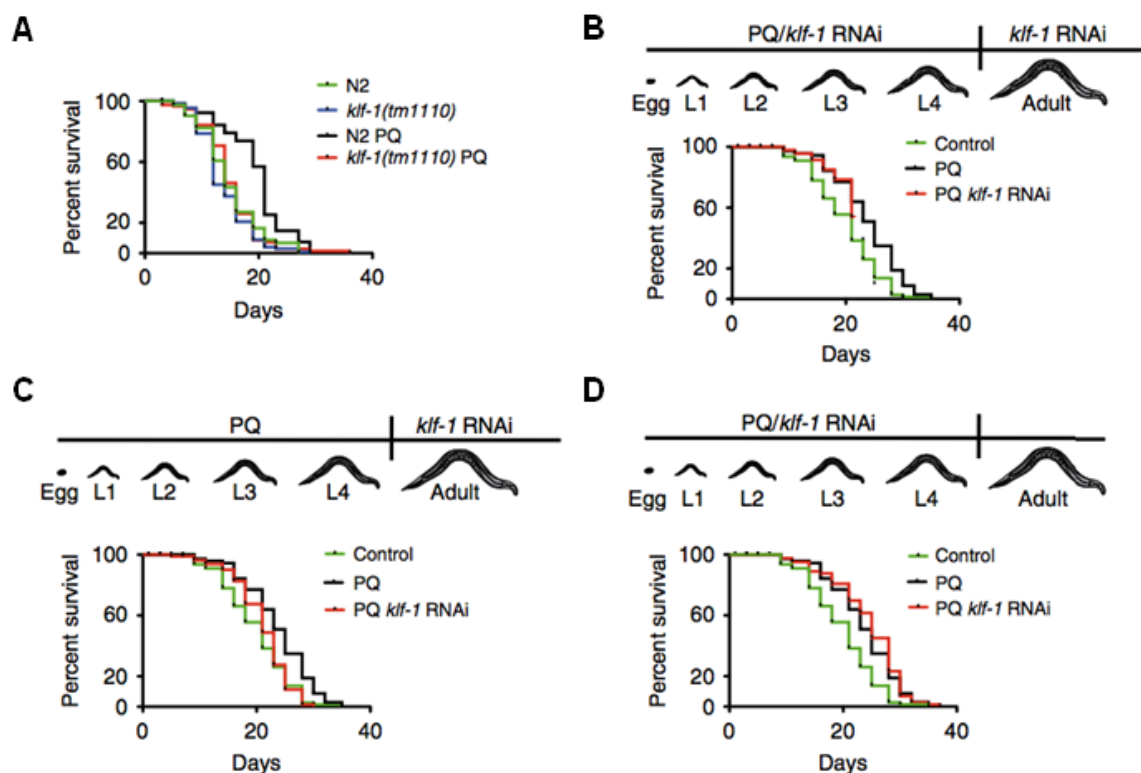


Fig. 3.3 Oxidative stress-induced longevity is inhibited by KLF-1 suppression during adulthood

Lifespan assays on worms exposed to 0.1mM paraquat (PQ) and *klf-1* RNAi. **A)** WT and *klf-1(tm1110)* worms grown whole life on PQ. **B-D)** WT worms grown until L4 on PQ and then were transferred to PQ-free plates. Worms were exposed to *klf-1* RNAi **B)** whole life. **C)** adulthood. **D)** larval stages. n=200 animals per condition. Data and figures obtained by Herholz et al. 2019.

Next, we questioned whether oxidative stress indeed plays a role in KLF-1 nuclear translocation in *isp-1;ctb-1* mutant. As oxidative stress is a result of imbalance between ROS production and accumulation of intracellular levels of ROS (Pizzino et al. 2017), we measured mtROS production. L4 *isp-1;ctb-1* animals demonstrated increased mtROS (Fig. 3.4.A). Interestingly, during adulthood *isp-1;ctb-1* animals showed less mtROS, supporting the described mitohormetic mechanism (Yun and Finkel 2014). To determine if this decreased mitochondrial ROS was not caused by reduced mitochondria, we also investigated mitochondrial (mito) mass. We observed an increased mito mass on D1 WT and *isp-1;ctb-1* animals, which was independent of KLF-1 (Fig. 3.4.B). Thus, ROS per mitochondria was increased in L4 *isp-1;ctb-1* and decreased in D1 *isp-1;ctb-1* animals in comparison to WT animals (Fig. 3.4.C).

To further explore whether oxidative stress plays a role in the KLF-1 nuclear translocation, we used NAC and Vit C, which both acts as antioxidants to inhibit the

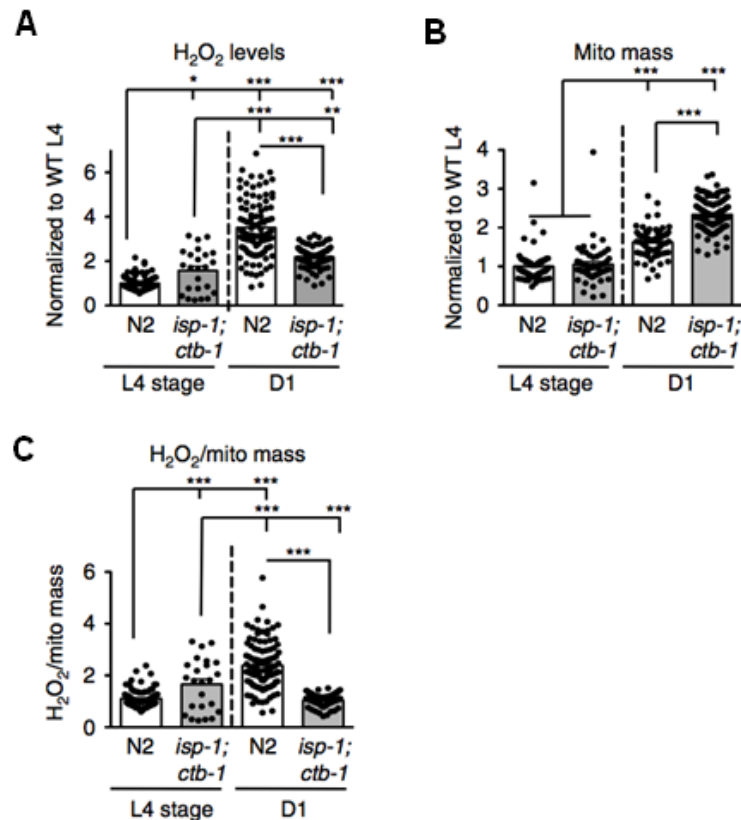


Fig. 3.4 *Isp-1;ctb-1* animals showed elevated H₂O₂ levels during L4

L4 and D1 WT and *isp-1;ctb-1* animals were exposed to EV and *klf-1* RNAi and stained with Mitotracker to measure mitochondrial ROS levels and mito mass. **A)** ROS levels visualized by Mitotracker Red CM-H₂XRos staining. **B)** Mito mass visualized by Deep Red Mitotracker staining. **C)** Ratio between H₂O₂ levels and mitochondrial mass. n=60 animals per condition. Data were normalized on L4 N2 stage and are presented as mean ± SEM. ***p<0.001, *p<0.005, one-way ANOVA with Turkey post hoc test. Data and figures obtained by Herholz et al. 2019. Figure is modified.

oxidative stress (Patananan et al. 2015; Desjardins et al. 2017; Yang and Hekimi 2010a). From now on, NAC and Vit C treatment will be referred to as antioxidant treatment. To determine if antioxidant treatment was able to reduce the number of oxidative stress-induced KLF-1-positive nuclei, we treated WT worms either with NAC or Vit C from egg stage. When the animals reached L4, we exposed them to 1 μM AA treatment and scored the KLF-1-positive nuclei on D1. The number of KLF-1-positive nuclei was decreased upon both antioxidant treatments (Fig. 3.5.A). Vit C treatment was able to clearly decrease KLF-1 presence in the nuclei to WT control levels, whereas NAC treatment would even further decrease the number of KLF-1-positive nuclei compared to WT control. Next, we investigated if the antioxidant treatment could also prevent the increased KLF-1-positive nuclei in *isp-1;ctb-1* mutant. Again, both

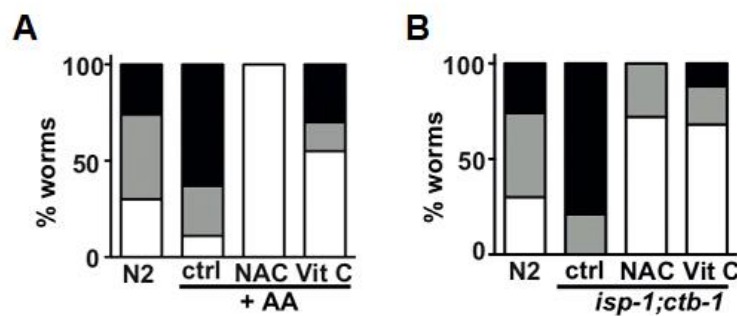


Fig. 3.5 Antioxidant treatment abolishes oxidative stress-induced KLF-1 nuclear localization.

Quantification of amount of KLF-1 nuclear localization upon control, 10mM NAC or 10mM Vit C treatment. **A)** WT animals treated with 1 μ M AA. **B)** *isp-1;ctb-1* animals. n=20 animals per condition. Figures obtained from Herholz et al. 2019.

antioxidant treatments were able to strongly reduce the number of KLF-1-positive nuclei in *isp-1;ctb-1* animals (Fig. 3.5.B). Collectively, these results clearly demonstrate that KLF-1 nuclear translocation in *isp-1;ctb-1* worms are caused by ROS signalling.

3.2 L3/L4-dependent ROS signalling is required for KLF-1 nuclear localization

Next, we wanted to elucidate when the oxidative stress signalling is required during the *C. elegans* lifespan to induce KLF-1 signalling cascade. We previously showed that KLF-1 nuclear translocation was exclusively needed during adulthood in the long lived *isp-1;ctb-1* mitomutant (Herholz et al. 2019). Remarkably, RNAi suppression of various ETC subunits during larval stages was proposed to induce longer lifespan (Dillin et al. 2002). This supports our observation in *isp-1;ctb-1* worms that clearly demonstrate increased mitochondrial ROS level during L4 (Fig. 3.4).

To determine when the ROS signal is required for the KLF-1-nuclear translocation in *isp-1;ctb-1* animals, we inhibited the ROS production of complex III during all larval stages and from late L3 by treatment with S3QEL-2 (Watson et al. 2021; Orr et al. 2015). S3QEL-2 is a selective inhibitor of the mitochondrial complex III Q_o site (Fig. 1.5) (Orr et al. 2015). Here, we show that upon inhibition of ROS production at complex III, the number of KLF-1-positive nuclei was steadily decreased in *isp-1;ctb-1* mutant (Fig. 3.6). Interestingly, inhibition from late L3 showed no altered number of KLF-1-positive nuclei (Fig. 3.6). This suggests that complex III-produced

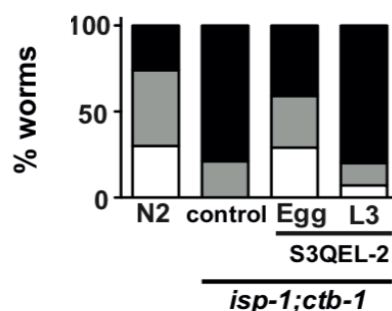


Fig 3.6 Complex III-ROS-production site inhibitor S3QEL-2 blocks KLF-1 nuclear localization during larvae stages

WT and *isp-1;ctb-1* worms were assayed for KLF-1 nuclear localization upon control or in the presence of 100 μ M S3QEL-2. Worms were treated either from egg stage or larvae L3 development stage and assayed at day 1 of adulthood. n=20 animals per condition. Figures obtained from Herholz et al. 2019.

ROS is needed before late L3 to translocate KLF-1 to the nucleus.

To further establish at which developmental stage the ROS signal is required for the KLF-1 nuclear translocation, we assayed the detoxification capacity of the animals. Upon KLF-1 nuclear translocation, CYPs and consequently detoxification capacity is activated (Herholz et al. 2019). To assay the detoxification capacity, we exposed WT and *isp-1;ctb-1* animals to high levels of H_2O_2 , which can induce damage to proteins via oxidative stress. These damaged proteins can be cleared by CYPs, which therefore correlates in H_2O_2 stress resistance. First, we exposed WT to AA, which translocates KLF-1 to the nucleus. We could demonstrate a significant increase of H_2O_2 stress resistance when worms were treated during L3 and L4 (Fig. 3.7.A). However, treatment during either L3 or L4 was insufficient to induce increased stress resistance. Thus, the KLF-1 nuclear translocation is L3 and L4 signal dependent. Second, we investigated *isp-1;ctb-1* animals upon S3QEL-2 treatment. We could confirm that whole larvae treatment decreases the increased H_2O_2 stress resistance seen in *isp-1;ctb-1* control (Fig. 3.7.B). Moreover, we could show that S3QEL-2 treatment only during L3 till D1 was enough to largely decrease the H_2O_2 stress resistance. Collectively, these data show that ROS signal during early L3 until young adults is required for the KLF-1 nuclear translocation.

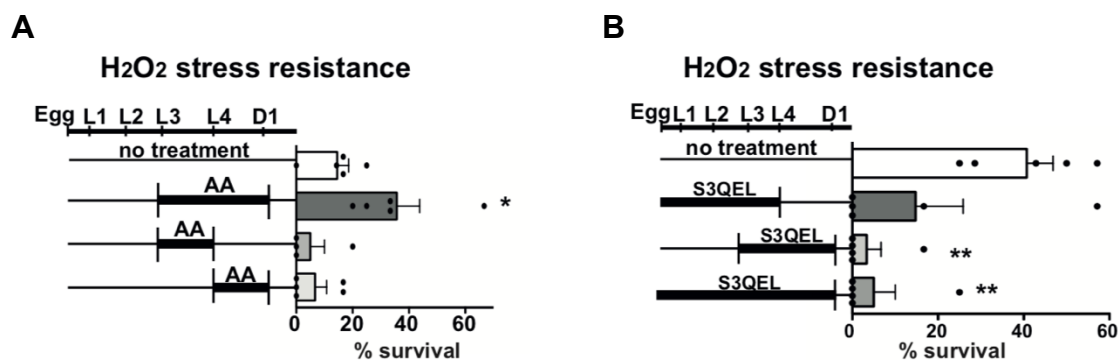


Fig 3.7 Redox signal is required during L3/L4

Animals were treated with 20 mM H₂O₂ at Day 1 and survival was analysed 4 h after treatment. **A)** WT worms were treated with 2 μ M AA at specific larvae stages. **B)** *isp-1;ctb-1* worms were treated with 100 μ M S3QEL-2 at specific larvae stages. Data are presented as mean \pm SEM. * p <0.05 and ** p <0.01, Student's T-test. n =100 animals per condition. Data and figures obtained by Herholz et al. 2019.

3.3 KLF-1 nuclear translocation is induced by mitochondrial produced ROS

After confirming that ROS translocates KLF-1 to the nucleus in our *isp-1;ctb-1* animals, we asked ourselves whether only complex III-derived ROS could translocate KLF-1 to the nucleus? As it was previously shown that mild mitochondrial dysfunction of some MRC subunits results in extended lifespan (Dillin et al. 2002; Tsang and Lemire 2002; C. Xu et al. 2018), we performed a screen to evaluate which specific mild mitochondrial dysfunction would induce KLF-1 nuclear translocation.

We exposed WT animals to either chemical or genetic inhibition of specific MRC subunits or we decreased the membrane potential (Table 3.1). To induce mild complex

Table 3.1. Overview of drugs and RNAi used for inducing mild mitochondrial dysfunction

Overview of used drugs (chemical inhibition) and RNAi (genetic inhibition) and their respectively inhibition site.

	Complex I	Complex II	Complex III	Complex IV	ATP synthase	Membrane potential
Chemical inhibition	Rot mitoPQ	Malonate	AA Myxo			FCCP
Genetic inhibition	<i>nuo-2</i>		<i>cyc-1</i>	<i>cco-1</i>	<i>atp-5</i>	

I dysfunction, we used 100 nM Rotenone and 5 μ M mitoPQ and *nuo-2* RNAi (N. Li et al. 2003; Sherer et al. 2003). Rotenone inhibits the transfer of electrons from the iron-sulphur subunits to ubiquinone, resulting in incomplete electron transfer to oxygen and ROS production (N. Li et al. 2003; Sherer et al. 2003; Robb et al. 2015; Grad and Lemire 2004). MitoPQ is a mitochondrial matrix-targeted redox cyler, which induces superoxide at the flavin site of complex I (Robb et al. 2015). Mild complex II dysfunction was induced by exposing the worms to 25 mM Malonate which is a competitive inhibitor of succinate dehydrogenase (Gutman 1978; Dervartanian and Veeger 1964; Chouchani et al. 2014). For complex III dysfunction, worms were treated with 2 μ M AA and 50 μ M Myxothiazol and *cyc-1* RNAi (Davoudi et al. 2014; Gerth et al. 1980; Slater 1973; Butler et al. 2010). Myxothiazol binds at the Qo site and is a competitive inhibitor of ubiquinol. *Cyc-1* is the *C. elegans* homolog of cytochrome C. Both suppressions block the electron transfer flow, either to the Rieske Iron-Sulfur complex or to the complex IV (Dillin et al. 2002). To induce complex IV or ATP synthase dysfunction, worms were treated with either *cco-1* or *atp-5* (ATP synthase subunit-5) RNAi (Bennett, Wende, et al. 2014; Dillin et al. 2002; Yoneda et al. 2004; Nagro et al. 2014; C. Xu et al. 2018). Finally, the role of membrane potential was evaluated by treatment with 5 μ M FCCP, an uncoupler agent which transports protons across the mitochondrial inner membrane (Benz and McLaughlin 1983) and therefore decreases the proton gradient.

So, to determine the effect of the different drug treatments, L4 WT animals were transferred to NGM plates containing different drugs. D1 animals were imaged and number of KLF-1-positive nuclei was scored (Fig. 3.8.A). Upon treatment with rotenone, mitoPQ, AA and myxothiazol, the number of KLF-1-positive nuclei was strongly increased (Fig. 3.8.B). Whereas treatment with malonate and FCCP were unable to induce KLF-1 nuclear translocation. Thus, drugs that induce mild dysfunction of complex I and complex III seem to result in KLF-1 nuclear translocation. Next, we investigated the effect of the different MRC RNAi. We grew the animals on plates with either control, *nuo-2*, *cyc-1*, *cco-1* or *atp-5* RNAi and scored them on D1. Corresponding with the drug treatment, genetic inhibition of complex I and complex III by *nuo-2* and *cyc-1* RNAi, respectively, increased the number of KLF-1-positive nuclei (Fig 3.8.C), whereas *atp-5* RNAi did not induce KLF-1 nuclear translocation. Curiously, also *cco-1* suppression translocated KLF-1 to the nucleus. It was described that complex IV could produce ROS (Reichart et al. 2019; Adam-Vizi 2005; Kadenbach 2021). Taken together, our results strongly suggest that mild suppression of

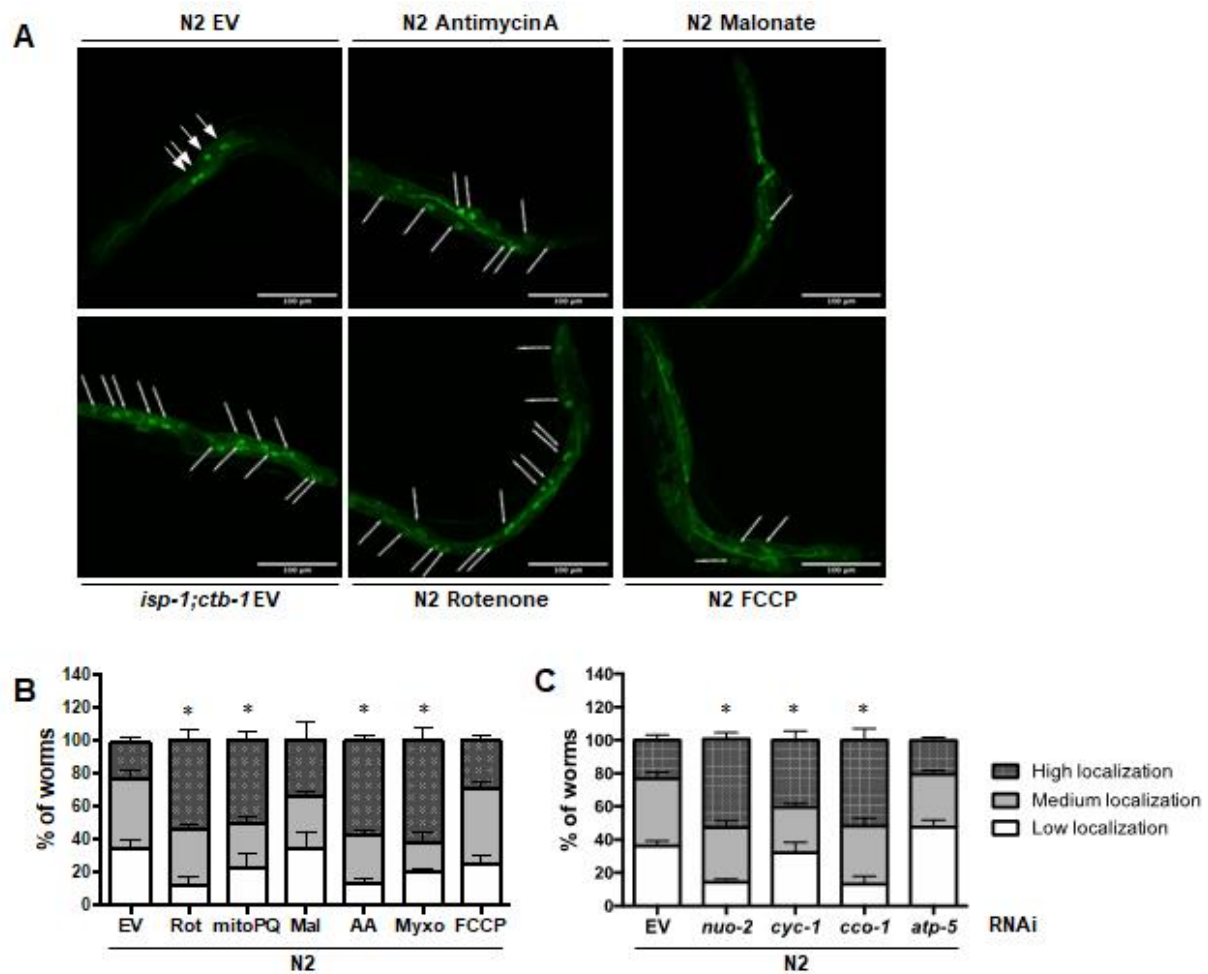


Fig 3.8 ROS-producing ETC complexes are responsible for KLF-1 nuclear localization.

Number of KLF-1-positive nuclei in one-day-old WT and *isp-1;ctb-1* animals were scored upon either chemical inhibition or genetic inhibition of the electron transport chain complexes, ATP synthase or mitochondrial membrane potential. For chemical inhibition treatment, worms were transferred during L4 on NGM plates containing drugs. The drug concentrations used were 100 nM Rotenone (Rot), 5 μ M mitoparaquat (mitoPQ), 25 mM Malonate (Mal), 2 μ M AA, 10 μ M myxothiazol (Myxo) or 5 μ M FCCP. For genetic inhibition, worms were bleached on NGM plates with L4440, *nuo-2*, *cyc-1*, *cco-1* or *atp-5* RNAi. **A)** Representative pictures of KLF-1 expression in WT and *isp-1;ctb-1* worms upon either drugs or RNAi. Arrows represent KLF-1-positive nuclei. **B)** Quantification of amount of KLF-1 nuclear localization in WT and *isp-1;ctb-1* worms upon suppressions. $n=30$ worms per condition. $*p<0.05$, Student's T-test. Modified from Hermeling et al. 2022.

mitochondrial complexes I, III and IV, which are responsible for ROS production, can translocate KLF-1 to the nucleus, whereas suppression of complex V or membrane potential could not (Q. Chen et al. 2003; Kowaltowski et al. 2009; Reichart et al. 2019).

Next, as suppression of both ROS production sites complex I and III were able to translocate KLF-1 to the nucleus, we wanted to investigate whether mild

suppression of other ROS production sites may also result in KLF-1 nuclear translocation. Whereas mitochondria are the prime source of endogenous ROS in the cell, at least two other organelles are also able to produce ROS, namely peroxisomes and ER (Del Río and López-Huertas 2016; Banerjee et al. 2011). Peroxisomal ROS is mainly produced by β -oxidation of very long chain fatty acids (Kakimoto et al. 2015; Handler and Thurman 1987). As this is one of the main functions of peroxisomes, this organelle has an elaborated antioxidant machinery to respond to elevated ROS levels. The antioxidant response in peroxisomes depends on SODs, PRDX, GPX, NADPH-generating dehydrogenases and catalase (Tiew, Sheahan, and Rose 2015; Pascual-Ahuir, Manzanares-Estreder, and Proft 2017). ER-derived ROS is closely linked to ER protein-folding homeostasis (Banerjee et al. 2011; Zeeshan et al. 2016). During the protein-folding process, disulphide bonds are formed by oxidation of thiol groups on cysteine of peptides. This results in H_2O_2 production during ER stress, which may lead to H_2O_2 accumulation. As peroxisomal H_2O_2 is mainly controlled by detoxification capacity of catalase (Cogoni and Macino 1999), we downregulated catalase with *ctl-1* and *ctl-2* RNAi to induce elevated H_2O_2 levels in WT animals (Fig. 3.9.A). Interestingly, upon *ctl-1* RNAi WT animals showed an increased number of KLF-1-positive nuclei whereas *ctl-2* or peroxisomal assembly factor 5 (*prx-5*) RNAi showed no significant difference to WT control. To evaluate the role of ER-derived ROS, we induced ER stress in WT worms by using 50 μ M tunicamycin, an inhibitor of biosynthesis of N-linked glycans (Banerjee et al. 2011). Tunicamycin treatment has been shown to

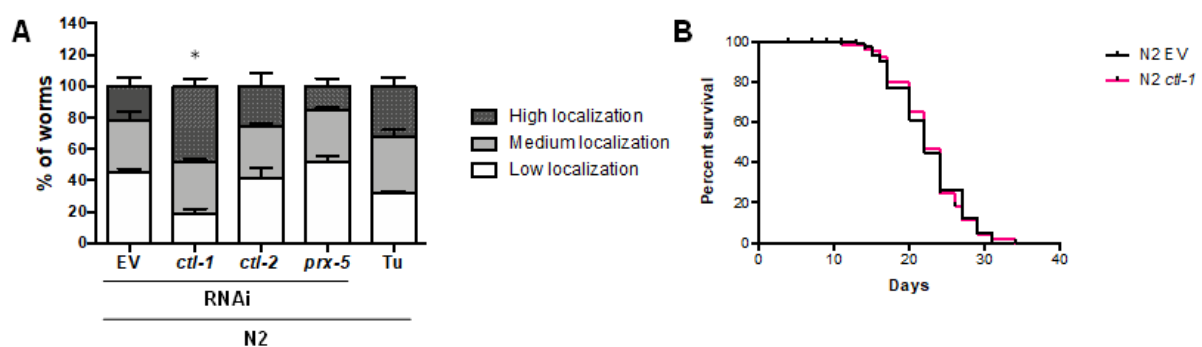


Fig 3.9 Peroxisomal and ER-derived ROS are unable to induce KLF-1-mediated longevity.

A) Quantification of amount of KLF-1 nuclear localization in WT animals upon RNAi or tunicamycin (Tu) treatment. For RNAi, worms were treated whole life with either catalase-1 (*ctl-1*), catalase-2 (*ctl-2*) or peroxisomal assembly factor 5 (*prx-5*). For Tu treatment, worms were bleached on control plates and transferred during L4 to plates containing 50 μ M tunicamycin. $n=30$ worms per condition. **B)** Lifespan of WT worms on RNAi plates with either L4440 or *ctl-1* RNAi. $n=200$ worms per condition. * $p<0.05$, Student's T-test. Modified from Hermeling et al. 2022.

increase the levels of misfolded proteins and therefore causing ER stress. However, tunicamycin treatment caused no increase in number of KLF-1-positive nuclei (Fig. 3.9.A). This suggests ER-derived ROS plays no role in the KLF-1 translocation to the nucleus.

As *ctl-1* RNAi showed an increase of KLF-1 translocation to the nucleus, we performed a lifespan assay on WT worms to establish if the peroxisomal ROS-induced nuclear KLF-1 is inducing long-lived phenotype. However, WT worms on control and *ctl-1* RNAi were not significantly different (Fig. 3.9.B). Thus, increased peroxisomal ROS is not sufficient to induce KLF-1-mediated longevity.

Finally, we wanted to determine if the KLF-1 nuclear translocation upon mild suppression of the MRC were all dependent on ROS (Fig. 3.8). To validate this hypothesis, we assayed the number of KLF-1-positive nuclei upon mild suppression of complex I by *nuo-2* RNAi and complex IV by *cco-1* RNAi in the presence of the antioxidant Vit C. Treatment with Vit C was able to decrease the presence of KLF-1 in the nucleus to WT levels (Fig. 3.10). In summary, our results show that mild suppression of mitochondrial complexes I, III and IV translocate KLF-1 to the nucleus by mitochondrial produced ROS.

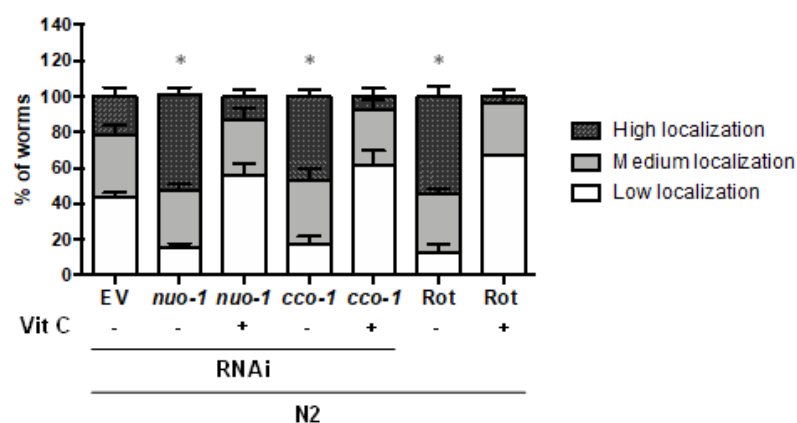


Fig 3.10 KLF-1 is translocated to the nucleus by mtROS.

Number of KLF-1-positive nuclei nuclear in one-day-old WT animals upon control, *nuo-2* or *cco-1* RNAi or 100 nM Rot treatment, with or without the presence of 10 mM Vit C. n=30 worms per condition.

* $p < 0.05$, Student's T-test. Modified from Hermeling et al. 2022.

3.4 E3 ligase WWP-1 is activating KLF-1, however it is not part of the KLF-1-induced longevity pathway

The HECT ubiquitin E3 ligase WWP-1 is a regulator of DR-induced lifespan by interacting with KLF-1 by monoubiquitylation (Carrano et al. 2009; Carrano, Dillin, and Hunter 2014). Therefore, we were interested if WWP-1 plays a role in our long-lived mitomutant. Firstly, we treated WT worms that expressed KLF-1 tagged to YFP with control or *wwp-1* RNAi from egg stage until adulthood. WT animals showed an increased number of KLF-1-positive nuclei upon *wwp-1* RNAi (Fig. 3.11). This suggests that WWP-1 inhibits KLF-1 translocation to the nucleus. Secondly, to test if WWP-1 interaction with KLF-1 was redox signalling dependent, we treated WT animals in the presence of *wwp-1* RNAi with either NAC or Vit C (Fig. 3.11). Both treatments showed significant increase of KLF-1-positive nuclei compared to WT EV. However, unlike what we observed in *isp-1;ctb-1* animals, both treatments were unable to reduce KLF-1-positive nuclei to WT levels. Thus, *wwp-1* depletion is likely translocating KLF-1 to the nucleus in a different mode of mechanism than in *isp-1;ctb-1* animals.

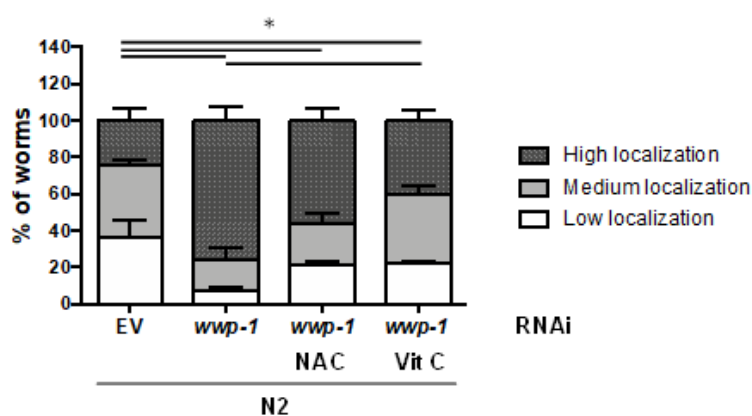


Fig. 3.11 *Wwp-1* depletion subcellular translocate KLF-1 in a non-redox dependent manner

Quantification of number of KLF-1 nuclei in day 1 of adulthood WT animals upon EV or *wwp-1* RNAi with or without the presence of 10 mM NAC or 10 mM Vit C. n=30 worms per condition. * $p < 0.05$, Student's T-test. Modified from Hermeling et al. 2022

WWP-1 is described as a HECT ubiquitin E3 ligase which can target protein for proteasomal degradation by polyubiquitylate (Huang et al. 2000; Cao et al. 2011; Zhi and Chen 2012), we hypothesized that WWP-1 targets KLF-1 for degradation. To test this, we inhibited the proteasome to determine if this would result in increased KLF-1-positive nuclei similar as inhibition of *wwp-1*. To block the proteasome, we used Bor,

a reversible inhibitor of the 26S (Chauhan et al. 2005; D. Chen et al. 2011). To determine if the Bor treatment worked to inhibit proteasome degradation, we used an *in vivo* degradation assay as described by Segref et al. (Segref, Torres, and Hoppe 2011). For this assay we used worms expressing a non-cleavable ubiquitin which is N-terminally fused to GFP (UbV-GFP) under the *sur-5* promoter. In WT animals this construct is targeted for degradation, whereas upon inhibition of the degradation system the GFP is stabilized. When we treated WT worms with 10 μ M Bor, we showed an increase in GFP signal in comparison with untreated WT worms (Fig. 3.12.A). Next, we treated worms from eggs stage with *wwp-1* RNAi and when the worms reached L4 we transferred them to plates containing 10 μ M Bor. After 24 hours, the worms were imaged. Surprisingly, treatment with Bor would rather decrease the number of KLF-1-positive nuclei in control WT worms (Fig. 3.12.B). Upon *wwp-1* RNAi there was no significant difference between control and Bor treatment. This suggests that WWP-1 mechanism of KLF-1 nuclear translocation is not dependent on proteasomal degradation.

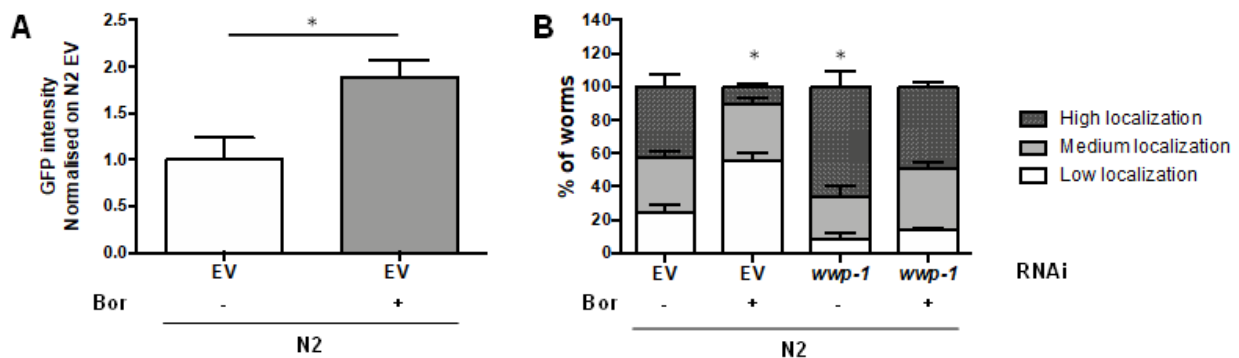


Fig 3.12 KLF-1 is not regulated by WWP-1-induced proteasomal degradation

A) UbV-GFP intensity in one-day-old WT animals upon control or 10 μ M Bortezomib treatment. Worms were treated from larvae L4 with Bortezomib. $n=25$ worms per condition. Data was normalised on N2 EV. $*p<0.05$, Student's T-test. **B)** Quantification of KLF-1-positive nuclei in WT animals upon EV or *WWP-1* RNAi with or without 10 μ M Bortezomib. $n=30$ worms per condition. $*p<0.05$, Student's T-test. Modified from Hermeling et al. 2022.

As *wwp-1* depletion translocates KLF-1 to the nucleus, we explored if the presence of nuclear KLF-1 will also result in increased CYPs expression, altered lipid levels and increased longevity as in our *isp-1;ctb-1* mutant (Herholz et al. 2019). Firstly, we analysed the transcript levels of *cyp*, which were increased in *isp-1;ctb-1* mutant (Herholz et al. 2019). Most of the *cyps* levels show no significant difference between WT control and *wwp-1* RNAi, whereas all *cyps* levels were significantly increased in

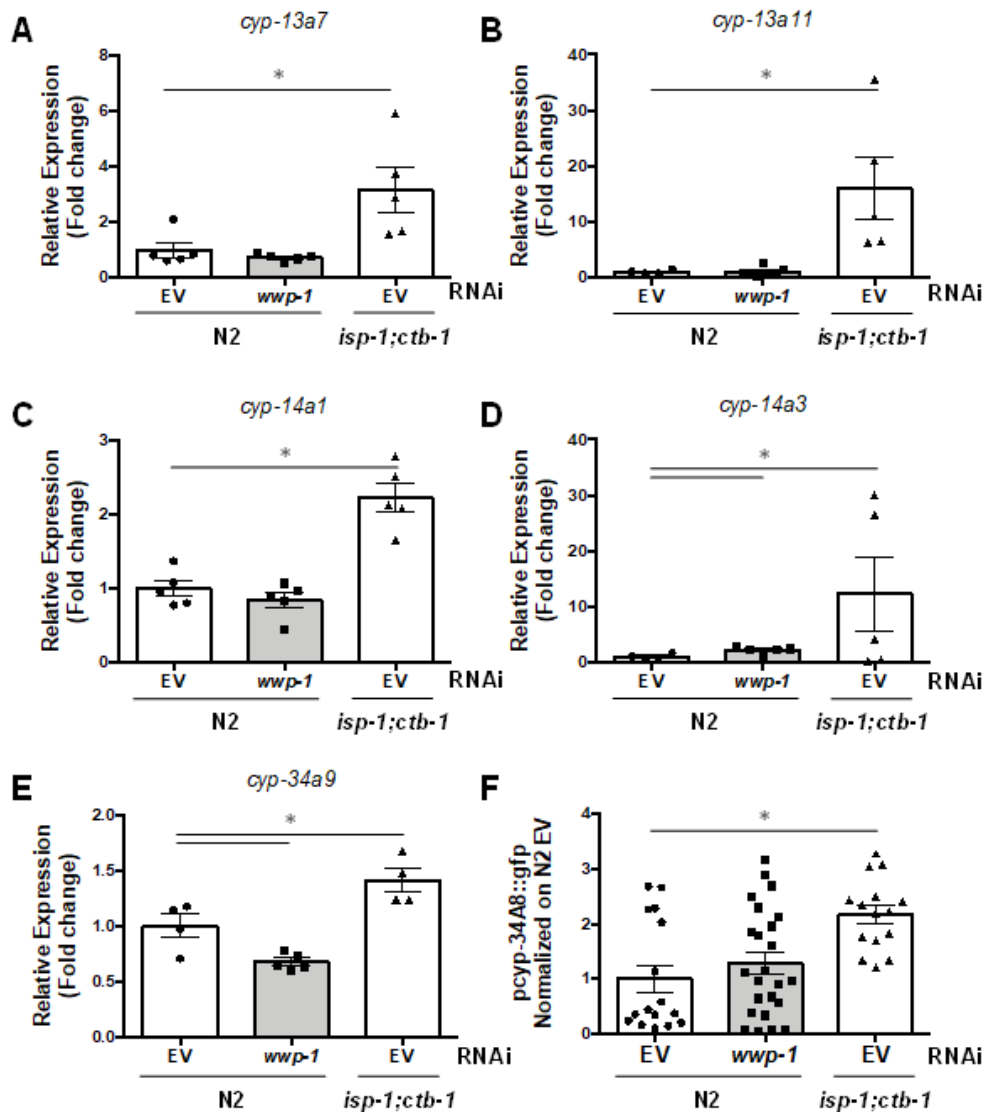


Fig 3.13 WWP-1-mediated KLF-1 nuclear localization is not inducing *cyps*

CYPs expressions were investigated in WT and *isp-1;ctb-1* animals with or without *wwp-1* RNAi. **A-E)** *cyps* expression levels were assessed by qPCR at first day of adulthood. *n*=4 per condition. **A)** *cyp-13a7*. **B)** *cyp-13a11*. **C)** *cyp-14a1*. **D)** *cyp-14a3*. **E)** *cyp-34a9*. **F)** *pcyp-34a8-GFP* intensity measured on one-day-old animals. *n*=20 per condition. **A-F)** Data was normalized on N2 EV and presented as mean \pm SEM. **p*<0.05, Student's T-test. Modified from Hermeling et al. 2022.

isp-1;ctb-1 mutant (Fig. 3.13.A-E). *Cyp-34a9* was even decreased upon *wwp-1* depletion (Fig. 3.13.E). Only *cyp-14a3* showed a significant two-fold increase upon *wwp-1* RNAi in comparison to control. However, in *isp-1;ctb-1* mutant *cyp-14a3* was increased almost twenty-fold (Fig. 3.13.D). Secondly, we further evaluate the CYPs expression by using a reporter strain in which the *gfp* expression was driven by *cyp-34a8* promoter. As expected, *gfp* levels were increased in *isp-1;ctb-1* mutant (Fig. 3.13.F). However, in WT animals there was no significant difference upon *wwp-1* RNAi.

Therefore, CYPs are not induced upon WWP-1-mediated KLF-1 nuclear translocation. Thirdly, we also evaluated the lipid levels, as we and others have shown that KLF-1 regulates various lipid genes (Hashmi et al. 2008; Herholz et al. 2019). Animals were treated with 5 μ M BODIPY 493/503 for 1h and green fluorescence was measured by microscopy (Klapper et al. 2011; Palgunow, Klapper, and Do 2012). *Isp-1;ctb-1* mutants showed a decreased lipid levels in comparison to WT worms, which was KLF-1 dependent as *klf-1* RNAi in *isp-1;ctb-1* mutant rescues the lipid levels (Fig. 3.14.A). *Wwp-1* RNAi did not significantly alter lipid levels in WT worms. Lastly, we assessed the lifespan of WT and *isp-1;ctb-1* animals upon *wwp-1* RNAi. WT worms on *wwp-1* RNAi showed no difference in lifespan with WT control (Fig. 3.14.B). Moreover, *wwp-1* depletion had no effect on *isp-1;ctb-1* lifespan (Fig. 3.14.C). In summary, we showed that *wwp-1* depletion results in translocation of KLF-1 to the nucleus, however this does not induce increased *cyps* levels, decreased lipid level and prolonged lifespan as we showed for *isp-1;ctb-1* mutant.

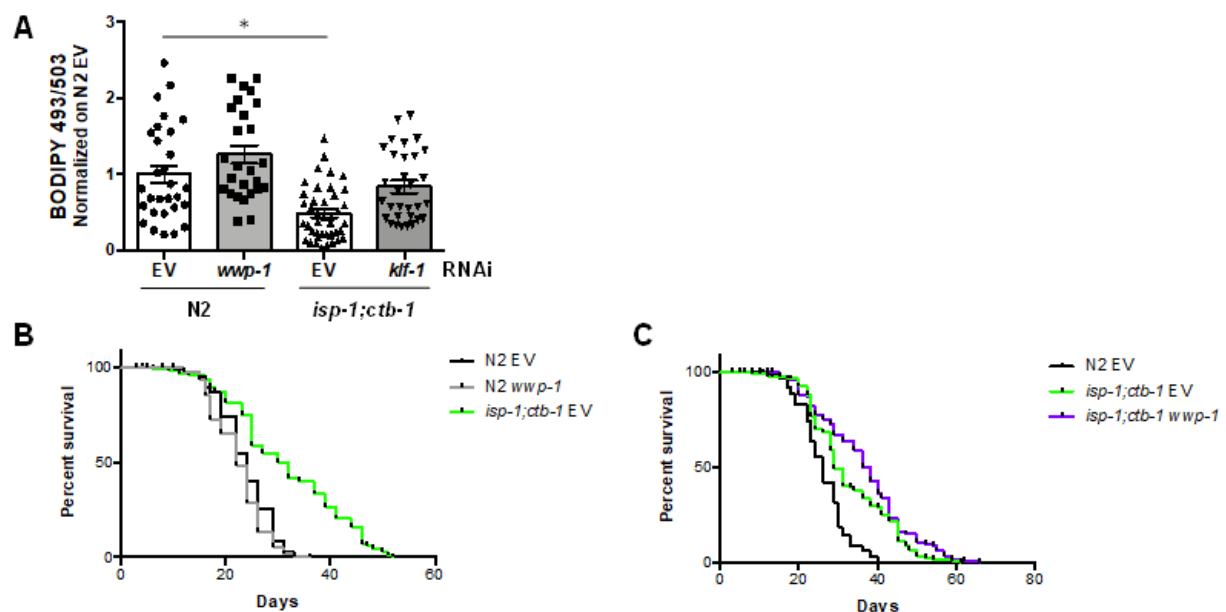


Fig 3.14 WWP-1 interaction with KLF-1 is not responsible for the increased lifespan in *isp-1;ctb-1* worms

Fat levels and lifespans were investigated in WT and *isp-1;ctb-1* animals with or without *wwp-1* RNAi.

A) Worms were treated for 1h with BODIPY 493/503 and afterwards fluorescence intensity was measured on one-day-old animals. Data was normalized on N2 EV and presented as mean \pm SEM. $n=25$ per condition. $*p<0.05$, Student's T-test. **B-C)** lifespans. $n=200$ animals per condition. **B)** Data obtained by Linda Baumann. Modified from Hermeling et al. 2022.

3.5 The role of mitochondrial SOD-3 and PRDX-3 in KLF-1 nuclear translocation

Since we showed that KLF-1 nuclear translocation in *isp-1;ctb-1* mutant is ROS-dependent, we next investigated the mitochondrial redox signalling. The main question we wanted to answer was how the mitochondrial ETC-originated superoxide anion radicals result in a stable redox signalling for the KLF-1 nuclear translocation. We investigated if exogenous treatment with ROS would be able to induce KLF-1 nuclear translocation. As most ROS molecules are highly unstable and reactive and therefore unsuited to act as a stable signal, we focused on the most stable ROS molecule: H_2O_2 (Sies 2014). Hydrogen peroxide has been recognized as ROS signalling molecule since it was found 50 years ago to be physiologically present at low steady-state levels in respiring eukaryotic cells (Sies 1993; di Marzo, Chisci, and Giovannoni 2018; P. K. Jensen 1966). Indeed, treatment of WT animals with 10 mM H_2O_2 resulted in an increased number of KLF-1-positive nuclei (Fig. 3.15).

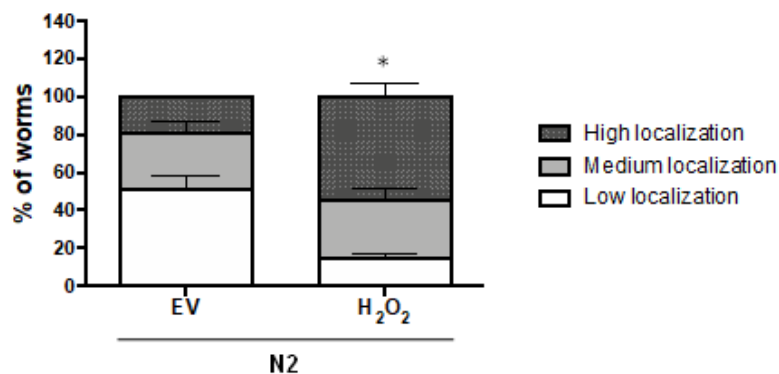


Fig 3.15 ROS molecule H_2O_2 translocate KLF-1 to the nucleus

Number of KLF-1-positive nuclei in WT worms with or without 10 mM H_2O_2 treatment. One-day-old WT worms were imaged after treatment with 10 mM H_2O_2 for 30 minutes. $n=30$ animals per condition. * $p<0.05$, Student's T-test. Modified from Hermeling et al. 2022.

The metabolizing of $\text{O}_2^{\cdot-}$ into H_2O_2 is performed by the SODs (Fridovich 1995; Buettner 2011). These SODs are the key cellular antioxidants against ROS-induced injury as they are highly reactive to free radicals. Furthermore, they are highly conserved across all biological kingdoms and have different subcellular compartmentalization. In *C. elegans*, five different *sods* are present, namely *sod-1* to *sod-5* (Doonan et al. 2008; Horspool and Chang 2017; L. T. Jensen and Culotta 2005; Fujii et al. 1998; Back, Braeckman, and Matthijssens 2012; Sakamoto and Imai 2017).

Here, we focused on the well-described cytosolic *sod-1* and mitochondrial *sod-2* and *sod-3* whereas the lesser-described *sod-4* and *sod-5* are suggested to be localized in extracellular space and cytosol, respectively, of specific subset of neurons (Gems and Doonan 2009; Fujii et al. 1998). Interestingly, we observed a strongly decreased KLF-1 nuclear translocation in *isp-1;ctb-1* mutant upon *sod-3* RNAi treatment whereas either suppression of *sod-1* or *sod-2* did not alter the level of KLF-1 nuclear translocation (Fig. 3.16.A). Additionally, a simultaneous suppression of the mitochondrial *sod-2* and *sod-3* showed a decreased KLF-1 nuclear translocation.

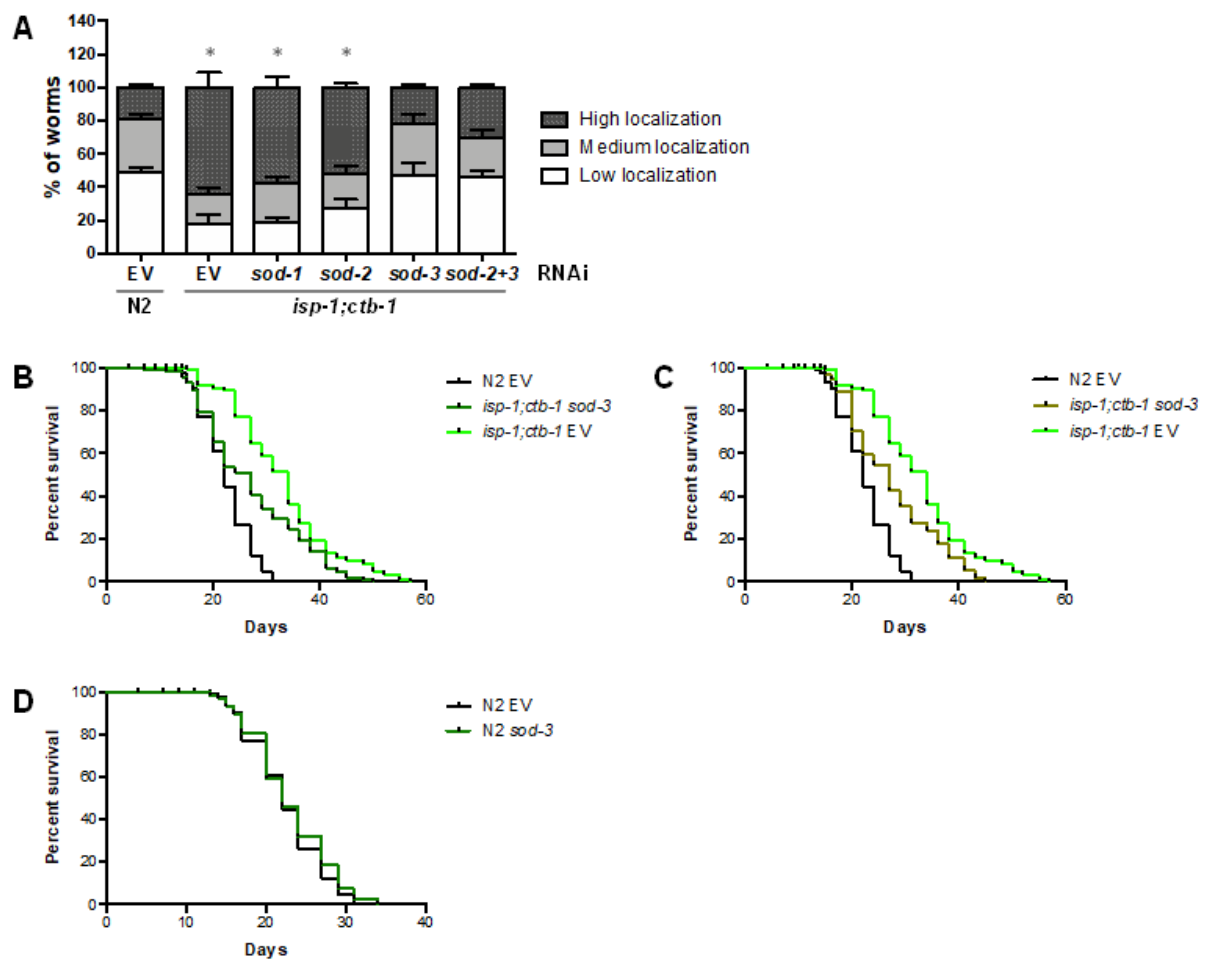


Fig 3.16 Mitomutant-induced longevity is mediated by *sod-3*

A) Number of KLF-1-positive nuclei was assayed at day 1 of adulthood in WT and *isp-1;ctb-1* animals upon control, *sod-1*, *sod-2*, *sod-3* and combined *sod-2* and *sod-3* RNAi. Data were normalized on N2 D1 and are presented as mean \pm SEM. $*p < 0.05$ $n=30$ animals per condition. $*p < 0.05$, Student's T-test
B-D) WT and *isp-1;ctb-1* lifespans on control and *sod-3* RNAi. $n=200$ worms per condition. **B)** WT and *isp-1;ctb-1* animals were treated whole lifespan with RNAi. **C)** WT and *isp-1;ctb-1* animals were treated during larvae stages with RNAi. At day 1 of adulthood animals were transferred to control plates.. **D)** WT animals were treated whole lifespan with EV and *sod-3* RNAi. Modified from Hermeling et al. 2022.

Lifespan experiments revealed an impact of *sod-3* depletion on *isp-1;ctb-1* longevity (Fig. 3.16.B). *sod-3* depletion decreased the lifespan of *isp-1;ctb-1* mutant, whereas the same suppression in WT animals did not alter their lifespan. Moreover, suppression with *sod-3* RNAi only during larvae stages was sufficient to decrease *isp-1;ctb-1* lifespan (Fig. 3.16.C). While, lifespan of WT animals demonstrated no significant difference upon *sod-3* RNAi (Fig. 3.16.D).

As we could show that *sod-3* depletion may mediate the mitomutant-induced lifespan, we wanted to determine the expression levels of the *sods*. Interestingly, *sod-2* and especially *sod-3* were highly induced in *isp-1;ctb-1* mutant (Fig. 3.17). This is similar *daf-2* long-lived mutants, where *sod-3* is highly induced and controlled by DAF-16 transcription factor (L. Zhao et al. 2017; Senchuk et al. 2018). KLF-1 is not directly regulating expression of cytosolic *sod-1*, or the mitochondrial *sod-2* or *sod-3*, as *klf-1* depletion in *isp-1;ctb-1* animals only prevents the early upregulation of the *sods*. However, at day 5 of adulthood expression levels of the *sods* genes were unchanged upon *klf-1* depletion (Fig. 3.17). Altogether, this shows that *sod-3* is highly induced in *isp-1;ctb-1* animals and likely responsible for converting $O_2^{\cdot-}$ to H_2O_2 to act as a second messenger to induce KLF-1 nuclear translocation and increased lifespan.

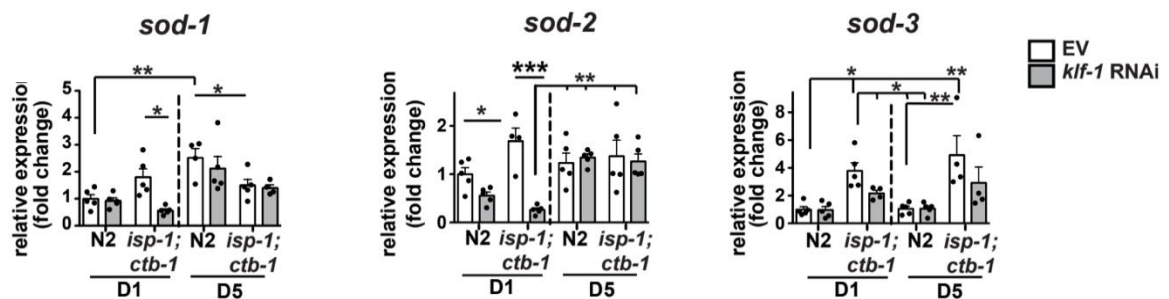


Fig 3.17 KLF-1-independent increased *sod-2* and *sod-3* expression in D1 *isp-1;ctb-1* mutant

The expression of *sod-1*, *sod-2* and *sod-3* was confirmed by qPCR at day 1 and day 5 of adulthood in WT and *isp-1;ctb-1* animals. n=4 samples per condition. Data were normalized on N2 D1 and are presented as mean \pm SEM. **p*<0.05, ***p*<0.01 and ****p*<0.001, one-way ANOVA with Tukey post hoc test. Data and figure were obtained by Herholz et al. 2019.

In order to determine what signalling steps act downstream of increased H_2O_2 levels, we first hypothesized that H_2O_2 is reduced by redox enzymes (di Marzo, Chisci, and Giovannoni 2018; Sies 2014). Two major redox enzyme families are responsible for reducing H_2O_2 , namely GPX and PRDX (Johnston and Ebert 2012; Z. A. Wood et al. 2003; Margis et al. 2008). Both redox enzymes use their cysteines to reduce H_2O_2 by forming dithiols. Afterward, GPX is reduced by glutathione, while PRDX is reduced

by the thioredoxin redox (TRX) system. In *C. elegans*, we have eight GPXs (*gpx-1* to *gpx-8*) and three PRDXs (*prdx-2*, *prdx-3* and *prdx-6*) (Ferguson and Bridge 2019). Interestingly, whereas the nematode GPX contains a cysteine, the mammalian homolog contains the more-redox sensitive selenocysteine (Sakamoto et al. 2014). To test our hypothesis, we performed *gpx* and *prdx* RNAi on WT worms in the presence of AA. While, we observed no clear alterations in KLF-1 nuclear translocation in WT worms on AA upon *gpx* RNAi, we observed increased KLF-1-positive nuclei upon *prdx-3* and *prdx-6* RNAi (data not shown). As *prdx* depletion resulted in an opposite trend than expected, our hypothesis is that *prdx* is necessary for the H₂O₂ reduction. Therefore, we decided to focus on the PRDX family members.

The PRDX family has three members, namely cytosolic *prdx-2* and mitochondrial *prdx-3* and lesser described *prdx-6* (Gruber et al. 2015). Based on the fact that *prdx-3* and *prdx-6* RNAi demonstrated an increase in KLF-1 nuclear translocation in the presence of AA, we wanted to determine if *prdx* depletion alone was enough to translocate KLF-1 to the nucleus. Indeed, *prdx-3* RNAi translocates KLF-1 towards the nucleus in WT animals (Fig. 3.18). Whereas *prdx-6* RNAi showed no clear difference with control. Altogether, these data suggest *prdx-3* depletion results in a decreased H₂O₂ reduction capacity, which may lead to increased H₂O₂ in the mitochondria.

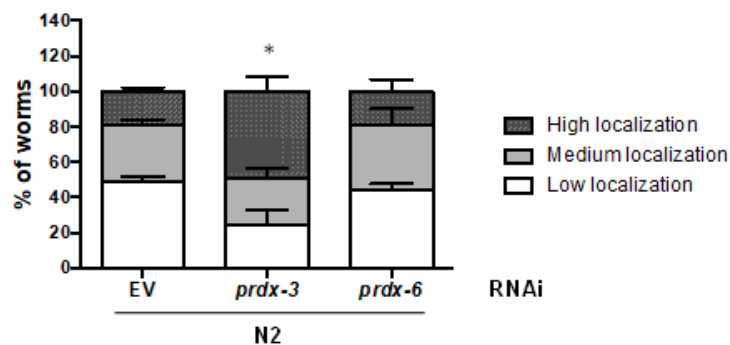


Fig 3.18 KLF-1 is translocated to the nucleus when *prdx-3* is depleted

A) Number of KLF-1 nuclei in one-day-old WT animals upon control (EV), *prdx-2* and *prdx-6* RNAi on day 1 of adulthood. n=30 per condition. **p*<0.05, Student's T-test. Modified from Hermeling et al. 2022.

As we hypothesised that *prdx-3* depletion leads to increased H₂O₂ levels, we then investigated if this depletion could result in prolonged lifespan in WT animals. We performed lifespan assay on WT and *prdx-3(gk529)* animals (Olá Hová et al. 2008) and we showed that *prdx-3(gk529)* mutant have a clear increased lifespan (Fig.

3.19.A). We also included *prdx-2(gk169)* mutant (Olá Hová et al. 2008) to establish if the lifespan effect was similar to *prdx-3(gk529)* mutant. *Prdx-2* depletion demonstrated a strong decrease in lifespan, which was also previously be observed (Oláhová et al. 2008). The lifespan of *prdx-3(gk529)* mutant was ROS and KLF-1 dependent (Fig. 3.19.B). In summary, *prdx-3* depletion induces KLF-1 nuclear translocation and ROS- and KLF-1-mediated longevity, which is likely due to decreased H_2O_2 reduction.

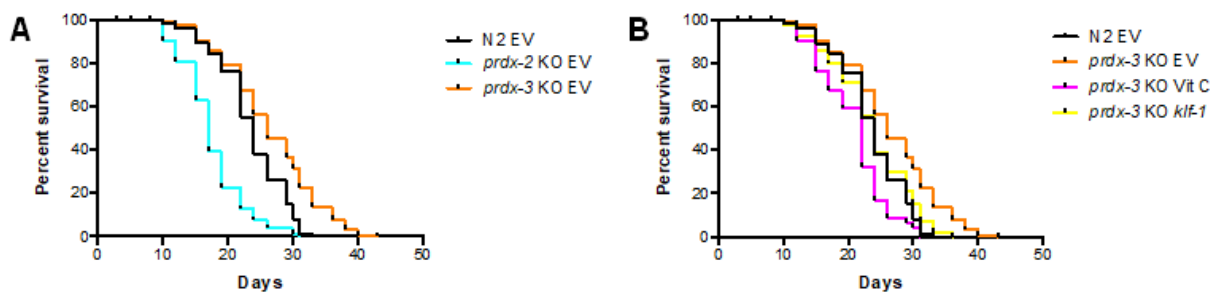


Fig 3.19 *Prdx-3* depletion results in ROS-induced and KLF-1-mediated longevity

Lifespan assay on WT, *prdx-2(gk169)* and *prdx-3(gk529)* animals. $n=200$ animals per condition **A)** Lifespan assays on EV RNAi. **B)** Lifespan assay on EV with or without 10 mM Vit C and *klf-1* RNAi. Modified from Hermeling et al. 2022.

3.6 L4 *isp-1;ctb-1* animals have increased mitochondrial H_2O_2 release what results in increased oxidative cytosolic redox state.

Next, we wanted to ascertain whether H_2O_2 is released from the mitochondria into the cytosol. As the ROS signal is late larval dependent (Herholz et al. 2019), we decided to investigate H_2O_2 levels during L4. For this purpose, we expressed the genetically encoded H_2O_2 sensor, roGFP2-Orp1, in WT and *isp-1;ctb-1* worms. This redox-sensitive sensor, which is pH independent, acts through dithiol-disulphide exchange between the H_2O_2 molecule and roGFP2 (Braeckman et al. 2016; Maremonti et al. 2020; Roma et al. 2018). RoGFP2 has dual excitation (405- and 488-nm), where reduced roGFP2 is excited by 405-nm while oxidized roGFP2 is excited by 488-nm (Braeckman et al. 2016). To address the mitochondrial H_2O_2 release in cytosol, we tagged this construct to *tomm20* under the muscle promoter *myo-3*, to express this construct at the OMM (Kaufmann et al. 2003). When we imaged D1 WT animals, we saw mitochondria in both channels of roGFP2 (Fig. 3.20.A). To validate the roGFP2 method, we treated the WT worms with 10 mM H_2O_2 . This resulted in an increased oxidized roGFP2 ratio (Fig. 3.20.B). Next, we exposed WT to 5 mM DTT, as reduced

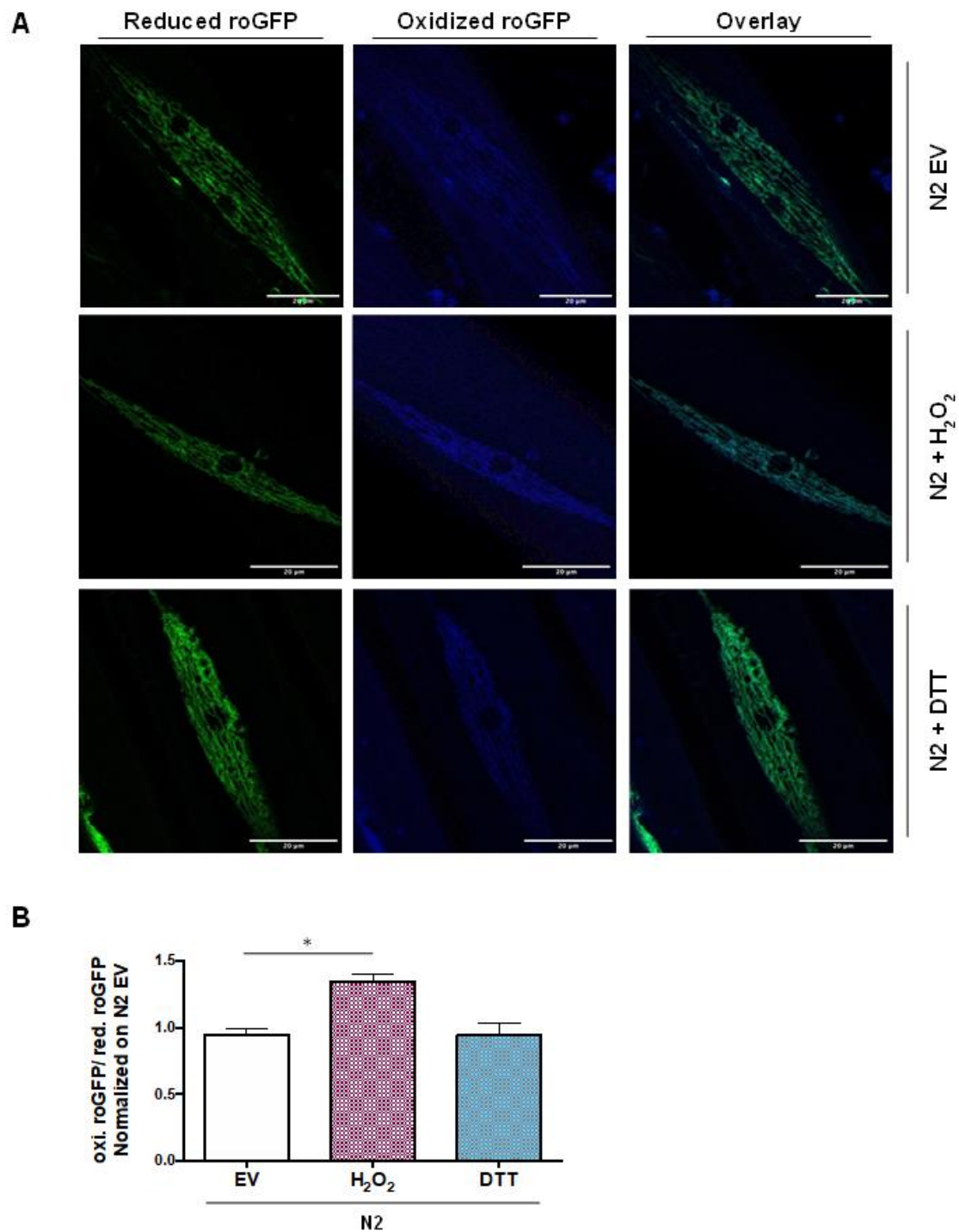


Fig 3.20 *Isp-1;ctb-1* mutants demonstrate increased oxidative roGFP2 in muscle

A) Representative pictures of L4 WT animals expressing *pmyo3::tom20::rogfp₂-Orp1*. Reduced *rogfp₂* was measured on 420-nm excitation, while oxidized *rogfp₂* was measured on 500-nm excitation. Scale bar 20 μ m. **B)** Quantification of **A**. WT animals were either treated with control (EV), 10 mM H₂O₂, 5 mM DTT. DTT and H₂O₂ treatment was just performed before imaging. Data shown is the ratio between oxidized versus reduced *rogfp₂*. n=3 per condition. Data were normalized on N2 EV and are presented as mean \pm SEM. * p <0.05, Student's T-test. Modified from Hermeling et al. 2022.

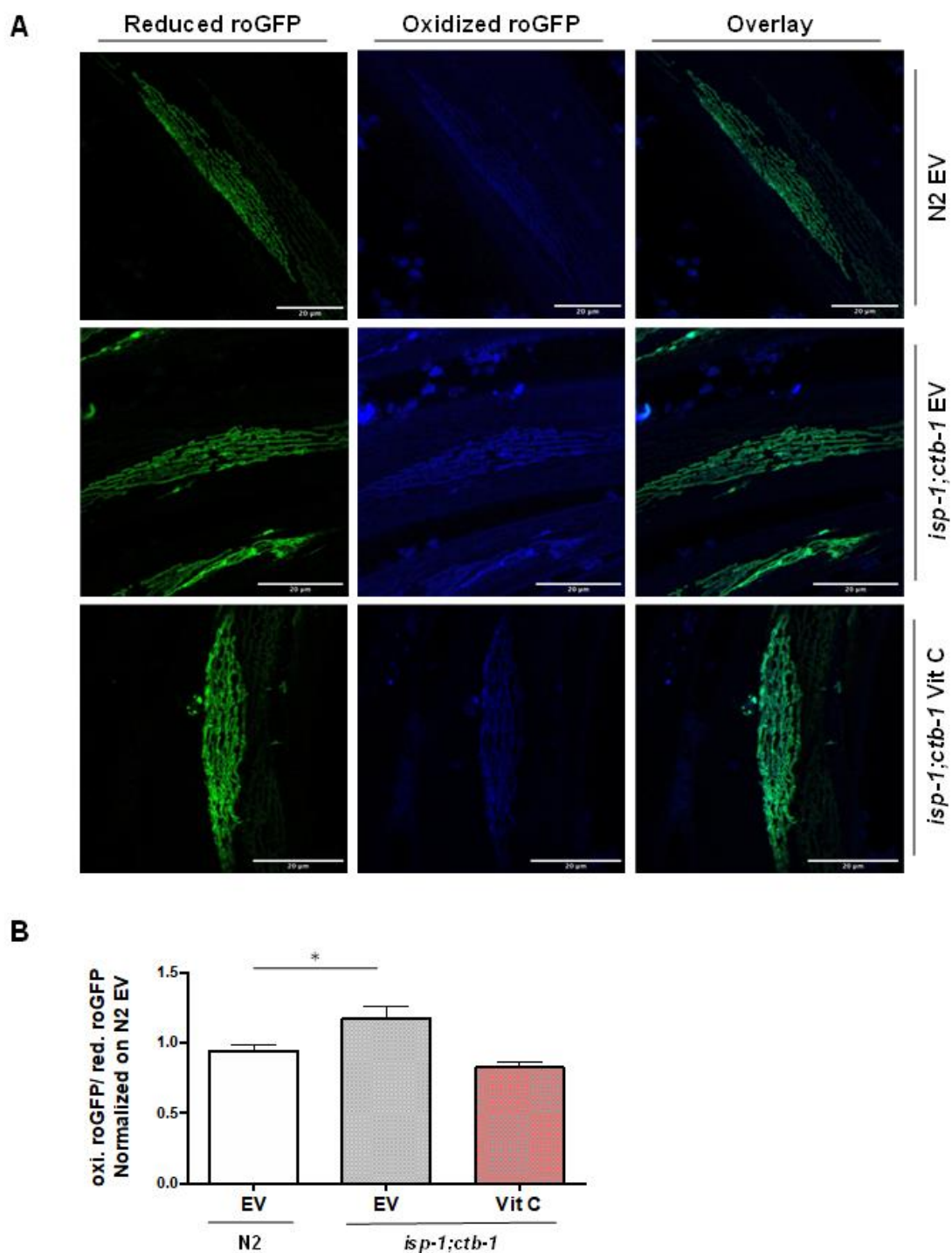


Fig 3.21 *Isp-1;ctb-1* mutants demonstrate increased oxidative roGFP2 in muscle

A) Representative pictures of L4 WT and *isp-1;ctb-1* animals expressing *pmyo3::tom20::roGFP2-Orp1*. Scale bar 20 μ m. **B)** Quantification of **A**. WT animals were either treated with control (EV). *Isp-1;ctb-1* animals were either treated with control (EV) or 10 mM Vit C. Vit C treatment was whole life. Data shown is the ratio between oxidized versus reduced roGFP2. Normalized on N2 EV. n=3 per condition. Data were normalized on N2 EV and are presented as mean \pm SEM. * $p < 0.05$, Student's T-test. Modified from Hermeling et al. 2022.

control (A. Seo et al. 2013), which is similar to WT control (Fig. 3.20.B). Thus, these data prove that the roGFP2 method works for determining the redox state at the OMM site, which correlates with the local H_2O_2 levels.

When we imaged L4 *isp-1;ctb-1* animals, we saw an increased mitochondrial H_2O_2 release (Fig. 3.21.A). Treatments with Vit C were able to diminish this increase to WT levels (Fig. 3.21.B). So, the roGFP2 construct illustrates the redox state at the OMM and therefore the mitochondrial H_2O_2 release, which is increased in muscle of *isp-1;ctb-1* mutant.

As *klf-1* is mainly gut expressed (Herholz et al. 2019), we expressed the *tomm20::rogfp2-orp1* under the gut promoter *pvha-6*. However, when we imaged this construct, we were unable to detect the oxidized roGFP2 signal due to autofluorescence of the gut bacteria (Fig. 3.22) (Clokey and Jacobson 1986; Coburn and Gems 2013). Therefore, we decided to switch to immunoblotting as the formation of disulphide bridge results in different molecular weights of roGFP2 (Reuter et al. 2019). We were able to detect the different bands of reduced and oxidized roGFP2 (Fig. 3.23.A) and they correlate with control treatment, namely DTT treatment as reduced control and H_2O_2 treatment as oxidized control in WT worms (Fig. 3.23.B).

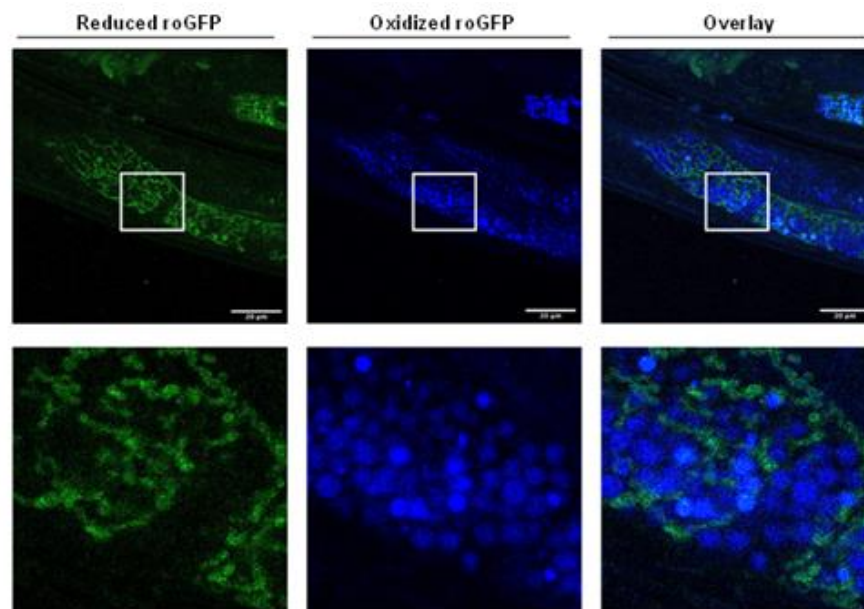


Fig 3.22 Increased mitochondrial H_2O_2 excretion into cytosol during L4 in *isp-1;ctb-1* mutant.

Representative pictures of one-day-old WT animals expressing *pvha::tom20::rogfp2-Orp1*. Reduced *rogfp2* was measured on 405-nm excitation, while oxidized *rogfp2* was measured on 488-nm excitation. Overlay is merged picture of reduced and oxidized roGFP2. Lower panels illustrate zoom in of white box in upper panels. Scale bar 20 μm . Modified from Hermeling et al. 2022.

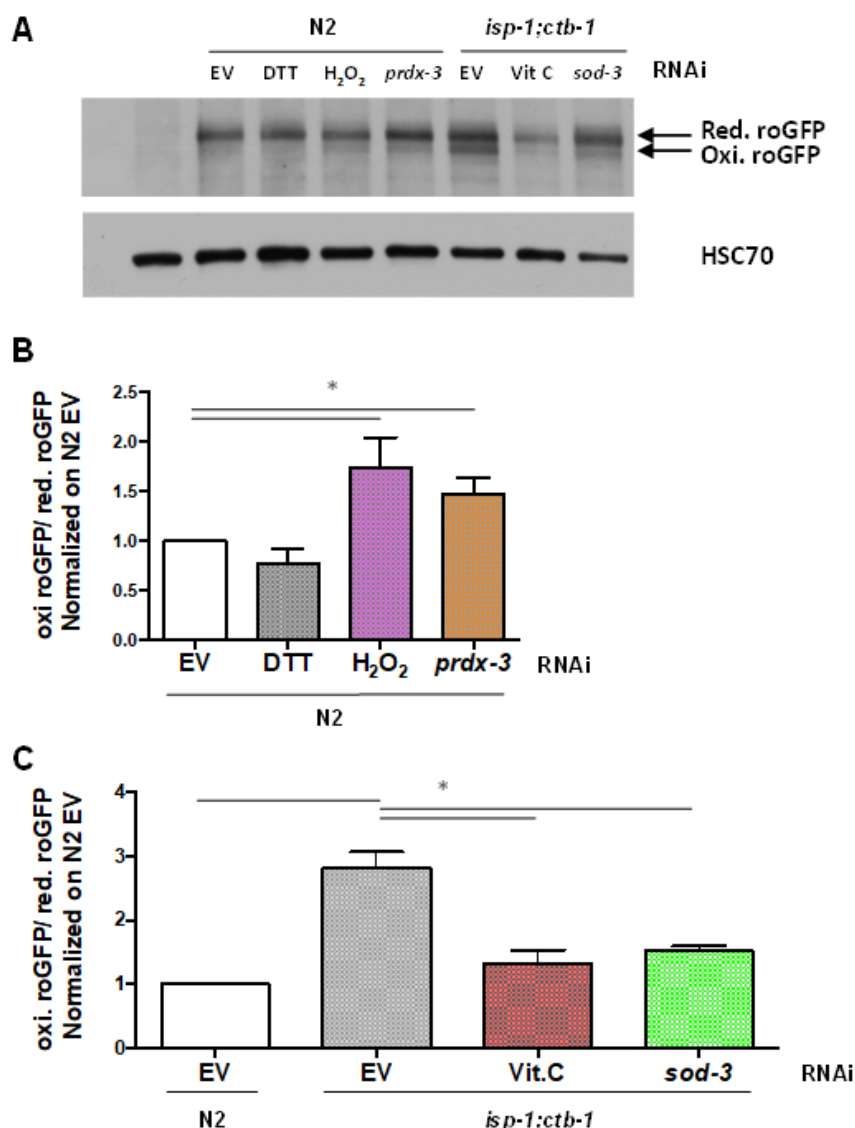


Fig 3.23 Increased mitochondrial H₂O₂ excretion into cytosol during L4 in *isp-1;ctb-1* mutant.

A) Immunoblot of whole worm lysates of L4 WT and *isp-1;ctb-1* animals for GFP antibody. Animals were expressing *pmyo3::tom20::rogfp2*. For loading control anti-HSC70 antibody was used. WT animals were either treated with control (EV), *prdx-3* RNAi, 5 mM dithiothreitol (DTT) or 10 mM H₂O₂. DTT and H₂O₂ treatment was just performed before imaging. *isp-1;ctb-1* animals were treated with control (EV), 10 mM Vit C or *sod-3* RNAi **B-C)** Quantification of **A**. **B** WT. **C:** *isp-1;ctb-1* animals. Data shown is the ratio between oxidized versus reduced roGFP2 corrected for HSC70 and normalized on N2 EV. n=3 per condition. Data are presented as mean ± SEM. **p*<0.05, Student's T-test. Modified from Hermeling et al. 2022.

Prdx-3 RNAi increased the oxidized roGFP2, suggesting *prdx-3* depletion results in increased mitochondrial H₂O₂ release (Fig. 3.23.B). Interestingly, comparing WT with *isp-1;ctb-1* animals also showed an increased amount of oxidized roGFP2 (Fig. 3.23.C). This demonstrates that L4 *isp-1;ctb-1* mutant has higher mitochondrial H₂O₂

release than L4 WT. Furthermore, this increase is diminished by either *sod-3* suppression or antioxidant treatment (Fig. 3.23.C). Taken together, these results show that mitochondrial H_2O_2 release is the ROS signal for increased lifespan, which is mediated by SOD-3 and PRDX-3.

Next, we wanted to determine if the increased mitochondrial H_2O_2 release in *isp-1;ctb-1* mutant affects the overall cytosolic redox state of the worm. In order to

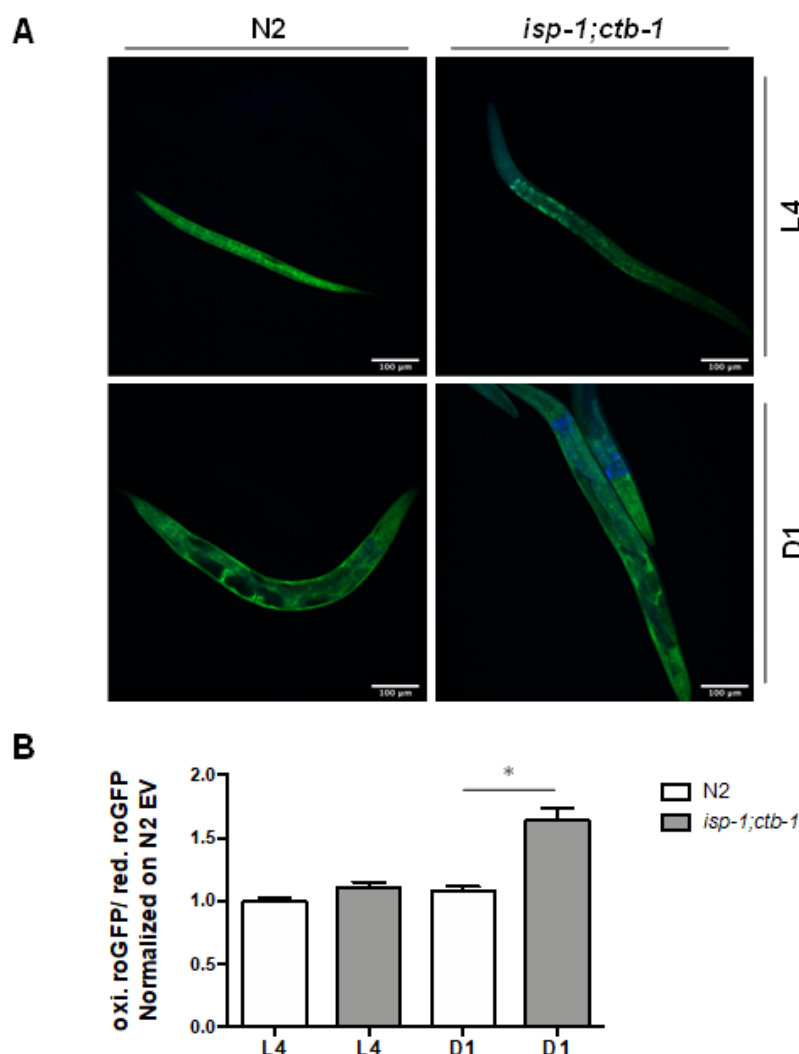


Fig 3.24 One-day-old *isp-1;ctb-1* animals have increased oxidized cytosolic environment

A) Representative pictures of L4 and D1 WT and *isp-1;ctb-1* animals expressing *grx1::roGFP₂*. Reduced roGFP₂ was measured on 490-nm excitation and visualized in green, while oxidized roGFP₂ was measured on 405-nm excitation and visualized in blue. Scale bar 100 μ m. **B)** Quantification of **A**. L4 and D1 WT and *isp-1;ctb-1* animals. Data shown is the ratio between oxidized versus reduced roGFP₂ and normalized on N2 L4. n=25 animals per condition. Data are presented as mean \pm SEM. * p <0.05, Student's T-test. Modified from Hermeling et al. 2022.

investigate this, we used a cytosolic GRX1-roGFP2- Orp1 sensor (Müller et al. 2017). This sensor is expressed under the *rpl-17* promoter and works similarly to the *tomm20::rogfp2::orp1 construct*. When we analysed the redox state in L4 WT and *isp-1;ctb-1* mutant, we did not detect any difference between the two conditions (Fig. 3.24). L4 *isp-1;ctb-1* mutant showed a mild, but not significant increased oxidized redox state. Also, there is no difference between L4 and D1 WT worms. Interestingly, D1 *isp-1;ctb-1* mutant demonstrated a strongly increased oxidized cytosolic redox state (Fig. 3.24.B). In summary, D1 *isp-1;ctb-1* mutant has an increased oxidized cytosolic redox environment.

3.7 VDAC-1 is facilitating H₂O₂ transport across membranes

As we showed that mitochondrial H₂O₂ is responsible for KLF-1 nuclear translocation by strongly increasing the oxidized cytosolic state, we next investigated how H₂O₂ can translocate out of the mitochondria into the cytosol. As diffusion of H₂O₂ across membranes is limited, consequently active transport is required (Bienert, Schjoerring, and Jahn 2006). It has been suggested that aquaporins and VDAC play a vital role in ROS transport (DeHart et al. 2018; L. Zhang et al. 2020; Bienert, Schjoerring, and Jahn 2006; Cordeiro 2015). Therefore, we performed a RNAi screen on *isp-1;ctb-1* worms by depleting aquaporins (*aqp-1* till *aqp-12*) (Ni et al. 2017; A. Seo et al. 2013) and *vdac-1* (Uozumi et al. 2015) to assay the number of KLF-1-positive nuclei on D1. Whereas the various aquaporin RNAi showed no alteration in KLF-1-positive nuclei (data not shown), *vdac-1* RNAi showed a strong decrease in KLF-1 nuclear translocation (Fig. 3.25.A). Furthermore, *vdac-1* depletion reduced the lifespan of *isp-1;ctb-1* worms (Fig. 3.25.B). Moreover, *vdac-1* depletion during larvae stages was sufficient to reduce the *isp-1;ctb-1* lifespan (Fig. 3.25.C), whereas WT demonstrated no significant alteration between control and *vdac-1* depletion (Fig. 3.25.D). Next, we utilized our *tomm20-roGFP2* strain to validate that VDAC-1 is responsible for H₂O₂ transport across the OMM. *Vdac-1* depletion demonstrated a decreased oxidative roGFP2 ratio, although this decrease was not significant (Fig. 3.26). In summary, this data strongly suggests that *vdac-1* is part of the KLF-1 nuclear translocation by facilitating transport of H₂O₂ across the OMM. Altogether, these results emphasizes the role of SOD-3, PRDX-3 and VDAC-1 in ROS signalling (Fig. 3.27).

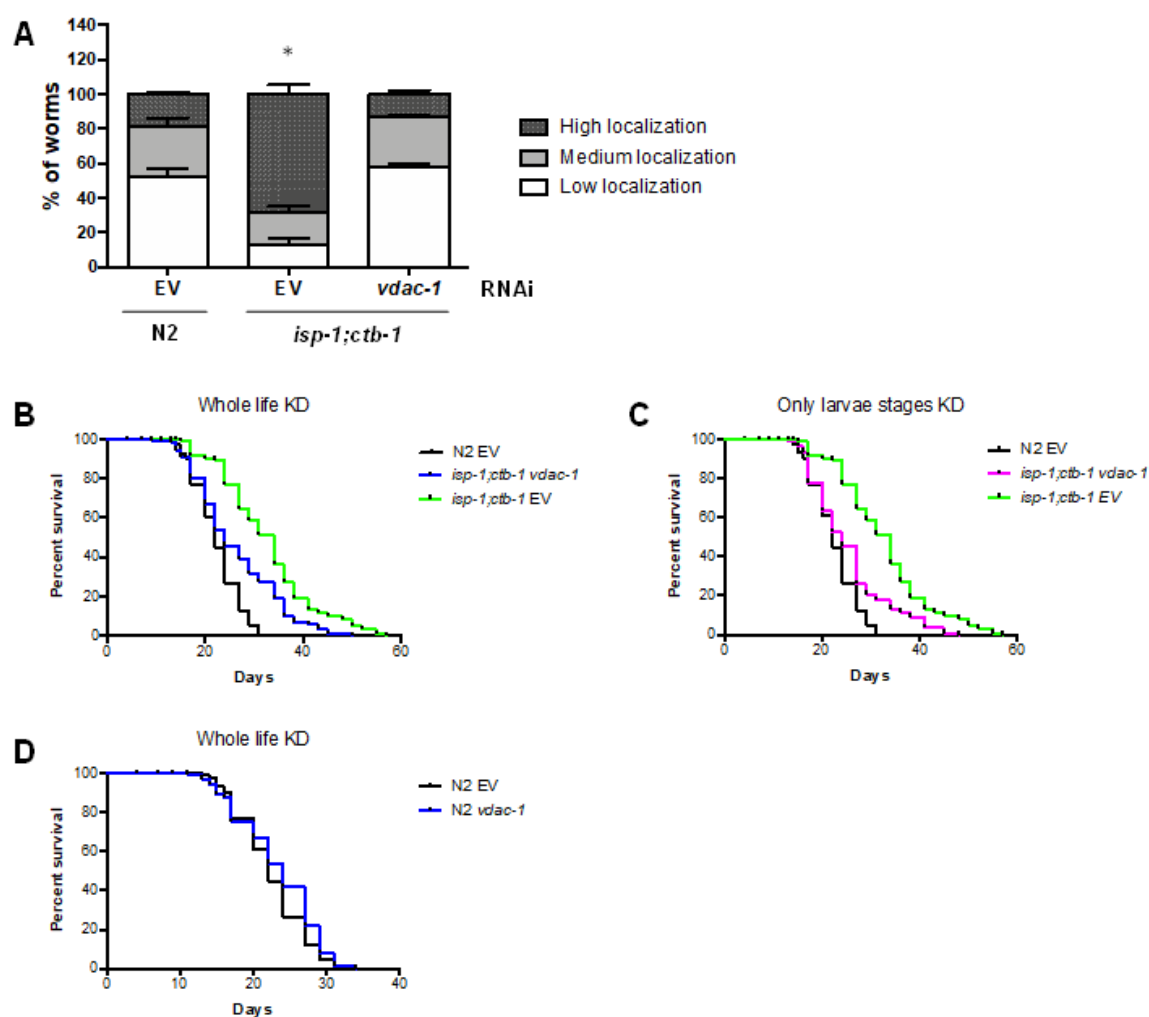


Fig 3.25 *Vdac-1* depletion inhibits KLF-1 nuclear translocation and diminish increased *isp-1;ctb-1* lifespan

A) Quantification of KLF-1-positive nuclear localization on day 1 of adulthood in WT and *isp-1;ctb-1* animals upon control or *vdac-1* RNAi. $n=30$ animals per condition. $*p < 0.05$, Student's T-test. **B-D)** WT and *isp-1;ctb-1* lifespans on *vdac-1* RNAi. $n=200$ worms per condition. **B)** WT and *isp-1;ctb-1* animals were treated whole lifespan with RNAi. **C)** WT and *isp-1;ctb-1* animals were treated during larvae stages with RNAi. At day 1 of adulthood animals were transferred to control plates. **D)** WT animals were treated whole lifespan with *vdac-1* RNAi. Modified from Hermeling et al. 2022.

3.8 SOD-3, PRDX-3 and VDAC-1 regulates CYPs-induced xenobiotic detoxification response

As we have shown that SOD-3, PRDX-3 and VDAC-1 regulate KLF-1 nuclear translocation and lifespan, we wanted to determine if these enzymes also regulate

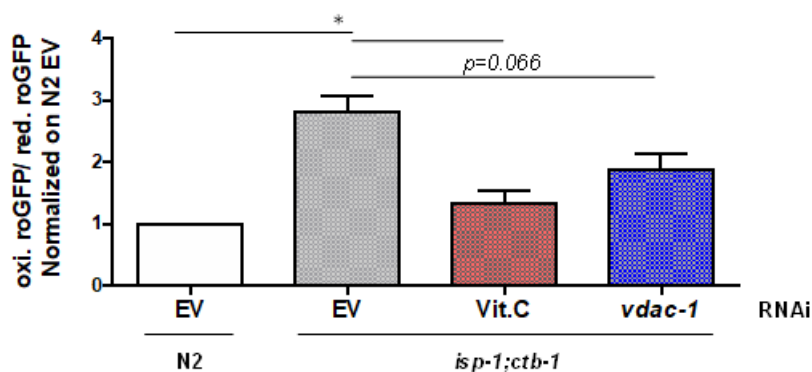


Fig 3.26 VDAC-1 may be part of mitochondrial H_2O_2 transport across OMM.

Quantification of immunoblot of whole worm lysates of L4 WT and *isp-1;ctb-1* animals expressing *pmyo3::tom20::rogfp2*. Used antibodies were anti-GFP and anti-HSC70 (loading control). WT animals were either treated with control (EV) and *isp-1;ctb-1* animals were treated with control (EV), or *vdac-1* RNAi. Data shown is the ratio between oxidized versus reduced *rogfp2* corrected for HSC70 and normalized on N2 EV. $n=3$ per condition. Data are presented as mean \pm SEM. * $p<0.05$, Student's T-test. Modified from Hermeling et al. 2022.

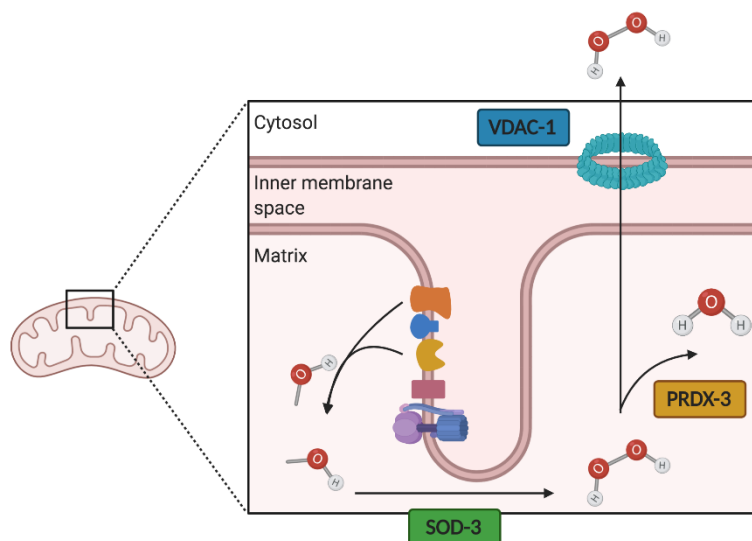


Fig 3.27 Schematic overview of proposed mitochondrial signalling cascade

Signalling cascade in mitochondria: Upon mild ETC dysfunction, O_2^- is generated and metabolized into H_2O_2 by SOD-3. H_2O_2 can be either reduced by PRDX-3 into water or exported across the OMM by VDAC-1, which results in a oxidized cytosolic redox environment. Figure made with Bioscript.com. Modified from Hermeling et al. 2022.

CYPs expression and alter the xenobiotic detoxification capacity as we saw in our long-lived *isp-1;ctb-1* mutant. To determine the *cyp* levels, we assayed *cyp-34a8* expression, using the transcriptional reporter *pcyp-34a8::gfp*. *Prdx-3* depletion results in a twofold increased *cyp34a8* expression (Fig. 3.28). In agreement with

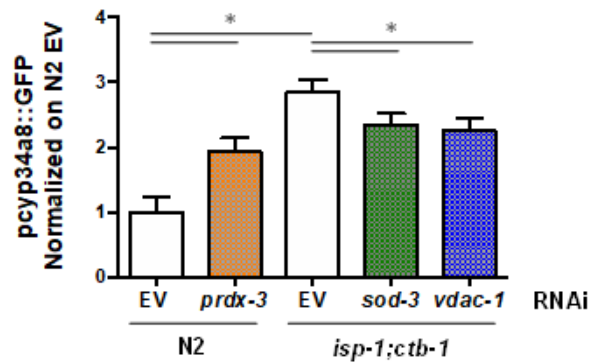


Fig 3.28 SOD-3, PRDX-3 and VDAC-1 regulates *cyp34a8* expression

Pcyp34a8::gfp expression was measured on one-day-old WT and *isp-1;ctb-1* worms upon control (EV), *prdx-3*, *sod-3* or *vdac-1* RNAi. $n=20$ animals per condition. Data were normalized on N2 EV and are presented as mean \pm SEM. $*p<0.05$, Student's T-test. Modified from Hermeling et al. 2022.

previous work, *cyp-34a8* expression in *isp-1;ctb-1* mutant is three-fold increased. Interestingly, *sod-3* or *vdac-1* depletion decreases *cyp-34a8* levels in *isp-1;ctb-1* mutant (Fig. 3.28).

The upregulation of CYPs should benefit the xenobiotic detoxification capacity in WT animals, while downregulation should diminish this capacity in *isp-1;ctb-1* mutant. To further investigate this, we exposed the animals to two xenobiotic assays. First, we exposed worms to 1 mM levamisole, a paralysing agent. *Prdx-3* depletion animals showed an increased tolerance to paralysation than control animals (Fig. 3.29.A). Similarly, *isp-1;ctb-1* mutant has an increased tolerance to paralysation. However, this tolerance is decreased upon *sod-3* and *vdac-1* depletion (Fig. 3.29.C). Second, we treated worms with microtubule-targeting vinblastine, an antimitotic drug. Here, *prdx-3* depletion animals reached further developmental stages than WT control (Fig. 3.29.B). Also, *isp-1;ctb-1* animals have reached further developmental stages than WT (Fig. 3.29.D). *Sod-3* and *vdac-1* depletion diminishes this increased tolerance in *isp-1;ctb-1* mutant. In summary, consistent with the increased *cyp34a8* expression, *prdx-3* depletion increases the xenobiotic detoxification capacity in WT worms, whereas in *isp-1;ctb-1* mutant upon *sod-3* and *vdac-1* depletion, decreases the xenobiotic detoxification capacity, which is consistent with the decreased *cyp* expression.

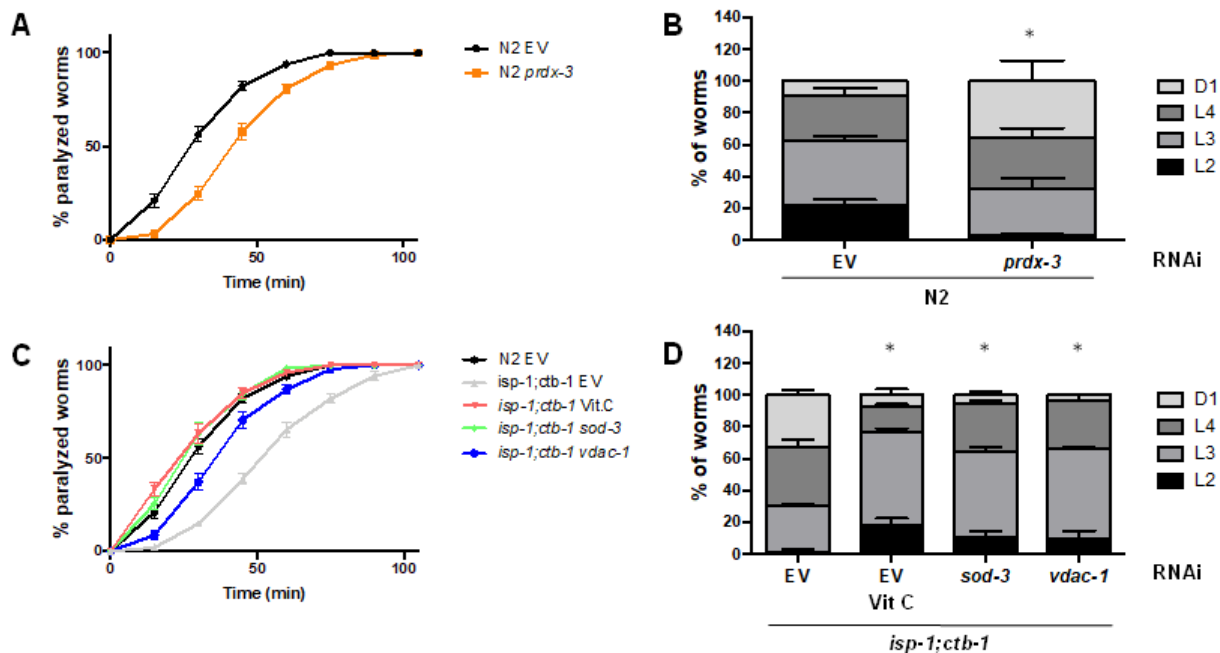


Fig 3.29 *Prdx-3* depletion induce, whereas *sod-3* and *vdac-1* depletion inhibits xenobiotic detoxification response

WT animals were grown on either control (EV) or *prdx-3* RNAi (**A, B**) and *isp-1;ctb-1* animals were grown on either control (EV), *sod-3* or *vdac-1* RNAi or 10 mM Vit C (**C, D**) Animals were transferred on the fourth day of adulthood on plates containing 1 mM of levamisole. Worms were assayed every 15 min for movement and failing to move was counted as paralyzed. n=80 animals per condition. Data are presented as mean \pm SEM. ** $p < 0.01$, Student's T-test. **B, D**) L1 larvae WT animals were grown in liquid with and without 100 μ M vinblastine. When untreated vinblastine WT animals reached first day (D1) of adulthood, the treated vinblastine animals were assayed for developmental stages. n=200 animals per condition. Data are presented as mean \pm SEM. * $p < 0.05$, Student's T-test. Modified from Hermeling et al. 2022.

3.9 Indirect thiol modification is responsible for KLF-1 nuclear translocation

Oxidative modifications of proteins have been described to be closely linked to alteration of intracellular redox state. As we have shown that *isp-1;ctb-1* animals have a more oxidized redox state (Fig. 3.24), we investigated the role of oxidative modifications of proteins in our mutant. We primarily focused on thiols of cystines as the balance between cysteine and cystine is a well-established H_2O_2 -inducable oxidative modification (Calvo, Ayté, and Hidalgo 2013; Riemer et al. 2015). When

cysteine gets oxidized by ROS, the sulfhydryl group is metabolized into sulfenic acid which is highly reactive to form cystine through disulphide bond formation. To gain deeper insights into the role of cystine bonds, we used DTT, a widely used treatment to reduce disulphide bonds and ultimately cystine into cysteine. Interestingly, treatment with DTT was able to decrease the amount of KLF-1 nuclear translocation in both WT and *isp-1;ctb-1* worms (Fig. 3.30). These data suggest that thiol modification of cysteine into cystine is part of the KLF-1 nuclear translocation pathway. However, this also gives rise to the question if this modification is directly on one of the cysteines of KLF-1 or rather on one of the cysteines on a protein in the KLF-1 nuclear translocation pathway.

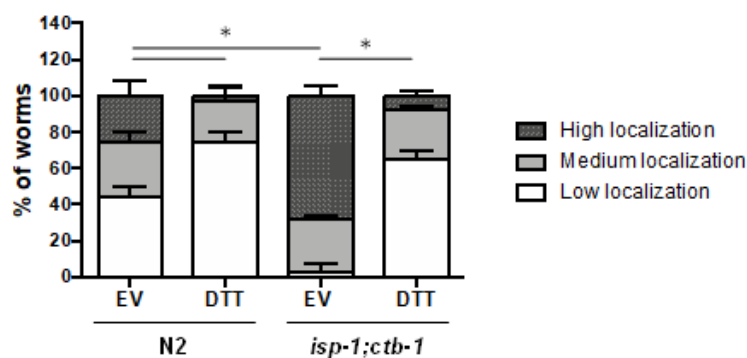


Fig 3.30 Formation of disulphide bonds are required for KLF-1 nuclear translocation

Number of KLF-1-positive nuclei in one-day-old WT and *isp-1;ctb-1* animals with or without 5 mM DTT treatment. DTT treatment was just performed before imaging. n=30 animals per condition. Data are presented as mean \pm SEM. * $p < 0.05$, Student's T-test. Modified from Hermeling et al. 2022.

In order to analyse whether the oxidation-induced thiol modifications are directly modifying the cysteines on KLF-1 we analysed changes in cysteine redox states by shift assay (Habich and Riemer 2017; Pant, Oh, and Mysore 2021; Cobley and Husi 2020). Reduced cysteines were captured by treatment with 20 mM NEM, a small membrane-permeable thiol-reactive probe to block reduced thiols, whereas oxidized cysteines were captured by treatment with 20 mM mm(PEG)24, a large thiol-reactive probe (Fig. 3.31). D1 worms were treated with NEM, frozen, lysed and proteins were treated with mm(PEG)24 before running the samples on Western blot. Consequently, the different sizes between thiol-reactive probes result in a shift in kDa size, which correlate to the redox state of the cysteines (Fig. 3.31). However, the results obtained from the shift assay were very inconclusive as observed bands of KLF-1-YFP showed different patterns between experiments (Fig. 3.32.A). Moreover, treatments with antioxidants, NAC or Vit C, and S3QEL-3 were not showing difference from *isp-1;ctb-*

1 control (Fig. 3.32.B). Next, we used a different tag, namely FLAG, on KLF-1 to determine whether another tag or different antibody would improve the consistency of

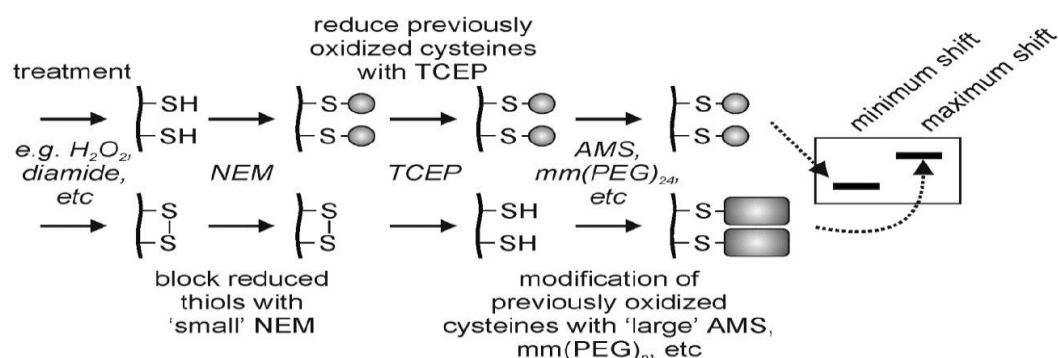


Fig 3.31 Schematic illustration showing protocol of shift assay

Determination of redox state of thiol group by treatment with NEM, TCEP and mm(PEG)24. NEM captures reduced cysteines, while mm(PEG)24 captures oxidized cysteines. Figure obtained from Habich and Riemer 2017.

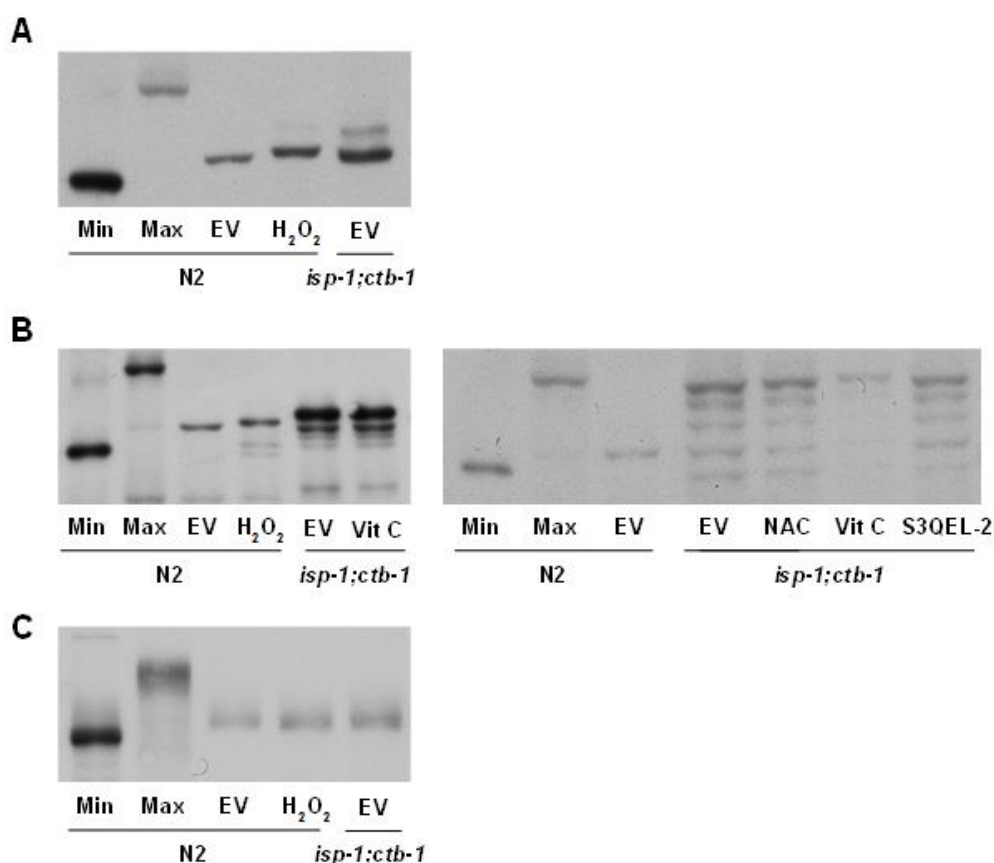


Fig 3.32 Shift assay resulted in inconclusive results

Western blot of one-day-old WT and *isp-1;ctb-1* animals **A-B**) Animals expressing *klf-1::YFP*. **A**) WT and *isp-1;ctb-1* animals treated with control (EV) RNAi or 10 mM H_2O_2 . **B**) *isp-1;ctb-1* animals treated with 10 mM NAC, 10 mM Vit C or 100 μ M S3QEL-2. **C**) Animals expressing *klf-1::FLAG*.

our shift assay results. FLAG tag has been described as a relatively small protein tag and therefore less likely to influence protein behaviour. Unfortunately, KLF-1-FLAG demonstrated similar inconclusive pattern (Fig. 3.32.C). Therefore, we concluded this method was unsuited for our model and hypothetical setup. In summary, we were unable to detect alterations in cysteine redox state of KLF-1 by using the shift assay.

As we were unable to detect thiol modification on KLF-1 by using the shift assay, we decided to study the thiol modifications on cysteine of KLF-1 by mutagenesis. As one of the cysteines was part of a predicted nuclear localization sequence (NLS) (cNLS Mapper) (Kosugi et al. 2009), we focussed on investigating this cysteine (Fig. 3.33.A).

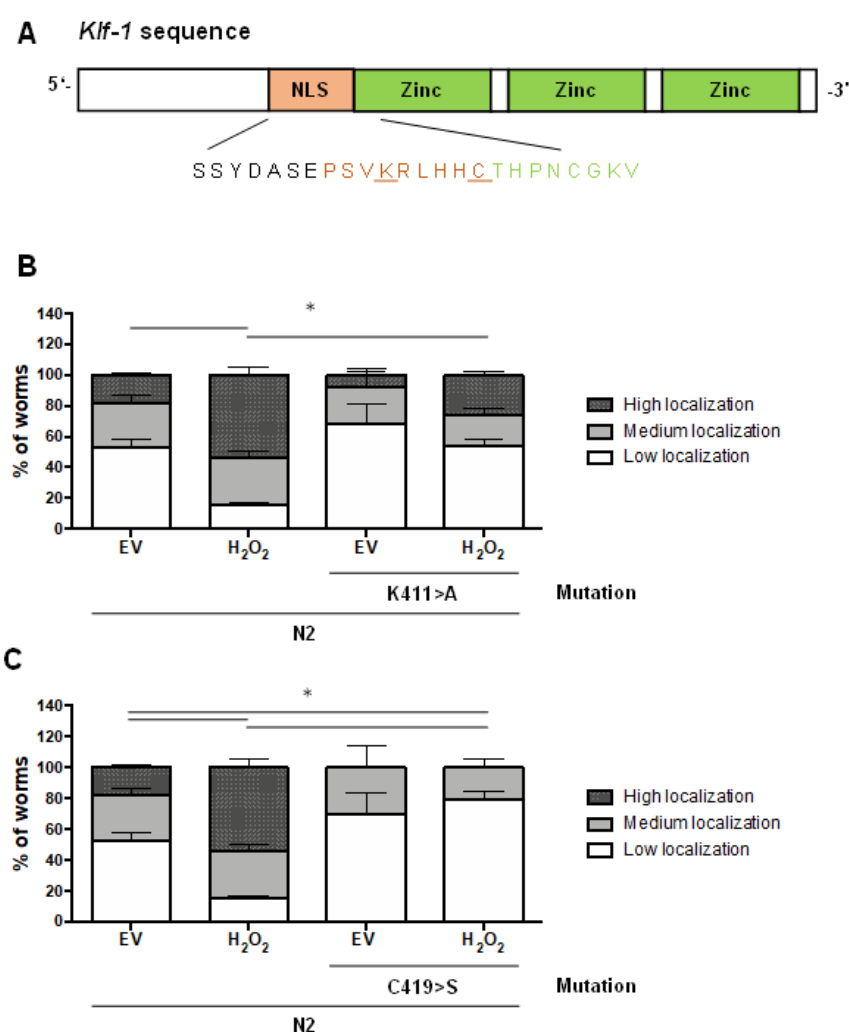


Fig 3.33 H₂O₂-induced KLF-1 nuclear translocation is dependent on the NLS and cysteine 419

A) *Klf-1* sequence with nuclear localization sequence (NLS) and zinc finger domains highlighted **B)** Number of KLF-1-positive nuclei in one-day-old WT animals with KLF-1 mutations at respectively lysine (K) 411 and cysteine (C) 419 to alanine (A) or serine (S) with or without 10 mM H₂O₂ treatment. n=30 animals per condition. Data are presented as mean \pm SEM. ** p <0.01, Student's T-test. Modified from Hermeling et al. 2022.

In addition, this cysteine was situated at the start of the first zinc finger domain. Firstly, we mutated lysine (K) 411 into alanine (A) to determine if this K is indeed part of NLS and required for KLF-1 nuclear translocation. The positive charged lysine in NLS is supposed to strongly binds to importin (Melén et al. 2003), which transports protein across the nuclear membrane. Secondly, we proceeded by mutagenizing cysteine (C) 419 into serine (S) to structurally mimic cysteine without the thiol. When we exposed animals to H_2O_2 treatment, both mutated KLFs demonstrated a strongly reduced number of KLF-1- positive nuclei (Fig. 3.33.B and 3.33.C). This data suggest that the predicted NLS and cysteine are indeed necessary for ROS-induced KLF-1 nuclear translocation.

Next, we wanted to determine if this decrease in nuclear KLF-1 presence was caused by decreased thiol modification capacity or by protein instability. Therefore, we used *wwp-1* RNAi, as we have shown that WWP-1 regulates KLF-1 nuclear translocation in a non-ROS dependent manner (Fig. 3.11). Surprisingly, also *wwp-1*

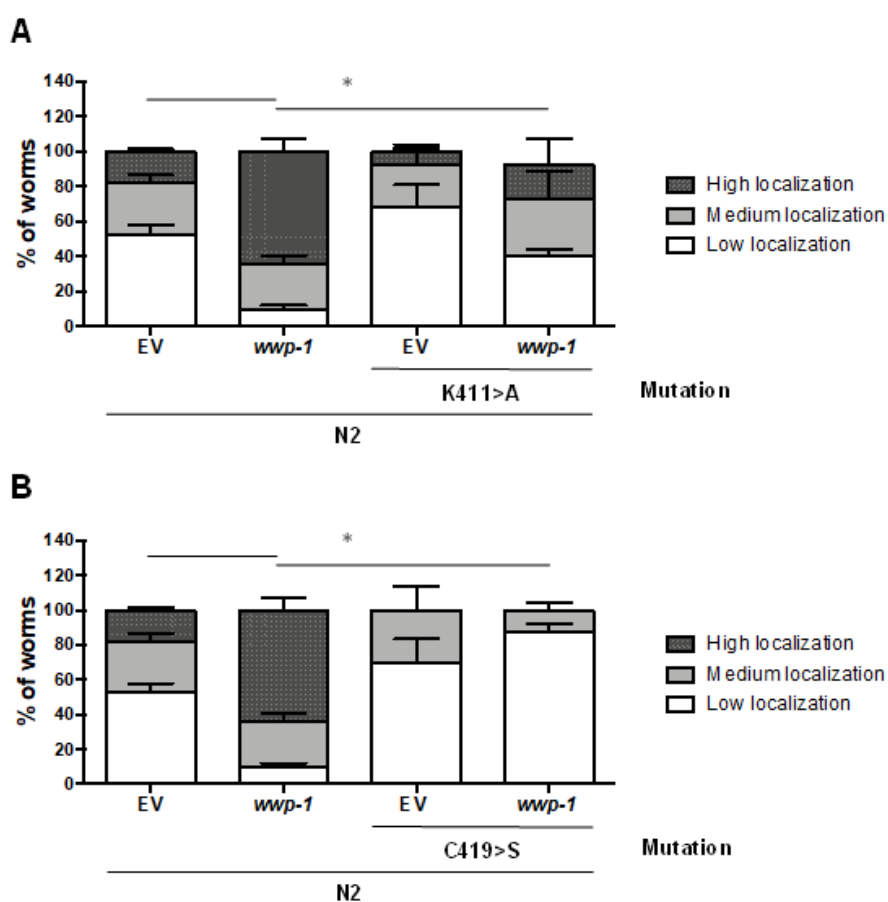


Fig 3.34 Mutagenesis of NLS and cysteine 419 decreases WWP-1-mediated KLF-1 nuclear translocation

A) *Klf-1* sequence with nuclear localization sequence (NLS) and zinc finger domains highlighted **B)** Number of KLF-1-positive nuclei in one-day-old WT animals with KLF-1 mutations at respectively lysine (K) 411 and cysteine (C) 419 to alanine (A) or serine (S) exposed to EV or *wwp-1* RNAi. n=30 animals per condition. Data are presented as mean \pm SEM. ** $p < 0.01$, Student's T-test. Modified from Hermeling et al. 2022.

depletion resulted in decreased KLF-1 presence in the nucleus in both KLF-1 mutants (Fig.3.34). So, although the nuclear localization of KLF-1 was reduced upon H_2O_2 treatment, also *wwp-1* RNAi showed a decrease in KLF-1-positive nuclei, suggesting that C 419 could also be required for KLF-1 protein structure and stability.

3.10 Thiol alteration-sensitive p38 MAPK components: SEK-1 and NSY-1

To analyse whether one of the upstream components in KLF-1 nuclear translocation are regulated by oxidized-induced thiol modification, we first had to find potential interaction partners. To achieve this, we performed a CO-IP and consequently mass spectrometry on WT and *isp-1;ctb-1* animals expressing *klf-1-FLAG*. The potential interaction partners are enlisted in Supplementary Table. 2. We decided to focus on SAPK/ERK kinase-1 (SEK-1), a mitogen-activated protein kinase (MAPK) kinase, as it was previously been proposed to regulate transcription factors and the p38 MAPK signalling cascade is thiol modification sensitive (Fig. 3.35). As SEK-1 was reported to function together with upstream kinase Neuronal SYmmetry-1 (NSY-1), which is the ortholog of human MAPKKK, we investigated the KLF-1 nuclear translocation in WT and *isp-1;ctb-1* animals upon *nsy-1* and *sek-1* RNAi.

Interestingly, while *nsy-1* and *sek-1* depletion in WT animals had no effect, suppression in *isp-1;ctb-1* mutant significantly decreased the KLF-1 nuclear translocation (Fig. 3.36). Thus, this suggests that p38 MAPK signalling might be involved in the regulation of KLF-1 nuclear translocation.

Next, we wanted to investigate the missing link between increased H_2O_2 levels and activation of NSY-1. One of the proposed mechanisms of H_2O_2 activation of NSY-1 is via the redox enzyme TRX (Saitoh et al. 1998; Pramanik and Srivastava 2012). In mammals, TRX inhibits AKS1, the mammalian homolog of NSY-1 by forming a TRX/ASK1 complex. Upon availability of H_2O_2 , TRX undergoes thiol modification and

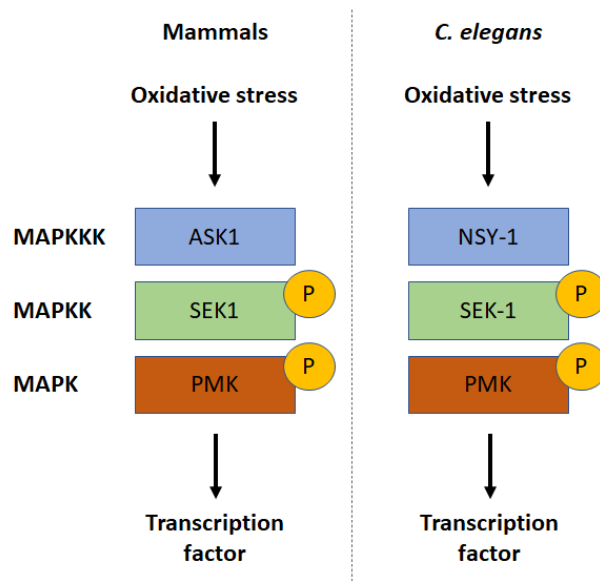


Fig 3.35 Schematic overview of the p38 MAPK signalling cascade

The p38 MAPK proteins: (left) mammals, (right) *C. elegans*.

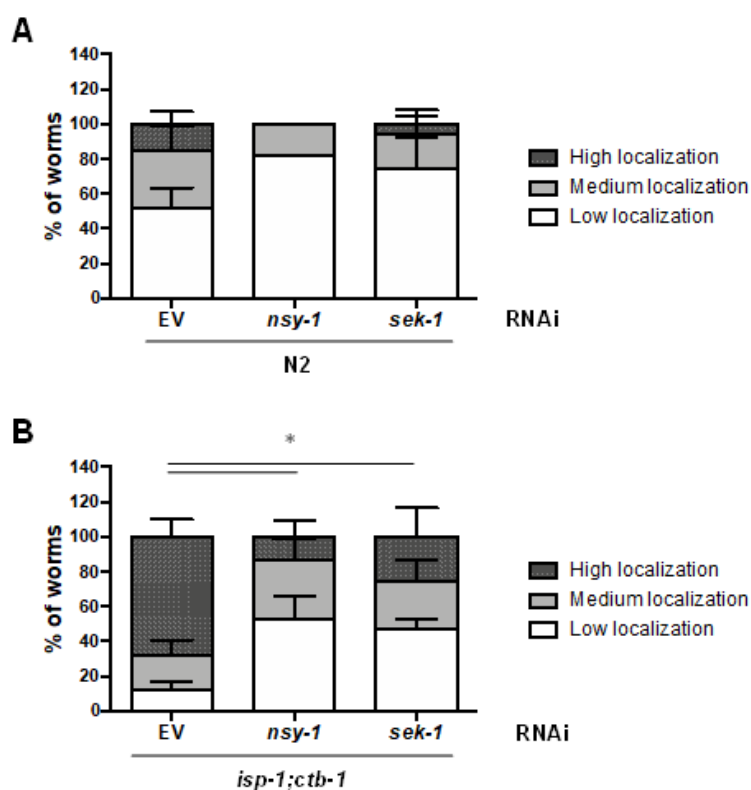


Fig 3.36 p38 MAPK signalling pathway is mediated KLF-1 nuclear translocation

Number of KLF-1-positive nuclei in one-day-old WT and *isp-1;ctb-1* animals with either EV, *nsy-1* or *sek-1* RNAi. **A)** WT animals. **B)** *isp-1;ctb-1* animals. n=30 animals per condition. n=10 animals for WT *nsy-1* RNAi condition. Data are presented as mean \pm SEM. * $p < 0.05$, Student's T-test. Modified from Hermeling et al. 2022.

releases and activates ASK1 (Saitoh et al. 1998; Pramanik and Srivastava 2012). To determine if nematode TRX plays a role in KLF-1 nuclear translocation, we performed TRX suppression in WT and *isp-1;ctb-1* animals. *C. elegans* have 5 isomers of TRX, namely *trx-1*, *trx-2*, *trx-3*, *trx-4* and *trx-5*. Remarkably, *trx-4* RNAi showed a slight increased trend in WT worms, which was also observed in WT worms treated with AA (Fig. 3.37.A) (Cores 2015). However, upon *trx-1* and *trx-4* RNAi KLF-1 nuclear translocation is diminished in *isp-1;ctb-1* animals, which is contradictory to WT animals (Fig. 3.37.B). In summary, TRX seems to regulate KLF-1 nuclear translocation, however the exact mechanism remains unclear.

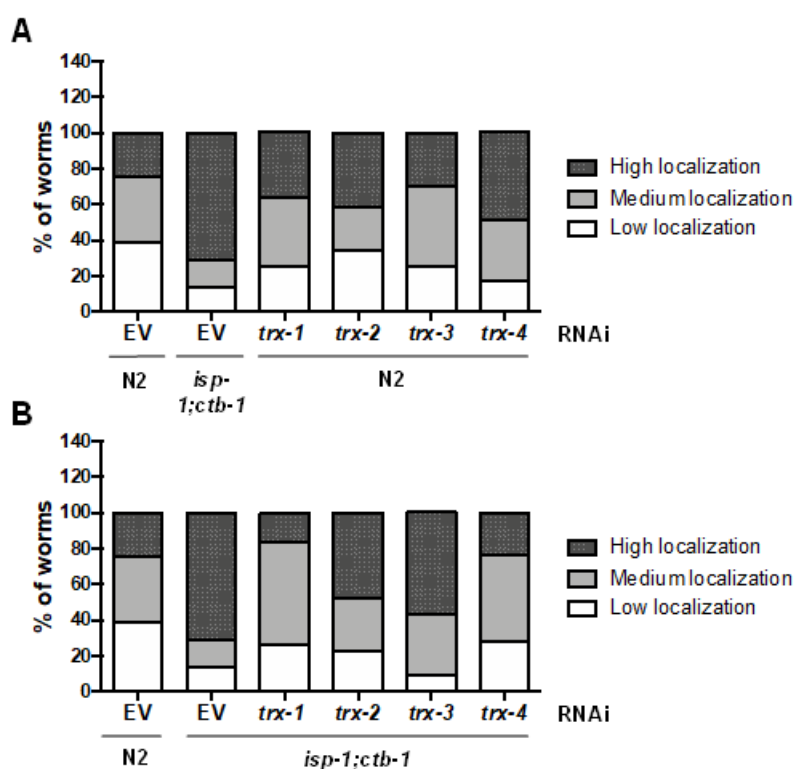


Fig 3.37 TRX-1 and TRX-4 may regulate KLF-1 nuclear translocation via NSY-1

Analyses of number of KLF-1-positive nuclei in one-day-old WT and *isp-1;ctb-1* animals with either EV, *trx-1*, *trx-2*, *trx-3* or *trx-4* RNAi. **A)** WT animals. **B)** *isp-1;ctb-1* animals. n=20 animals per condition. All experiments were only performed only twice. Data are presented as mean. Modified from Hermeling et al. 2022.

3.11 KLF-1 nuclear translocation is regulated by conserved MAPK component; PMK-3.

Next, we further investigated p38 MAPK genes as potential candidates for the KLF-1 nuclear translocation pathway. P38 MAPK signalling cascade is activated by

oxidative stress and involves MAPKKK/NSY-1 and MAPKK/SEK-1 (Tanaka-Hino et al. 2002; Hoyt et al. 2017; Sagasti et al. 2001). This cascade results in activation of downstream effector kinase PMK-1. We performed a kinases and phosphatases screen to find candidates for the KLF-1 nuclear translocation pathway upon AA treatment (Cores 2015). Worms were grown on RNAi of specific candidates and when they were D1 they were exposed to AA and scored for KLF-1-positive nuclei. Among these genes, we assayed many of the kinases belonging to the p38 MAPK family. The strongest decrease in AA-induced KLF-1 nuclear translocation was detected with *pmk-3* (Cores 2015).

In order to test if PMKs are also regulatory in our *isp-1;ctb-1* mutant, we investigated KLF-1 nuclear translocation in WT and *isp-1;ctb-1* animals upon *pmk* RNAi. Suppression of *pmk-1*, *pmk-2* or *pmk-3* did not induce KLF-1 nuclear translocation in WT animals (Fig. 3.38.A). Remarkably, suppression of all three *pmk* members resulted in a reduced KLF-1 nuclear translocation in *isp-1;ctb-1* animals (Fig. 3.38.B). Furthermore, combined *pmk-1*, *pmk-2* and *pmk-3* (*pmks*) RNAi showed a strong reduction of KLF-1 nuclear localization. In addition to the effect demonstrated on nuclear localization, *pmk-1*, *pmk-2* and *pmk-3* depletion reduced the lifespan of *isp-1;ctb-1* animals (Fig. 3.39.A). While *pmk-1* and *pmk-2* depletion demonstrated a stronger effect on longevity than *pmk-3* depletion, they also decreased the lifespan of

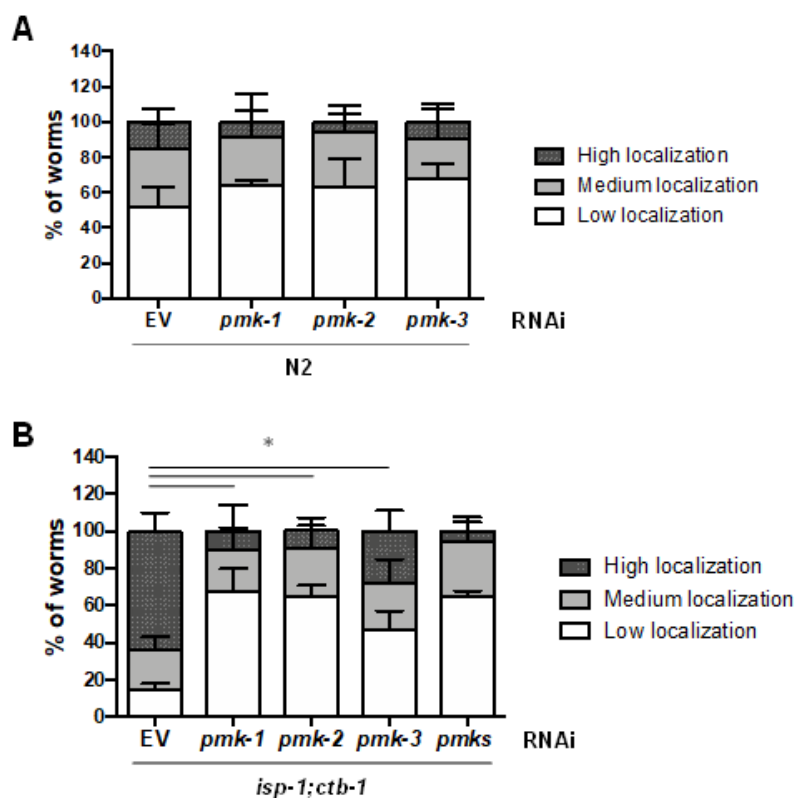
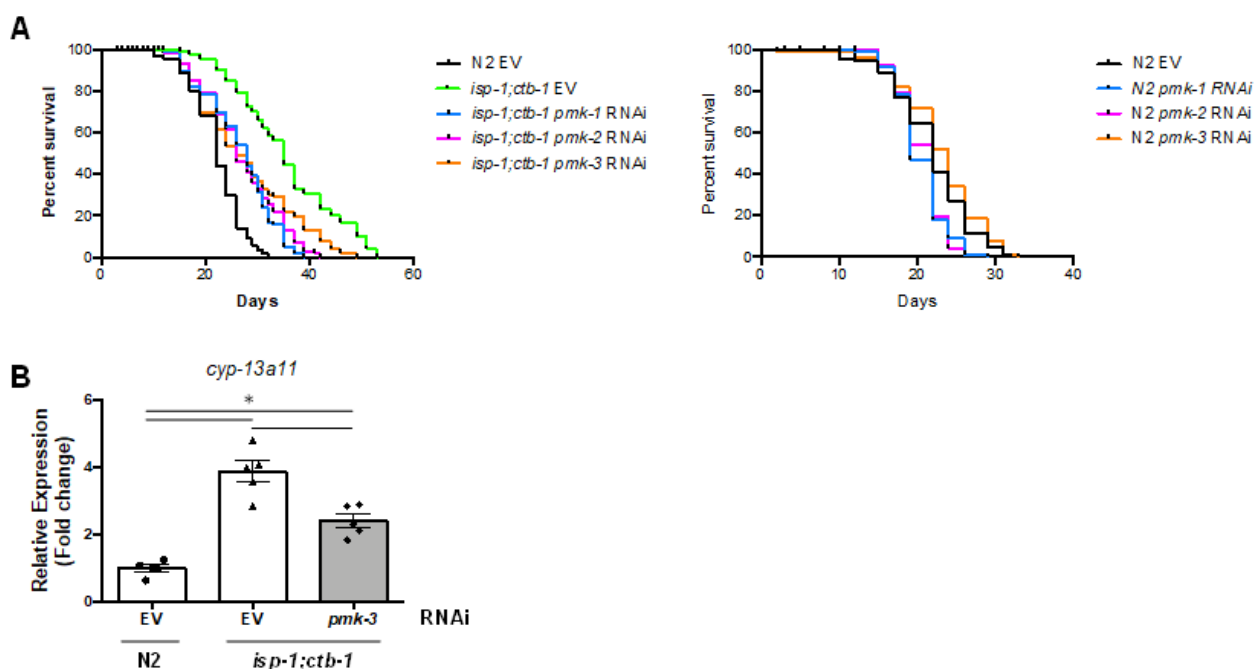


Fig 3.38 PMKs mediate the nuclear localization of KLF-1 in *isp-1;ctb-1* mutant

KLF-1 nuclear translocation assayed by number of KLF-1-positive nuclei in WT and *isp-1;ctb-1* animals on day 1 of adulthood. RNAi was either EV, *pmk-1*, *pmk-2* or *pmk-3* RNAi. **A)** WT animals. **B)** *isp-1;ctb-1* animals. For *pmks* treatment all three *pmks* were combined. $n=30$ animals per condition. $n=10$ animals for *isp-1;ctb-1 pmks* condition. Data are presented as mean \pm SEM. $*p<0.05$, Student's T-test. Modified from Hermeling et al. 2022.

WT animals (Fig. 3.39.A). Moreover, WT animals upon *pmk-1* and *pmk-2* depletion looked paler and were less moving in comparison to animals on *pmk-3* RNAi. Therefore, suggesting PMK-3 as mediator of longevity in *isp-1;ctb-1* mutant. This reduction of longevity seems to correlate with decreased *cyp* expression levels in *isp-1;ctb-1* animals as our lab previously demonstrated (Cores 2015). In short, expression levels of *cyp-13a11* and *cyp-13a7* were reduced by *pmk-1*, *pmk-2* or *pmk-3* depletion in *isp-1;ctb-1* animals. While *cyp-14a1* levels showed a decrease only upon *pmk-3* depletion. Overall the strongest reduction, which resulted in similar expression levels as *klf-1* depletion, was achieved by *pmk-3* suppression. This, we confirmed with qPCR of *cyp-13a11* (Fig. 3.39.B). Altogether, this data reinforced the idea of *pmk-3* as

**Fig 3.39 PMK-3 is mediating cyps-induced longevity**

A) WT (right) and *isp-1;ctb-1* (left) lifespans on control and *pmk-1*, *pmk-2* or *pmk-3* RNAi. $n=200$ worms per condition. **B)** *cyp-13a11* expression levels was assessed by qPCR at first day of adulthood in one-day-old WT and *isp-1;ctb-1* animals upon control or *pmk-3* RNAi. $n=4$ per condition. Data were normalized on N2 EV and are presented as mean \pm SEM. $*p<0.05$, Student's T-test. Modified from Hermeling et al. 2022.

regulator of the KLF-1 nuclear translocation in *isp-1;ctb-1* mitomutants.

Despite the evidence that p38 MAPK signalling is regulating KLF-1 nuclear translocation, the mechanism of activation is still unclear. Therefore, to identify potential phosphorylation sites on KLF-1, we analysed the *klf-1* sequence using NetPhos 3.1 (Blom et al. 2004), a serine, threonine, tyrosine phosphorylation sites prediction server, and focussed on p38 MAPK specific candidates. We found three predicted phosphorylation site candidates on KLF-1, namely serine (S) 39, serine 280 and tyrosine 178. Next, we mutagenized S39 and S280 of the *klf-1-yfp* construct into alanine (A), due to their high phosphorylation score. The mutagenesis of S into A should result into an inactive phosphorylated mutant. When we expressed these constructs in *C. elegans*, only S39 expressed YFP signal and therefore we focussed on S39 (Fig. 3.40.A). The S39>A mutant upon H₂O₂ treatment was unable to translocate KLF-1 to the nucleus (Fig 3.36.B). Next, we mutagenized S39 in aspartate acid (D), to mimic a constitutively active phosphorylation form. However, this active form was insufficient to increase the number of nuclear KLF-1 (Fig. 3.40.B).

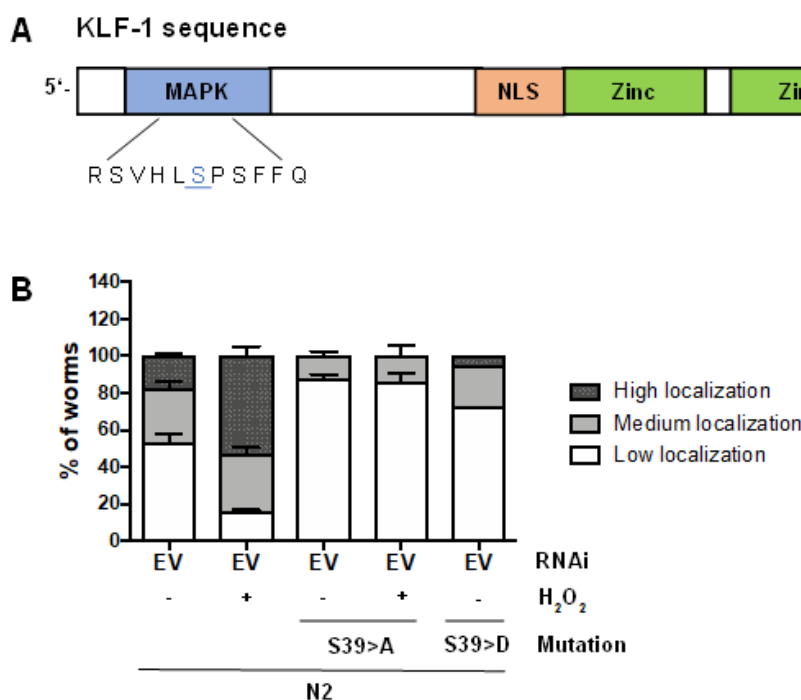


Fig 3.40 PMK-3 is regulating KLF-1 nuclear translocation by phosphorylation of serine 39

A) *Klf-1* sequence with p38 MAPK site, nuclear localization sequence (NLS) and zinc finger domains highlighted **B)** Number of KLF-1-positive nuclei in one-day-old WT animals with KLF-1 mutations at respectively serine 39 to alanine (A) or aspartic acid (D) with or without 10 mM H₂O₂ treatment. n=30 animals per condition. n=10 animals for S39>D EV condition. Data are presented as mean ± SEM.

***p*<0.01, Student's T-test.

Further investigation is required to determine if this is due to increased protein instability, decreased protein import or if multiple MAPK sites requires phosphorylation to translocate KLF-1 to the nucleus.

4. Discussion

We have shown that ETC complexes I and III generate ROS during L4, which is essential to translocate KLF-1 to the nucleus. Moreover, we demonstrated *de novo* data that ROS compound H_2O_2 is used as second messenger, through regulation of SOD-3, PRDX-3 and VDAC-1. SOD-3 is generating H_2O_2 by metabolises of $O_2^{\cdot-}$, PRDX-3 is reducing H_2O_2 and VDAC-1 is transporting H_2O_2 . This L4 ROS pulse induces a strongly increased oxidized cytosolic redox state in D1 *isp-1;ctb-1* animals. Finally, we provide evidence that p38 MAPK pathway and especially PMK-3 might sense the oxidized redox state and be responsible for regulating KLF-1 nuclear localization by phosphorylation (Fig. 3.41).

4.1 Identification of mtROS as inducer of KLF-1-mediated mitohormesis

We observed that KLF-1 is located in the nucleus in D1 *isp-1;ctb-1* mitomutant, while in WT animals the KLF-1 was mainly present in the cytosol (Fig. 3.1). This correlates with the role of transcription factors as “nuclear messengers”, as they convert signals into alteration in gene transcription (Adcock and Caramori 2009). ETC suppression during developmental stages has been reported to be necessary for longevity (Durieux, Wolff, and Dillin 2011). Similar, mild oxidative stress during larval

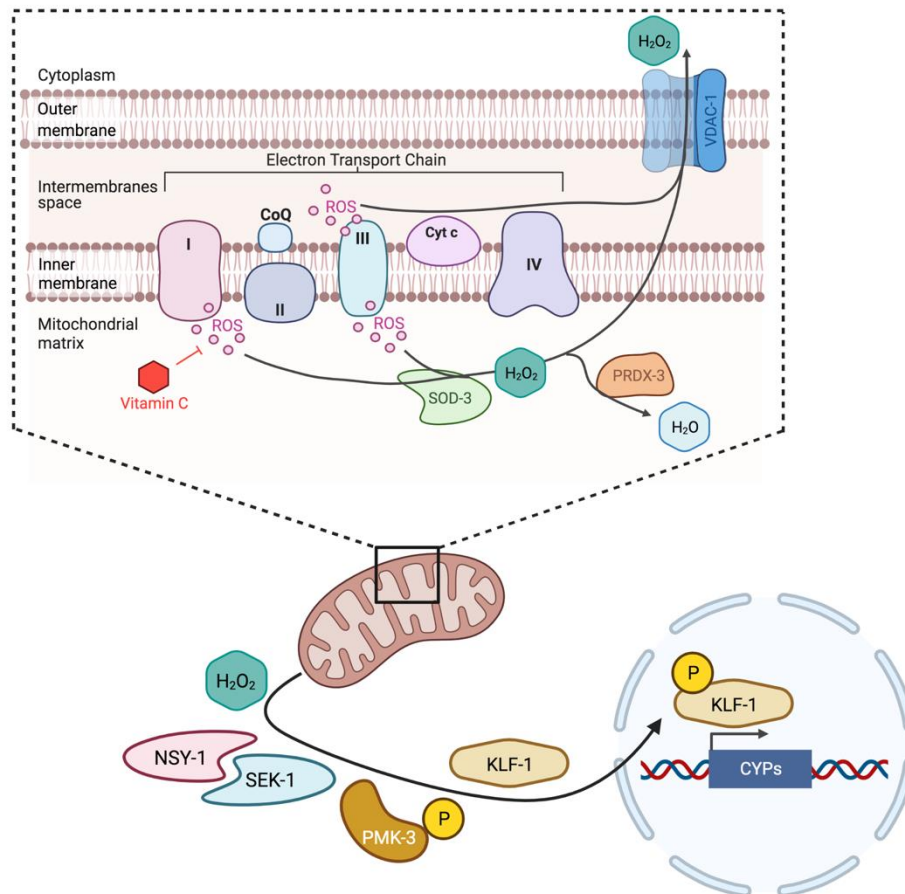


Fig 3.41 Overview of KLF-1 activation in *C. elegans*

The figure represents a simplified version of the mechanism behind KLF-1 activation, based on our results. Created with BioRender.com. Modified from Hermeling et al. 2022.

was sufficient to induce prolonged lifespan (Rascón and Harrison 2010). Therefore, we hypothesised that oxidative stress translocates KLF-1 to the nucleus in *isp-1;ctb-1* mutant. Indeed, the KLF-1 nuclear translocation was increased in WT animals when inducing oxidative stress in developmental stages by treatment with PQ and AA (Fig. 3.2). Moreover, treatment with antioxidants was sufficient to diminish the nuclear translocation of KLF-1 in mitomutant *isp-1;ctb-1* (Fig. 3.5). Furthermore, oxidative stress during larval stages was sufficient to induce longer lifespan in WT animals, while not in the *klf-1(tm1110)* mutant (Fig. 3.3). Altogether, this suggests oxidative stress in the form of ROS as activator during developmental stages, which translocate transcriptional factor KLF-1 to the nucleus during adulthood, which we previously suggest as a key characteristic for longevity (Herholz et al. 2019).

An array of our data suggests a mitohormesis process in *isp-1;ctb-1* mutant: (I) The amount of oxidative damaged proteins, measured by carbonylation, is decreased in day-five-old animals, (II) Increased resistance due to elevated expression of genes

encoding proteins involved in phase I xenobiotic detoxification, particularly CYPs, (III) increased mitochondrial ROS production in L4 *isp-1;ctb-1* animals (Fig. 3.4) (Herholz et al. 2019). This suggests L4-produced H₂O₂ may be the low stress signal required for activation of hormesis. This proof of principle has already been described in *C. elegans*, for example *memo-1* depletion increases NADPH oxidases-produced ROS and induces increased transcriptional levels of UGTs and GSTs (de Haes et al. 2014). Blocking the early low stress signal, by inhibiting mitochondrial complex III-produced ROS during late larval stages decreases oxidative stress resistance in *isp-1;ctb-1* mutant (Fig. 3.6 and 3.7.B). Lastly, WT animals have increased oxidative stress resistance only upon late larval AA treatment, which serves as early low stress signal (Fig. 3.7.A). This is all in agreement with the mitohormetic theory (Yun and Finkel 2014).

Our study showed that life-extending mitohormetic response as observed in our mitochondrial dysfunctional model arise from a signalling pulse of mtROS between L3 and D1 (Fig. 3.6 and 3.7). Remarkably, this correlates with the developmental phases when the majority of somatic mitochondrial biogenesis occurs (I. Bratic et al. 2009) and when the aerobic respiration peaks in development (Vanfleteren and de Vreese 1996; Penkov et al. 2020; Smith and Sturmey 2013). Both processes can lead to increased mtROS production, which may explain the origin of our signalling pulse. This phenotype was observed by others that stress during late developmental stages is sufficient to extend lifespan (D. K. Woo and Shadel 2011; Rea, Ventura, and Johnson 2007).

We could translocate KLF-1 to the nucleus upon Rot, mitoPQ, AA and Myxo treatment and *nuo-2*, *cyc-1* and *cco-1* RNAi during L4 (Fig. 3.8). This activation was ROS-dependent, as key ROS-producing complexes, such as complex I and III (Scialò, Fernández-Ayala, and Sanz 2017; Chouchani et al. 2014) were involved and antioxidant treatment diminished this activation (Fig. 3.10). Interestingly, the nuclear KLF-1 inducers *nuo-2*, *cyc-1* and *cco-1* have previously been described as inducers of longevity (Rea, Ventura, and Johnson 2007) and they exhibit increased mtROS (Yang and Hekimi 2010a). Moreover, *cco-1*-induced longevity was reported to be mediated by p38 MAPK components NSY-1 and PMK-1 (Bennett et al. 2017). While *atp-5* suppression was observed to induce longevity (C. Xu et al. 2018), we observed no effect on KLF-1 location. This difference might be explained by the fact that ETC-mediated longevity is dependent on ROS signalling, while ATP synthase-mediated

longevity is dependent on TOR signalling (C. Xu et al. 2018). Surprisingly, altered ATP levels are not necessarily correlated with lifespan extension (Jeremy Michael van Raamsdonk et al. 2010; Copeland et al. 2009). Thus, *atp-5* depletion or complex V dysfunction might activate a different longevity assurance pathway than KLF-1 and CYPs. The treatment with uncoupler FCCP suggests KLF-1 nuclear translocation is mitochondrial membrane potential independent. While some authors have shown with redox-active probes that low doses of FCCP stimulate mitochondrial H₂O₂ production (Zybovykh, Straud, and Roth 2010; Z. Wu et al. 2018; Brennan et al. 2006), it has been suggested that this increase is rather a FCCP-induced redistribution of already oxidized probes than enhanced O₂^{•−} generation (Budd, Castilho, and Nicholls 1997). FCCP is more commonly known for decreasing ROS production, as O₂^{•−} generation is strongly dependent on membrane potential (S. Cadenas 2018; Brand et al. 2016; Hagal Rottenberg, Covian, and Trumpower 2009). Moreover, it has been observed that FCCP induces mitophagy, which was observed to reduce ROS levels (Kane et al. 2018; Berezhnov et al. 2016). We could further investigate the relationship between FCCP treatment and mitochondrial ROS production in our model with our TOMM20-roGFP2 sensor.

4.2 WWP-1: an alternative pathway of KLF-1 activation

WWP-1, the *C. elegans* E3 ligase and orthologous to mammalian WWP1 pathway, was shown to be a positive regulator of DR-induced longevity (Carrano et al. 2009; Huang et al. 2000). E3 ligases are key components of targeting substrate proteins by ubiquitin, as post-modification or as targeting for degradation (Song et al. 2020; Balaji and Hoppe 2020). Interestingly, ubiquitinated proteome rewiring was linked to lifespan (Koyuncu et al. 2021). The mammalian WWP1 was demonstrated to target various KLFs for proteasome-dependent degradation by polyubiquitylation, for example KLF2 and KLF5 (X. Zhang, Srinivasan, and Lingrel 2004; Ceshi Chen et al. 2005; Conkright, Wani, and Lingrel 2001). However, the *C. elegans* HECT domain family ligase acts upstream of KLF-1 by poly-monoubiquitylation (Carrano, Dillin, and Hunter 2014). It is still unclear how WWP-1-mediated ubiquitylation could affect KLF-1 (Carrano, Dillin, and Hunter 2014). We could show that depletion of WWP-1 translocates KLF-1 to the nucleus in WT animals (Fig. 3.11). Proteasomal degradation appears to not impact KLF-1 translocation, as we observed no clear increase of KLF-

1 level upon proteasomal inhibition via Bor treatment (Fig. 3.12). Therefore, our data suggest that WWP-1 is a negative regulator of KLF-1, independent of proteasome degradation. This suggests WWP-1-mediated ubiquitylation either causes inhibition of KLF-1 translocation towards the nucleus or that WWP-1 is present in the nucleus and induces the nuclear export of KLF-1. Interestingly, the mammalian WWP1 is expressed in the cytoplasm, early endosomes and nucleus, while not having any nuclear localization signal (C. Chen et al. 2008; S. R. Seo et al. 2004). Moreover, KLF5 co-localizes with WWP1 in the nucleus to form a protein complex (Ceshi Chen et al. 2005). However, the mechanism behind WWP-1 targeting KLF-1 remains unclear and further investigation is required. Therefore, it would be highly interesting to investigate the localization of WWP-1 under different conditions and to understand in what subcellular compartment WWP-1 interacts with KLF-1.

The role of WWP-1 on longevity remains puzzling, as conflicting results have been reported. WWP-1 was suggested to work parallel to DAG-16 in IIS mutant longevity (Samuelson, Carr, and Ruvkun 2007; C. S. Chen et al. 2010). Meanwhile, WWP-1-mediated modulation of KLF-1 was reported to be specific for DR-mediated longevity, as *wwp-1* RNAi in insulin/IGF-1 signalling mutant or mitomutant had no effect on their lifespan (Carrano et al. 2009). This discrepancy could be explained by the use of different *wwp-1* suppression, for example *wwp-1* RNAi versus *wwp-1(ok1102)* mutant or *daf-2(e1368)* versus *daf-2(e1370)* alleles. Others suggested that WWP-1 together with E2 ligase UBC-18 can modulate both stress response and DR pathways (Carrano and Hunter 2015). Upon DR KLF-1 is poly- monoubiquitylated by WWP-1/UBC-18 complex and thereby inducing DR-induced longevity, while upon stress an unknown substrate is ubiquitylated which induced the DAF-16-induced longevity by increasing stress resistance. This would be in agreement with the WWP-1 modulation on lifespan of WT animals (Fig. 3.13.H), as *wwp-1* suppression reduces lifespan in stress environments, like lifespans at 25°C or pore-forming toxin or pathogens (C. S. Chen et al. 2010; Carrano et al. 2009). Our study demonstrates that WWP-1 in our *isp-1;ctb-1* mitomutant animals likewise had no regulatory function, as *wwp-1* RNAi had no effect on *cyps* expression levels (Fig. 3.13) and *isp-1;ctb-1* longevity (Fig. 3.14). Therefore, our data suggest that WWP-1 indeed regulates subcellular localization of KLF-1, however it has no role in mitomutant-induced longevity. The difference between the WWP-1 and mitomutant-mediated KLF-1 pathways is probably caused by ROS signalling, as antioxidant treatment showed that WWP-1 regulation is not directly

altered (Fig. 3.11). Further analysis needs to be performed to determine the exact role of WWP-1 and its interplay with KLF-1 in longevity.

Klf-1 is expressed in hypodermis and some neurons but mainly in the intestine, which is key tissue for lipid storage and metabolism in *C. elegans* (Brock, Browse, and Watts 2006; Hashmi et al. 2008). It was observed that *klf-1* RNAi in WT animals resulted in an increased fat storage (Hashmi et al. 2008; Brock, Browse, and Watts 2006). Both KLF-2 and KLF-3 have been reported to be important for lipid metabolism (Ling et al. 2017). *Klf-2* is expressed in the intestine and therefore linked to lipid metabolism. KLF-3 has been shown to control β -oxidation of FA and autophagy (J. Zhang et al. 2013; Ling et al. 2017; J. Zhang et al. 2011). Altogether, these observations emphasise KLFs at the interplay of lipid metabolism in *C. elegans*. Our data supports previous reports that KLF-1 expression regulates lipid storage and metabolism, as higher levels of KLF-1 results in a decreased lipid levels, in the form of neutral lipids, in our *isp-1;ctb-1* mitomutant animals (Fig.3.14.A). This was dependent on increased nuclear presence of KLF-1, as *klf-1* RNAi restored lipid levels. Interestingly, the *wwp-1* is expressed in the intestine and regulation of DR-induced longevity was reported to be site-specific at intestine by tissue-specific feeding of *klf-1* RNAi (Carrano et al. 2009; Carrano, Dillin, and Hunter 2014). In our data *wwp-1* suppression in WT animals had no effect on lipid levels (Fig.3.14.A), however this assay only assayed neutral lipid storage. More in depth investigation is required to determine the role of WWP-1 and KLF-1 on the lipid metabolism and the effect on longevity.

4.3 Regulation of mtROS release

We used the roGFP2-Orp1 probe to create a *de novo* OMM H₂O₂ sensor by adding a *tomm20* targeting sequence to the probe. TOMM20 is a mitochondrial import receptor at the OMM facing the cytosol (Siillner et al. 1969; Abe et al. 2000) and therefore positioning this sensor just outside of the mitochondria. This sensor is a novel and much needed method of measuring H₂O₂ levels just on the outside of mitochondria in the cytosol and therefore enabling us to follow mtROS release into the cytosol. For example, we could demonstrate in the muscle the increased oxidization at the outside of the mitochondria by treatment with H₂O₂ (Fig. 3.20). This method enabled us to directly show an increased mtROS release into the cytosol in *isp-1;ctb-1* during L4

(Fig. 3.21). Consequently, this highlighted mtROS as signalling pulse. While in gut we could not use the sensor for imaging, due to autofluorescence of the gut bacteria (Fig. 3.22), we could demonstrate increases oxidized roGFP2-Orp1 in L4 *isp-1;ctb-1* mutant by immunoblot (Fig. 3.23). Moreover, we could determine the role of mitochondrial *prdx-3*, *sod-3* and *vdac-1* in KLF-1 nuclear localization (Fig. 3.27). *Prdx-3* suppression induces increased mtROS release in L4 WT animals (Fig. 3.23.B), which is likely due to decreased H₂O₂ reducing capacity. *Sod-3* and *vdac-1* RNAi inhibit mitochondrial H₂O₂ release, which is probably due to decreased H₂O₂ generation (Fig. 3.23.C) and reduced transport capacity, respectively (Fig. 3.26).

The role of PRDX and SOD are well-described as redox enzymes and are previously connected to signalling cascades and longevity (W. bin Wu et al. 2016; Oláhová et al. 2008; Jeremy M. van Raamsdonk and Hekimi 2009; Z. Wu et al. 2018). PRDX-2 has been described as key regulator of metformin and insulin/IGF-1-induced longevity (de Haes et al. 2014; Oláhová and Veal 2015). While we observed a decreased lifespan in *prdx-2* mutants, it remains a possibility that PRDX-2 plays a role in KLF-1 activation (Fig.3.17). In our RNAi screen, we were lacking *prdx-2* RNAi and consequently did not show the direct effect of PRDX-2 on KLF-1 activation as we only investigated the lifespan (Fig.3.16). Moreover, in our co-IP we observed PRDX-2 being pulled down in all our samples, even the negative control without *klf-1-FLAG* construct (Fig. 3.32). This suggests our FLAG antibody has an affinity for PRDX-2 and therefore interfering with the co-IP. To address this, it would be interesting to determine the effect of *prdx-2* depletion in our mitomutant by crossing *prdx-2* mutants in *isp-1;ctb-1*. We showed that *prdx-3* depletion results in increased mtROS release, improved xenobiotic detoxification capacity and longer lifespan, which is KLF-1 and CYPs-dependent (Fig. 3.19, 3.25. and 3.26). Contradictory, others observed no longer lifespan and less oxidative stress resistance in WT animals upon *prdx-3* suppression (Ranjan et al. 2013). These differences may be explained by the use of RNAi versus mutants, as both inhibitions probably result in different mtROS levels in the mitochondrial matrix. Furthermore, the *prdx-3* RNAi efficiency may vary. The nuclear translocation of KLF-1 by mtROS is probably threshold-dependent, as low mtROS level is probably insufficient to induce translocation of KLF-1 and high mtROS level is harmful. Therefore, different levels of mtROS results in various effects. Similarly, antioxidants have been demonstrated to have a beneficial U-shaped dose-response (Desjardins et

al. 2017). To further elucidate the beneficial threshold level of mtROS, it will be interesting to design an IMM redox sensor to further investigate this.

Remarkably, worms without *sods* expression are viable and showed a normal lifespan. However, these animals are highly sensitive to various stresses (Jeremy Michael van Raamsdonk and Hekimi 2012; Jeremy M. van Raamsdonk and Hekimi 2009). Moreover, PQ-induced longevity was described to be *sod-3*-dependent (Yee, Yang, and Hekimi 2014). This is in agreement with our data, whereas *sod-3* suppression in WT animals resulted in a normal lifespan and SOD-3 is necessary in *isp-1;ctb-1* to maintain their increased xenobiotic detoxification response (Fig. 3.29). Others demonstrated that overexpression (OE) of *sod-1* results in increased steady-state H₂O₂ levels *in vivo* and longer lifespan in WT animals, which is DAF-16 dependent (Cabreiro et al. 2011). Interestingly, simultaneous overexpression of H₂O₂ reducing enzymes *ctl-1*, *ctl-2* and *ctl-3* in *sod-1* OE animals had no effect on the increased lifespan (Cabreiro et al. 2011). It might be that H₂O₂ signalling happens locally (K. Chen et al. 2008; H. A. Woo et al. 2010) and therefore peroxisomal catalase would not reduce it. The role of catalases on second messenger H₂O₂ remains unclear.

Previously, H₂O₂ was often believed to diffuse across membranes. However, some membranes are poorly permeable (Bienert, Schjoerring, and Jahn 2006). Thus, this suggests H₂O₂ membrane permeability is either dependent on the lipid composition of the membrane or available transporter or channels. The first described transporters of H₂O₂ were the aquaporins (Bienert, Schjoerring, and Jahn 2006; Cordeiro 2015; Miller et al. 2010). Recent studies in cancer research introduced VDAC as new potential transporter of H₂O₂ across the OMM (L. Zhang et al. 2020; DeHart et al. 2018). While aquaporin depletion had no effect on KLF-1 nuclear localization in *isp-1;ctb-1* mitomutant, *vdac-1* RNAi diminished the presence of KLF-1 in the nucleus (Fig. 3.25) and downstream *cyp* expression (Fig. 3.28 and 3.29). However, the exact mechanism of how VDAC is transporting mtROS remains unclear. As VDAC can either facilitate transport as part of the mitochondrial permeable transition pore (mPTP) or mitochondrial VDAC pores (Hagai Rottenberg and Hoek 2017; J. Kim et al. 2019). Remarkably, it has been observed that long-lived mammals correlate with decreased gene expression and protein levels of complex I subunits, such as NDUFV2 and NDUFS4, and low abundance of VDAC expression (Mota-Martorell et al. 2020). This is in agreement with the observation that *vdac-1* OE in *C. elegans* shortens lifespan (Zhou et al. 2019). Altogether, these observations might suggest a role for VDAC in

longevity of ETC mutants. Moreover, *vdac-1* OE mutant is highly sensitive to oxidative stressor PQ (Zhou et al. 2019). *Vdac-1* OE might increase the capacity of H₂O₂ transport and consequently increase the cytosolic mtROS levels. These levels become harmful instead of being inducers of cytoprotective mechanisms. This again emphasizes the importance of achieving the correct threshold of ROS levels. Further experiments should aim to unravel the exact role of VDAC as mtROS transporter and its role in longevity.

Previously, ROS was viewed as oxidative stress and associated with various diseases, such as diabetes, cancer and neurodegenerative disorders (Wiederkehr and Wollheim 2006; Tatsuta and Langer 2008; Ristow and Williams 2006). Nowadays, H₂O₂ is widely implicated in longevity through reversible oxidation of thiol proteins (Parvez et al. 2018; Forman, Maiorino, and Ursini 2010; M. P. Murphy et al. 2011; Kiley and Storz 2004; Winterbourn and Hampton 2008). However, the remaining challenge for redox signalling is in understanding how H₂O₂ can oxidize particular signalling pathways. In other words, how is H₂O₂ signalling specificity achieved? Potential mechanisms that might influence specificity are pH-mediated thiol reactivity (pK_a), H₂O₂ diffusion, H₂O₂ production sites, redox enzymes and peroxymonocarbonate (Winterbourn 2020; Ferrer-Sueta et al. 2011). Based on current evidence, it is likely that multiple mechanisms play a role. There is still much to learn and advances in techniques, like thiol proteomics could help identify the mechanisms behind redox signalling on thiol proteins.

4.4 PMK pathway regulates KLF-1-mediated longevity

Our analysis of potential KLF-1 interaction partners via co-IP led to the identification of the homolog of p38 MAPKK component SEK-1 (Fig. 3.32). This kinase is part of the p38 MAPK signalling pathway (Fig 3.25) and has previously been described as regulator of transcription factors upon oxidative stress, namely DAF-16, RNT-1 and SKN-1 (Inoue et al. 2005a; Kondo et al. 2005; K. Lee et al. 2012). Moreover, SEK-1 was described in DR-induced longevity, as it induces a xenobiotic detoxification program (Chamoli et al. 2020). The p38 MAPK pathway has been well characterized as sensor of different kind of cellular stresses and inflammatory cytokines (Kyriakis and Avruch 2012). Together with the upstream kinase ASK, orthologous of nematode *nsy-1*, and the downstream kinases *pmk-1*, *pmk-2* and *pmk-*

3, this pathway is required for the activation of innate immunity and function and differentiation of specific neurons (Chuang and Bargmann 2005; Sagasti et al. 2001; Tanaka-Hino et al. 2002; Hoyt et al. 2017).

Further analysis of the PMKs on lifespan and *cyps* expression levels in *isp-1;ctb-1* mutant underlined PMK-3 as key regulators of KLF-1 nuclear localization (Fig. 3.38). While *pmk-1* and *pmk-2* RNAi demonstrated reduced presence of KLF-1 in the nucleus in *isp-1;ctb-1* animals (Fig.3.38), not all downstream CYPs were reduced (Fig.3.39.B) (Cores 2015). Moreover, we observed decreased lifespan in WT animals upon *pmk-1* and *pmk-2* RNAi (Fig.3.39), which suggests toxicity due to suppression. This might cause the decreased lifespan in *isp-1;ctb-1* animals. Therefore, PMK-1 and PMK-2 seem not to directly regulate longevity in *isp-1;ctb-1*. In agreement with our data, PMK-3 is previously been described as key regulator in mitomutant-induced longevity, which was suggested to be under the control of SEK-3 (Munkácsy et al. 2016). The authors described the mitochondrial-associated degradation pathway, including SEK-3 and PMK-3, as necessary for longevity in *isp-1(qm150)*. Interestingly, they also found SEK-1 in their targeted screen for factors regulating reporter gene *Ptbb-GFP* expression in *isp-1(qm150)* mutant by RNAi (Munkácsy et al. 2016). However, they only investigated the effect of *pmk-3* RNAi on lifespan of different mitomutants. Therefore, it would be interesting to investigate the role of SEK-3 in *isp-1;ctb-1* longevity. The use of *pmk-3* RNAi or *pmk-3(ok169)* mutant was sufficient to diminish increased lifespan in genetic and RNAi-induced mitomutant, including *isp-1(qm150)*, *nuo-6(qm200)*, *nuo-2* and *cco-1* RNAi (Munkácsy et al. 2016). This complements our data that *nuo-2* and *cco-1* RNAi induce KLF-1 nuclear localization (Fig. 3.8) and suggests similar PMK-3 regulation as in *isp-1;ctb-1* animals. The sensing of oxidative stress by NSY-1 and activation of p38 MAPK has been described in mammals and *C. elegans* (An and Blackwell 2003; Hourihan et al. 2016; Naji et al. 2018). While the exact mechanism of activation remains unclear, the thiol side chain of NSY-1 is strongly suggests to be the key activation side (Saitoh et al. 1998). This is in agreement with our observation that DTT treatment decrease the presence of KLF-1 in the nucleus in *isp-1;ctb-1* mutant (Fig. 3.27). This suggests that oxidized thiol modification is necessary for KLF-1 nuclear localization and this modification might be on NSY-1. It remains a possibility that thiol modification on KLF-1 plays a role in KLF-1 nuclear translocation, as we were unable to detect alterations by using the shift assay (Fig. 3.32).

Nowadays, there are three theories on how NSY-1 via thiol modification is activated. The first theory suggests that locally generated ROS can directly target and recruit NSY-1 (Hourihan et al. 2016). To test this possibility in our model, we need to evaluate the *nsy-1* expression and locally recruitment to OMM in WT and *isp-1;ctb-1* mutant. Our results that peroxisomal and ER-produced ROS are insufficient to induce KLF-1-mediated longevity support this hypothesis (Fig. 3.9). The second theory suggests TRX forms a complex with ASK1, mammalian homolog of NSY-1 and hereby blocks the activation. Oxidation of H₂O₂-sensitive TRX through disulphide bridge formation between Cys32 and Cys35 dislocates and activates ASK1 (Saitoh et al. 1998; Pramanik and Srivastava 2012). Contradictory, while we demonstrated that inhibition of TRX-4 further increased the KLF-1 nuclear localization upon AA treatment in WT animals (Cores 2015), we also observed decreased presence of KLF-1 in the nucleus in *isp-1;ctb-1* animals upon *trx-1* and *trx-4* RNAi (Fig. 3.33). Therefore, further research should focus on the role of TRX in KLF-1 nuclear localization. The third theory suggests PRDX, mainly PRDX-2 as cellular cytosolic H₂O₂ sensor which relays H₂O₂ signalling on NSY-1 via thiol modification (Quintin, Aspert, and Charvin 2021; Zhao and Wang, n.d.; de Haes et al. 2014b; G. Li et al. 2016).

Phosphorylation is a well-described mechanism of regulation activity of transcriptional factors. Especially, the rearranging of transcriptional factors between cytoplasm and nucleus is regulated by phosphorylation/dephosphorylation events that rely either on targeting interaction partners or on altering the recognition of the NLS or nuclear export signal (NES) on transcriptional factors. It has been suggested that phosphorylation events increase the recognition of the NLS by nuclear importers (Harreman et al. 2004; Nardozzi et al. 2010). Some mammalian KLFs have been described to possess NLS or NES. For example, SUMOylated KLF5 is mainly nuclear localized via inhibition of NES (Du et al. 2008), the NLS of KLF8 is phosphorylation sensitive (Mehta et al. 2009) and KLF6 subcellular localization, which possesses both a NLS and NES, depends on splicing variants (Rodríguez et al. 2010). The evidence for NES in KLF-1 nuclear localization seems limited as according to NES predictor LocNES NES probability on KLF-1 is low (NES score 0.206) (D. Xu et al. 2015). Nematode KLF-1 has a NLS and our data suggests phosphorylation promotes the recognition of this NLS, as we detect less nuclear KLF-1 upon mutagenesis of the phosphorylation site S29 (Fig. 3.36). Moreover, mutagenesis of NLS site K411 and C419 (Fig. 3.30 and 3.31) in mutated NLS results in decreased nuclear *klf-1* expression

upon H₂O₂ treatment and *wwp-1* RNAi. While we cannot exclude that the decreased presence of KLF-1 in the nucleus is due to conformational changes of the protein instead of suppression of KLF-1 nuclear localization signalling cascade. Our results strongly suggest that the NLS of KLF-1 is required for the nuclear targeting and the recognition is phosphorylation dependent. We tried to induce the translocation of KLF-1 to the nucleus by mutagenesis S29 in D, which might result in a constitutively active phosphorylated KLF-1. However, it seems phosphorylation of S29 is insufficient to translocate KLF-1 to the nucleus (Fig. 3.40.B). Another possibility is that both predicted phosphorylation sites are required to be phosphorylated.

The xenobiotic detoxification mechanism consists of three-phase, namely phase I till III (Settivari et al. 2017). KLF-1 is a regulator of phase I detoxification response genes, the *cyps* (Herholz et al. 2019), while transcription factor skinhead-1 or SKN-1 is a regulator of phase II detoxification response genes, mainly the *ugt* and *gst* genes (Naji et al. 2018; An and Blackwell 2003). Transcriptional factor SKN-1 is the homolog of mammalian mitochondrial transcription regulator NRF (Virbasius, Virbasius, and Scarpulla 1993) and it does not regulate the expression of most *cyp* genes (Oliveira et al. 2009; Herholz et al. 2019). Interestingly, *pmk-1* has been described as upstream regulator of SKN-1 mediated detoxification response (Inoue et al. 2005). In insulin/IGF-1 mutant SKN-1 is a negative regulator of longevity by inhibiting DAF-16 through PMK-1 (Deng et al. 2020; Troemel et al. 2006). As both transcriptional factors KLF-1 and SKN-1 are induced by oxidative stress, finetuning of the detoxification response may be performed by PMK-1 and PMK-3. However, the exact mechanism remains unclear. Altogether, these observations establish p38 MAPK signalling cascade as key regulator of lifespan through finetuning the xenobiotic response gene program.

4.6 Summary

In summary, in this work we identify the redox pathway that activates transcriptional factor KLF-1, the essential regulator of the mitomutant longevity (Fig.3.37). We placed mtROS as key signalling pulse during developmental stages, which is regulated by mitochondrial redox enzymes PRDX-3 and SOD-3. With the utilization of our *de novo* mitochondrial H₂O₂ release sensor, we further emphasised the role of VDAC-1 as ROS transporter and H₂O₂ as second messenger. Moreover,

we showed that p38 MAPK signalling cascade might be a central position in regulating lifespan in *C. elegans* mitomutants. This pathway seems to be, at least partially, conserved, as mammalian KLFs are activated by oxidative stress and regulated by phosphorylation and p38 MAPK signalling. Altogether, our work further expands the fundamental understanding of lifespan regulation. Further efforts should focus on more in depth research about ROS signalling and thiol regulation. Especially, to establish whether our results extend to mammalian system and if our observations could be used for therapeutic strategies against age-associated diseases.

References

- Abe, Yoshito, Toshihiro Shodai, Takanori Muto, Katsuyoshi Mihara, Hisayoshi Torii, Shuh-ichi Nishikawa, Toshiya Endo, and Daisuke Kohda. 2000. "Structural Basis of Presequence Recognition by The Mitochondrial Protein Import Receptor Tom20." *Cell* 100: 551–60.
- Adam-Vizi, Vera. 2005. "Production of Reactive Oxygen Species in Brain: Contribution by Electron Transport Chain and Non–Electron Transport Chain Sources." *Antioxidants & Redox Signaling* 7 (9): 1140–49.
- Adcock, Ian M, and Gaetano Caramori. 2009. "Transcription Factors." In *Asthma and COPD*, 373–80.
- Aleman, J., M. J. de la Cruz, I. Roncero, and Miquel J. 1988. "Effects of Aging on Respiration, ATP Levels and Calcium Transport in Rat Liver Mitochondria. Response to Theophylline." *Exp Gerontol* 23: 25–34.
- Altmann, Richard. 1890. *Die Elementarorganismen Und Ihre Beziehungen Zu Den Zellen*. De Gruyter. <https://doi.org/doi:10.1515/9783112366967>.
- Alzheimer, A, Hans Fö, ; Rstl, and Raymond Levy. 1991. "On Certain Peculiar Diseases of Old Age Translated and with an Introduction By." *History of Psychiatry*.
- Amador-Noguez, Daniel, Kazuo Yagi, Susan Venable, and Gretchen Darlington. 2004. "Gene Expression Profile of Long-Lived Ames Dwarf Mice and Little Mice." *Aging Cell* 3 (6): 423–41. <https://doi.org/10.1111/j.1474-9728.2004.00125.x>.
- An, Jae Hyung, and T. Keith Blackwell. 2003. "SKN-1 Links C. Elegans Mesendodermal Specification to a Conserved Oxidative Stress Response." *Genes and Development* 17 (15): 1882–93. <https://doi.org/10.1101/gad.1107803>.
- Arum, Oge, Michael S. Bonkowski, Juliana S. Rocha, and Andrzej Bartke. 2009. "The Growth Hormone Receptor Gene-Disrupted Mouse Fails to Respond to an Intermittent Fasting Diet." *Aging Cell* 8 (6): 756–60. <https://doi.org/10.1111/j.1474-9726.2009.00520.x>.
- Ashrafi, G., and T. L. Schwarz. 2013. "The Pathways of Mitophagy for Quality Control and Clearance of Mitochondria." *Cell Death and Differentiation*. <https://doi.org/10.1038/cdd.2012.81>.
- Åslund, Fredrik, Ming Zheng, Jon Beckwith, and Gisela Storz. 1999. "Regulation of the OxyR Transcription Factor by Hydrogen Peroxide and the Cellular Thiol-Disulfide Status." *Proc. Natl Acad. Sci. USA* 96: 6161–65. www.pnas.org.
- Avery, Leon, and Boris B Shtonda. 2003. "Food Transport in the C. Elegans Pharynx."
- Babior, B. M., R. S. Kipnes, and J. T. Curnutte. 1973. "Biological Defense Mechanisms. The Production by Leukocytes of Superoxide, a Potential Bactericidal Agent." *The Journal of Clinical Investigation* 52 (3): 741–44. <https://doi.org/10.1172/JCI107236>.
- Back, Patricia, Bart P. Braeckman, and Filip Matthijssens. 2012. "ROS in Aging Caenorhabditis Elegans: Damage or Signaling?" *Oxidative Medicine and Cellular Longevity* 2012. <https://doi.org/10.1155/2012/608478>.
- Balaban, Robert S., Shino Nemoto, and Toren Finkel. 2005. "Mitochondria, Oxidants, and Aging." *Cell*. Cell Press. <https://doi.org/10.1016/j.cell.2005.02.001>.
- Balaji, Vishnu, and Thorsten Hoppe. 2020. "Regulation of E3 Ubiquitin Ligases by Homotypic and Heterotypic Assembly." *F1000Research*. F1000 Research Ltd. <https://doi.org/10.12688/f1000research.21253.1>.

- Balchin, David, Manajit Hayer-Hartl, and F. Ulrich Hartl. 2016. "In Vivo Aspects of Protein Folding and Quality Control." *Science*. American Association for the Advancement of Science. <https://doi.org/10.1126/science.aac4354>.
- Bandara, Aloka B., Joshua C. Drake, and David A. Brown. 2021. "Complex II Subunit SDHD Is Critical for Cell Growth and Metabolism, Which Can Be Partially Restored with a Synthetic Ubiquinone Analog." *BMC Molecular and Cell Biology* 22 (1). <https://doi.org/10.1186/s12860-021-00370-w>.
- Banerjee, Aditi, Jing Yu Lang, Mien Chie Hung, Krishanu Sengupta, Sushanta K. Banerjee, Krishna Baksi, and Dipak K. Banerjee. 2011. "Unfolded Protein Response Is Required in Nu/Nu Mice Microvasculature for Treating Breast Tumor with Tunicamycin." *Journal of Biological Chemistry* 286 (33): 29127–38. <https://doi.org/10.1074/jbc.M110.169771>.
- Barondes, S, M Nirenberg, G Spyrides, F Lipmann, W Gilbert, A Ishihama, N Mizuno, et al. 1963. "The Maintenance of the Accuracy of Protein Synthesis and Its Relevance to Ageing." *J. Mol. Biol.* Vol. 49.
- Bartke, Andrzej. 2008. "Insulin and Aging." *Cell Cycle*. Taylor and Francis Inc. <https://doi.org/10.4161/cc.7.21.7012>.
- Bedard, Karen, and Karl-Heinz Krause. 2007. "The NOX Family of ROS-Generating NADPH Oxidases: Physiology and Pathophysiology." <https://doi.org/10.1152/physrev.00044.2005.-For>.
- Belousov, Vsevolod v., Arkady F. Fradkov, Konstantin A. Lukyanov, Dmitry B. Staroverov, Konstantin S. Shakhbazov, Alexey v. Terskikh, and Sergey Lukyanov. 2006. "Genetically Encoded Fluorescent Indicator for Intracellular Hydrogen Peroxide." *Nature Methods* 3 (4): 281–86. <https://doi.org/10.1038/nmeth866>.
- Bennett, Christopher F., and Matt Kaeberlein. 2014. "The Mitochondrial Unfolded Protein Response and Increased Longevity: Cause, Consequence, or Correlation?" *Experimental Gerontology* 56: 142–46. <https://doi.org/10.1016/j.exger.2014.02.002>.
- Bennett, Christopher F., Jane J. Kwon, Christine Chen, Joshua Russell, Kathlyn Acosta, Nikolay Burnaevskiy, Matthew M. Crane, et al. 2017. "Transaldolase Inhibition Impairs Mitochondrial Respiration and Induces a Starvation-like Longevity Response in *Caenorhabditis Elegans*." *PLoS Genetics* 13 (3). <https://doi.org/10.1371/journal.pgen.1006695>.
- Bennett, Christopher F., Helen vander Wende, Marissa Simko, Shannon Klum, Sarah Barfield, Haeri Choi, Victor v. Pineda, and Matt Kaeberlein. 2014. "Activation of the Mitochondrial Unfolded Protein Response Does Not Predict Longevity in *Caenorhabditis Elegans*." *Nature Communications* 5 (March). <https://doi.org/10.1038/ncomms4483>.
- Bennett, Christopher F, Helen Vander Wende, Marissa Simko, Shannon Klum, Haeri Choi, Victor V Pineda, Matt Kaeberlein, and Cellular Biology Program. 2014. "Activation of the Mitochondrial Unfolded Protein Response Does Not Predict Longevity in *Caenorhabditis Elegans* Christopher," no. 206. <https://doi.org/10.1038/ncomms4483.Activation>.
- Benz, R., and S. McLaughlin. 1983. "The Molecular Mechanism of Action of the Proton Ionophore FCCP (Carbonylcyanide p-Trifluoromethoxyphenylhydrazine)." *Biophysical Journal* 41 (3): 381–98. [https://doi.org/10.1016/S0006-3495\(83\)84449-X](https://doi.org/10.1016/S0006-3495(83)84449-X).
- Berezhnov, Alexey v., Marc P.M. Soutar, Evgeniya I. Fedotova, Maria S. Frolova, Helene Plun-Favreau, Valery P. Zinchenko, and Andrey Y. Abramov. 2016. "Intracellular PH Modulates Autophagy and Mitophagy." *Journal of Biological Chemistry* 291 (16): 8701–8. <https://doi.org/10.1074/jbc.M115.691774>.

- Bienert, Gerd P., Jan K. Schjoerring, and Thomas P. Jahn. 2006. "Membrane Transport of Hydrogen Peroxide." *Biochimica et Biophysica Acta - Biomembranes*. <https://doi.org/10.1016/j.bbamem.2006.02.015>.
- Bisby, Roger H. 1990. "Reactions of a Free Radical Intermediate in the Oxidation of Amodiaquine." *Biochemical Pharmacology* 39 (12): 2051–53.
- Black, Adrian R, Jennifer D Black, and Jane Azizkhan-Clifford. 2001. "Sp1 and Krü Ppel-Like Factor Family of Transcription Factors in Cell Growth Regulation and Cancer." *JOURNAL OF CELLULAR PHYSIOLOGY*. Vol. 188.
- Blom, Nikolaj, Thomas Sicheritz-Pontén, Ramneek Gupta, Steen Gammeltoft, and Søren Brunak. 2004. "Prediction of Post-Translational Glycosylation and Phosphorylation of Proteins from the Amino Acid Sequence." *PROTEOMICS* 4 (6): 1633–49. <https://doi.org/https://doi.org/10.1002/pmic.200300771>.
- Bodnar, Andrea G, Michel Ouellette, Maria Frolkis, Shawn E Holt, Choy-Pik Chiu, Gregg B Morin, Calvin B Harley, Jerry W Shay, Serge Lichtsteiner, and Woodring E Wright. 1998. "Extension of Life-Span by Introduction of Telomerase into Normal Human Cells." *Science* 279: 349–52. <https://www.science.org>.
- Bonini, Marcelo G., Cristina Rota, Aldo Tomasi, and Ronald P. Mason. 2006. "The Oxidation of 2',7'-Dichlorofluorescein to Reactive Oxygen Species: A Self-Fulfilling Prophecy?" *Free Radical Biology and Medicine* 40 (6): 968–75. <https://doi.org/10.1016/j.freeradbiomed.2005.10.042>.
- Braeckman, Bart P., Arne Smolders, Patricia Back, and Sasha de Henau. 2016. "In Vivo Detection of Reactive Oxygen Species and Redox Status in *Caenorhabditis Elegans*." *Antioxidants & Redox Signaling* 25 (10): 577–92. <https://doi.org/10.1089/ars.2016.6751>.
- Brand, Martin D. 2010. "The Sites and Topology of Mitochondrial Superoxide Production." *Experimental Gerontology* 45 (7–8): 466–72. <https://doi.org/10.1016/j.exger.2010.01.003>.
- . 2016. "Mitochondrial Generation of Superoxide and Hydrogen Peroxide as the Source of Mitochondrial Redox Signaling." *Free Radical Biology and Medicine*. Elsevier Inc. <https://doi.org/10.1016/j.freeradbiomed.2016.04.001>.
- Brand, Martin D., Renata L.S. Goncalves, Adam L. Orr, Leonardo Vargas, Akos A. Gerencser, Martin Borch Jensen, Yves T. Wang, et al. 2016. "Suppressors of Superoxide-H₂O₂ Production at Site IQ of Mitochondrial Complex I Protect against Stem Cell Hyperplasia and Ischemia-Reperfusion Injury." *Cell Metabolism* 24 (4): 582–92. <https://doi.org/10.1016/j.cmet.2016.08.012>.
- Bratic, Ana, and Nils Göran Larsson. 2013. "The Role of Mitochondria in Aging." *Journal of Clinical Investigation*. <https://doi.org/10.1172/JCI64125>.
- Bratic, Ivana, Jürgen Hench, Johan Henriksson, Adam Antebi, Thomas R. Bürglin, and Aleksandra Trifunovic. 2009. "Mitochondrial DNA Level, but Not Active Replicase, Is Essential for *Caenorhabditis Elegans* Development." *Nucleic Acids Research* 37 (6): 1817–28. <https://doi.org/10.1093/nar/gkp018>.
- Bratic, Ivana, and Aleksandra Trifunovic. 2010. "Mitochondrial Energy Metabolism and Ageing." *Biochimica et Biophysica Acta - Bioenergetics*. <https://doi.org/10.1016/j.bbabi.2010.01.004>.
- Brenda, C. 1898. "Weitere Mittelungen Über Die Mitochondria ." *Verh Physiol Ges Berlin*.
- Brennan, Jonathan P., Richard Southworth, Rodolfo A. Medina, Sean M. Davidson, Michael R. Duchon, and Michael J. Shattock. 2006. "Mitochondrial Uncoupling, with Low Concentration FCCP, Induces ROS-Dependent Cardioprotection Independent of KATP

- Channel Activation." *Cardiovascular Research* 72 (2): 313–21.
<https://doi.org/10.1016/j.cardiores.2006.07.019>.
- Brenner, S. 1974. "The Genetics of *Caenorhabditis Elegans*." *Genetics*, no. 77: 71–94.
- . 1988. *Foreword. The Nematode Caenorhabditis Elegans*. Edited by W. B. Wood. Cold Spring Harbor, NY: Cold Spring Harbor Laboratory Press.
- Brenner, Sydney. 2002. "The Worm's Turn." *Current Biology* 12 (21): R713.
- Briston, Thomas, Malcolm Roberts, Sian Lewis, Ben Powney, James M. Staddon, Gyorgy Szabadkai, and Michael R. Duchen. 2017. "Mitochondrial Permeability Transition Pore: Sensitivity to Opening and Mechanistic Dependence on Substrate Availability." *Scientific Reports* 7 (1). <https://doi.org/10.1038/s41598-017-10673-8>.
- Brock, Trisha J., John Browse, and Jennifer L. Watts. 2006. "Genetic Regulation of Unsaturated Fatty Acid Composition in *C. Elegans*." *PLoS Genetics* 2 (7): 0997–1005.
<https://doi.org/10.1371/journal.pgen.0020108>.
- Brouillette, Scott, Ravi K. Singh, John R. Thompson, Alison H. Goodall, and Nilesh J. Samani. 2003. "White Cell Telomere Length and Risk of Premature Myocardial Infarction." *Arteriosclerosis, Thrombosis, and Vascular Biology* 23 (5): 842–46.
<https://doi.org/10.1161/01.ATV.0000067426.96344.32>.
- Brunet, Anne, Azad Bonni, Michael J Zigmund, Michael Z Lin, Peter Juo, Linda S Hu, Michael J Anderson, Karen C Arden, John Blenis, and Michael E Greenberg. 1999. "Akt Promotes Cell Survival by Phosphorylating and Inhibiting a Forkhead Transcription Factor." *Cell*. Vol. 96.
- Budd, Samantha L., Roger F. Castilho, and David G. Nicholls. 1997. "Mitochondrial Membrane Potential and Hydroethidine-Monitored Superoxide Generation in Cultured Cerebellar Granule Cells." *FEBS Letters* 415 (1): 21–24. [https://doi.org/10.1016/S0014-5793\(97\)01088-0](https://doi.org/10.1016/S0014-5793(97)01088-0).
- Buettner, Garry R. 2011. "Superoxide Dismutase in Redox Biology: The Roles of Superoxide and Hydrogen Peroxide." *Anticancer Agents Med Chem* 11 (4): 341–46.
- Buffenstein, Rochelle. 2005. "The Naked Mole-Rat: A New Long-Living Model for Human Aging Research." <https://academic.oup.com/biomedgerontology/article/60/11/1369/623073>.
- Butler, Jeffrey A., Natascia Ventura, Thomas E. Johnson, and Shane L. Rea. 2010. "Long-Lived Mitochondrial (Mit) Mutants of *Caenorhabditis Elegans* Utilize a Novel Metabolism." *The FASEB Journal* 24: 4977–88.
- Cabreiro, Filipe, Daniel Ackerman, Ryan Doonan, Caroline Araiz, Patricia Back, Diana Papp, Bart P. Braeckman, and David Gems. 2011. "Increased Life Span from Overexpression of Superoxide Dismutase in *Caenorhabditis Elegans* Is Not Caused by Decreased Oxidative Damage." *Free Radical Biology and Medicine* 51 (8): 1575–82.
<https://doi.org/10.1016/j.freeradbiomed.2011.07.020>.
- Caciali, Pietro, Christopher B. Mahony, Tim Petzold, Patrizia Bordignon, Anne Laure Rougemont, and Julien Y. Bertrand. 2021. "A Connexin/Ifi30 Pathway Bridges HSCs with Their Niche to Dampen Oxidative Stress." *Nature Communications* 12 (1).
<https://doi.org/10.1038/s41467-021-24831-0>.
- Cadenas, Enrique, Kelvin J A Davies, Bernhard Kadenbach, Susanne Arnold, Icksoo Lee, and Elisabeth Bender. 2000. "Mitochondrial Energy Metabolism Is Regulated via Nuclear-Coded Subunits of Cytochrome c Oxidase."
- Cadenas, Susana. 2018. "Mitochondrial Uncoupling, ROS Generation and Cardioprotection." *Biochimica et Biophysica Acta - Bioenergetics*. Elsevier B.V.
<https://doi.org/10.1016/j.bbabi.2018.05.019>.

- Cai, Hua. 2005. "Hydrogen Peroxide Regulation of Endothelial Function: Origins, Mechanisms, and Consequences." *Cardiovascular Research*. <https://doi.org/10.1016/j.cardiores.2005.06.021>.
- Calabrese, Edward J. 2018. "Hormesis: Path and Progression to Significance." *International Journal of Molecular Sciences*. MDPI AG. <https://doi.org/10.3390/ijms19102871>.
- Calvo, Isabel A., José Ayté, and Elena Hidalgo. 2013. "Reversible Thiol Oxidation in the H₂O₂-Dependent Activation of the Transcription Factor Pap1." *Journal of Cell Science* 126 (10): 2279–84. <https://doi.org/10.1242/jcs.124370>.
- Camara, Amadou K.S., Yi Fan Zhou, Po Chao Wen, Emad Tajkhorshid, and Wai Meng Kwok. 2017. "Mitochondrial VDAC1: A Key Gatekeeper as Potential Therapeutic Target." *Frontiers in Physiology* 8 (JUN): 1–18. <https://doi.org/10.3389/fphys.2017.00460>.
- Cao, Xiaoxiao, Lixiang Xue, Limin Han, Liwei Ma, Tianda Chen, and Tanjun Tong. 2011. "WW Domain-Containing E3 Ubiquitin Protein Ligase 1 (WWP1) Delays Cellular Senescence by Promoting P27 Kip1 Degradation in Human Diploid Fibroblasts." *Journal of Biological Chemistry* 286 (38): 33447–56. <https://doi.org/10.1074/jbc.M111.225565>.
- Capalde, Roderick A., Robert Aggeler, Paola Turina, and Stephan Wilkens. 1994. "Coupling between Catalytic Sites and the Proton Channel in FiFo-Type ATPases." *TIBS*.
- Capozza, G, F Guerriep, G Vendemiale, E Altomare, and S Papa. 1994. "Age Related Changes of the Mitochondrial Energy Metabolism in Rat Liver and Heart." *Arch. Gerontol. Geriatr.*
- Carrano, Andrea C., Andrew Dillin, and Tony Hunter. 2014. "A Krüppel-like Factor Downstream of the E3 Ligase WWP-1 Mediates Dietary-Restriction-Induced Longevity in *Caenorhabditis Elegans*." *Nature Communications* 5 (May). <https://doi.org/10.1038/ncomms4772>.
- Carrano, Andrea C., and Tony Hunter. 2015. "Fitting WWP-1 in the Dietary Restriction Network." *Cell Cycle*. Taylor and Francis Inc. <https://doi.org/10.1080/15384101.2015.1032642>.
- Carrano, Andrea C., Zheng Liu, Andrew Dillin, and Tony Hunter. 2009. "A Conserved Ubiquitination Pathway Determines Longevity in Response to Diet Restriction." *Nature* 460 (7253): 396–99. <https://doi.org/10.1038/nature08130>.
- Carroll, Joe, Ian M. Fearnley, Richard J. Shannon, Judy Hirst, and John E. Walker. 2003. "Analysis of the Subunit Composition of Complex I from Bovine Heart Mitochondria." *Molecular & Cellular Proteomics : MCP* 2 (2): 117–26. <https://doi.org/10.1074/mcp.M300014-MCP200>.
- Cawthon, Richard M, Smith Ken R, Elizabeth O'Brien, Anna Sivatchenko, and Richard A Kerber. 2003. "Association between Telomere Length in Blood and Mortality in People Aged 60 Years or Older." *The Lancet* 361: 393–95. www.thelancet.com.
- Cecchini, Gary. 2003. "Function and Structure of Complex II of the Respiratory Chain." *Annual Review of Biochemistry*. <https://doi.org/10.1146/annurev.biochem.72.121801.161700>.
- . 2013. "Respiratory Complex II: Role in Cellular Physiology and Disease." *Biochimica et Biophysica Acta - Bioenergetics*. <https://doi.org/10.1016/j.bbabi.2013.02.010>.
- Chabi, Béatrice, Vladimir Ljubcic, Keir J. Menzies, Julianna H. Huang, Ayesha Saleem, and David A. Hood. 2008. "Mitochondrial Function and Apoptotic Susceptibility in Aging Skeletal Muscle." *Aging Cell* 7 (1): 2–12. <https://doi.org/10.1111/j.1474-9726.2007.00347.x>.
- Chamberlain, Jeffrey S, and Guy M Benian. 2000. "Muscular Dystrophy: The Worm Turns to Genetic Disease." *Current Biology*. Vol. 10.

- Chamoli, Manish, Anita Goyala, Syed Shamsh Tabrez, Atif Ahmed Siddiqui, Anupama Singh, Adam Antebi, Gordon J. Lithgow, Jennifer L. Watts, and Arnab Mukhopadhyay. 2020. "Polyunsaturated Fatty Acids and P38-MAPK Link Metabolic Reprogramming to Cytoprotective Gene Expression during Dietary Restriction." *Nature Communications* 11 (1). <https://doi.org/10.1038/s41467-020-18690-4>.
- Chance, Britton. 1961. "The Interaction of Energy and Electron Transfer Reactions in Mitochondria II." *THE JOURNAL OF BIOLOGICAL CHEMISTRY*. Vol. 236.
- Chapman, Tracey, and Linda Partridge. 1996. "Female Fitness in *Drosophila Melanogaster*: An Interaction between the Effect of Nutrition and of Encounter Rate with Males." *Proc. R. Soc. Lond. B*. 263: 755–59.
- Chauhan, Dharminder, Laurence Catley, Guilan Li, Klaus Podar, Teru Hideshima, Mugdha Velankar, Constantine Mitsiades, et al. 2005. "A Novel Orally Active Proteasome Inhibitor Induces Apoptosis in Multiple Myeloma Cells with Mechanisms Distinct from Bortezomib." *Cancer Cell* 8 (5): 407–19. <https://doi.org/10.1016/j.ccr.2005.10.013>.
- Chen, C., Z. Zhou, R. Liu, Y. Li, P. B. Azmi, and A. K. Seth. 2008. "The WW Domain Containing E3 Ubiquitin Protein Ligase 1 Upregulates ErbB2 and EGFR through RING Finger Protein 11." *Oncogene* 27 (54): 6845–55. <https://doi.org/10.1038/onc.2008.288>.
- Chen, Ceshi, Xiaodong Sun, Peng Guo, Xue Yuan Dong, Pooja Sethi, Xiaohong Cheng, Jun Zhou, et al. 2005. "Human Kruppel-like Factor 5 Is a Target of the E3 Ubiquitin Ligase WWP1 for Proteolysis in Epithelial Cells." *Journal of Biological Chemistry* 280 (50): 41553–61. <https://doi.org/10.1074/jbc.M506183200>.
- Chen, Chang Shi, Audrey Bellier, Cheng Yuan Kao, Ya Luen Yang, Huan da Chen, Ferdinand C.O. Los, and Raffi v. Aroian. 2010. "WWP-1 Is a Novel Modulator of the DAF-2 Insulin-like Signaling Network Involved in Pore-Forming Toxin Cellular Defenses in *Caenorhabditis Elegans*." *PLoS ONE* 5 (3). <https://doi.org/10.1371/journal.pone.0009494>.
- Chen, D., M. Frezza, S. Schmitt, J. Kanwar, and Q. P. Dou. 2011. "Bortezomib as the First Proteasome Inhibitor Anticancer Drug: Current Status and Future Perspectives." *Current Cancer Drug Targets* 11 (3): 239–53. <https://doi.org/10.2174/156800911794519752>.
- Chen, Di, Patrick Wai Lun Li, Benjamin A. Goldstein, Waijiao Cai, Emma Lynn Thomas, Fen Chen, Alan E. Hubbard, Simon Melov, and Pankaj Kapahi. 2013. "Germline Signaling Mediates the Synergistically Prolonged Longevity Produced by Double Mutations in Daf-2 and Rsk-1 in *C. Elegans*." *Cell Reports* 5 (6): 1600–1610. <https://doi.org/10.1016/j.celrep.2013.11.018>.
- Chen, Kai, Michael T. Kirber, Hui Xiao, Yu Yang, and John F. Keaney. 2008. "Regulation of ROS Signal Transduction by NADPH Oxidase 4 Localization." *Journal of Cell Biology* 181 (7): 1129–39. <https://doi.org/10.1083/jcb.200709049>.
- Chen, Qun, Edwin J. Vazquez, Shadi Moghaddas, Charles L. Hoppel, and Edward J. Lesnefsky. 2003. "Production of Reactive Oxygen Species by Mitochondria: Central Role of Complex III." *Journal of Biological Chemistry* 278 (38): 36027–31. <https://doi.org/10.1074/jbc.M304854200>.
- Cheng, Gang, Monika Zielonka, Brian Dranka, Suresh N. Kumar, Charles R. Myers, Brian Bennett, Alexander M. Garces, et al. 2018. "Detection of Mitochondria-Generated Reactive Oxygen Species in Cells Using Multiple Probes and Methods: Potentials, Pitfalls, and the Future." *Journal of Biological Chemistry* 293 (26): 10363–80. <https://doi.org/10.1074/jbc.RA118.003044>.
- Chin, Randall M., Xudong Fu, Melody Y. Pai, Laurent Vergnes, Heejun Hwang, Gang Deng, Simon Diep, et al. 2014. "The Metabolite α -Ketoglutarate Extends Lifespan by Inhibiting

- ATP Synthase and TOR." *Nature* 510 (7505): 397–401.
<https://doi.org/10.1038/nature13264>.
- Chinnery, Patrick Francis, and Gavin Hudson. 2013. "Mitochondrial Genetics." *British Medical Bulletin*. <https://doi.org/10.1093/bmb/ldt017>.
- Cho, Kyung Jin, Ji Min Seo, and Jae Hong Kim. 2011. "Bioactive Lipoyxygenase Metabolites Stimulation of NADPH Oxidases and Reactive Oxygen Species." *Molecules and Cells*.
<https://doi.org/10.1007/s10059-011-1021-7>.
- Choi, Hee-Jung, Seung-Jun Kim, Partha Mukhopadhyay, Sayeon Cho, Joo-Rang Woo, Gisela Storz, and Seong-Eon Ryu. 2001. "Structural Basis of the Redox Switch in the OxyR Transcription Factor." *Cell* 105 (1): 103–13.
- Chouchani, Edward T., Victoria R. Pell, Edoardo Gaude, Dunja Aksentijević, Stephanie Y. Sundier, Ellen L. Robb, Angela Logan, et al. 2014. "Ischaemic Accumulation of Succinate Controls Reperfusion Injury through Mitochondrial ROS." *Nature* 515 (7527): 431–35.
<https://doi.org/10.1038/nature13909>.
- Chuang, Chiou Fen, and Cornelia I. Bargmann. 2005. "A Toll-Interleukin 1 Repeat Protein at the Synapse Specifies Asymmetric Odorant Receptor Expression via ASK1 MAPKKK Signaling." *Genes and Development* 19 (2): 270–81.
<https://doi.org/10.1101/gad.1276505>.
- Cichanover, Aaron. 2005. "Intracellular Protein Degradation: From a Vague Idea Thru the Lysosome and the Ubiquitin-Proteasome System and onto Human Diseases and Drug Targeting." *Cell Death and Differentiation*. <https://doi.org/10.1038/sj.cdd.4401692>.
- Clancy, David J., David Gems, Ernst Hafen, Sally J. Leivers, and Linda Partridge. 2002. "Dietary Restriction in Long-Lived Dwarf Flies." *Science*.
<https://doi.org/10.1126/science.1069366>.
- Clokey, George v., and Lewis A. Jacobson. 1986. "The Autofluorescent 'Lipofuscin Granules' in the Intestinal Cells of *Caenorhabditis Elegans* Are Secondary Lysosomes." *Mechanisms of Ageing and Development* 35 (1): 79–94. [https://doi.org/10.1016/0047-6374\(86\)90068-0](https://doi.org/10.1016/0047-6374(86)90068-0).
- Cobley, James Nathan, and Holger Husi. 2020. "Immunological Techniques to Assess Protein Thiol Redox State: Opportunities, Challenges and Solutions." *Antioxidants* 9 (4): 1–25.
<https://doi.org/10.3390/antiox9040315>.
- Coburn, Cassandra, and David Gems. 2013. "The Mysterious Case of the c. *Elegans* Gut Granule: Death Anthranilic Acid and the Kynurenine Pathway." *Frontiers in Genetics* 4 (AUG): 1–4. <https://doi.org/10.3389/fgene.2013.00151>.
- Cochemé, Helena M., and Michael P. Murphy. 2008. "Complex I Is the Major Site of Mitochondrial Superoxide Production by Paraquat." *Journal of Biological Chemistry* 283 (4): 1786–98. <https://doi.org/10.1074/jbc.M708597200>.
- Cogoni, Carlo, and Giuseppe Macino. 1999. "A Cytosolic Catalase Is Needed to Extend Adult Lifespan in *C. Elegans* Daf-C and Clk-1 Mutants." *Nature* 399: 162–66.
<https://doi.org/10.1038/nature01425>.
- Cohen, Alan A. 2018. "Aging across the Tree of Life: The Importance of a Comparative Perspective for the Use of Animal Models in Aging." *Biochimica et Biophysica Acta - Molecular Basis of Disease*. Elsevier B.V. <https://doi.org/10.1016/j.bbadis.2017.05.028>.
- Commoner, Barry, Jonathan Townsend, and George E Pake. 1954. "Free Radicals in Biological Materials." *Nature* 11 (10): 689–91.
- Conkright, Michael D., Maqsood A. Wani, and Jerry B. Lingrel. 2001. "Lung Krüppel-like Factor Contains an Autoinhibitory Domain That Regulates Its Transcriptional Activation

- by Binding WWP1, an E3 Ubiquitin Ligase." *Journal of Biological Chemistry* 276 (31): 29299–306. <https://doi.org/10.1074/jbc.M103670200>.
- Copeland, Jeffrey M., Jaehyoung Cho, Thomas Lo, Jae H. Hur, Sepehr Bahadorani, Tagui Arabyan, Jason Rabie, Jennifer Soh, and David W. Walker. 2009. "Extension of *Drosophila* Life Span by RNAi of the Mitochondrial Respiratory Chain." *Current Biology* 19 (19): 1591–98. <https://doi.org/10.1016/j.cub.2009.08.016>.
- Cordeiro, Rodrigo M. 2015. "Molecular Dynamics Simulations of the Transport of Reactive Oxygen Species by Mammalian and Plant Aquaporins." *Biochimica et Biophysica Acta - General Subjects* 1850 (9): 1786–94. <https://doi.org/10.1016/j.bbagen.2015.05.007>.
- Cores, Estela Cepeda. 2015. "KLF-1 Mediates Mitohormesis by Orchestrating a Xenobiotic Detoxification Response Essential for Longevity in *C. Elegans*."
- Corsi, Ann K., Bruce Wightman, and Martin Chalfie. 2015. "A Transparent Window into Biology: A Primer on *Caenorhabditis Elegans*." *Genetics* 200 (2): 387–407. <https://doi.org/10.1534/genetics.115.176099>.
- Cristina, David, Michael Cary, Adam Lunceford, Catherine Clarke, and Cynthia Kenyon. 2009. "A Regulated Response to Impaired Respiration Slows Behavioral Rates and Increases Lifespan in *Caenorhabditis Elegans*." *PLoS Genetics* 5 (4). <https://doi.org/10.1371/journal.pgen.1000450>.
- Culetto, Emmanuel, and David B Sattelle. 2000. "A Role for *Caenorhabditis Elegans* in Understanding the Function and Interactions of Human Disease Genes." *Human Molecular Genetics*. Vol. 9. http://www.sanger.ac.uk/Projects/C_elegans/.
- Cullingford, Timothy E., Matthew J. Butler, Andrew K. Marshall, El Li Tham, Peter H. Sugden, and Angela Clerk. 2008. "Differential Regulation of Krüppel-like Factor Family Transcription Factor Expression in Neonatal Rat Cardiac Myocytes: Effects of Endothelin-1, Oxidative Stress and Cytokines." *Biochimica et Biophysica Acta - Molecular Cell Research* 1783 (6): 1229–36. <https://doi.org/10.1016/j.bbamcr.2008.03.007>.
- Dancy, Beverley M., Margaret M. Sedensky, and Philip G. Morgan. 2014. "Effects of the Mitochondrial Respiratory Chain on Longevity in *C. Elegans*." *Experimental Gerontology*. Elsevier Inc. <https://doi.org/10.1016/j.exger.2014.03.028>.
- D'Autr aux, Beno t, and Michel B. Toledano. 2007. "ROS as Signalling Molecules: Mechanisms That Generate Specificity in ROS Homeostasis." *Nature Reviews Molecular Cell Biology*. <https://doi.org/10.1038/nrm2256>.
- Davoudi, Mina, Jukka Kallij rvi, Sanna Marjavaara, Heike Kotarsky, Eva Hansson, Per Lev  en, and Vineta Fellman. 2014. "A Mouse Model of Mitochondrial Complex III Dysfunction Induced by Myxothiazol." *Biochemical and Biophysical Research Communications* 446 (4): 1079–84. <https://doi.org/10.1016/j.bbrc.2014.03.058>.
- DeHart, David N., Diana Fang, Kareem Heslop, Li Li, John J. Lemasters, and Eduardo N. Maldonado. 2018. "Opening of Voltage Dependent Anion Channels Promotes Reactive Oxygen Species Generation, Mitochondrial Dysfunction and Cell Death in Cancer Cells." *Biochemical Pharmacology* 148 (February): 155–62. <https://doi.org/10.1016/j.bcp.2017.12.022>.
- Delaunay, Agnes, Anne-Dominique Isnard, and Michel B Toledano. 2000. "H₂O₂ Sensing through Oxidation of the Yap1 Transcription Factor." *The EMBO Journal* 19: 5157–66.
- Deng, Jianhui, Yuxi Dai, Haiqing Tang, and Shanshan Pang. 2020. "SKN-1 Is a Negative Regulator of DAF-16 and Somatic Stress Resistance in *C. Elegans*." *G3: Genes, Genomes, Genetics* 10 (4). <https://doi.org/10.1534/g3.120.401203>.

- Derisbourg, Maxime J., Laura E. Wester, Ruth Baddi, and Martin S. Denzel. 2021. "Mutagenesis Screen Uncovers Lifespan Extension through Integrated Stress Response Inhibition without Reduced mRNA Translation." *Nature Communications* 12 (1). <https://doi.org/10.1038/s41467-021-21743-x>.
- Dervartanian, D. V., and C. Veeger. 1964. "STUDIES ON SUCCINATE DEHYDROGENASE. I. SPECTRAL PROPERTIES OF THE PURIFIED ENZYME AND FORMATION OF ENZYME-COMPETITIVE INHIBITOR COMPLEXES." *Biochimica et Biophysica Acta* 92 (November): 233–47.
- Desjardins, David, Briseida Cacho-Valadez, Ju Ling Liu, Ying Wang, Callista Yee, Kristine Bernard, Arman Khaki, Lionel Breton, and Siegfried Hekimi. 2017. "Antioxidants Reveal an Inverted U-Shaped Dose-Response Relationship between Reactive Oxygen Species Levels and the Rate of Aging in *Caenorhabditis Elegans*." *Aging Cell* 16 (1): 104–12. <https://doi.org/10.1111/accel.12528>.
- Dikic, Ivan. n.d. "Proteasomal and Autophagic Degradation Systems." <https://doi.org/10.1146/annurev-biochem>.
- Dillin, Andrew, Ao Lin Hsu, Nuno Arantes-Oliveira, Joshua Lehrer-Graiwer, Honor Hsin, Andrew G. Fraser, Ravi S. Kamath, Julie Ahringer, and Cynthia Kenyon. 2002. "Rates of Behavior and Aging Specified by Mitochondrial Function during Development." *Science* 298 (5602): 2398–2401. <https://doi.org/10.1126/science.1077780>.
- Distelmaier, Felix, Werner J.H. Koopman, Lambertus P. van den Heuvel, Richard J. Rodenburg, Ertan Mayatepek, Peter H.G.M. Willems, and Jan A.M. Smeitink. 2009. "Mitochondrial Complex i Deficiency: From Organelle Dysfunction to Clinical Disease." *Brain*. Oxford University Press. <https://doi.org/10.1093/brain/awp058>.
- Doonan, Ryan, Joshua J. McElwee, Filip Matthijssens, Glenda A. Walker, Koen Houthoofd, Patricia Back, Andrea Matscheski, Jacques R. Vanfleteren, and David Gems. 2008. "Against the Oxidative Damage Theory of Aging: Superoxide Dismutases Protect against Oxidative Stress but Have Little or No Effect on Life Span in *Caenorhabditis Elegans*." *Genes and Development* 22 (23): 3236–41. <https://doi.org/10.1101/gad.504808>.
- Dourado, Daniel F.A.R., Marcel Swart, and Alexandra T.P. Carvalho. 2018. "Why the Flavin Adenine Dinucleotide (FAD) Cofactor Needs To Be Covalently Linked to Complex II of the Electron-Transport Chain for the Conversion of FADH₂ into FAD." *Chemistry - A European Journal* 24 (20): 5246–52. <https://doi.org/10.1002/chem.201704622>.
- Du, James X., Agnieszka B. Bialkowska, Beth B. McConnell, and Vincent W. Yang. 2008. "SUMOylation Regulates Nuclear Localization of Krüppel-like Factor 5." *Journal of Biological Chemistry* 283 (46): 31991–2. <https://doi.org/10.1074/jbc.M803612200>.
- Dudkina, Natalya v., Stephanie Sunderhaus, Egbert J. Boekema, and Hans Peter Braun. 2008. "The Higher Level of Organization of the Oxidative Phosphorylation System: Mitochondrial Supercomplexes." *Journal of Bioenergetics and Biomembranes*. <https://doi.org/10.1007/s10863-008-9167-5>.
- Durieux, Jenni, Suzanne Wolff, and Andrew Dillin. 2011. "The Cell-Non-Autonomous Nature of Electron Transport Chain-Mediated Longevity." *Cell* 144 (1): 79–91. <https://doi.org/10.1016/j.cell.2010.12.016>.
- Ermakova, Yulia G., Dmitry S. Bilan, Mikhail E. Matlashov, Natalia M. Mishina, Ksenia N. Markvicheva, Oksana M. Subach, Fedor v. Subach, et al. 2014. "Red Fluorescent Genetically Encoded Indicator for Intracellular Hydrogen Peroxide." *Nature Communications* 5. <https://doi.org/10.1038/ncomms6222>.
- Esterberg, Robert, Tor Linbo, Sarah B. Pickett, Patricia Wu, Henry C. Ou, Edwin W. Rubel, and David W. Raible. 2016. "Mitochondrial Calcium Uptake Underlies ROS Generation

- during Aminoglycoside-Induced Hair Cell Death." *Journal of Clinical Investigation* 126 (9): 3556–66. <https://doi.org/10.1172/JCI84939>.
- Faggioli, Francesca, Tao Wang, Jan Vijg, and Cristina Montagna. 2012. "Chromosome-Specific Accumulation of Aneuploidy in the Aging Mouse Brain." *Human Molecular Genetics* 21 (24): 5246–53. <https://doi.org/10.1093/hmg/dds375>.
- Fan, Liyan, David R. Sweet, Domenick A. Prosdocimo, Vinesh Vinayachandran, Ernest R. Chan, Rongli Zhang, Olga Ilkayeva, et al. 2021. "Muscle Krüppel-like Factor 15 Regulates Lipid Flux and Systemic Metabolic Homeostasis." *Journal of Clinical Investigation* 131 (4). <https://doi.org/10.1172/JCI139496>.
- Félix, Marie Anne, Alyson Ashe, Joséphine Piffaretti, Guang Wu, Isabelle Nuez, Tony Bêlicard, Yanfang Jiang, et al. 2011. "Natural and Experimental Infection of *Caenorhabditis* Nematodes by Novel Viruses Related to Nodaviruses." *PLoS Biology* 9 (1). <https://doi.org/10.1371/journal.pbio.1000586>.
- Félix, Marie Anne, and Fabien Dubeau. 2012. "Population Dynamics and Habitat Sharing of Natural Populations of *Caenorhabditis Elegans* and *C. Briggsae*." *BMC Biology* 10 (June). <https://doi.org/10.1186/1741-7007-10-59>.
- Feng, Jinliu, Frédéric Bussière, and Siegfried Hekimi. 2001. "Mitochondrial Electron Transport Is a Key Determinant of Life Span in *Caenorhabditis Elegans*." *Developmental Cell* 1 (5): 633–44. [https://doi.org/10.1016/S1534-5807\(01\)00071-5](https://doi.org/10.1016/S1534-5807(01)00071-5).
- Ferguson, Gavin Douglas, and Wallace John Bridge. 2019. "The Glutathione System and the Related Thiol Network in *Caenorhabditis Elegans*." *Redox Biology* 24 (December 2018): 101171. <https://doi.org/10.1016/j.redox.2019.101171>.
- Ferrer-Sueta, Gerardo, Bruno Manta, Horacio Botti, Rafael Radi, Madia Trujillo, and Ana Denicola. 2011. "Factors Affecting Protein Thiol Reactivity and Specificity in Peroxide Reduction." *Chemical Research in Toxicology*. American Chemical Society. <https://doi.org/10.1021/tx100413v>.
- Fielenbach, Nicole, and Adam Antebi. 2008. "C. *Elegans* Dauer Formation and the Molecular Basis of Plasticity." *Genes and Development*. <https://doi.org/10.1101/gad.1701508>.
- Figueiredo, Pedro Alexandre, Scott K. Powers, Rita M. Ferreira, Hans Joachim Appell, and José A. Duarte. 2009. "Aging Impairs Skeletal Muscle Mitochondrial Bioenergetic Function." *Journals of Gerontology - Series A Biological Sciences and Medical Sciences* 64 (1): 21–33. <https://doi.org/10.1093/gerona/gln048>.
- Foreman, Julia, Vadim Demidchik, John H F Bothwell, Panagiota Mylona, Henk Miedema, Miguel Angel Torresk{, Paul Linstead, et al. 2003. "Reactive Oxygen Species Produced by NADPH Oxidase Regulate Plant Cell Growth." www.nature.com/nature.
- Forman, Henry Jay, Matilde Maiorino, and Fulvio Ursini. 2010. "Signaling Functions of Reactive Oxygen Species." *Biochemistry*. <https://doi.org/10.1021/bi9020378>.
- Forsberg, Lars A., Chiara Rasi, Hamid R. Razzaghian, Geeta Pakalapati, Lindsay Waite, Krista Stanton Thilbeault, Anna Ronowicz, et al. 2012. "Age-Related Somatic Structural Changes in the Nuclear Genome of Human Blood Cells." *American Journal of Human Genetics* 90 (2): 217–28. <https://doi.org/10.1016/j.ajhg.2011.12.009>.
- Fridovich, Irwin. 1995. "Superoxide Radical and Superoxide Dismutases." *Annu Rev Biochem* 64: 97–112.
- Fujii, Michihiko, Naoaki Ishii, Atsuhiko Joguchi, Kayo Yasuda, and Dai Ayusawa. 1998. "A Novel Superoxide Dismutase Gene Encoding Membrane-Bound and Extracellular Isoforms by Alternative Splicing in *Caenorhabditis Elegans*." *DNA Research* 5 (1): 25–30. <https://doi.org/10.1093/dnares/5.1.25>.

- Furchgott, Robert F., and John v. Zawadzki. 1980. "The Obligatory Role of Endothelial Cells in the Relaxation of Arterial Smooth Muscle by Acetylcholine." *Nature* 288: 373–76.
- Garcia-Fernandez, Maria, Inma Sierra, Juan E. Puche, Lucia Guerra, and Inma Castilla-Cortazar. 2011. "Liver Mitochondrial Dysfunction Is Reverted by Insulin-like Growth Factor II (IGF-II) in Aging Rats." *Journal of Translational Medicine* 9 (1). <https://doi.org/10.1186/1479-5876-9-123>.
- Gaschler, Michael M., and Brent R. Stockwell. 2017. "Lipid Peroxidation in Cell Death." *Biochemical and Biophysical Research Communications*. Elsevier B.V. <https://doi.org/10.1016/j.bbrc.2016.10.086>.
- Gatt, Ariana P., Olivia F. Duncan, Johannes Attems, Paul T. Francis, Clive G. Ballard, and Joseph M. Bateman. 2016. "Dementia in Parkinson's Disease Is Associated with Enhanced Mitochondrial Complex I Deficiency." *Movement Disorders* 31 (3): 352–59. <https://doi.org/10.1002/mds.26513>.
- Ge, Chun, Bei Cao, Dong Feng, Fang Zhou, Jingwei Zhang, Na Yang, Siqi Feng, Guangji Wang, and Jiye Aa. 2017. "The Down-Regulation of SLC7A11 Enhances ROS Induced P-Gp over-Expression and Drug Resistance in MCF-7 Breast Cancer Cells." *Scientific Reports* 7 (1). <https://doi.org/10.1038/s41598-017-03881-9>.
- Gechev, Tsanko S., and Jacques Hille. 2005. "Hydrogen Peroxide as a Signal Controlling Plant Programmed Cell Death." *Journal of Cell Biology*. <https://doi.org/10.1083/jcb.200409170>.
- Geiszt, Miklós, and Thomas L. Leto. 2004. "The Nox Family of NAD(P)H Oxidases: Host Defense and Beyond." *Journal of Biological Chemistry*. <https://doi.org/10.1074/jbc.R400024200>.
- Geletyuk, V I, V N J Kazachenko, M E Krouse, G T Schneider, P W Gage, H Oberleithner, G Giebisch, et al. 1982. "Nitric Oxide Release Accounts for the Biological Activity of Endothelium-Derived Relaxing Factor." *Greger, R. & Schlatter, E. Pflugers Arch. Ges. Physiol.* Vol. 86.
- Gems, David, and Ryan Doonan. 2009. "Antioxidant Defense and Aging in C. Elegans: Is the Oxidative Damage Theory of Aging Wrong?" *Cell Cycle* 8 (11): 1681–87. <https://doi.org/10.4161/cc.8.11.8595>.
- Gems, David, and Linda Partridge. 2013. "Genetics of Longevity in Model Organisms: Debates and Paradigm Shifts." *Annual Review of Physiology*. <https://doi.org/10.1146/annurev-physiol-030212-183712>.
- Gerschman, Rebeca, Daniel L Gilbert, Sylvanus W Nye, Peter Dwyer, and Wallace O Fenn2. 1954. "Oxygen Poisoning and X-Irradiation: A Mechanism in Common I." *Science*. Vol. 119. <https://www.science.org>.
- Gerth, K., H. Irschik, H. Reichenbach, and W. Trowitzsch. 1980. "Myxothiazol, an Antibiotic from Myxococcus Fulvus (Myxobacterales): I. Cultivation, Isolation, Physico-Chemical and Biological Properties." *The Journal of Antibiotics* 33 (12): 1474–79. <https://doi.org/10.7164/antibiotics.33.1474>.
- Giorgi, Carlotta, Saverio Marchi, and Paolo Pinton. 2018. "The Machineries, Regulation and Cellular Functions of Mitochondrial Calcium." *Nature Reviews Molecular Cell Biology*. Nature Publishing Group. <https://doi.org/10.1038/s41580-018-0052-8>.
- Gladyshev, Vadim N. 2014. "The Free Radical Theory of Aging Is Dead. Long Live the Damage Theory!" *Antioxidants and Redox Signaling* 20 (4): 727–31. <https://doi.org/10.1089/ars.2013.5228>.
- Grad, Leslie I., and Bernard D. Lemire. 2004. "Mitochondrial Complex I Mutations in Caenorhabditis Elegans Produce Cytochrome c Oxidase Deficiency, Oxidative Stress and

- Vitamin-Responsive Lactic Acidosis." *Human Molecular Genetics* 13 (3): 303–14.
<https://doi.org/10.1093/hmg/ddh027>.
- Grandison, Richard C., Matthew D.W. Piper, and Linda Partridge. 2009. "Amino-Acid Imbalance Explains Extension of Lifespan by Dietary Restriction in *Drosophila*." *Nature* 462 (7276): 1061–64. <https://doi.org/10.1038/nature08619>.
- Green, Cara L., Dudley W. Lamming, and Luigi Fontana. 2021. "Molecular Mechanisms of Dietary Restriction Promoting Health and Longevity." *Nature Reviews Molecular Cell Biology*. Nature Research. <https://doi.org/10.1038/s41580-021-00411-4>.
- Green, Rebecca A, Anjon Audhya, Andrei Pozniakovsky, Alexander Dammermann, Hayley Pemble, Joost Momen, Nathan Portier, Anthony Hyman, Arshad Desai, and Karen Oegema. 2008. "Expression and Imaging of Fluorescent Proteins in the *C. Elegans* Gonad and Early Embryo." In *Fluorescent Proteins*, 85:179–218. Methods in Cell Biology. Academic Press. [https://doi.org/https://doi.org/10.1016/S0091-679X\(08\)85009-1](https://doi.org/https://doi.org/10.1016/S0091-679X(08)85009-1).
- Greer, Eric L., Dara Dowlatshahi, Max R. Banko, Judit Villen, Kimmi Hoang, Daniel Blanchard, Steven P. Gygi, and Anne Brunet. 2007. "An AMPK-FOXO Pathway Mediates Longevity Induced by a Novel Method of Dietary Restriction in *C. Elegans*." *Current Biology* 17 (19): 1646–56. <https://doi.org/10.1016/j.cub.2007.08.047>.
- Griffith, Jack D, Laurey Comeau, Soraya Rosenfield, Rachel M. Stansel, Alessandro Bianchi, Heidi Moss, and Titia de Lange. 1999. "Mammalian Telomeres End in a Large Duplex Loop." *Cell* 97: 503–14.
- Gruber, Jan, Ce Belle Chen, Sheng Fong, Li Fang Ng, Emelyne Teo, and Barry Halliwell. 2015. "Caenorhabditis Elegans: What We Can and Cannot Learn from Aging Worms." *Antioxidants and Redox Signaling* 23 (3): 256–79.
<https://doi.org/10.1089/ars.2014.6210>.
- Gutman, M. 1978. "Modulation of Mitochondrial Succinate Dehydrogenase Activity, Mechanism and Function." *Molecular and Cellular Biochemistry* 20 (1): 41–60.
<https://doi.org/10.1007/BF00229453>.
- Gutscher, Marcus, Mirko C. Sobotta, Guido H. Wabnitz, Seda Ballikaya, Andreas J. Meyer, Yvonne Samstag, and Tobias P. Dick. 2009. "Proximity-Based Protein Thiol Oxidation by H₂O₂-Scavenging Peroxidases." *Journal of Biological Chemistry* 284 (46): 31532–40.
<https://doi.org/10.1074/jbc.M109.059246>.
- Habich, Markus, and Jan Riemer. 2017. "Detection of Cysteine Redox States in Mitochondrial Proteins in Intact Mammalian Cells." In *Mitochondria: Practical Protocols*, edited by Dejana Mokranjac and Fabiana Perocchi, 105–38. New York, NY: Springer New York.
https://doi.org/10.1007/978-1-4939-6824-4_8.
- Hackenbrock, Charles R, Brad Chazotte, and Sharmila Shaila Gupte. 1986. "The Random Collision Model and a Critical Assessment of Diffusion and Collision in Mitochondrial Electron Transport." *Journal of Bioenergetics and Biomembranes*. Vol. 18.
- Haes, Wouter de, Lotte Frooninckx, Roel van Assche, Arne Smolders, Geert Depuydt, Johan Billen, Bart P. Braeckman, Liliane Schoofs, and Liesbet Temmerman. 2014. "Metformin Promotes Lifespan through Mitohormesis via the Peroxiredoxin PRDX-2." *Proceedings of the National Academy of Sciences of the United States of America* 111 (24).
<https://doi.org/10.1073/pnas.1321776111>.
- Hande, M Prakash, Enrique Samper, Peter Lansdorp, and María A Blasco. 1999. "Telomere Length Dynamics and Chromosomal Instability in Cells Derived from Telomerase Null Mice." *The Journal of Cell Biology*. Vol. 144. <http://www.jcb.org>.
- Handler, Jeffrey A., and Ronald G. Thurman. 1987. "Rates of H₂O₂ Generation from Peroxisomal β -Oxidation Are Sufficient to Account for Fatty Acid-Stimulated Ethanol

- Metabolism in Perfused Rat Liver." *Alcohol* 4 (2): 131–34.
[https://doi.org/10.1016/0741-8329\(87\)90011-5](https://doi.org/10.1016/0741-8329(87)90011-5).
- Hansen, Malene, Stefan Taubert, Douglas Crawford, Nataliya Libina, Seung Jae Lee, and Cynthia Kenyon. 2007. "Regulation of Yeast Replicative Span by TOR and Sch9 in Response to Nutrients." *Aging Cell* 6 (1): 95–110. <https://doi.org/10.1111/j.1474-9726.2006.00267.x>.
- Harel, Itamar, and Anne Brunet. 2016. "The African Turquoise Killifish: A Model for Exploring Vertebrate Aging and Diseases in the Fast Lane." In *Cold Spring Harbor Symposia on Quantitative Biology*, 80:275–79. Cold Spring Harbor Laboratory Press.
<https://doi.org/10.1101/sqb.2015.80.027524>.
- Harman, D. 1956. "Aging: A Theory Based on Free Radical and Radiation Chemistry." *Journal of Gerontology* 11 (3): 298–300.
- . 1972. "The Biologic Clock: The Mitochondria? ." *Journal of the American Geriatrics Society* 20: 145–47.
- Harreman, Michelle T., Trisha M. Kline, Heidi G. Milford, M. Beth Harben, Alec E. Hodel, and Anita H. Corbett. 2004. "Regulation of Nuclear Import by Phosphorylation Adjacent to Nuclear Localization Signals." *Journal of Biological Chemistry* 279 (20): 20613–21.
<https://doi.org/10.1074/jbc.M401720200>.
- Hartman, Phil S, Naoaki Ishii, Ernst-Bernhard Kayser, Phil G Morgan, and Margaret M Sedensky. 2001. "Mitochondrial Mutations Differentially Affect Aging, Mutability and Anesthetic Sensitivity in *Caenorhabditis Elegans*." *Mechanisms of Ageing and Development*. Vol. 122. www.elsevier.com/locate/mechagedev.
- Hashmi, Sarwar, Qiongmei Ji, Jun Zhang, Ranjit S Parhar, Cheng-Han Huang, Chris Brey, and Randy Gaugler. 2008. "A Krüppel-Like Factor in *Caenorhabditis Elegans* with Essential Roles in Fat Regulation, Cell Death, and Phagocytosis." www.liebertpub.com.
- Heidler, Tanja, Kai Hartwig, Hannelore Daniel, and Uwe Wenzel. 2010. "Caenorhabditis Elegans Lifespan Extension Caused by Treatment with an Orally Active ROS-Generator Is Dependent on DAF-16 and SIR-2.1." *Biogerontology* 11 (2): 183–95.
<https://doi.org/10.1007/s10522-009-9239-x>.
- Herbener, G. H. 1976. "A Morphometric Study of Age-Dependent Changes in Mitochondrial Population of Mouse Liver and Heart." *J Gerontol* 1: 8–12.
- Herholz, Marija, Estela Cepeda, Linda Baumann, Alexandra Kukat, Johannes Hermeling, Sarah Maciej, Karolina Szczepanowska, Victor Pavlenko, Peter Frommolt, and Aleksandra Trifunovic. 2019. "KLF-1 Orchestrates a Xenobiotic Detoxification Program Essential for Longevity of Mitochondrial Mutants." *Nature Communications* 10 (1).
<https://doi.org/10.1038/s41467-019-11275-w>.
- Hermeling, Johannes CW, Marija Herholz, Linda Baumann, Estela Cepeda Cores, Aleksandra Zečić, Thorsten Hoppe, Jan Riemer, and Aleksandra Trifunovic. 2022. "Mitochondria-Originated Redox Signalling Regulates KLF-1 to Promote Longevity in *Caenorhabditis Elegans*." *Redox Biology* 58 (December). <https://doi.org/10.1016/j.redox.2022.102533>.
- Hoekstra, Attje S., and Jean Pierre Bayley. 2013. "The Role of Complex II in Disease." *Biochimica et Biophysica Acta - Bioenergetics* 1827 (5): 543–51.
<https://doi.org/10.1016/j.bbabo.2012.11.005>.
- Hole, Paul S, Joanna Zabkiewicz, Chinmay Munje, Zarabeth Newton, Lorna Pearn, Paul White, Nuria Marquez, et al. 2013. "Overproduction of NOX-Derived ROS in AML Promotes Proliferation and Is Associated with Defective Oxidative Stress Signaling." *Blood* 122: 3322–30. <https://doi.org/10.1182/blood-2013-04>.

- Honjoh, Sakiko, Takuya Yamamoto, Masaharu Uno, and Eisuke Nishida. 2009. "Signalling through RHEB-1 Mediates Intermittent Fasting-Induced Longevity in *C. Elegans*." *Nature* 457 (7230): 726–30. <https://doi.org/10.1038/nature07583>.
- Horn, Susanne, Adina Figl, P. Sivaramakrishna Rachakonda, Christine Fischer, Antje Sucker, Andreas Gast, Stephanie Kadel, et al. 2013. "TERT Promoter Mutations in Familial and Sporadic Melanoma." *Science* 339 (6122): 959–61.
- Horspool, Alexander M., and Howard C. Chang. 2017. "Superoxide Dismutase SOD-1 Modulates *C. Elegans* Pathogen Avoidance Behavior." *Scientific Reports* 7 (February): 1–13. <https://doi.org/10.1038/srep45128>.
- Hourihan, John M., Lorenza E. Moronetti Mazzeo, L. Paulette Fernández-Cárdenas, and T. Keith Blackwell. 2016. "Cysteine Sulfenylation Directs IRE-1 to Activate the SKN-1/Nrf2 Antioxidant Response." *Molecular Cell* 63 (4): 553–66. <https://doi.org/10.1016/j.molcel.2016.07.019>.
- Houthoofd, Koen, Bart P Braeckman, Isabelle Lenaerts, Kristel Brys, Annemie de Vreese, Sylvie van Eygen, and Jacques R Vanfleteren. 2002. "No Reduction of Metabolic Rate in Food Restricted *Caenorhabditis Elegans*." *Experimental Gerontology* 37 (12): 1359–69. [https://doi.org/https://doi.org/10.1016/S0531-5565\(02\)00172-9](https://doi.org/https://doi.org/10.1016/S0531-5565(02)00172-9).
- Hoyt, Jill M., Samuel K. Wilson, Madhuri Kasa, Jeremy S. Rise, Irini Topalidou, and Michael Ailion. 2017. "The SEK-1 P38 MAP Kinase Pathway Modulates Gq Signaling in *Caenorhabditis Elegans*." *G3: Genes, Genomes, Genetics* 7 (9): 2979–89. <https://doi.org/10.1534/g3.117.043273>.
- Hsieh, Paishiun N., Guangjin Zhou, Yiyuan Yuan, Rongli Zhang, Domenick A. Prosdocimo, Panjamaporn Sangwung, Anna H. Borton, et al. 2017. "A Conserved KLF-Autophagy Pathway Modulates Nematode Lifespan and Mammalian Age-Associated Vascular Dysfunction." *Nature Communications* 8 (1). <https://doi.org/10.1038/s41467-017-00899-5>.
- Hu, Sunli, Chunwu Zhang, Libin Ni, Chongan Huang, Dingwen Chen, Keqing Shi, Haiming Jin, et al. 2020. "Stabilization of HIF-1 α Alleviates Osteoarthritis via Enhancing Mitophagy." *Cell Death and Disease* 11 (6). <https://doi.org/10.1038/s41419-020-2680-0>.
- Huang, Kai, Kirby D. Johnson, Andrei G. Petcherski, Thomas Vandergon, Eric A. Mosser, Neal G. Copeland, Nancy A. Jenkins, Judith Kimble, and Emery H. Bresnick. 2000. "A HECT Domain Ubiquitin Ligase Closely Related to the Mammalian Protein WWP1 Is Essential for *Caenorhabditis Elegans* Embryogenesis." *Gene* 252 (1–2): 137–45. [https://doi.org/10.1016/S0378-1119\(00\)00216-X](https://doi.org/10.1016/S0378-1119(00)00216-X).
- Ichimiya, Harumi, R Giselle Huet, Phil Hartman, Hisako Amino, Kiyoshi Kita, and Naoaki Ishii. n.d. "Complex II Inactivation Is Lethal in the Nematode *Caenorhabditis Elegans*." www.elsevier.com/locate/mito.
- Imataka, H., K. Sogawa, K. Yasumoto -i., Y. Kikuchi, K. Sasano, A. Kobayashi, M. Hayami, and Y. Fujii-Kuriyama. 1992. "Two Regulatory Proteins That Bind to the Basic Transcription Element (BTE), a GC Box Sequence in the Promoter Region of the Rat P-4501A1 Gene." *EMBO Journal* 11 (10): 3663–71. <https://doi.org/10.1002/j.1460-2075.1992.tb05451.x>.
- Inoue, Hideki, Naoki Hisamoto, Hyung An Jae, Riva P. Oliveira, Eisuke Nishida, T. Keith Blackwell, and Kunihiro Matsumoto. 2005. "The *C. Elegans* P38 MAPK Pathway Regulates Nuclear Localization of the Transcription Factor SKN-1 in Oxidative Stress Response." *Genes and Development* 19 (19): 2278–83. <https://doi.org/10.1101/gad.1324805>.
- Ishii, N. 2000. "Oxidative Stress and Aging in *Caenorhabditis Elegans*." *Free Radical Research* 33 (6): 857–64. <https://doi.org/10.1080/10715760000301371>.

- Ishii, Naoaki, Kiyoko Takahashi, Satoru Tomita, Tetsuo Keino, Shuji Honda, Kazuhiro Yoshino, and Kenshi Suzuki. 1990. "A Methyl Viologen-Sensitive Mutant of the Nematode *Caenorhabditis Elegans*." *Mutation Research*. Vol. 237.
- Iwata, So, Joong W Lee, Kengo Okada, John Kyongwon Lee, Momi Iwata, Bjarne Rasmussen, Thomas A Link, S Ramaswamy, and Bing K Jap. 1998. "Complete Structure of the 11-Subunit Bovine Mitochondrial Cytochrome Bc 1 Complex." *Science* 281: 64–71. <https://www.science.org>.
- Jang, Youngmok C., Viviana I. Pérez, Wook Song, Michael S. Lustgarten, Adam B. Salmon, James Mele, Wenbo Qi, et al. 2009. "Overexpression of Mn Superoxide Dismutase Does Not Increase Life Span in Mice." *Journals of Gerontology - Series A Biological Sciences and Medical Sciences* 64 (11): 1114–25. <https://doi.org/10.1093/gerona/glp100>.
- Jensen, Laran T., and Valeria Cizewski Culotta. 2005. "Activation of CuZn Superoxide Dismutases from *Caenorhabditis Elegans* Does Not Require the Copper Chaperone CCS." *Journal of Biological Chemistry* 280 (50): 41373–79. <https://doi.org/10.1074/jbc.M509142200>.
- Jensen, P. K. 1966. "Antimycin-Insensitive Oxidation of Succinate and Reduced Nicotinamide-Adenine Dinucleotide in Electron-Transport Particles. II. Steroid Effects." *Biochimica et Biophysica Acta* 122 (2): 167–74.
- John Barton, By P, John E Packer, and Ritchie J Sims. 1961. "Kinetics of the Reaction of Hydrogen Peroxide with Cysteine and Cyste-Amine." *J. Phys. Chena*. Vol. 1.
- Johnston, Andrew D., and Paul R. Ebert. 2012. "The Redox System in *C. Elegans*, a Phylogenetic Approach." *Journal of Toxicology* 2012. <https://doi.org/10.1155/2012/546915>.
- Kaczynski, Joanna A, Abigail A Conley, Martin Fernandez Zapico, Sharon M Delgado, Jin-San Zhang, and Raul Urrutia. 2002. "Functional Analysis of Basic Transcription Element (BTE)-Binding Protein (BTEB) 3 and BTEB4, a Novel Sp1-like Protein, Reveals a Subfamily of Transcriptional Repressors for the BTE Site of the Cytochrome P4501A1 Gene Promoter." *Biochemical Journal* 366 (3): 873–82. <https://doi.org/10.1042/bj20020388>.
- Kadenbach, Bernhard. 2021. "Complex IV – The Regulatory Center of Mitochondrial Oxidative Phosphorylation." *Mitochondrion*. Elsevier B.V. <https://doi.org/10.1016/j.mito.2020.10.004>.
- Kaeberlein, Matt, Wilson R. Powers, and Kristan K. Steffen. 2005. "Regulation of Yeast Replicative Span by TOR and Sch9 in Response to Nutrients." *Science* 310 (5751): 1193–96. <https://doi.org/10.1126/science.1119238>.
- Kakimoto, Pâmela A.H.B., Fábio K. Tamaki, Ariel R. Cardoso, Sandro R. Marana, and Alicia J. Kowaltowski. 2015. "H₂O₂ Release from the Very Long Chain Acyl-CoA Dehydrogenase." *Redox Biology* 4: 375–80. <https://doi.org/10.1016/j.redox.2015.02.003>.
- Kamath, Ravi S., and Julie Ahringer. 2003. "Genome-Wide RNAi Screening in *Caenorhabditis Elegans*." *Methods* 30 (4): 313–21. [https://doi.org/10.1016/S1046-2023\(03\)00050-1](https://doi.org/10.1016/S1046-2023(03)00050-1).
- Kamath, Ravi S., Andrew G. Fraser, Yan Dong, Gino Poulin, Richard Durbin, Monica Gotta, Alexander Kanapin, et al. 2003. "Systematic Functional Analysis of the *Caenorhabditis Elegans* Genome Using RNAi." *Nature* 421 (6920): 231–37. <https://doi.org/10.1038/nature01278>.
- Kandoth, Pramod K., and Melissa G. Mitchum. 2013. "War of the Worms: How Plants Fight Underground Attacks." *Current Opinion in Plant Biology*. <https://doi.org/10.1016/j.pbi.2013.07.001>.

- Kane, Mariame Selma, Aurelien Paris, Philippe Codron, Julien Cassereau, Vincent Procaccio, Guy Lenaers, Pascal Reynier, and Arnaud Chevrollier. 2018. "Current Mechanistic Insights into the CCCP-Induced Cell Survival Response." *Biochemical Pharmacology*. Elsevier Inc. <https://doi.org/10.1016/j.bcp.2017.12.018>.
- Kapahi, Pankaj, Brain M. Zid, Tony Harper, Daniel Koslover, Viveca Sapin, and Seymour Benzer. 2004. "Regulation of Lifespan InDrosophilaby Modulation of Genes in the TOR Signaling Pathway." *Current Biology* 14: 885–90. <https://doi.org/10.1016/j>.
- Karlsson, Markus, Tino Kurz, Ulf T. Brunk, Sven E. Nilsson, and Christina I. Frennesson. 2010. "What Does the Commonly Used DCF Test for Oxidative Stress Really Show?" *Biochemical Journal* 428 (2): 183–90. <https://doi.org/10.1042/BJ20100208>.
- Kaufmann, Thomas, Sarah Schlipf, Javier Sanz, Karin Neubert, Reuven Stein, and Christoph Borner. 2003. "Characterization of the Signal That Directs Bcl-XL, but Not Bcl-2, to the Mitochondrial Outer Membrane." *Journal of Cell Biology* 160 (1): 53–64. <https://doi.org/10.1083/jcb.200210084>.
- Kayser, Ernst Bernhard, Phil G. Morgan, Charles L. Hoppel, and Margaret M. Sedensky. 2001. "Mitochondrial Expression and Function of GAS-1 in Caenorhabditis Elegans." *Journal of Biological Chemistry* 276 (23): 20551–58. <https://doi.org/10.1074/jbc.M011066200>.
- Kayser, Ernst-Bernhard, Phil G Morgan, and Margaret M Sedensky. 2004. "Mitochondrial Complex I Function Affects Halothane Sensitivity in Caenorhabditis Elegans." *Anesthesiology*. Vol. 101. <http://pubs.asahq.org/anesthesiology/article-pdf/101/2/365/356352/0000542-200408000-00017.pdf>.
- Kenyon, Cynthia. 2010. "A Pathway That Links Reproductive Status to Lifespan in Caenorhabditis Elegans." In *Annals of the New York Academy of Sciences*, 1204:156–62. Blackwell Publishing Inc. <https://doi.org/10.1111/j.1749-6632.2010.05640.x>.
- Kenyon, Cynthia J. 2010. "The Genetics of Ageing." *Nature*. <https://doi.org/10.1038/nature08980>.
- Kevei, Éva, and Thorsten Hoppe. 2014. "Ubiquitin Sets the Timer: Impacts on Aging and Longevity." *Nature Publishing Group*. <https://doi.org/10.1016/j.cmet>.
- Kharade, Sujay v., Nitish Mittal, Shankar P. Das, Pratima Sinha, and Nilanjan Roy. 2005. "Mrg19 Depletion Increases S. Cerevisiae Lifespan by Augmenting ROS Defence." *FEBS Letters* 579 (30): 6809–13. <https://doi.org/10.1016/j.febslet.2005.11.017>.
- Khodakarami, Amirabbas, Isabel Saez, Johanna Mels, and David Vilchez. 2015. "Mediation of Organismal Aging and Somatic Proteostasis by the Germline." *Frontiers in Molecular Biosciences*. Frontiers Media S.A. <https://doi.org/10.3389/fmolb.2015.00003>.
- Khraiwesh, Husam, José A. López-Domínguez, Guillermo López-Lluch, Plácido Navas, Rafael de Cabo, Jon J. Ramsey, José M. Villalba, and José A. González-Reyes. 2013. "Alterations of Ultrastructural and Fission/Fusion Markers in Hepatocyte Mitochondria from Mice Following Calorie Restriction with Different Dietary Fats." *Journals of Gerontology - Series A Biological Sciences and Medical Sciences* 68 (9): 1023–34. <https://doi.org/10.1093/gerona/glt006>.
- Kiley, Patricia J., and Gisela Storz. 2004. "Exploiting Thiol Modifications." *PLoS Biology*. <https://doi.org/10.1371/journal.pbio.0020400>.
- Kim, Jeonghan, Rajeev Gupta, Luz P Blanco, Shutong Yang, Anna Shteinfer-Kuzmine, Kening Wang, Jun Zhu, et al. 2019. "VDAC Oligomers Form Mitochondrial Pores to Release MtDNA Fragments and Promote Lupus-like Disease." *Science* 366: 1531–36. <https://www.science.org>.

- Kim, Yujin E., Mark S. Hipp, Andreas Bracher, Manajit Hayer-Hartl, and F. Ulrich Hartl. 2013. "Molecular Chaperone Functions in Protein Folding and Proteostasis." *Annual Review of Biochemistry*. <https://doi.org/10.1146/annurev-biochem-060208-092442>.
- Kirkwood, Thomas B.L., and Axel Kowald. 2012. "The Free-Radical Theory of Ageing - Older, Wiser and Still Alive: Modelling Positional Effects of the Primary Targets of ROS Reveals New Support." *BioEssays* 34 (8): 692–700. <https://doi.org/10.1002/bies.201200014>.
- Klapper, Maja, Madeleine Ehmke, Daniela Palgunow, Mike Böhme, Christian Matthäus, Gero Bergner, Benjamin Dietzek, Jürgen Popp, and Frank Döring. 2011. "Fluorescence-Based FRET and Vital Staining of Lipid Droplets in *Caenorhabditis Elegans* Reveal Fat Stores Using Microscopy and Flow Cytometry Approaches Oil Red O Staining" 52. <https://doi.org/10.1194/jlr.D011940>.
- Koh, Kwi Hye, Xian Pan, Wei Zhang, Alan McLachlan, Raul Urrutia, and Hyunyoung Jeong. 2014. "Krüppel-Like Factor 9 Promotes Hepatic Cytochrome P450 2D6 Expression during Pregnancy in CYP2D6-Humanized Mice." *Molecular Pharmacology* 86 (6): 727. <https://doi.org/10.1124/mol.114.093666>.
- Komori, M, K Nishio, M Kitada, K Shiramatsu, K Muroya, M Soma, K Nagashima, et al. 1993. "Gene Structure of CYP3A4, an Adult-Specific Form of Cytochrome P450 in Human Livers, and Its Transcriptional Control CYP3A4 Is the Adult-Specific Form of Cytochrome P450 in Human Livers." *Eur. J. Biochem.* Vol. 218.
- Kondo, Masaki, Sumino Yanase, Takamasa Ishii, Philip S. Hartman, Kunihiro Matsumoto, and Naoaki Ishii. 2005. "The P38 Signal Transduction Pathway Participates in the Oxidative Stress-Mediated Translocation of DAF-16 to *Caenorhabditis Elegans* Nuclei." *Mechanisms of Ageing and Development* 126 (6–7): 642–47. <https://doi.org/10.1016/j.mad.2004.11.012>.
- Koopman, Werner J.H., Peter H.G.M. Willems, Jan A.M. M Smeitink, and D Ph. 2012. "Monogenic Mitochondrial Disorders." *The New England Journal of Medicine* 366 (12): 1132–41. <https://doi.org/10.1056/NEJMra1012478>.
- Kosugi, Shunichi, Masako Hasebe, Masaru Tomita, and Hiroshi Yanagawa. 2009. "Systematic Identification of Cell Cycle-Dependent Yeast Nucleocytoplasmic Shuttling Proteins by Prediction of Composite Motifs." *Proceedings of the National Academy of Sciences of the United States of America* 106 (25): 10171–76. <https://doi.org/10.1073/pnas.0900604106>.
- Kotamraju, Srigiridhar, Shasi v. Kalivendi, Eugene Konorev, Christopher R. Chitambar, Joy Joseph, and B. Kalyanaraman. 2004. "Oxidant-Induced Iron Signaling in Doxorubicin-Mediated Apoptosis." *Methods in Enzymology* 378 (January): 362–82. [https://doi.org/10.1016/S0076-6879\(04\)78026-X](https://doi.org/10.1016/S0076-6879(04)78026-X).
- Kowaltowski, Alicia J., Nadja C. de Souza-Pinto, Roger F. Castilho, and Anibal E. Vercesi. 2009. "Mitochondria and Reactive Oxygen Species." *Free Radical Biology and Medicine* 47 (4): 333–43. <https://doi.org/10.1016/j.freeradbiomed.2009.05.004>.
- Koyuncu, Seda, Rute Loureiro, Hyun Ju Lee, Prerana Wagle, Marcus Krueger, and David Vilchez. 2021. "Rewiring of the Ubiquitinated Proteome Determines Ageing in *C. Elegans*." *Nature* 596 (7871): 285–90. <https://doi.org/10.1038/s41586-021-03781-z>.
- Kuang, Jujiao, and Paul R Ebert. 2012. "The Failure to Extend Lifespan via Disruption of Complex II Is Linked to Preservation of Dynamic Control of Energy Metabolism." *Mitochondrion* 12 (2): 280–87. <https://doi.org/https://doi.org/10.1016/j.mito.2011.10.003>.

- Kubben, Nard, Weiqi Zhang, Lixia Wang, Ty C. Voss, Jiping Yang, Jing Qu, Guang Hui Liu, and Tom Misteli. 2016. "Repression of the Antioxidant NRF2 Pathway in Premature Aging." *Cell* 165 (6): 1361–74. <https://doi.org/10.1016/j.cell.2016.05.017>.
- Kühlbrandt, Werner. 2015. "Structure and Function of Mitochondrial Membrane Protein Complexes." *BMC Biology*. BioMed Central Ltd. <https://doi.org/10.1186/s12915-015-0201-x>.
- Kumsta, Caroline, Jessica T. Chang, Reina Lee, Ee Phie Tan, Yongzhi Yang, Rute Loureiro, Elizabeth H. Choy, et al. 2019. "The Autophagy Receptor P62/SQST-1 Promotes Proteostasis and Longevity in *C. Elegans* by Inducing Autophagy." *Nature Communications* 10 (1). <https://doi.org/10.1038/s41467-019-13540-4>.
- Kyriakis, John M, and Joseph Avruch. 2012. "Mammalian MAPK Signal Transduction Pathways Activated by Stress and Inflammation: A 10-Year Update." *Physiol Rev* 92: 689–737. <https://doi.org/10.1152/physrev.00028.2011.-The>.
- Lakowski, Bernard, and Siegfried Hekimi. 1996. "Determination of Life-Span in *Caenorhabditis Elegans* by Four Clock Genes." *Science* 272 (5264): 1010–13. <https://doi.org/10.1126/science.272.5264.1010>.
- . 1998. "The Genetics of Caloric Restriction in *Caenorhabditis Elegans*." *Proceedings of the National Academy of Sciences of the United States of America* 95 (22): 13091–96. <https://doi.org/10.1073/pnas.95.22.13091>.
- Lambert, A J, and B J Merry. 2004. "Effect of Caloric Restriction on Mitochondrial Reactive Oxygen Species Production and Bioenergetics: Reversal by Insulin." *Am J Physiol Regul Integr Comp Physiol* 286: 71–79. <https://doi.org/10.1152/ajp>.
- Larsson, Nils Göran. 2010. "Somatic Mitochondrial DNA Mutations in Mammalian Aging." *Annual Review of Biochemistry*. <https://doi.org/10.1146/annurev-biochem-060408-093701>.
- Larsson, Nils-Göran, and David A Clayton. 1995. "Molecular Genetic Aspects of Human Mitochondrial Disorders." www.annualreviews.org.
- Lee, Jin Won, and John D. Helmann. 2006. "The PerR Transcription Factor Senses H₂O₂ by Metal-Catalysed Histidine Oxidation." *Nature* 440 (7082): 363–67. <https://doi.org/10.1038/nature04537>.
- Lee, Kiho, Jiwon Shim, Jaebum Bae, Young Joon Kim, and Junho Lee. 2012. "Stabilization of RNT-1 Protein, Runt-Related Transcription Factor (RUNX) Protein Homolog of *Caenorhabditis Elegans*, by Oxidative Stress through Mitogen-Activated Protein Kinase Pathway." *Journal of Biological Chemistry* 287 (13): 10444–52. <https://doi.org/10.1074/jbc.M111.314146>.
- Lee, Siu Sylvia, Raymond Y.N. Lee, Andrew G. Fraser, Ravi S. Kamath, Julie Ahringer, and Gary Ruvkun. 2003. "A Systematic RNAi Screen Identifies a Critical Role for Mitochondria in *C. Elegans* Longevity." *Nature Genetics* 33 (1): 40–48. <https://doi.org/10.1038/ng1056>.
- Lencina, Andrea M., Thierry Franza, Matthew J. Sullivan, Glen C. Ulett, Deepak S. Ipe, Philippe Gaudu, Robert B. Gennis, and Lici A. Schurig-Briccio. 2018. "Type 2 NADH Dehydrogenase Is the Only Point of Entry for Electrons into the *Streptococcus Agalactiae* Respiratory Chain and Is a Potential Drug Target." *MBio* 9 (4). <https://doi.org/10.1128/mBio.01034-18>.
- Li, Jian, Michael Stouffs, Lena Serrander, Botond Banfi, Esther Bettiol, Yves Charnay, Klaus Steger, Karl-Heinz Krause, and Marisa E Jaconi. 2006. "The NADPH Oxidase NOX4 Drives Cardiac Differentiation: Role in Regulating Cardiac Transcription Factors and MAP Kinase Activation." *Molecular Biology of the Cell* 17: 3978–88. <https://doi.org/10.1091/mbc.E05-06>.

- Li, Nianyu, Kathy Ragheb, Gretchen Lawler, Jennie Sturgis, Bartek Rajwa, J. Andres Melendez, and J. Paul Robinson. 2003. "Mitochondrial Complex I Inhibitor Rotenone Induces Apoptosis through Enhancing Mitochondrial Reactive Oxygen Species Production." *Journal of Biological Chemistry* 278 (10): 8516–25. <https://doi.org/10.1074/jbc.M210432200>.
- Li, Pengying, Dongyang Zhang, Lingxiao Shen, Kelei Dong, Meiling Wu, Zhouluo Ou, and Dongyun Shi. 2016. "Redox Homeostasis Protects Mitochondria through Accelerating ROS Conversion to Enhance Hypoxia Resistance in Cancer Cells." *Scientific Reports* 6 (March). <https://doi.org/10.1038/srep22831>.
- Li, Ying, Wei Xu, Michael W. McBurney, and Valter D. Longo. 2008. "SirT1 Inhibition Reduces IGF-I/IRS-2/Ras/ERK1/2 Signaling and Protects Neurons." *Cell Metabolism* 8 (1): 38–48. <https://doi.org/10.1016/j.cmet.2008.05.004>.
- Lin, Weiwei, Na Yuan, Zhen Wang, Yan Cao, Yixuan Fang, Xin Li, Fei Xu, et al. 2015. "Autophagy Confers DNA Damage Repair Pathways to Protect the Hematopoietic System from Nuclear Radiation Injury." *Scientific Reports* 5 (July). <https://doi.org/10.1038/srep12362>.
- Ling, Jun, Christopher Brey, Megan Schilling, Farah Lateef, Zenaida P. Lopez-Dee, Kristopher Fernandes, Kavita Thiruchelvam, et al. 2017. "Defective Lipid Metabolism Associated with Mutation in Klf-2 and Klf-3: Important Roles of Essential Dietary Salts in Fat Storage." *Nutrition and Metabolism* 14 (1). <https://doi.org/10.1186/s12986-017-0172-8>.
- Lithgow, Gordon J., Tiffany M. White, Simon Melov, and Thomas E. Johnson. 1995. "Thermotolerance and Extended Life-Span Conferred by Single-Gene and Induced by Thermal Stress." *Genetics* 92: 7540–44.
- Loeb, Jacques, and J H Northrop. 1911. "What Determines the Duration of Life in Metazoa?" *PNAS* 62 (17): 382–86.
- López-Otín, Carlos, Maria A. Blasco, Linda Partridge, Manuel Serrano, and Guido Kroemer. 2013. "The Hallmarks of Aging." *Cell*. Elsevier B.V. <https://doi.org/10.1016/j.cell.2013.05.039>.
- Lu, Jun, and Arne Holmgren. 2014. "The Thioredoxin Antioxidant System." *Free Radical Biology and Medicine*. Elsevier Inc. <https://doi.org/10.1016/j.freeradbiomed.2013.07.036>.
- Maiorino, Matilde, Fulvio Ursini, Valentina Bosello, Stefano Toppo, Silvio C.E. Tosatto, Pierluigi Mauri, Katja Becker, et al. 2007. "The Thioredoxin Specificity of Drosophila GPx: A Paradigm for a Peroxiredoxin-like Mechanism of Many Glutathione Peroxidases." *Journal of Molecular Biology* 365 (4): 1033–46. <https://doi.org/10.1016/J.JMB.2006.10.033>.
- Mallipattu, Sandeep K., Sylvia J. Horne, Vivette D'Agati, Goutham Narla, Ruijie Liu, Michael A. Frohman, Kathleen Dickman, et al. 2015. "Krüppel-like Factor 6 Regulates Mitochondrial Function in the Kidney." *Journal of Clinical Investigation* 125 (3): 1347–61. <https://doi.org/10.1172/JCI77084>.
- Maremonti, Erica, Dag Markus Eide, Lisa M. Rossbach, Ole Christian Lind, Brit Salbu, and Dag Anders Brede. 2020. "In Vivo Assessment of Reactive Oxygen Species Production and Oxidative Stress Effects Induced by Chronic Exposure to Gamma Radiation in Caenorhabditis Elegans." *Free Radical Biology and Medicine* 152 (September 2019): 583–96. <https://doi.org/10.1016/j.freeradbiomed.2019.11.037>.

- Margis, Rogerio, Christophe Dunand, Felipe K. Teixeira, and Marcia Margis-Pinheiro. 2008. "Glutathione Peroxidase Family - An Evolutionary Overview." *FEBS Journal* 275 (15): 3959–70. <https://doi.org/10.1111/j.1742-4658.2008.06542.x>.
- Markvicheva, Kseniya N., Dmitry S. Bilan, Natalia M. Mishina, Andrey Yu Gorokhovatsky, Leonid M. Vinokurov, Sergey Lukyanov, and Vsevolod v. Belousov. 2011. "A Genetically Encoded Sensor for H₂O₂ with Expanded Dynamic Range." *Bioorganic and Medicinal Chemistry* 19 (3): 1079–84. <https://doi.org/10.1016/j.bmc.2010.07.014>.
- Martínez-Revelles, Sonia, María S. Avendaño, Ana B. García-Redondo, Yolanda Álvarez, Andrea Aguado, Jose v. Pérez-Girón, Laura García-Redondo, et al. 2013. "Reciprocal Relationship between Reactive Oxygen Species and Cyclooxygenase-2 and Vascular Dysfunction in Hypertension." *Antioxidants and Redox Signaling* 18 (1): 51–65. <https://doi.org/10.1089/ars.2011.4335>.
- Marzo, Noemi di, Elisa Chisci, and Roberto Giovannoni. 2018. "The Role of Hydrogen Peroxide in Redox-Dependent Signaling: Homeostatic and Pathological Responses in Mammalian Cells." *Cells* 7 (10): 156. <https://doi.org/10.3390/cells7100156>.
- Masoro, E J. 2002. *Caloric Restriction*. Edited by Edward J Masoro. *Caloric Restriction*. Research Profiles in Aging. Amsterdam: Elsevier. <https://doi.org/https://doi.org/10.1016/B978-044451162-1/50000-X>.
- Masoro, Edward J. 2009. "Caloric Restriction-Induced Life Extension of Rats and Mice: A Critique of Proposed Mechanisms." *Biochimica et Biophysica Acta (BBA) - General Subjects* 1790 (10): 1040–48. <https://doi.org/https://doi.org/10.1016/j.bbagen.2009.02.011>.
- Matoba, Keiichiro, Yuan Lu, Rongli Zhang, Eric R. Chen, Panjamaporn Sangwung, Benlian Wang, Domenick A. Prosdocimo, and Mukesh K. Jain. 2017. "Adipose KLF15 Controls Lipid Handling to Adapt to Nutrient Availability." *Cell Reports* 21 (11): 3129–40. <https://doi.org/10.1016/j.celrep.2017.11.032>.
- Matsuno-Yagi, A, and Y Hatefi. 1985. "Studies on the Mechanism of Oxidative Phosphorylation. Catalytic Site Cooperativity in ATP Synthesis." *Journal of Biological Chemistry* 260 (27): 14424–27. [https://doi.org/10.1016/S0021-9258\(17\)38584-8](https://doi.org/10.1016/S0021-9258(17)38584-8).
- Mazat, Jean Pierre, Anne Devin, and Stéphane Ransac. 2020. "Modelling Mitochondrial ROS Production by the Respiratory Chain." *Cellular and Molecular Life Sciences*. Springer. <https://doi.org/10.1007/s00018-019-03381-1>.
- McConnell, Beth B., and Vincent W. Yang. 2010. "Mammalian Krüppel-Like Factors in Health and Diseases." *Physiological Reviews*. <https://doi.org/10.1152/physrev.00058.2009>.
- McElwee, Joshua J., Eugene Schuster, Eric Blanc, James H. Thomas, and David Gems. 2004. "Shared Transcriptional Signature in *Caenorhabditis Elegans* Dauer Larvae and Long-Lived *Daf-2* Mutants Implicates Detoxification System in Longevity Assurance." *Journal of Biological Chemistry* 279 (43): 44533–43. <https://doi.org/10.1074/jbc.M406207200>.
- Mehta, Tina S., Heng Lu, Xianhui Wang, Alison M. Urvalek, Kim Hang H. Nguyen, Farah Monzur, Jojo D. Hammond, Jameson Q. Ma, and Jihe Zhao. 2009. "A Unique Sequence in the N-Terminal Regulatory Region Controls the Nuclear Localization of KLF8 by Cooperating with the C-Terminal Zinc-Fingers." *Cell Research* 19 (9): 1098–1109. <https://doi.org/10.1038/cr.2009.64>.
- Meinhardt, S. W., X. H. Yang, B. L. Trumpower, and T. Ohnishi. 1987. "Identification of a Stable Ubisemiquinone and Characterization of the Effects of Ubiquinone Oxidation-Reduction Status on the Rieske Iron-Sulfur Protein in the Three-Subunit Ubiquinol-Cytochrome c Oxidoreductase Complex of *Paracoccus Denitrificans*." *Journal of*

- Biological Chemistry* 262 (18): 8702–6. [https://doi.org/10.1016/s0021-9258\(18\)47471-6](https://doi.org/10.1016/s0021-9258(18)47471-6).
- Melén, Krister, Riku Fagerlund, Jacqueline Franke, Matthias Köhler, Leena Kinnunen, and Ilkka Julkunen. 2003. “Importin α Nuclear Localization Signal Binding Sites for STAT1, STAT2, and Influenza A Virus Nucleoprotein.” *Journal of Biological Chemistry* 278 (30): 28193–200. <https://doi.org/10.1074/jbc.M303571200>.
- Mello, C. C., J. M. Kramer, D. Stinchcomb, and V. Ambros. 1991. “Efficient Gene Transfer in *C. Elegans*: Extrachromosomal Maintenance and Integration of Transforming Sequences.” *EMBO Journal* 10 (12): 3959–70. <https://doi.org/10.1002/j.1460-2075.1991.tb04966.x>.
- Melo, Justine A., and Gary Ruvkun. 2012. “Inactivation of Conserved *C. Elegans* Genes Engages Pathogen- and Xenobiotic-Associated Defenses.” *Cell* 149 (2): 452–66. <https://doi.org/10.1016/j.cell.2012.02.050>.
- Michaelis, L. 1939. “Free Radicals as Intermediate Steps of Oxidation-Reduction.” *Cold Spring Harb Symp Quant Biol* 7: 33–49.
- Mignolet-Spruyt, Lorin, Enjun Xu, Niina Idänheimo, Frank A. Hoeberichts, Per Mühlenbock, Mikael Brosche, Frank van Breusegem, and Jaakko Kangasjärvi. 2016. “Spreading the News: Subcellular and Organellar Reactive Oxygen Species Production and Signalling.” *Journal of Experimental Botany*. Oxford University Press. <https://doi.org/10.1093/jxb/erw080>.
- Miller, Evan W, Bryan C Dickinson, Christopher J Chang, C J C Designed, and B C D Performed. 2010. “Aquaporin-3 Mediates Hydrogen Peroxide Uptake to Regulate Downstream Intracellular Signaling.” *CHEMISTRY BIOCHEMISTRY* 107 (36): 15681–86. <https://doi.org/10.1073/pnas.1005776107/-/DCSupplemental>.
- Miranda-Vizueté, Antonio, and Elizabeth A. Veal. 2017. “Caenorhabditis Elegans as a Model for Understanding ROS Function in Physiology and Disease.” *Redox Biology*. Elsevier B.V. <https://doi.org/10.1016/j.redox.2016.12.020>.
- Mitchell, Sarah J., Morten Scheibye-Knudsen, Dan L. Longo, and Rafael de Cabo. 2015. “Animal Models of Aging Research: Implications for Human Aging and Age-Related Diseases.” *Annual Review of Animal Biosciences* 3 (February): 283–303. <https://doi.org/10.1146/annurev-animal-022114-110829>.
- Miyadera, Hiroko, Hisako Amino, Akira Hiraishi, Hikari Taka, Kimie Murayama, Hideto Miyoshill, Kimitoshi Sakamoto, Naoaki Ishii, Siegfried Hekimi, and Kiyoshi Kita. 2001. “Altered Quinone Biosynthesis in the Long-Lived Clk-1 Mutants of *Caenorhabditis Elegans*.” *Journal of Biological Chemistry* 276 (11): 7713–16. <https://doi.org/10.1074/jbc.C000889200>.
- Miyadera, Hiroko, Kazuro Shiomi, Hideaki Ui, Yuichi Yamaguchi, Rokuro Masuma, Hiroshi Tomoda, Hideto Miyoshi, Arihiro Osanai, Kiyoshi Kita, and Satoshi O Mura. 2003. “Atpenins, Potent and Specific Inhibitors of Mitochondrial Complex II (Succinate-Ubiquinone Oxidoreductase).” *BIOCHEMISTRY Downloaded at Buchhandlung Bouvier on November*. Vol. 100. www.pnas.org/cgi/doi/10.1073/pnas.0237315100.
- Morais, Vanessa A., Patrik Verstreken, Anne Roethig, Joél Smet, An Snellinx, Mieke Vanbrabant, Dominik Haddad, et al. 2009. “Parkinson’s Disease Mutations in PINK1 Result in Decreased Complex I Activity and Deficient Synaptic Function.” *EMBO Molecular Medicine* 1 (2): 99–111. <https://doi.org/10.1002/emmm.200900006>.
- Morgan, Bruce, Koen van Laer, Theresa N.E. Owusu, Daria Ezeriņa, Daniel Pastor-Flores, Prince Saforo Amponsah, Anja Tursch, and Tobias P. Dick. 2016. “Real-Time Monitoring

- of Basal H₂O₂ Levels with Peroxiredoxin-Based Probes." *Nature Chemical Biology* 12 (6): 437–43. <https://doi.org/10.1038/nchembio.2067>.
- Morgan, Phil G., M. Margaret, and M. D. Sedensky. 1994. "Mutations Conferring New Patterns of Sensitivity to Volatile Anesthetics in *Caenorhabditis Elegans*." *Anesthesiology* 81: 888–98.
- Morgan, Phil G, Margaret Sedensky, and Philip M Meneely. 1990. "Multiple Sites of Action of Volatile Anesthetics in *Caenorhabditis Elegans* (Genetics/Mutations/Anesthesia)." *Proc. Natl. Acad. Sci. USA* 87: 2965–69.
- Mota-Martorell, Natalia, Mariona Jove, Irene Pradas, Isabel Sanchez, José Gómez, Alba Naudi, Gustavo Barja, and Reinald Pamplona. 2020. "Low Abundance of NDUFV2 and NDUFS4 Subunits of the Hydrophilic Complex I Domain and VDAC1 Predicts Mammalian Longevity." *Redox Biology* 34 (July). <https://doi.org/10.1016/j.redox.2020.101539>.
- Muftuoglu, Meltem, Junko Oshima, Cayetano Kobbe, Wen Hsing Cheng, Dru F. Leistriz, and Vilhelm A. Bohr. 2008. "The Clinical Characteristics of Werner Syndrome: Molecular and Biochemical Diagnosis." *Human Genetics*. <https://doi.org/10.1007/s00439-008-0562-0>.
- Mukherjee, Abhisek, Diego Morales-Scheiing, Peter C Butler, and Claudio Soto. 2015. "Type 2 Diabetes as a Protein Misfolding Disease." *Trends in Molecular Medicine* 21 (7): 439–49. <https://doi.org/https://doi.org/10.1016/j.molmed.2015.04.005>.
- Müller, Alexandra, Jannis F. Schneider, Adriana Degrossoli, Nataliya Lupilova, Tobias P. Dick, and Lars I. Leichert. 2017. "Systematic in Vitro Assessment of Responses of RoGFP2-Based Probes to Physiologically Relevant Oxidant Species." *Free Radical Biology and Medicine* 106 (February): 329–38. <https://doi.org/10.1016/j.freeradbiomed.2017.02.044>.
- Muller, Florian L., Arthur G. Roberts, Michael K. Bowman, and David M. Kramer. 2003. "Architecture of the Q-o Site of the Cytochrome Bc₁ Complex Probed by Superoxide Production." *Biochemistry* 42 (21): 6493–99. <https://doi.org/10.1021/bi0342160>.
- Munkácsy, Erin, Maruf H. Khan, Rebecca K. Lane, Megan B. Borrer, Jae H. Park, Alex F. Bokov, Alfred L. Fisher, Christopher D. Link, and Shane L. Rea. 2016. "DLK-1, SEK-3 and PMK-3 Are Required for the Life Extension Induced by Mitochondrial Bioenergetic Disruption in *C. Elegans*." *PLoS Genetics* 12 (7). <https://doi.org/10.1371/journal.pgen.1006133>.
- Munkácsy, Erin, and Shane L. Rea. 2014. "The Paradox of Mitochondrial Dysfunction and Extended Longevity." *Experimental Gerontology*. Elsevier Inc. <https://doi.org/10.1016/j.exger.2014.03.016>.
- Muñoz-Tremblay, Lauren. 2015. "Role of Metabolic Shifts in Protection from Mutation Damage: Characterizing Mitochondrial Membrane Potential in *C. Elegans* Gas-1 Mutants." *McNair Scholars Online Journal* 9 (1). <https://doi.org/10.15760/mcnair.2015.101>.
- Murphy, Coleen T, Steven A Mccarroll, Cornelia I Bargmann, Andrew Fraser, Ravi S Kamath, Julie Ahringer, Hao Li, and Cynthia Kenyon. 2003. "Genes That Act Downstream of DAF-16 to Influence the Lifespan of *Caenorhabditis Elegans*." www.nature.com/nature.
- Murphy, Michael P., Arne Holmgren, Nils Göran Larsson, Barry Halliwell, Christopher J. Chang, Balaraman Kalyanaraman, Sue Goo Rhee, et al. 2011. "Unraveling the Biological Roles of Reactive Oxygen Species." *Cell Metabolism*. <https://doi.org/10.1016/j.cmet.2011.03.010>.
- Nagro, Christopher Del, Yang Xiao, Linda Rangell, Mike Reichelt, and Thomas O'Brien. 2014. "Depletion of the Central Metabolite NAD Leads to Oncosis-mediated Cell Death."

- Journal of Biological Chemistry* 289 (51): 35182–92.
<https://doi.org/10.1074/jbc.M114.580159>.
- Nagy, Péter, and Michael T. Ashby. 2007. “Reactive Sulfur Species: Kinetics and Mechanisms of the Oxidation of Cysteine by Hypohalous Acid to Give Cysteine Sulfenic Acid.” *Journal of the American Chemical Society* 129 (45): 14082–91.
<https://doi.org/10.1021/ja0737218>.
- Naji, Ali, John Houston, Caroline Skalley Rog, Ali al Hatem, Saba Rizvi, and Ransome van der Hoeven. 2018. “The Activation of the Oxidative Stress Response Transcription Factor SKN-1 in Caenorhabditis Elegans by Mitis Group Streptococci.” *PLoS ONE* 13 (8).
<https://doi.org/10.1371/journal.pone.0202233>.
- Nardoizzi, Jonathan, Nikola Wenta, Noriko Yasuhara, Uwe Vinkemeier, and Gino Cingolani. 2010. “Molecular Basis for the Recognition of Phosphorylated STAT1 by Importin A5.” *Journal of Molecular Biology* 402 (1): 83–100.
<https://doi.org/10.1016/j.jmb.2010.07.013>.
- Neupane, Prashant, Sudina Bhujju, Nita Thapa, and Hitesh Kumar Bhattarai. 2019. “ATP Synthase: Structure, Function and Inhibition.” *Biomolecular Concepts* 10 (1): 1–10.
<https://doi.org/10.1515/bmc-2019-0001>.
- Ni, Zi Xin, Jian Min Cui, Nian Zhang Zhang, and Bao Quan Fu. 2017. “Structural and Evolutionary Divergence of Aquaporins in Parasites (Review).” *Molecular Medicine Reports* 15 (6): 3943–48. <https://doi.org/10.3892/mmr.2017.6505>.
- Nietzel, Thomas, Marlene Elsässer, Cristina Ruberti, Janina Steinbeck, José Manuel Ugalde, Philippe Fuchs, Stephan Wagner, et al. 2019. “The Fluorescent Protein Sensor RoGFP2-Orp1 Monitors in Vivo H₂O₂ and Thiol Redox Integration and Elucidates Intracellular H₂O₂ Dynamics during Elicitor-Induced Oxidative Burst in Arabidopsis.” *New Phytologist* 221 (3): 1649–64. <https://doi.org/10.1111/nph.15550>.
- Nijtmans, Leo G J, Petr Klement, Josef Houck, and Coby van den Bogert. 1995. “Biochemical et Biohvsica Acta Assembly of Mitochondrial ATP Synthase in Cultured Human Cells: Implications for Mitochondrial Diseases.” *Biochimica et Biophysics Acta*. Vol. 1272.
- Oeppen, Jim, and James W. Vaupel. 2002. “Broken Limits to Life Expectancy.” *Science*.
<https://doi.org/10.1126/science.1069675>.
- Ogrunc, M., R. di Micco, M. Lontos, L. Bombardelli, M. Mione, M. Fumagalli, V. G. Gorgoulis, and F. D’Adda Di Fagagna. 2014. “Oncogene-Induced Reactive Oxygen Species Fuel Hyperproliferation and DNA Damage Response Activation.” *Cell Death and Differentiation* 21 (6): 998–1012. <https://doi.org/10.1038/cdd.2014.16>.
- Olá Hová, Monika, Sarah R Taylor, Siavash Khazaipoul, Jinling Wang, Brian A Morgan, Kunihiro Matsumoto, T Keith Blackwell, and Elizabeth A Veal. 2008. “A Redox-Sensitive Peroxiredoxin That Is Important for Longevity Has Tissue-and Stress-Specific Roles in Stress Resistance.” www.pnas.org/cgi/content/full/.
- Oláhová, Monika, Sarah R. Taylor, Siavash Khazaipoul, Jinling Wang, Brian A. Morgan, Kunihiro Matsumoto, T. Keith Blackwell, and Elizabeth A. Veal. 2008. “A Redox-Sensitive Peroxiredoxin That Is Important for Longevity Has Tissue- and Stress-Specific Roles in Stress Resistance.” *Proceedings of the National Academy of Sciences of the United States of America* 105 (50): 19839–44. <https://doi.org/10.1073/pnas.0805507105>.
- Oláhová, Monika, and Elizabeth A. Veal. 2015. “A Peroxiredoxin, PRDX-2, Is Required for Insulin Secretion and Insulin/IIS-Dependent Regulation of Stress Resistance and Longevity.” *Aging Cell* 14 (4): 558–68. <https://doi.org/10.1111/accel.12321>.
- Oliveira, Riva P., Jess Porter Abate, Kieran Dilks, Jessica Landis, Jasmine Ashraf, Coleen T. Murphy, and T. Keith Blackwell. 2009. “Condition-Adapted Stress and Longevity Gene

- Regulation by *Caenorhabditis Elegans* SKN-1/Nrf." *Aging Cell* 8 (5): 524–41.
<https://doi.org/10.1111/j.1474-9726.2009.00501.x>.
- Orr, Adam L, Leonardo Vargas, Carolina N Turk, Janine E Baaten, Jason T Matzen, Victoria J Dardov, Stephen J Attle, et al. 2015. "Suppressors of Superoxide Production from Mitochondrial Complex III" 11 (11): 834–36.
<https://doi.org/10.1038/nchembio.1910.Suppressors>.
- Pak, Valeriy v., Daria Ezerina, Olga G. Lyublinskaya, Brandán Pedre, Pyotr A. Tyurin-Kuzmin, Natalie M. Mishina, Marion Thauvin, et al. 2020. "Ultrasensitive Genetically Encoded Indicator for Hydrogen Peroxide Identifies Roles for the Oxidant in Cell Migration and Mitochondrial Function." *Cell Metabolism* 31 (3): 642-653.e6.
<https://doi.org/10.1016/j.cmet.2020.02.003>.
- Palgunow, Daniela, Maja Klapper, and Frank Do. 2012. "Dietary Restriction during Development Enlarges Intestinal and Hypodermal Lipid Droplets in *Caenorhabditis Elegans*" 7 (11). <https://doi.org/10.1371/journal.pone.0046198>.
- Pan, Kally Z., Julia E. Palter, Aric N. Rogers, Anders Olsen, Di Chen, Gordon J. Lithgow, and Pankaj Kapahi. 2007. "Inhibition of mRNA Translation Extends Lifespan in *Caenorhabditis Elegans*." *Aging Cell* 6 (1): 111–19. <https://doi.org/10.1111/j.1474-9726.2006.00266.x>.
- Pant, Bikram Datt, Sunhee Oh, and Kirankumar S. Mysore. 2021. "Protocol for Determining Protein Cysteine Thiol Redox Status Using Western Blot Analysis." *STAR Protocols* 2 (2): 100566. <https://doi.org/10.1016/j.xpro.2021.100566>.
- Papa, Sergio, Pietro Luca Marino, Giuseppe Capitanio, Antonio Gaballo, Domenico de Rasmio, Anna Signorile, and Vittoria Petruzzella. 2012. "The Oxidative Phosphorylation System in Mammalian Mitochondria." *Advances in Mitochondrial Medicine* 942: 3–37.
- Parvez, Saba, Marcus J.C. Long, Jesse R. Poganik, and Yimon Aye. 2018. "Redox Signaling by Reactive Electrophiles and Oxidants." *Chemical Reviews*. American Chemical Society.
<https://doi.org/10.1021/acs.chemrev.7b00698>.
- Pascual-Ahuir, Amparo, Sara Manzanares-Estreder, and Markus Proft. 2017. "Pro- and Antioxidant Functions of the Peroxisome-Mitochondria Connection and Its Impact on Aging and Disease." *Oxidative Medicine and Cellular Longevity* 2017.
<https://doi.org/10.1155/2017/9860841>.
- Patananan, Alexander N, Lauren M Budenholzer, Maria E Pedraza, Eric R Torres, N Adler, and Steven G Clarke. 2015. "The Invertebrate *Caenorhabditis Elegans* Biosynthesizes Ascorbate." *Biochemical and Biophysical Research Communications*, no. 569: 32–44.
<https://doi.org/10.1016/j.abb.2015.02.002.The>.
- Pearl, R. 1928. "The Rate of Living Theory."
- Pearson, Richard J., Laura Morf, and Upinder Singh. 2013. "Regulation of H₂O₂ Stress-Responsive Genes through a Novel Transcription Factor in the Protozoan Pathogen *Entamoeba Histolytica*." *Journal of Biological Chemistry* 288 (6): 4462–74.
<https://doi.org/10.1074/jbc.M112.423467>.
- Pedre, Brandán, David Young, Daniel Charlier, Álvaro Mourenza, Leonardo Astolfi Rosado, Laura Marcos-Pascual, Khadija Wahni, et al. 2018. "Structural Snapshots of OxyR Reveal the Peroxidatic Mechanism of H₂O₂ Sensing." *Proceedings of the National Academy of Sciences of the United States of America* 115 (50): E11623–32.
<https://doi.org/10.1073/pnas.1807954115>.
- Pei, Jimin, and Nick v. Grishin. 2013. "A New Family of Predicted Krüppel-like Factor Genes and Pseudogenes in Placental Mammals." *PLoS ONE* 8 (11).
<https://doi.org/10.1371/journal.pone.0081109>.

- Penkov, Sider, Bharath Kumar Raghuraman, Cihan Erkut, Jana Oertel, Roberta Galli, Eduardo Jacobo Miranda Ackerman, Daniela Vorkel, et al. 2020. "A Metabolic Switch Regulates the Transition between Growth and Diapause in *C. Elegans*." *BMC Biology* 18 (1). <https://doi.org/10.1186/s12915-020-0760-3>.
- Pfanner, Nikolaus, Bettina Warscheid, and Nils Wiedemann. 2019. "Mitochondrial Proteins: From Biogenesis to Functional Networks." *Nature Reviews Molecular Cell Biology*. Nature Publishing Group. <https://doi.org/10.1038/s41580-018-0092-0>.
- Pizzino, Gabriele, Natasha Irrera, Mariapaola Cucinotta, Giovanni Pallio, Federica Mannino, Vincenzo Arcoraci, Francesco Squadrito, Domenica Altavilla, and Alessandra Bitto. 2017. "Oxidative Stress: Harms and Benefits for Human Health." *Oxidative Medicine and Cellular Longevity* 2017. <https://doi.org/10.1155/2017/8416763>.
- Pollak, Nina M., Matthew Hoffman, Ira J. Goldberg, and Konstantinos Drosatos. 2018. "Krüppel-Like Factors: Crippling and Uncrippling Metabolic Pathways." *JACC: Basic to Translational Science*. Elsevier Inc. <https://doi.org/10.1016/j.jacbts.2017.09.001>.
- Poole, Leslie B., P. Andrew Karplus, and Al Claiborne. 2004. "Protein Sulfenic Acids in Redox Signaling." *Annual Review of Pharmacology and Toxicology*. <https://doi.org/10.1146/annurev.pharmtox.44.101802.121735>.
- Powers, Evan T., Richard I. Morimoto, Andrew Dillin, Jeffery W. Kelly, and William E. Balch. 2009. "Biological and Chemical Approaches to Diseases of Proteostasis Deficiency." *Annual Review of Biochemistry*. <https://doi.org/10.1146/annurev.biochem.052308.114844>.
- Poyton, Robert O, and Joan E McEwen. 1996. "Crosstalk between Nuclear and Mitochondrial Genomes." *Atmu. Rev. Bimheni*. Vol. 19. www.annualreviews.org.
- Pramanik, Kartick C., and Sanjay K. Srivastava. 2012. "Apoptosis Signal-Regulating Kinase 1-Thioredoxin Complex Dissociation by Capsaicin Causes Pancreatic Tumor Growth Suppression by Inducing Apoptosis." *Antioxidants and Redox Signaling* 17 (10): 1417–32. <https://doi.org/10.1089/ars.2011.4369>.
- Prosdocimo, Domenick A., Jenine E. John, Lilei Zhang, Elizabeth S. Efraim, Rongli Zhang, Xudong Liao, and Mukesh K. Jain. 2015. "KLF15 and PPAR α Cooperate to Regulate Cardiomyocyte Lipid Gene Expression and Oxidation." *PPAR Research* 2015 (February). <https://doi.org/10.1155/2015/201625>.
- Pujol, Claire, Ivana Bratic-Hench, Marija Sumakovic, Jürgen Hench, Arnaud Mourier, Linda Baumann, Victor Pavlenko, and Aleksandra Trifunovic. 2013. "Succinate Dehydrogenase Upregulation Destabilize Complex I and Limits the Lifespan of Gas-1 Mutant." *PLoS ONE* 8 (3). <https://doi.org/10.1371/journal.pone.0059493>.
- Quintin, Sophie, Theo Aspert, and Gilles Charvin. 2021. "Distinct Mechanisms Underlie H2O2 Sensing in *C. Elegans* Head and Tail." *BioRxiv*.
- Raamsdonk, Jeremy M. van, and Siegfried Hekimi. 2009. "Deletion of the Mitochondrial Superoxide Dismutase Sod-2 Extends Lifespan in *Caenorhabditis Elegans*." *PLoS Genetics* 5 (2). <https://doi.org/10.1371/journal.pgen.1000361>.
- Raamsdonk, Jeremy Michael van, and Siegfried Hekimi. 2012. "Superoxide Dismutase Is Dispensable for Normal Animal Lifespan." *Proceedings of the National Academy of Sciences of the United States of America* 109 (15): 5785–90. <https://doi.org/10.1073/pnas.1116158109>.
- Raamsdonk, Jeremy Michael van, Yan Meng, Darius Camp, Wen Yang, Xihua Jia, Claire Bénard, and Siegfried Hekimi. 2010. "Decreased Energy Metabolism Extends Life Span in *Caenorhabditis Elegans* without Reducing Oxidative Damage." *Genetics* 185 (2): 559–71. <https://doi.org/10.1534/genetics.110.115378>.

- Ranjan, Manickaratnam, Jan Grubern, Li Fang Ng, and Barry Halliwell. 2013. "Repression of the Mitochondrial Peroxiredoxin Antioxidant System Does Not Shorten Life Span but Causes Reduced Fitness in *Caenorhabditis Elegans*." *Free Radical Biology and Medicine* 63: 381–89. <https://doi.org/10.1016/j.freeradbiomed.2013.05.025>.
- Rascón, Brenda, and Jon F. Harrison. 2010. "Lifespan and Oxidative Stress Show a Non-Linear Response to Atmospheric Oxygen in *Drosophila*." *Journal of Experimental Biology* 213 (20): 3441–48. <https://doi.org/10.1242/jeb.044867>.
- Rea, Shane L., Natascia Ventura, and Thomas E. Johnson. 2007. "Relationship between Mitochondrial Electron Transport Chain Dysfunction, Development, and Life Extension in *Caenorhabditis Elegans*." *PLoS Biology* 5 (10): 2312–29. <https://doi.org/10.1371/journal.pbio.0050259>.
- Reichart, Gesine, Johannes Mayer, Cindy Zehm, Timo Kirschstein, Tursonjan Tokay, Falko Lange, Simone Baltrusch, et al. 2019a. "Mitochondrial Complex IV Mutation Increases Reactive Oxygen Species Production and Reduces Lifespan in Aged Mice." *Acta Physiologica* 225 (4). <https://doi.org/10.1111/apha.13214>.
- . 2019b. "Mitochondrial Complex IV Mutation Increases Reactive Oxygen Species Production and Reduces Lifespan in Aged Mice." *Acta Physiologica* 225 (4). <https://doi.org/10.1111/apha.13214>.
- Reuter, Wilhad Hans, Thorsten Masuch, Na Ke, Marine Lenon, Meytal Radzinski, Vu Van Loi, Guoping Ren, et al. 2019. "Utilizing Redox-Sensitive GFP Fusions to Detect in Vivo Redox Changes in a Genetically Engineered Prokaryote." *Redox Biology* 26 (July): 0–9. <https://doi.org/10.1016/j.redox.2019.101280>.
- Riemer, Jan, Markus Schwarzländer, Marcus Conrad, and Johannes M. Herrmann. 2015. "Thiol Switches in Mitochondria: Operation and Physiological Relevance." *Biological Chemistry*. Walter de Gruyter GmbH. <https://doi.org/10.1515/hsz-2014-0293>.
- Rieske, J. S., S. H. Lipton, H. Baum, and H. I. Silman. 1967. "Factors Affecting the Binding of Antimycin A to Complex 3 of the Mitochondrial Respiratory Chain." *Journal of Biological Chemistry* 242 (21): 4888–96. [https://doi.org/10.1016/s0021-9258\(18\)99453-6](https://doi.org/10.1016/s0021-9258(18)99453-6).
- Río, Luis A. Del, and Eduardo López-Huertas. 2016. "ROS Generation in Peroxisomes and Its Role in Cell Signaling." *Plant and Cell Physiology* 57 (7): 1364–76. <https://doi.org/10.1093/pcp/pcw076>.
- Ristow, Michael, and Kathrin Schmeisser. 2014. "Mitohormesis: Promoting Health and Lifespan by Increased Levels of Reactive Oxygen Species (ROS)." *Dose-Response* 12 (2): 288–341. <https://doi.org/10.2203/dose-response.13-035.Ristow>.
- Ristow, Michael, and Lippincott Williams. 2006. "Oxidative Metabolism in Cancer Growth." <http://journals.lww.com/co-clinicalnutrition>.
- Robb, Ellen L., Justyna M. Gawel, Dunja Aksentijević, Helena M. Cochemé, Tessa S. Stewart, Maria M. Shchepinova, He Qiang, et al. 2015. "Selective Superoxide Generation within Mitochondria by the Targeted Redox Cyclor MitoParaquat." *Free Radical Biology and Medicine* 89: 883–94. <https://doi.org/10.1016/j.freeradbiomed.2015.08.021>.
- Rodenburg, Richard J. 2016. "Mitochondrial Complex I-Linked Disease." *Biochimica et Biophysica Acta - Bioenergetics* 1857 (7): 938–45. <https://doi.org/10.1016/j.bbabi.2016.02.012>.
- Rodríguez, Estefanía, Nana Aburjania, Nolan M. Priedigkeit, Analisa Difeo, and John A. Martignetti. 2010. "Nucleo-Cytoplasmic Localization Domains Regulate Krü Ppel-like Factor 6 (KLF6) Protein Stability and Tumor Suppressor Function." *PLoS ONE* 5 (9): 1–13. <https://doi.org/10.1371/journal.pone.0012639>.

- Roger, Andrew J., Sergio A. Muñoz-Gómez, and Ryoma Kamikawa. 2017. "The Origin and Diversification of Mitochondria." *Current Biology*. Cell Press. <https://doi.org/10.1016/j.cub.2017.09.015>.
- Rogina, Blanka, and Stephen L Helfand. 2004. "Sir2 Mediates Longevity in the Fly through a Pathway Related to Calorie Restriction." www.pnas.org/cgi/doi/10.1073/pnas.0404184101.
- Roma, Leticia Prates, Marcel Deponte, Jan Riemer, and Bruce Morgan. 2018. "Mechanisms and Applications of Redox-Sensitive Green Fluorescent Protein-Based Hydrogen Peroxide Probes." *Antioxidants and Redox Signaling* 29 (6): 552–68. <https://doi.org/10.1089/ars.2017.7449>.
- Rossi, Filippo, Della Bianca, and Pietro de Togni. 1985. "Mechanisms and Functions of the Oxygen Radicals Producing Respiration of Phagocytes." *Comp. Immun. Microbiol. Infect. Dis.* Vol. 8.
- Rota, Cristina, Colin F. Chignell, and Ronald P. Mason. 1999. "Evidence for Free Radical Formation during the Oxidation of 2'-7'-Dichlorofluorescein to the Fluorescent Dye 2'-7'-Dichlorofluorescein by Horseradish Peroxidase:: Possible Implications for Oxidative Stress Measurements." *Free Radical Biology and Medicine* 27 (7–8): 873–81. [https://doi.org/10.1016/S0891-5849\(99\)00137-9](https://doi.org/10.1016/S0891-5849(99)00137-9).
- Rottenberg, Hagai, and Jan B. Hoek. 2017. "The Path from Mitochondrial ROS to Aging Runs through the Mitochondrial Permeability Transition Pore." *Aging Cell*. Blackwell Publishing Ltd. <https://doi.org/10.1111/accel.12650>.
- Rottenberg, Hagai, Raul Covian, and Bernard L. Trumpower. 2009. "Membrane Potential Greatly Enhances Superoxide Generation by the Cytochrome Bc1 Complex Reconstituted into Phospholipid Vesicles." *Journal of Biological Chemistry* 284 (29): 19203–10. <https://doi.org/10.1074/jbc.M109.017376>.
- Rual, Jaen François, Julian Ceron, John Koreth, Tong Hao, Anne Sophie Nicot, Tomoko Hirozane-Kishikawa, Jean Vandenhoute, et al. 2004. "Toward Improving Caenorhabditis Elegans Phenome Mapping with an ORFeome-Based RNAi Library." *Genome Research* 14 (10 B): 2162–68. <https://doi.org/10.1101/gr.2505604>.
- Sablina, Anna A., Andrei v. Budanov, Galina v. Ilyinskaya, Larissa S. Agapova, Julia E. Kravchenko, and Peter M. Chumakov. 2005. "The Antioxidant Function of the P53 Tumor Suppressor." *Nature Medicine* 11 (12): 1306–13. <https://doi.org/10.1038/nm1320>.
- Sagasti, A, N Hisamoto, J Hyodo, M Tanaka-Hino, K Matsumoto, and C I Bargmann. 2001. "The CaMKII UNC-43 Activates the MAPKKK NSY-1 to Execute a Lateral Signaling Decision Required for Asymmetric Olfactory Neuron Fates." *Cell* 105 (2): 221–32.
- Saitoh, Masao, Hideki Nishitoh, Makiko Fujii, Kohsuke Takeda, Kei Tobiume, Yasuhiro Sawada, Masahiro Kawabata, Kohei Miyazono, and Hidenori Ichijo. 1998. "Mammalian Thioredoxin Is a Direct Inhibitor of Apoptosis Signal-Regulating Kinase (ASK) 1." *The EMBO Journal*. Vol. 17.
- Sakamoto, Taro, and Hirotaka Imai. 2017. "Hydrogen Peroxide Produced by Superoxide Dismutase SOD-2 Activates Sperm in Caenorhabditis Elegans." *Journal of Biological Chemistry* 292 (36): 14804–13. <https://doi.org/10.1074/jbc.M117.788901>.
- Sakamoto, Taro, Kana Maebayashi, Yasuhito Nakagawa, and Hirotaka Imai. 2014. "Deletion of the Four Phospholipid Hydroperoxide Glutathione Peroxidase Genes Accelerates Aging in Caenorhabditis Elegans." *Genes to Cells* 19 (10): 778–92. <https://doi.org/10.1111/gtc.12175>.

- Salo, Adrian Bøgh, Peter Husen, and Ilia A. Solov'Yov. 2017. "Charge Transfer at the Qo-Site of the Cytochrome Bc1 Complex Leads to Superoxide Production." *Journal of Physical Chemistry B* 121 (8): 1771–82. <https://doi.org/10.1021/acs.jpcc.6b10403>.
- Sampayo, James N., Anders Olsen, and Gordon J. Lithgow. 2003. "Oxidative Stress in *Caenorhabditis Elegans*: Protective Effects of Superoxide Dismutase/Catalase Mimetics." *Aging Cell* 2 (6): 319–26. <https://doi.org/10.1046/j.1474-9728.2003.00063.x>.
- Samuelson, Andrew v., Christopher E. Carr, and Gary Ruvkun. 2007. "Gene Activities That Mediate Increased Life Span of *C. Elegans* Insulin-like Signaling Mutants." *Genes and Development* 21 (22): 2976–94. <https://doi.org/10.1101/gad.1588907>.
- Sauer, Heinrich, Gohar Rahimi, Ju « Rgen Hescheler, and Maria Wartenberg. 2000. "Role of Reactive Oxygen Species and Phosphatidylinositol 3-Kinase in Cardiomyocyte Differentiation of Embryonic Stem Cells."
- Schmidt, Oliver, Nikolaus Pfanner, and Chris Meisinger. 2010. "Mitochondrial Protein Import: From Proteomics to Functional Mechanisms." *Nature Reviews Molecular Cell Biology*. <https://doi.org/10.1038/nrm2959>.
- Scialò, Filippo, Daniel J. Fernández-Ayala, and Alberto Sanz. 2017. "Role of Mitochondrial Reverse Electron Transport in ROS Signaling: Potential Roles in Health and Disease." *Frontiers in Physiology*. Frontiers Media S.A. <https://doi.org/10.3389/fphys.2017.00428>.
- Segref, Alexandra, Serena Torres, and Thorsten Hoppe. 2011. "A Screenable in Vivo Assay to Study Proteostasis Networks in *Caenorhabditis Elegans*." <https://doi.org/10.1534/genetics.111.126797>.
- Senchuk, Megan M., Dylan J. Dues, Claire E. Schaar, Benjamin K. Johnson, Zachary B. Madaj, Megan J. Bowman, Mary E. Winn, and Jeremy M. van Raamsdonk. 2018. "Activation of DAF-16/FOXO by Reactive Oxygen Species Contributes to Longevity in Long-Lived Mitochondrial Mutants in *Caenorhabditis Elegans*." *PLoS Genetics* 14 (3): 1–27. <https://doi.org/10.1371/journal.pgen.1007268>.
- Seo, Angie, Janelle L. Jackson, Jolene V. Schuster, and Didem Vardar-Ulu. 2013. "Using UV-Absorbance of Intrinsic Dithiothreitol (DTT) during RPHPLC as a Measure of Experimental Redox Potential in Vitro." *Anal Bioanal Chem*. 405 (19): 6379–84. <https://doi.org/10.1007/s00216-013-7063-2>.Using.
- Seo, Su Ryeon, François Lallemand, Nathalie Ferrand, Marcia Pessah, Sébastien L'Hoste, Jacques Camonis, and Azeddine Atfi. 2004. "The Novel E3 Ubiquitin Ligase Tiul1 Associates with TGIF to Target Smad2 for Degradation." *EMBO Journal* 23 (19): 3780–92. <https://doi.org/10.1038/sj.emboj.7600398>.
- Settivari, R.S., J.C. Rowlands, D.M. Wilson, S.M. Arnold, and P.J. Spencer. 2017. "Application of Evolving Computational and Biological Platforms for Chemical Safety Assessment." In *A Comprehensive Guide to Toxicology in Nonclinical Drug Development*, 843–73. Elsevier. <https://doi.org/10.1016/b978-0-12-803620-4.00032-3>.
- Shama, Silvian, Chi-Yung Lai, Jill M Antoniazzi, James C Jiang, and S Michal Jazwinski. 1998. "Heat Stress-Induced Life Span Extension in Yeast."
- Sherer, Todd B., Ranjita Betarbet, Claudia M. Testa, Byoung Boo Seo, Jason R. Richardson, Jin Ho Kim, Gary W. Miller, Takao Yagi, Akemi Matsuno-Yagi, and J. Timothy Greenamyre. 2003. "Mechanism of Toxicity in Rotenone Models of Parkinson's Disease." *Journal of Neuroscience* 23 (34): 10756–64. <https://doi.org/10.1523/jneurosci.23-34-10756.2003>.
- Shigenaga, Mark K, Toiy M Hagen, and Bruce N Ames. 1994. "Oxidative Damage and Mitochondrial Decay in Aging (Bioenergetics/Mitochondria DNA/Arwdbipn/Acetyl-L-Cnitlne/Neurodegeneration)." *Proc. Natl. Acad. Sci. USA*. Vol. 91.

- Shore, David E., Christopher E. Carr, and Gary Ruvkun. 2012. "Induction of Cytoprotective Pathways Is Central to the Extension of Lifespan Conferred by Multiple Longevity Pathways." *PLoS Genetics* 8 (7). <https://doi.org/10.1371/journal.pgen.1002792>.
- Shore, David E., and Gary Ruvkun. 2013. "A Cytoprotective Perspective on Longevity Regulation." *Trends in Cell Biology*. <https://doi.org/10.1016/j.tcb.2013.04.007>.
- Sierra, Felipe. 2016. "The Emergence of Geroscience as an Interdisciplinary Approach to the Enhancement of Health Span and Life Span." *Cold Spring Harbor Perspectives in Medicine* 6 (4). <https://doi.org/10.1101/cshperspect.a025163>.
- Sies, Helmut. 1993. "Strategies of Antioxidant Defense." *Eur. J. Biochem.* Vol. 215.
- . 2014. "Role of Metabolic H₂O₂ Generation: Redox Signaling and Oxidative Stress." *Journal of Biological Chemistry*. American Society for Biochemistry and Molecular Biology Inc. <https://doi.org/10.1074/jbc.R113.544635>.
- Siillner, Thomas, Gareth Griffiths, Rupert Pfaller, Nikolaus Pfanner, and Walter Neupert'. 1969. "MOM19, an Import Receptor for Mitochondrial Precursor Proteins." *Cell*. Vol. 59.
- Slater, E. C. 1973. "The Mechanism of Action of the Respiratory Inhibitor Antimycin." *Biochimica et Biophysica Acta* 301 (July): 129–54.
- Smith, Danielle G., and Roger G. Sturme. 2013. "Parallels between Embryo and Cancer Cell Metabolism." *Biochemical Society Transactions* 41 (2): 664–69. <https://doi.org/10.1042/BST20120352>.
- Sohal, Rajindar S., Richard Weindruch, J W Curtsinger, H H Fukui, D R Townsend, J W Vaupel, L Xiu, and Exp Gerontol. 1994. "Oxidative Stress, Caloric Restriction, and Aging." *Proc. Natl. Acad. Sci. USA*. Vol. 30. <https://www.science.org>.
- Solmaz, Sozanne R.N., and Carola Hunte. 2008. "Structure of Complex III with Bound Cytochrome C in Reduced State and Definition of a Minimal Core Interface for Electron Transfer." *Journal of Biological Chemistry* 283 (25): 17542–49. <https://doi.org/10.1074/jbc.M710126200>.
- Song, Ning Ning, Pengcheng Ma, Qiong Zhang, Lei Zhang, Huishan Wang, Longlong Zhang, Liang Zhu, Chun Hui He, Bingyu Mao, and Yu Qiang Ding. 2020. "Rnf220/Zc4h2-Mediated Monoubiquitylation of Phox2 Is Required for Noradrenergic Neuron Development." *Development (Cambridge, England)* 147 (6). <https://doi.org/10.1242/dev.185199>.
- Spinelli, Jessica B., and Marcia C. Haigis. 2018. "The Multifaceted Contributions of Mitochondria to Cellular Metabolism." *Nature Cell Biology*. Nature Publishing Group. <https://doi.org/10.1038/s41556-018-0124-1>.
- Stadtman, Earl R. 1992. "Protein Oxidation and Aging." *Science* 257: 1220–24.
- Steensel, B van, A Smogorzewska, and T de Lange. 1998. "TRF2 Protects Human Telomeres from End-to-End Fusions." *Cell* 92: 401–13.
- Stehling, Oliver, and Roland Lill. 2013. "The Role of Mitochondria in Cellular Iron-Sulfur Protein Biogenesis: Mechanisms, Connected Processes, and Diseases." *Cold Spring Harbor Perspectives in Biology* 5 (8). <https://doi.org/10.1101/cshperspect.a011312>.
- Steinbaugh, Michael J., Liou Y. Sun, Andrzej Bartke, and Richard A. Miller. 2012. "Activation of Genes Involved in Xenobiotic Metabolism Is a Shared Signature of Mouse Models with Extended Lifespan." *American Journal of Physiology - Endocrinology and Metabolism* 303 (4). <https://doi.org/10.1152/ajpendo.00110.2012>.
- Stewart, James Bruce, Christoph Freyer, Joanna L. Elson, Anna Wredenberg, Zekiye Cansu, Aleksandra Trifunovic, and Nils Göran Larsson. 2008. "Strong Purifying Selection in

- Transmission of Mammalian Mitochondrial DNA." *PLoS Biology* 6 (1): 0063–0071. <https://doi.org/10.1371/journal.pbio.0060010>.
- Stocco', D M, J Cascarano, and M A Wilson. 1977. "Quantitation of Mitochondria1 DNA, RNA, and Protein in Starved and Starved-Refed Rat Liver." *J Cell Physiol* 90 (2): 295–306.
- Sullivan, Lucas B., and Navdeep S Chandel. 2014. "Mitochondrial Reactive Oxygen Species and Cancer." *Cancer & Metabolism* 2 (17): 99–116. <https://doi.org/10.1186/2049-3002-2-17>.
- Sun, Fei, Xia Huo, Yujia Zhai, Aojin Wang, Jianxing Xu, Dan Su, Mark Bartlam, and Zihe Rao. 2005. "Crystal Structure of Mitochondrial Respiratory Membrane Protein Complex II." *Cell* 121 (7): 1043–57. <https://doi.org/10.1016/j.cell.2005.05.025>.
- Sun, Xiaojuan, Wei Dong Chen, and Yan Dong Wang. 2017. "DAF-16/FOXO Transcription Factor in Aging and Longevity." *Frontiers in Pharmacology*. Frontiers Media S.A. <https://doi.org/10.3389/fphar.2017.00548>.
- Suthammarak, Wichit, Phil G. Morgan, and Margaret M. Sedensky. 2010. "Mutations in Mitochondrial Complex III Uniquely Affect Complex I in *Caenorhabditis Elegans*." *Journal of Biological Chemistry* 285 (52): 40724–31. <https://doi.org/10.1074/jbc.M110.159608>.
- Takubo, Kaiyo, Ken-Ichi Nakamura, Naotaka Izumiyama, Eiki Furugori, Motoji Sawabe, Tomio Arai, Yuki Yoshi Esaki, et al. 2000. "Telomere Shortening With Aging in Human Liver." *Journal of Gerontology: BIOLOGICAL SCIENCES Copyright*. Vol. 55. <https://academic.oup.com/biomedgerontology/article/55/11/B533/563335>.
- Tampo, Yoshiko, Srigiridhar Kotamraju, Christopher R. Chitambar, Shasi v. Kalivendi, Agnes Keszler, and Joy Joseph B. Kalyanaraman. 2003. "Oxidative Stress-Induced Iron Signaling Is Responsible for Peroxide-Dependent Oxidation of Dichlorodihydrofluorescein in Endothelial Cells Role of Transferrin Receptor-Dependent Iron Uptake in Apoptosis." *Circulation Research* 92 (1): 56–63. <https://doi.org/10.1161/01.RES.0000048195.15637.AC>.
- Tanaka-Hino, Miho, Alvaro Sagasti, Naoki Hisamoto, Masato Kawasaki, Shunji Nakano, Jun Ninomiya-Tsuji, Cornelia I Bargmann, and Kunihiro Matsumoto. 2002. "SEK-1 MAPKK Mediates Ca 2+ Signaling to Determine Neuronal Asymmetric Development in *Caenorhabditis Elegans*." *EMBO Reports*. Vol. 3.
- Tapia, Patrick C. 2006. "Sublethal Mitochondrial Stress with an Attendant Stoichiometric Augmentation of Reactive Oxygen Species May Precipitate Many of the Beneficial Alterations in Cellular Physiology Produced by Caloric Restriction, Intermittent Fasting, Exercise and Dietary Phytonutrients: 'Mitohormesis' for Health and Vitality." *Medical Hypotheses* 66 (4): 832–43. <https://doi.org/10.1016/j.mehy.2005.09.009>.
- Tatsuta, Takashi, and Thomas Langer. 2008. "Quality Control of Mitochondria: Protection against Neurodegeneration and Ageing." *EMBO Journal*. <https://doi.org/10.1038/sj.emboj.7601972>.
- Tiew, Terence W.Y., Michael B. Sheahan, and Ray J. Rose. 2015. "Peroxisomes Contribute to Reactive Oxygen Species Homeostasis and Cell Division Induction in Arabidopsis Protoplasts." *Frontiers in Plant Science* 6 (AUG): 1–16. <https://doi.org/10.3389/fpls.2015.00658>.
- Timón-Gómez, Alba, Eva Nývltová, Luciano A. Abriata, Alejandro J. Vila, Jonathan Hosler, and Antoni Barrientos. 2018. "Mitochondrial Cytochrome c Oxidase Biogenesis: Recent Developments." *Seminars in Cell and Developmental Biology*. Elsevier Ltd. <https://doi.org/10.1016/j.semcd.2017.08.055>.

- Tralau, Tewes, and Andreas Luch. 2013. "The Evolution of Our Understanding of Endo-Xenobiotic Crosstalk and Cytochrome P450 Regulation and the Therapeutic Implications." *Expert Opinion on Drug Metabolism and Toxicology*. <https://doi.org/10.1517/17425255.2013.828692>.
- Trifunovic, Aleksandra, Anna Hansson, Anna Wredenberg, Anja T Rovio, Eric Dufour, Ivan Khvorostov, Johannes N Spelbrink, Rolf Wibom, Howard T Jacobs, and Nils-Gö Ran Larsson. 2005. "Somatic MtDNA Mutations Cause Aging Phenotypes without Affecting Reactive Oxygen Species Production." www.pnas.org/cgi/doi/10.1073/pnas.0508886102.
- Trifunovic, Aleksandra, Anna Wredenberg, Maria Falkenberg, Johannes N. Spelbrink, Anja T. Rovio, Carl E. Bruder, Mohammad Bohlooly-Y, et al. 2004. "Premature Ageing in Mice Expressing Defective Mitochondrial DNA Polymerase." *Nature* 429 (May): 417–23. <https://doi.org/10.1038/nature02544>.
- Troemel, Emily R., Stephanie W. Chu, Valerie Reinke, Siu Sylvia Lee, Frederick M. Ausubel, and Dennis H. Kim. 2006. "P38 MAPK Regulates Expression of Immune Response Genes and Contributes to Longevity in *C. Elegans*." *PLoS Genetics* 2 (11): 1725–39. <https://doi.org/10.1371/journal.pgen.0020183>.
- Tsang, William Y., and Bernard D. Lemire. 2002. "Mitochondrial Genome Content Is Regulated during Nematode Development." *Biochemical and Biophysical Research Communications* 291 (1): 8–16. <https://doi.org/10.1006/bbrc.2002.6394>.
- Tsang, William Y., Leanne C. Sayles, Leslie I. Grad, David B. Pilgrim, and Bernard D. Lemire. 2001. "Mitochondrial Respiratory Chain Deficiency in *Caenorhabditis Elegans* Results in Developmental Arrest and Increased Life Span." *Journal of Biological Chemistry* 276 (34): 32240–46. <https://doi.org/10.1074/jbc.M103999200>.
- Ulloa-Aguirre, Alfredo, Aylin C. Hanyaloglu, Teresa Zariñán, and Jo Ann Janovick. 2020. "Protein Homeostasis and Regulation of Intracellular Trafficking of G Protein-Coupled Receptors." In *Protein Homeostasis Diseases*, 247–77. Elsevier. <https://doi.org/10.1016/b978-0-12-819132-3.00012-9>.
- Uozumi, Takayuki, Masayuki Hamakawa, Yu ki Deno, Nobushige Nakajo, and Takaaki Hirotsu. 2015. "Voltage-Dependent Anion Channel (VDAC-1) Is Required for Olfactory Sensing in *Caenorhabditis Elegans*." *Genes to Cells* 20 (10): 802–16. <https://doi.org/10.1111/gtc.12269>.
- Ushio-Fukai, Masuko. 2006. "Redox Signaling in Angiogenesis: Role of NADPH Oxidase." *Cardiovascular Research*. <https://doi.org/10.1016/j.cardiores.2006.04.015>.
- Vanfleteren, J. R., and A. de Vreese. 1996. "Rate of Aerobic Metabolism and Superoxide Production Rate Potential in the Nematode *Caenorhabditis Elegans*." *J Exp Zool.* 274 (2): 93–100.
- Vellai, T., K. Takacs-Vellai, Y. Zhang, A. L. Kovacs, L. Orosz, and F. Muller. 2003. "Influence of TOR Kinase on Lifespan in *C. Elegans*." *Nature Genetics* 426: 620–21. <http://arxiv.org/abs/cond-mat/0304695>.
- Virbasius, Ching-Man A, Joseph v Virbasius, and Richard C Scarpulla. 1993. "NRF-1, an Activator Involved in Nuclear-Mitochondrial Interactions, Utilizes a New DNA-Binding Domain Conserved in a Family of Developmental Regulators."
- Vringer, Esme, and Stephen W.G. Tait. 2019. "Mitochondria and Inflammation: Cell Death Heats Up." *Frontiers in Cell and Developmental Biology*. Frontiers Media S.A. <https://doi.org/10.3389/fcell.2019.00100>.
- Watson, Mark A., Blaine Pattavina, Tyler A.U. Hilsabeck, Jose Lopez-Dominguez, Pankaj Kapahi, and Martin D. Brand. 2021. "S3QELs Protect against Diet-Induced Intestinal

- Barrier Dysfunction." *Aging Cell*, no. May 2020: 1–10.
<https://doi.org/10.1111/ace.13476>.
- Wiederkehr, Andreas, and Claes B. Wollheim. 2006. "Minireview: Implication of Mitochondria in Insulin Secretion and Action." *Endocrinology*.
<https://doi.org/10.1210/en.2006-0057>.
- Wilson, Shelly R, Aditya D Joshi, and Cornelis J Elferink. 2013. "The Tumor Suppressor Kruppel-Like Factor 6 Is a Novel Aryl Hydrocarbon Receptor DNA Binding Partner." *Journal of Pharmacology and Experimental Therapeutics* 345 (3): 419.
<https://doi.org/10.1124/jpet.113.203786>.
- Winterbourn, Christine C. 2018. "Biological Production, Detection, and Fate of Hydrogen Peroxide." *Antioxidants and Redox Signaling*. Mary Ann Liebert Inc.
<https://doi.org/10.1089/ars.2017.7425>.
- . 2020. "Hydrogen Peroxide Reactivity and Specificity in Thiol-Based Cell Signalling." *Biochemical Society Transactions*. Portland Press Ltd.
<https://doi.org/10.1042/BST20190049>.
- Winterbourn, Christine C., and Mark B. Hampton. 2008. "Thiol Chemistry and Specificity in Redox Signaling." *Free Radical Biology and Medicine*.
<https://doi.org/10.1016/j.freeradbiomed.2008.05.004>.
- Wong, Anne, Paula Boutis, Siegfried Hekimi, and Penfield Ave. 1995. "Mutations in the Elk-1 Gene of *Caenorhabditis Elegans* Affect Developmental and Behavioral Timing."
- Woo, Dong Kyun, and Gerald S. Shadel. 2011. "Mitochondrial Stress Signals Revise an Old Aging Theory." *Cell*. Elsevier B.V. <https://doi.org/10.1016/j.cell.2010.12.023>.
- Woo, Hyun Ae, Sun Hee Yim, Dong Hae Shin, Dongmin Kang, Dae Yeul Yu, and Sue Goo Rhee. 2010. "Inactivation of Peroxiredoxin I by Phosphorylation Allows Localized H₂O₂ Accumulation for Cell Signaling." *Cell* 140 (4): 517–28.
<https://doi.org/10.1016/j.cell.2010.01.009>.
- Wood, Zachary A., Ewald Schröder, J. Robin Harris, and Leslie B. Poole. 2003. "Structure, Mechanism and Regulation of Peroxiredoxins." *Trends in Biochemical Sciences* 28 (1): 32–40. [https://doi.org/10.1016/S0968-0004\(02\)00003-8](https://doi.org/10.1016/S0968-0004(02)00003-8).
- Wu, Wei bin, Ramkumar Menon, Yue Ying Xu, Jiu Ru Zhao, Yan Lin Wang, Yuan Liu, and Hui Juan Zhang. 2016. "Downregulation of Peroxiredoxin-3 by Hydrophobic Bile Acid Induces Mitochondrial Dysfunction and Cellular Senescence in Human Trophoblasts." *Scientific Reports* 6 (December). <https://doi.org/10.1038/srep38946>.
- Wu, Ziyun, Megan M. Senchuk, Dylan J. Dues, Benjamin K. Johnson, Jason F. Cooper, Leira Lew, Emily Machiela, et al. 2018. "Mitochondrial Unfolded Protein Response Transcription Factor ATF5-1 Promotes Longevity in a Long-Lived Mitochondrial Mutant through Activation of Stress Response Pathways." *BMC Biology* 16 (1).
<https://doi.org/10.1186/s12915-018-0615-3>.
- Xu, Chen, Woosoon Hwang, Dae Eun Jeong, Youngjae Ryu, Chang Man Ha, Seung Jae v. Lee, Lulu Liu, and Zhi Ming He. 2018. "Genetic Inhibition of an ATP Synthase Subunit Extends Lifespan in *C. Elegans*." *Scientific Reports* 8 (1): 1–14. <https://doi.org/10.1038/s41598-018-32025-w>.
- Xu, Darui, Kara Marquis, Jimin Pei, Szu Chin Fu, Tolga Całatay, Nick v. Grishin, and Yuh Min Chook. 2015. "LocNES: A Computational Tool for Locating Classical NESs in CRM1 Cargo Proteins." *Bioinformatics* 31 (9): 1357–65.
<https://doi.org/10.1093/bioinformatics/btu826>.

- Yanagida, Atsushi, Kazuhiro Sogawa, Ken-ichi Yasumoto, and Yoshiaki Fujii Kuriyama. 1990. "A Novel Cis-Acting DNA Element Required for a High Level of Inducible Expression of the Rat P-450c Gene." *MOLECULAR AND CELLULAR BIOLOGY*.
- Yanase, Sumino, Kayo Yasuda, and Naoaki Ishii. 2002. "Adaptive Responses to Oxidative Damage in Three Mutants OfCaenorhabditis Elegans (Age-1, Mev-1 and Daf-16) That Affect Lifespan." *Mechanisms of Ageing and Development* 123: 1579–87.
- Yang, Wen, and Siegfried Hekimi. 2010a. "A Mitochondrial Superoxide Signal Triggers Increased Longevity in Caenorhabditis Elegans." *PLoS Biology* 8 (12). <https://doi.org/10.1371/journal.pbio.1000556>.
- . 2010b. "Two Modes of Mitochondrial Dysfunction Lead Independently to Lifespan Extension in Caenorhabditis Elegans." *Aging Cell* 9 (3): 433–47. <https://doi.org/10.1111/j.1474-9726.2010.00571.x>.
- Yee, Callista, Wen Yang, and Siegfried Hekimi. 2014. "The Intrinsic Apoptosis Pathway Mediates the Pro-Longevity Response to Mitochondrial ROS in C Elegans." *Cell* 157 (4): 897–909. <https://doi.org/10.1016/j.cell.2014.02.055>.
- Yoneda, Takunari, Cristina Benedetti, Fumihiko Urano, Scott G. Clark, Heather P. Harding, and David Ron. 2004. "Compartment-Specific Perturbation of Protein Handling Activates Genes Encoding Mitochondrial Chaperones." *Journal of Cell Science* 117 (18): 4055–66. <https://doi.org/10.1242/jcs.01275>.
- Yun, Jeanho, and Toren Finkel. 2014. "Mitohormesis." *Cell Metabolism*. Cell Press. <https://doi.org/10.1016/j.cmet.2014.01.011>.
- Yusoff, Abdul Aziz Mohamed, Farizan Ahmad, Zamzuri Idris, Hasnan Jaafar, and Jafri Malin Abdullah. 2015. "Understanding Mitochondrial DNA in Brain Tumorigenesis." In *Molecular Considerations and Evolving Surgical Management Issues in the Treatment of Patients with a Brain Tumor*. InTech. <https://doi.org/10.5772/58965>.
- Zeeshan, Hafiz Maher Ali, Geum Hwa Lee, Hyung Ryong Kim, and Han Jung Chae. 2016. "Endoplasmic Reticulum Stress and Associated ROS." *International Journal of Molecular Sciences* 17 (3): 1–20. <https://doi.org/10.3390/ijms17030327>.
- Zhang, Bingfang, Lei Wang, Aisheng Zhan, Min Wang, Lanxiang Tian, Weixiang Guo, and Yongxin Pan. 2021. "Long-Term Exposure to a Hypomagnetic Field Attenuates Adult Hippocampal Neurogenesis and Cognition." *Nature Communications* 12 (1). <https://doi.org/10.1038/s41467-021-21468-x>.
- Zhang, Jun, Razan Bakheet, Ranjit S. Parhar, Cheng Han Huang, M. Mahmood Hussain, Xiaoyue Pan, Shahid S. Siddiqui, and Sarwar Hashmi. 2011. "Regulation of Fat Storage and Reproduction by Krüppel-like Transcription Factor KLF3 and Fat-Associated Genes in Caenorhabditis Elegans." *Journal of Molecular Biology* 411 (3): 537–53. <https://doi.org/10.1016/j.jmb.2011.06.011>.
- Zhang, Jun, Sanya Hashmi, Fatima Cheema, Nafla Al-Nasser, Razan Bakheet, Ranjit S. Parhar, Futwan Al-Mohanna, Randy Gaugler, M. Mahmood Hussain, and Sarwar Hashmi. 2013. "Regulation of Lipoprotein Assembly, Secretion and Fatty Acid β -Oxidation by Krüppel-like Transcription Factor, Klf-3." *Journal of Molecular Biology* 425 (15): 2641–55. <https://doi.org/10.1016/j.jmb.2013.04.020>.
- Zhang, Leilei, Danyelle M. Townsend, Morgan Morris, Eduardo N. Maldonado, Yu Lin Jiang, Ann Marie Broome, Jennifer R. Bethard, Lauren E. Ball, and Kenneth D. Tew. 2020. "Voltage-Dependent Anion Channels Influence Cytotoxicity of ME-344, a Therapeutic Isoflavone." *Journal of Pharmacology and Experimental Therapeutics* 374 (2): 308–18. <https://doi.org/10.1124/jpet.120.000009>.

- Zhang, Weiqing, Janiel M Shields, Kazuhiro Sogawa, Yoshiaki Fujii-Kuriyama, and Vincent W Yang. 1998. "The Gut-Enriched Krü Ppel-like Factor Suppresses the Activity of the CYP1A1 Promoter in an Sp1-Dependent Fashion*." <http://www.jbc.org>.
- Zhang, Wenjia, Xianglong Hu, Qi Shen, and Da Xing. 2019. "Mitochondria-Specific Drug Release and Reactive Oxygen Species Burst Induced by Polyprodrug Nanoreactors Can Enhance Chemotherapy." *Nature Communications* 10 (1). <https://doi.org/10.1038/s41467-019-09566-3>.
- Zhang, Xiaoling, Seetha v Srinivasan, and Jerry B. Lingrel. 2004. "WWP1-Dependent Ubiquitination and Degradation of the Lung Kruppel-like Factor, KLF2." *Elsevier* 316 (1): 139-148/.
- Zhao, Fang, and Qinghua Wang. 2012. "The Protective Effect of Peroxiredoxin II on Oxidative Stress Induced Apoptosis in Pancreatic β -Cells." <http://www.cellandbioscience.com/content/2/1/22>.
- Zhao, Liang, Yang Zhao, Ruihai Liu, Xiaonan Zheng, Min Zhang, Huiyuan Guo, Hao Zhang, and Fazheng Ren. 2017. "The Transcription Factor DAF-16 Is Essential for Increased Longevity in *C. Elegans* Exposed to *Bifidobacterium Longum* BB68." *Scientific Reports* 7 (1): 1–7. <https://doi.org/10.1038/s41598-017-07974-3>.
- Zhao, Quan, Jianghui Wang, Ilya v. Levichkin, Stan Stasinopoulos, Michael T. Ryan, and Nicholas J. Hoogenraad. 2002. "A Mitochondrial Specific Stress Response Inmammalian Cells." *The EMBO Journal* 21 (17): 4411–19.
- Zheng, Ming, Fredrik Aslund, and Gisela Storz. 1998. "Activation of the OxyR Transcription Factor by Reversible Disulfide Bond Formation." *Science* 279: 1718–21.
- Zhi, Xu, and Ceshi Chen. 2012. "WWP1: A Versatile Ubiquitin E3 Ligase in Signaling and Diseases." *Cellular and Molecular Life Sciences* 69 (9): 1425–34. <https://doi.org/10.1007/s00018-011-0871-7>.
- Zhou, Ben, Johannes Kreuzer, Caroline Kumsta, Lianfeng Wu, Kimberli J. Kamer, Lucydalila Cedillo, Yuyao Zhang, et al. 2019. "Mitochondrial Permeability Uncouples Elevated Autophagy and Lifespan Extension." *Cell* 177 (2): 299-314.e16. <https://doi.org/10.1016/j.cell.2019.02.013>.
- Zhu, Jian, Tsuyoshi Egawa, Syun Ru Yen, Linda Yu, and Chang An Yu. 2007. "Simultaneous Reduction of Iron-Sulfur Protein and Cytochrome BL during Ubiquinol Oxidation in Cytochrome Bc1 Complex." *Proceedings of the National Academy of Sciences of the United States of America* 104 (12): 4864–69. <https://doi.org/10.1073/pnas.0607812104>.
- Zybovych, Iryna O., Sarah Straud, and Michael G. Roth. 2010. "Mitochondrial Dysfunction Confers Resistance to Multiple Drugs in *Caenorhabditis Elegans*." *Molecular Biology of the Cell* 21: 956–69. <https://doi.org/10.1091/mbc.E09>.

Acknowledgements

Prof. Dr. Aleksandra Trifunovic, or better **Sandra**, thank you so much for accepting me in your lab back in 2017 and giving me the opportunity to work on this project. I am very grateful for your understanding, support and critical scientific comments during the PhD track, in my high and low moments. But above all, thank you for making the lab such a warm environment to be in. Your endless effort of socializing and creating events and meetings, especially the Christmas dinners at your place, are truly something I will always cherish.

Thank you to the members of my defence committee for their time and effort of evaluating this dissertation, **Prof. Dr. David Vilchez** and **Prof. Dr. Jan Riemer. Jan**, a special thank you for your valuable advice, support and being part of my thesis advise committee.

I would also like to thank **Prof. Dr. Thorsten Hoppe** for your valuable advice, support and being part of my thesis advise committee.

Katerina Vlantis, our coordinator of the mito-RTG, a big thank you for making Cologne such a warm meeting ground for mitochondrial students. Thank you for your effort, guidance and particularly your kindness.

Dr. Marija Herholz, thank you so much for sharing and teaching me your worm knowledge, your patience and your guidance, especially when I was lost in my PhD project. Without you and your help and effort this thesis would not be possible. You made my time in the lab and behind the microscope very enjoyable with your enthusiasm and chit-chat about David, the children and our mutual love for gardening. Thank you for sharing your stories and all the best to your family.

Linda Baumann thank you so much for all your help and introducing me in all the worm techniques in the lab. I enjoyed the many conversations with you, like about carnival or you making fun about the Dutch. Special thanks for keeping the lab working together with **Katharina Senft. Katha** thank you for your thoughtfulness.

Dr. Alexandra Kukat, thank you for your sympathy, parking help and providing a listening ear when needed.

My dear fellow lab PhD members, **Hien Roszivalová**, **Milica Popovic** and **Harshita Kaul**. Thank you so much for all the fun moments in and outside lab live, especially all our coffee and lunch dates, which I will always cherish. I am so grateful for your friendship and support during all this time. And do not forget, it is almost weekend on Wednesday! **Hien** thank you for all your kindness and openness, but moreover for all our fun little moments in the lab, like our sing-alongs. **Milica** thank you for all the great conversations and lively discussions, which were always a nice break during my day, and our shared love of music. **Harshita**, thank you for all your positive vibes and sharing your Indian culture in the lab.

I would like to thank my bachelor and master students, especially **Lea Isermann** and **Gregor Fink**. **Lea** it was great to see your development from student to PhD candidate in our lab. **Gregor**, I had a great time with you in the lab.

A big thank you to all the other present and former lab member of **AG Trifunovic**: **Franziska Baumann**, **Dr. Marijana Croon**, **Dr. Aleksandra Zečić**, **Dr. Eddy Hofsetz**, **Dr. Sophie Kaspar**, **Dr. Claire Pujol**, **Lance Chao Wu**, **Moritz Esser**, **Heike Brucherseifer**, **Elke Mainz** and **Anthanasios Katsalifis**. Especially, an exceptional big thank you to **Dr. Anastasia Rumyantseva**, **Dr. Sarah Miciej** and **Dr. Karolina Szczepanowska**. **Anastasia**, thank you so much for your companionship and all your help and advice when I struggled in the lab. **Sarah**, my first coffee buddy, I am so grateful for your help and attitude when I just entered the lab and I will never forget our Friday Disney madness. **Karolina**, thank you for always being open-minded for discussions and having time to clarify biochemistry techniques to me.

A special thanks to the labs of **AG Riemer**, **AG Hoppe**, **AG Rugarli**, **AG Vilchez** and **AG Schumacher** for sharing their knowledge, assistance and support.

The biggest thank you goes to all of my family and friends, especially to my parents. Lieve **pa** en **ma**, zonder jullie steun, ondersteuning, aanmoediging en liefde was ik nooit terecht gekomen waar ik nu ben. Ik ben enorm trots dat ik jullie zoon ben.

Mijn liefste **Romy**, al jouw steun, geduld en liefde zijn de reden dat mijn PhD succesvol afgerond is, zonder jou was dit onmogelijk geweest. Sorry voor de vele keren wanneer ik te druk was met werk. Ik kijk enorm uit naar onze bruiloft in 2022.

Appendix

Supplementary Table 1. Lifespan data and statistical analysis

Genotype	Condition	Mean±SE	Median survival	p value (Log-rank test)	Number of animals died/total
N2	EV	22.34±0.335	22		186/200
N2	<i>ctl-1</i>	22.46±0.422	22	ns 0.8232	114/125
N2	EV	23.66±0.358	24		193/200
N2	<i>wwp-1</i>	22.19±0.377	22	0.0078 ^a	168/200
<i>isp-1;ctb-1</i>	<i>wwp-1</i>	31.18±0.996	30	< 0.0001 ^a	119/176
N2	EV	26.15±0.471	26		164/200
<i>isp-1;ctb-1</i>	EV	32.54±0.938	29	< 0.0001 ^a	128/200
<i>isp-1;ctb-1</i>	<i>wwp-1</i>	36.30±0.992	38	< 0.0001 ^a	136/200
N2	EV	22.34±0.335	22		186/200
<i>isp-1;ctb-1</i>	<i>sod-3</i>	26.84±0.858	27	< 0.0001 ^a < 0.0001 ^b	126/200
<i>isp-1;ctb-1</i>	EV	32.64±0.856	34	< 0.0001 ^a	121/200
N2	EV	22.34±0.335	22		186/200
<i>isp-1;ctb-1</i>	<i>sod-3</i> /EV	27.52±0.795	27	< 0.0001 ^a < 0.0001 ^b	108/175
<i>isp-1;ctb-1</i>	EV	32.64±0.856	34	< 0.0001 ^a	121/200
N2	EV	22.34±0.335	22		186/200
N2	<i>sod-3</i>	22.84±0.403	22	ns 0.4796 ^a	155/175
N2	EV	23.47±0.408	24		166/175
<i>prdx 2</i>	EV	17.26±0.511	17	< 0.0001 ^a	87/100
<i>prdx 3</i>	EV	26.37±0.574	26	< 0.0001 ^a	156/175
N2	EV	23.47±0.408	24		166/175
<i>prdx-3</i>	EV	26.37±0.574	26	< 0.0001 ^a	156/175
<i>prdx 3</i>	Vit C	20.65±0.394	22	< 0.0001 ^a < 0.0001 ^c	173/175
<i>prdx 3</i>	<i>klf-1</i>	23.47±0.515	24	ns 0.8546	150/175

				< 0.0005 ^c	
N2	EV	22.34±0.335	22		186/200
<i>isp-1;ctb-1</i>	<i>vdac-1</i>	26.12±0.704	24	< 0.0001 ^a	147/200
<i>isp-1;ctb-1</i>	EV	32.64±0.856	34	< 0.0001 ^b	
<i>isp-1;ctb-1</i>	EV	32.64±0.856	34	< 0.0001 ^a	88/200
N2	EV	22.34±0.335	22		186/200
<i>isp-1;ctb-1</i>	<i>vdac-1</i> /EV	25.30±0.753	24	< 0.0001 ^a	112/200
<i>isp-1;ctb-1</i>	EV	32.64±0.856	34	< 0.0001 ^b	
<i>isp-1;ctb-1</i>	EV	32.64±0.856	34	< 0.0001 ^a	121/200
N2	EV	22.34±0.335	22		186/200
N2	<i>vdac-1</i>	23.23±0.396	24	ns 0.0629	188/200
N2	EV	22.11±0.366	22		180/200
<i>isp-1;ctb-1</i>	EV	35.42±0.847	35	< 0.0001 ^a	130/200
<i>isp-1;ctb-1</i>	<i>pmk-1</i>	26.38±0.626	28	< 0.0001 ^a	117/175
<i>isp-1;ctb-1</i>	<i>pmk-1</i>	26.38±0.626	28	< 0.0001 ^b	
<i>isp-1;ctb-1</i>	<i>pmk-2</i>	26.91±0.581	26	< 0.0001 ^a	160/200
<i>isp-1;ctb-1</i>	<i>pmk-2</i>	26.91±0.581	26	< 0.0001 ^b	
<i>isp-1;ctb-1</i>	<i>pmk-3</i>	27.67±0.939	26	< 0.0001 ^a	106/200
<i>isp-1;ctb-1</i>	<i>pmk-3</i>	27.67±0.939	26	< 0.0001 ^b	
N2	EV	22.11±0.366	22		86/200
N2	<i>pmk-1</i>	20.27±0.359	19	0.0182	81/100
N2	<i>pmk-2</i>	20.58±0.312	22	0.0272	92/100
N2	<i>pmk-3</i>	22.78±0.616	24	ns 0.1643	76/100

^a Log-Rank test compared to N2 EV

^b Log-Rank test compared to *isp-1;ctb-1* EV

^c Log-Rank test compared to *prdx-3* EV

Supplementary Table 2. Potential KLF-1 interaction partners

Gene	
acer-1	Acetyl-CoA deacylase
acdH-11	Acyl-CoA dehydrogenase family member 11
asp-6	Aspartic protease 6
atl-1	Serine/threonine-protein kinase ATR (EC 2.7.11.1) (ATM-like protein 1)
C46G7.2	Uncharacterized protein
CELE_D1054.3	SGS domain-containing protein
CELE_E01A2.1	GCS light chain (Gamma-ECS regulatory subunit)
CELE_F08B12.4	Uncharacterized protein
CELE_F25E2.2	Uncharacterized protein
CELE_F35D11.4	CYTH domain-containing protein
CELE_F36F2.1	Costars domain-containing protein
CELE_F39H2.3	GCV_T domain-containing protein
CELE_F40F8.5	Uncharacterized protein
CELE_F53H1.1	RNA helicase
CELE_F54B8.4	Uncharacterized protein
CELE_F57F4.4	Uncharacterized protein
CELE_R13H4.2	Uncharacterized protein
CELE_T05H10.1	USP domain-containing protein
CELE_T08D2.8	TOG domain-containing protein
CELE_T12B5.15	Uncharacterized protein
CELE_T12D8.10	Uncharacterized protein
CELE_T12D8.5	Uncharacterized protein
CELE_W10C8.5	Arginine kinase
CELE_Y32H12A.8	WD_REPEATS_REGION domain-containing protein
CELE_Y54E5A.5	Uncharacterized protein
CELE_Y69A2AR.18	Uncharacterized protein
CELE_ZC196.5	Uncharacterized protein
CELE_ZK1058.9	Uncharacterized protein
CELE_ZK1098.11	N-acetyltransferase domain-containing protein 1 (Protein NATD1)
CELE_ZK1307.8	Glucosidase 2 subunit beta (Glucosidase II subunit beta)
ccg-1	Conserved Cysteine/Glycine domain protein
cmd-1	Calmodulin (CaM)
cox-17	Cytochrome OXidase assembly protein
ctl-3	Catalase
ddx-17	RNA helicase
ddx-35	Probable ATP-dependent RNA helicase DHX35 homolog
dld-1	Dihydrolipoyl dehydrogenase, mitochondrial

dut-1	dUTP diphosphatase
E01A2.2	Serrate RNA effector molecule homolog (Arsenite-resistance protein 2 homolog)
egl-45	Eukaryotic translation initiation factor 3 subunit A (eIF3a)
eif-2 gamma	Protein-synthesizing GTPase
ensa-1	ENdoSulfine Alpha
erfa-3	Tr-type G domain-containing protein
erp-44	Endoplasmic reticulum resident protein 44.2
exc-15	Aldo_ket_red domain-containing protein
fli-1	Protein flightless-1 homolog
frm-1	Moesin/ezrin/radixin homolog 1
gei-15	GEX Interacting protein
gl-1	Germline survival defective-1
gpd-2	Glyceraldehyde-3-phosphate dehydrogenase 2 (GAPDH-2)
gsk-3	Glycogen synthase kinase-3
gspd-1	Glucose-6-phosphate 1-dehydrogenase (G6PD)
gst-7	Probable glutathione S-transferase 7
gst-1	Glutathione transferase omega-1
gta-1	Probable 4-aminobutyrate aminotransferase, mitochondrial
him-1	Structural maintenance of chromosomes protein 1
his-24	Histone 24
his-74	Histone H3.3-like type 2
hphd-1	Hydroxyacid-oxoacid transhydrogenase, mitochondrial (HOT)
hum-2	Dilute domain-containing protein
hum-5	Heavy chain, Unconventional Myosin (Myosin IA)
icd-2	Nascent polypeptide-associated complex subunit alpha (NAC-alpha)
ima-3	Importin subunit alpha-3 (Karyopherin subunit alpha-3)
immt-1	MICOS complex subunit MIC60-1
inx-12	Innexin-12 (Protein opu-12)
ketn-1	KETtin (Drosophila actin-binding) homolog (Kettin)
lea-1	Plant Late Embryo Abundant (LEA) related
lin-10	Protein lin-10
mct-3	MFS domain-containing protein
msh-2	DNA_MISMATCH_REPAIR_2 domain-containing protein
mthf-1	Probable methylenetetrahydrofolate reductase
nol-56	Nucleolar protein 56
nspd-1	Nematode Specific Peptide family, group D
pcca-1	Propionyl-CoA carboxylase alpha chain, mitochondrial (PCCase subunit alpha)
pck-1	Phosphoenolpyruvate carboxykinase (GTP)

pqn-52	Prion-like-(Q/N-rich)-domain-bearing protein
pyc-1	Pyruvate carboxylase 1
pygl-1	Alpha-1,4 glucan phosphorylase
rnr-1	Ribonucleoside-diphosphate reductase large subunit
rop-1	60 kDa SS-A/Ro ribonucleoprotein homolog
rpa-1	Probable replication factor A 73 kDa subunit (RP-A p73)
rpa-2	RPA_C domain-containing protein
sams-4	Probable S-adenosylmethionine synthase 4 (AdoMet synthase 4)
sek-1	Dual specificity mitogen-activated protein kinase kinase sek-1 (MAP kinase kinase sek-1)
sucl-1	Succinate--CoA ligase [ADP/GDP-forming] subunit alpha, mitochondrial
tag-18	Uncharacterized protein
ttr-17	TransThyretin-Related family domain
ucr-2.2	Peptidase_M16 domain-containing protein
ule-1	Uterine Lumin Expressed/localized
unc-18	Putative acetylcholine regulator unc-18
unc-27	Troponin I 2 (CeTNI-2) (TnI 2)
unc-78	Actin-interacting protein 1 (AIP1)
Y45F10C.2	UPF0375 protein Y45F10C.2
ZK1073.1	Uncharacterized protein
ZK353.9	PITH domain-containing protein ZK353.9

Erklärung

Hiermit versichere ich an Eides statt, dass ich die vorliegende Dissertation selbstständig und ohne die Benutzung anderer als der angegebenen Hilfsmittel und Literatur angefertigt habe. Alle Stellen, die wörtlich oder sinngemäß aus veröffentlichten und nicht veröffentlichten Werken dem Wortlaut oder dem Sinn nach entnommen wurden, sind als solche kenntlich gemacht. Ich versichere an Eides statt, dass diese Dissertation noch keiner anderen Fakultät oder Universität zur Prüfung vorgelegen hat; dass sie - abgesehen von unten angegebenen Teilpublikationen und eingebundenen Artikeln und Manuskripten - noch nicht veröffentlicht worden ist sowie, dass ich eine Veröffentlichung der Dissertation vor Abschluss der Promotion nicht ohne Genehmigung des Promotionsausschusses vornehmen werde. Die Bestimmungen dieser Ordnung sind mir bekannt. Darüber hinaus erkläre ich hiermit, dass ich die Ordnung zur Sicherung guter wissenschaftlicher Praxis und zum Umgang mit wissenschaftlichem Fehlverhalten der Universität zu Köln gelesen und sie bei der Durchführung der Dissertation zugrundeliegenden Arbeiten und der schriftlich verfassten Dissertation beachtet habe und verpflichte mich hiermit, die dort genannten Vorgaben bei allen wissenschaftlichen Tätigkeiten zu beachten und umzusetzen. Ich versichere, dass die eingereichte elektronische Fassung der eingereichten Druckfassung vollständig entspricht."

Teilpublikationen:

Marija Herholz, Estela Cepeda, Linda Baumann, Alexandra Kukat, **Johannes Hermeling**, Sarah Maciej, Karolina Szczepanowska, Victor Pavlenko, Peter Frommolt, Aleksandra Trifunovic, KLF-1 orchestrates a xenobiotic detoxification program essential for longevity of mitochondrial mutants, *Nature Communications*, Volume 10, 26 July 2019.

Johannes Hermeling, Marija Herholz, Linda Baumann, Estela Cepeda, Aleksandra Zečić, Thorsten Hoppe, Jan Riemer, Aleksandra Trifunovic, Mitochondria-originated redox signalling regulates KLF-1 to promote longevity in *Caenorhabditis elegans*, *Redox Biology*, Volume 58, December 2022.

Cologne, den 14.11.2021



Johannes Christiaan Wilhelmus Hermeling

Curriculum vitae

Johannes Christiaan Wilhelmus Hermeling, M.Sc

Personal data

Date of birth: 15.10.1991, Arnhem, Netherlands
Nationality: Dutch
Address: Leonard Stassenstraat 2, 6417XP Heerlen
Email: johannes.hermeling@uk-koeln.de

Professional data

07.2017-01.2022 **PhD Candidate** at Prof. Dr. Aleksandra Trifunovic lab, CECAD Research center, University of Cologne, Germany
09.2014-06.2017 **Master of Science** in Medical Biology, Radboud University Nijmegen, Netherlands
09.2010-12.2015 **Bachelor of Science** in Biology, Radboud University Nijmegen, Netherlands
09.2004-06.2010 **High school graduate** at the Lorentz Lyceum, Arnhem, Netherlands

Conferences

30-01.09.2021 CRC Mito-RTG retreat, CECAD Research Center, Cologne, Germany. Part of organizer team
21-24.09.2021 EMBO workshop: Mitochondrial homeostasis and human disease, Girona, Spain. Poster presentation
06-07.02.2019 CMMC Annual Retreat, Nuembrecht, Germany. Poster presentation
12-13.04.2018 CRC Mito-RTG retreat, Ahrweiler, Germany
05-06.10.2017 CRC 1218 Retreat, Vaals, Netherlands. Poster presentation

Languages

English Highly proficient in speech and written
Dutch Native speaker

Publications

Mitochondria-originated redox signalling regulates KLF-1 to promote longevity in *Caenorhabditis elegans*. **Hermeling JCW.**, Herholz, M., Baumann L., Cepeda E., Zečić, A., Hoppe, T., Riemer, J., Trifunovic, A. Redox Biology, Volume 58, December 2022.

KLF-1 orchestrates a xenobiotic detoxification program essential for longevity of mitochondrial mutants. Herholz, M., Cepeda, E. Baumann, L. Kukat, A. **Hermeling, JCW.** Maciej, S. Szczepanowska, K. Pavlenko, V. Frommolt, P. Trifunovic, A., Nature Communications, Volume 10, 25 July 2019.

Mitochondrial inhibition triggers mitophagy-dependent necroptosis and ferroptosis in melanoma cells. Bast, F. van Oppen, L. Schockel, L. Bossenbroek, H. Van Ernst-de Vries, S. **Hermeling, JCW.** Grefte, S. Kopitz, C. Heroult, M. Willems, P. Koopman, W. Cell Death & Disease, Volume 8, Issue 3, 30 March 2017.

Seminars, workshops and training

23-30.11.2021	Communication, collaboration in science & academia - Dr. Ben Hartwig, Neuroblitz
07-13.04.2021	Data Analysis with R - Introduction to R Programming - Rick Scavetta, Scavetta Academy
08-10.02.2021	Skills for Project Leaders - Sabine Lerch, soft skills for science
18.01-22.02.2021	Patenting - Prof. Dr. Peter Schreier
24.8-04.09-2020	Career Mentoring and Management - Ruth Willmott, Bioscript
19-21.08.2020	Advanced Scientific Writing workshop, Writing Publishable Research Articles - Ruth Willmott, Bioscript
26-28.03.2018	Introduction workshop ImageJ, FIJI, Cellprofiler - Peter Zentis, CECAD Image Facility
07.2017-Now	MitoClub, monthly lecture series of mitochondrial biology
07.2017-Now	WIP seminars, biweekly lecture series of research project of CECAD Research center



Johannes Christiaan Wilhelmus Hermeling

21.12.22